POLYMODAL SENSATION IN THE VISUAL SYSTEM:

IMPLICATIONS FOR RETINAL FUNCTION

AND DISEASE

by

Daniel Aaron Ryskamp

A dissertation submitted to the faculty of
The University of Utah
in partial fulfillment of the requirements for the degree of

Doctor of Philosophy

Interdepartmental Program in Neuroscience

The University of Utah

December 2014

The University of Utah Graduate School

STATEMENT OF DISSERTATION APPROVAL

The following faculty members served as the supervisory committee chair and members for the dissertation of **Daniel Aaron Ryskamp**. Dates at right indicate the members' approval of the dissertation.

David Križaj, Chair		**08/01/2014** Date Approved
Richard Rabbitt, Member		**08/01/2014** Date Approved
Ning Tian, Member		**08/01/2014** Date Approved
Andres Villu Maricq, Member		**08/01/2014** Date Approved
Karen Wilcox, Member		**08/01/2014** Date Approved

The dissertation has also been approved by **Richard Dorsky**

Chair of the Department/School/College of **Neuroscience**

and by David B. Kieda, Dean of The Graduate School.

ABSTRACT

Progressive retinal ganglion cell (RGC) degeneration in glaucoma, the leading cause of permanent vision loss, is commonly caused by elevated intraocular pressure (IOP). Neuroprotective treatments complementing current IOP-reducing therapies could improve glaucoma management (Chapters 1, 3). IOP elevations induce glial reactivity (Chapter 4) and dysregulate RGC calcium (Chapters 2-3, 5-7), contributing to RGC degeneration (Chapters 5, 7), but it is unknown how glaucomatous forces perturb RGC and glial Ca^{2+} homeostasis. We discovered that mouse RGCs and Müller glia respond to osmotic pressure and tensile stretch with a cytosolic Ca^{2+} elevation that is primarily mediated by opening of the mechanosensitive cation channel transient receptor potential vanilloid 4 (TRPV4; Chapters 5-7). We therefore hypothesized that TRPV4 activation by glaucomatous forces drives RGC excitotoxicity. Consistent with this, intraocular injection of a selective TRPV4 agonist (GSK1016790A) induced mouse RGC loss (Chapter 7). This was prevented by systemic administration of a selective TRPV4 antagonist (HC-067047). Sustained exposure to glaucomatous mechanical strain caused RGC apoptosis, which was rescued by Ca^{2+} chelation or pharmacological/genetic TRPV4 antagonism, indicating that Ca^{2+} influx via TRPV4 is required for mechanical excitotoxicity (Chapter 7). Furthermore, RGCs and Müller glia swell during the progression of glaucoma and other blinding conditions, indicating the presence of aberrant osmotic gradients and loss of volume control. We found that RGC and Müller

cell swelling is exacerbated by TRPV4-dependent Ca^{2+} influx. Swelling differentially activated TRPV4 in neurons and glia, the later of which required phospholipase A2-dependent production of 5,6-EET, an endogenous TRPV4 agonist. The water channel aquaporin 4 (AQP4) facilitated water entry, which enhanced glial TRPV4 activation (Chapter 6). Finally, we found that TRPV4 antagonism in mouse and primate glaucoma models lowered IOP to normal levels, potentially by promoting fluid drainage from the eye via the trabecular meshwork (TM). Although IOP elevation for eight weeks caused mouse RGC loss, this was prevented by daily treatment with a TRPV4 antagonist (Chapter 7). TRPV4 inhibition, therefore, simultaneously lowers IOP and increases RGC resilience. This, together with our finding that TRPV4 is expressed in human RGCs, Müller glia and TM cells (Chapters 6, 7), makes TRPV4 an attractive therapeutic target for prevention of glaucoma.

To John and Carrie Ryskamp for teaching me to explore and think freely, to Dory Ryskamp for sparking my interest in the brain, to Steffen Werner for germinating my passion for research and to Jade Francetich for love, support and comic relief.

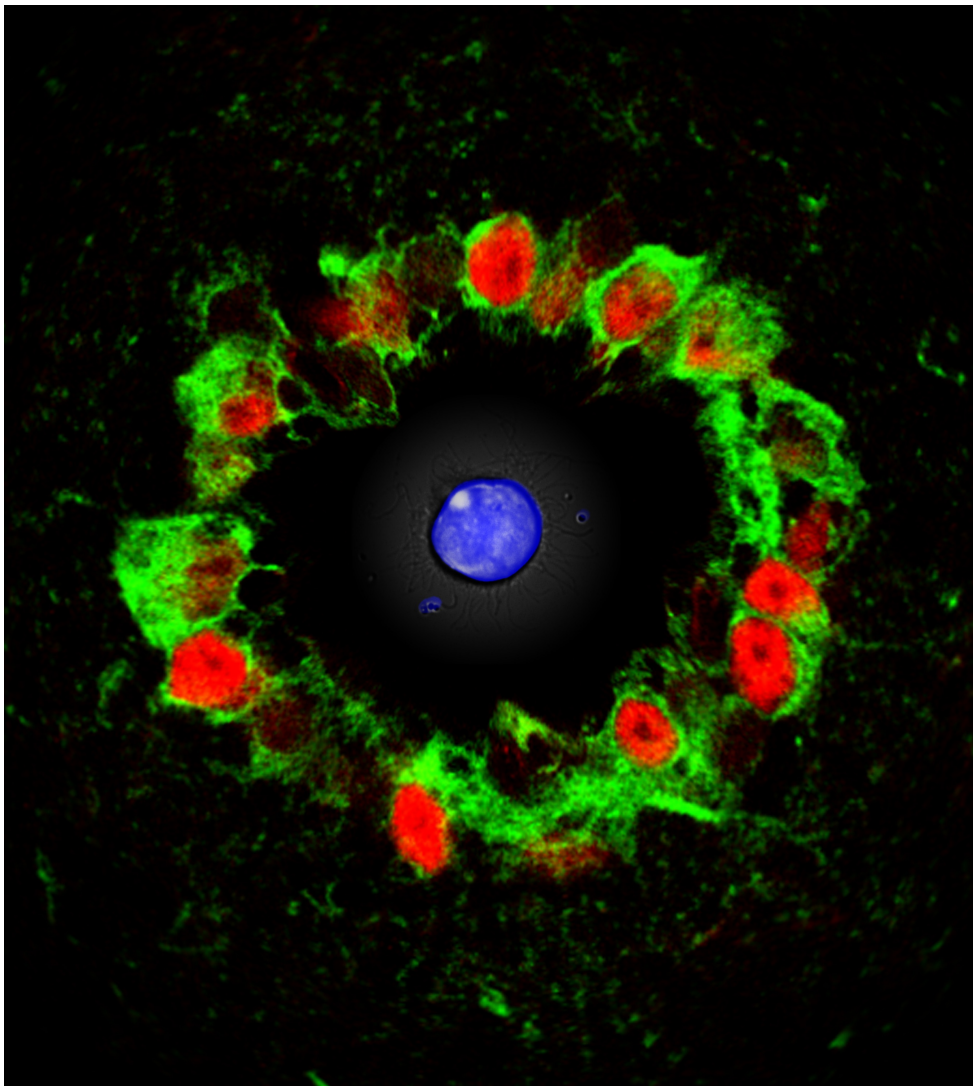

This frontispiece illustrates retinal ganglion cells, which are vulnerable to intraocular pressure in glaucoma, expressing the force-sensitive and calcium-permeable ion channel Transient Receptor Potential Vanilloid 4 (TRPV4), a phenomenon that may explain how intraocular forces dysregulate calcium in retinal ganglion cells and cause their degeneration. The concentric arrangement symbolizes the appearance of pressure phosphenes, which may be generated through mechanical activation of TRPV4. This image is a collage of TRPV4-immunofluoresence (green) in retinal ganglion cells (red Brn3a^{+} nuclei) and a brightfield/epifluorescence image of a *Thy1*:CFP^{+} RGC (blue).

"The eye obviously has fire within, for when the eye is struck fire flashes out."

— Alcmaeon of Croton, 5th century B.C., *On the history of deformation phosphenes and the idea of internal light generated in the eye for the purpose of vision* (Grüsser and Hagner, 1990, p. 58).

TABLE OF CONTENTS

LIST OF ABBREVIATIONS

$[Ca^{2+}]_i$: concentration of cytosolic/intracellular calcium

2-AG: 2-arachidonoylglycerol

5,6-EET: 5'6'-epoxyeicosatrienoic acid

AA: arachidonic acid

AEA: anandamide

AMPA: α-Amino-3-hydroxy-5-methyl-4-isoxazolepropionic acid

ATP: adenosine triphosphate

BBB: blood brain barrier

BRB: blood retina barrier

$[Ca^{2+}]_i$: intracellular calcium concentration

CB1: cannabinoid receptor type I

CB2: cannabinoid receptor type II

CNS: central nervous system

DAG: diacylglycerol

ER: endoplasmic reticulum

FAAH: fatty acid amide hydrolase

GCL: ganglion cell layer

GFAP: glial fibrillary acidic protein

Glut: glutamate

GMP: guanosine monophosphate

GPCR: G protein-coupled receptor

GSK101: GSK1016790A

GWAS: genome wide association studies

HC-06: HC-067047

HEK: human embryonic kidney

HpETEs: hydroperoxyeicosatetraenoic acids

HTS: hypotonic stimulation

IOP: intraocular pressure

ILM: inner limiting membrane

INL: inner nuclear layer

IPL: inner plexiform layer

IR: immunoreactivity

IS: inner segments

LGN: lateral geniculate nucleus

LO: lipoxygenase

mGluR: metabotropic glutamate receptor

MT: middle temporal

μG: microglia

MG: Müller glia

NADA: N-arachidonoyl dopamine

NAPE: N-acylphosphatidylethanolamine

NAPE-PLD: NAPE-specific phospholipase D

NFL: nerve fiber layer

NMDA: N-methyl-D-aspartate

OLM: outer limiting membrane

ONH: optic nerve head

ONL: outer nuclear layer

OPL: outer plexiform layer

OS: outer segments

PBS: phosphate-buffered saline

PEA: N-palmitoylethanolamide

PIP2: phosphatidylinositol 4,5-bisphosphate

PKC: protein kinase C

PLA2: phospholipase A2

PLC: phospholipase C

POAG: primary open-angle glaucoma

PNS: peripheral nervous system

PR: photoreceptor

RGC: retinal ganglion cell

RGCL: retinal ganglion cell layer

RT: room temperature

RT-PCR: Real-time polymerase chain reaction

TBI: traumatic brain injury

TLR: toll-like receptor

TOI: traumatic ocular injury

TRPM1: transient receptor potential melastatin 1

TRPV1: transient receptor potential vanilloid 1

TRPV4: transient receptor potential vanilloid 4

V1: primary visual cortex

ACKNOWLEDGEMENTS

I am deeply appreciative of the guidance, feedback and support provided by my mentor, David Krizaj, over the last five years. I joined his lab with limited experience in cellular and molecular physiology, but he cultivated a research environment in which I thrived. From the start, he allowed me to take over a promising project that has budded into several fruitful research directions and led to the preparation and publication of many manuscripts in addition to the identification of a promising therapeutic target for glaucoma. He was always available for questions and promptly responded to my emails and requests. Moreover, he proactively monitored my progress and helped in any way possible, from providing experimental and conceptual suggestions to buying reagents to support my research, even when my ideas were somewhat fanciful. Through his guidance, I learned how to efficiently approach science while maintaining rigor and opportunistic watchfulness. He generously sought out and provided me with many opportunities ranging from going to other labs to learn new techniques to conference attendance. His help in conference abstract composition undoubtedly improved my odds at securing travel grants and paper presentations. In addition to passing on his skills as a raconteur, he imparted his knack for poetic and thoughtful story telling in conversations, presentations and scientific writing. Beyond research training, he allowed me to instruct undergraduates, graduate students and even postdoctoral fellows to gain teaching experience. He enthusiastically supported my academic training outside of the lab and

was patient and understanding when extracurricular or personal activities slowed my research. For all of these reasons and more, I thank David Krizaj from the bottom of my heart for his outstanding involvement in my career and life development. Most importantly, I am grateful to David for demonstrating an inspirational and unrestrained enthusiasm for discovery, innovation and academic progress while maintaining a passion for adventure, friendship and the richness of life.

My labmates also deserve special thanks for their involvement in my training and for their contributions to this research. Peter Barabas comprehensively taught me lab techniques and procedures. He tirelessly answered my exhaustive list of questions and always stopped what he was doing to help me when needed. In particular, he taught me how to systematically troubleshoot and to creatively develop solutions for experimental and scientific problems. Peter helped David to develop the theoretical and experimental groundwork for my research project, suggesting TRPV4 as a candidate retinal ganglion cell (RGC) mechanosensor. In particular, David Krizaj, Paul Witkovsky, Peter Barabas, Helen Huang, Wei Xing and Wolfgang Liedtke generated the preliminary data suggesting the expression of TRPV4 in RGCs. My early experiments with Peter Barabas and later, just myself, demonstrated the functional expression of TRPV4 in RGCs and Müller glia. Amber Frye worked closely with me to investigate the role of TRPV4 in the pathogenesis of glaucoma using rodent and primate models of glaucoma. After making the initial discovery together that TRPV4 activity is required for pathological elevations of intraocular pressure and that TRPV4 is functional in trabecular meshwork cells, Amber worked diligently to quantify the extent of RGC loss in glaucoma models, identify new drugs/formulations for TRPV4 inhibition and to characterize TRPV4 physiology and

function in trabecular meshwork cells. Her tenacious motivation to master difficult experiments and techniques is inspirational and has enriched my work ethic. Amber and Tünde Molnar in particular taught me the importance of friendship and teamwork for effective scientific progress and emotional/social wellbeing. Tünde taught me the basics of electrophysiology and was instrumental in helping me to collect, analyze and interpret retina-specific data from high-speed pressure clamp experiments, a technique taught to me by Fred Sachs' lab (with help from Phil Gottlieb, Tom Suchyna, Radhakrishnan Gnanasambandam, Chilman Bae, Chris Nicolai, and Stephen Besch). Andrew Jo helped me with several calcium and volume imaging experiments, even after staying up all night. Shiwani Chauhan and Erik Soderborg helped me to collect and analyze data on RGC apoptosis. Sarah Redmon helped me to examine TRP channel function in microglia and to review literature on ocular and brain injuries. Anthony Iuso taught me more about the importance of membrane lipids in the regulation of TRP channel activity. Tam Phuong taught me about molecular biology techniques. I am grateful to everyone that has worked in and with David Krizaj's lab for help with projects as well as for their collective creation of such enjoyable memories.

I also thank many others at the University of Utah for participating in my training. Mary Lucero, a prior committee member, helped me to better evaluate scientific literature and electrophysiological experiments in classes and with a small journal club on the olfactory system. Ed Levine served on my committee during my qualifying exam and provided advice on NRSA grant applications. My current advisory committee members, including David Krizaj, Rick Rabbit, Ning Tian, Villu Maricq and Karen Wilcox, provided me with excellent experimental and conceptual advice and sharpened my ability

to think critically and practically. Tracy Marble helped to keep me on track in the neuroscience program. Anthea Letsou, Dean Li, Stephen Lessnick, Anne Moon, and Kevin Whitehead provided extensive training in translational research through the HHMI Med into Grad Program. David Shprecher allowed me to shadow him during his visits with patients that have Huntington's disease, Parkinson's disease, progressive supranuclear palsy, and other movement disorders. This invaluable experience is helping me to design my future postdoctoral research with Ilya Bezprozvanny. Jeff Anderson, Bradley Greger, Annette Fleckenstein and students in their labs facilitated my transition from research on cognitive neuroscience to cellular and molecular neuroscience. Bryan Jones taught me about computational and internet-based tools for research and self-promotion. Al Light and his lab taught me about pain research and how to isolate dorsal root neurons. Stefan Pulst taught me about spinal cerebellar ataxias, a relevant subject for my postdoctoral research. Gary Schoenwolf improved my scientific and grant writing through workshops. Kevin Breen, Jared Nielson, James Tucker, Felix Vazquez-Chona, Renee Bend and Lisa Briona were particularly helpful in preparing me for my qualifying exam. Eerik Elias helped to teach me about electrophysiology and whole-cell recording of RGCs. Other members of Ning Tian's lab taught me how to induce glaucoma using the microbead occlusion model and how to culture primary retinal cells. Micah Frerck taught me a great deal regarding the biophysics of infrared neural stimulation and has been fun to collaborate with. The Center for Teaching and Learning Excellence and in particular, Rai Farrelly, improved my ability to teach. Chris Rodesch taught me a great deal about microscopy, ImageJ and macros. In addition to providing new research opportunities, Chris Reilly taught me about recombinant overexpression systems and high-throughput

drug screening. He also provided several recombinant cell lines for ongoing experiments. Thank you all and thank you to the several other excellent course instructors and faculty members. Finally, thank you to many neuroscience, bioengineering, biology, molecular biology, biochemistry, physiology, geology, paleontology, atmospheric science and MD/PhD students for making graduate school so fun!

This work was supported by the HHMI Med into Grad scholarship (DR), NIH (T32DC008553, DR; EY13870, EY022076, P30EY014800 Vision Core grant, DK), Department of Defense W81XWH-12-1-0244, the International Retina Research Foundation, the Richard H. Chartrand Foundation, State of Utah TCIP, Glaucoma Research Foundation, the Foundation Fighting Blindness, the Moran TIGER award, and unrestricted grants from Research to Prevent Blindness to the Moran Eye Institute.

Reprint permissions were approved for Chapters 2 (Cells and MDPI), 3 (Current Eye Research and Informa Healthcare), 4 (Experimental Eye Research and Elsevier, LTD) and 5 (The Journal of Neuroscience) as well as for the appendix (Pharmacology Research & Perspectives and Wiley).

CHAPTER 1

AN INTRODUCTION TO POLYMODAL SENSATION IN THE RETINA AND ITS RELATION TO GLAUCOMA

This chapter discusses the nature of polymodal sensation in the visual system and its implications for retinal function and disease. Concepts regarding mechanosensation in the eye, retinal Transient Receptor Potential (TRP) channel physiology and the pathogenesis of glaucoma will be discussed. This chapter also introduces the rationale for this research and the primary hypothesis that glaucomatous forces perturb retinal ganglion cell and glial calcium signaling by overactivation of the mechanosensitive TRP Vanilloid 4 (TRPV4) cation channel, resulting in glial reactivity and retinal ganglion cell (RGC) excitotoxicity.

1.1 Polymodal Sensation in the Visual System

Sensory systems (e.g., vision, hearing, touch, taste, smell) encode more than the external world, they monitor and adapt to the physical and chemical environment in which they exist. For example, in addition to transducing and processing light information, cells in the retina respond to physical forces. However, very little is known about the physiological mechanisms that mediate mechanosensation in retinal cells. This section provides a brief overview of the visual system, a historical perspective on theories of vision and how mechanically induced percepts of light might be generated by the same molecular mechanisms that affect RGC vulnerability to intraocular pressure (IOP) in glaucoma.

1.1.1 Overview of the Visual System

Visual perception allows sighted animals to rapidly gather information from their surroundings, enabling them to efficiently navigate through and interact with their external environment. Visible light (electromagnetic radiation of wavelengths between ~400 and 800 nm), when reflected or emitted by objects in space to the eye, is focused by the cornea, pupil and lens onto the retina, creating an image that is transduced by photoreceptors in the outer retina into chemical and electric signals that are ultimately processed by the retina and brain for visual perception to occur.

In mammals, phototransduction occurs in photoreceptor outer segments when an absorbed photon converts the chromophore 11-*cis* retinal to all-*trans* retinal within a rhodopsin (in dim-light sensitive rod photoreceptors) or a cone opsin (in bright-light and color sensitive cone photoreceptors) G-protein coupled receptor. This triggers a

biochemical cascade that closes cyclic guanosine monophosphate (GMP)-gated cation channels, which are active in the absence of light (generating the "dark current"). This hyperpolarizes photoreceptors situated in the outer nuclear layer (ONL), reducing voltage-gated calcium influx into their synaptic terminals, which decreases vesicular release of glutamate within the outer plexiform layer (OPL). Bipolar cells relay this information to RGCs as it is processed through parallel horizontal cell pathways within the OPL and serial activation of amacrine cell processes in the inner plexiform layer (IPL; Livingston, 2002). Although there are several types of bipolar cells, they are generally divided into two classes, ON (light responsive) bipolar cells and OFF (light responsive) bipolar cells. While OFF bipolar cells are depolarized by glutamatergic input from photoreceptors by activation of α-Amino-3-hydroxy-5-methyl-4-isoxazolepropionic acid (AMPA), kainate and N-methyl-D-aspartate (NMDA) ionotropic receptors, ON bipolar cells are hyperpolarized by metabotropic glutamate receptor 6 (mGluR6)-mediated inhibition of transient receptor potential melastatin 1 (TRPM1) cation channels (Shen et al., 2009; Morgan et al., 2009). Release of glutamate from bipolar cell terminals in the IPL drives depolarization of postsynaptic amacrine cells and RGCs. Amacrine cells, which are located in both the inner nuclear layer (INL) and the ganglion cell layer (GCL) shape the receptive field and response properties of RGCs. These features are also shaped by the morphology and connectivity of RGC dendritic arbors as well as the convergence/divergence of information flow through the retina. RGCs are the only cell type that conveys visual information from the retina to the brain. Although there are several types of RGCs, they are generally classified as ON, OFF, or mixed ON-OFF RGCs (responsive to light turning on or off). They are further functionally characterized

as transient or sustained depending on the duration of their response to changes in light levels and by their response selectively (e.g., stimulus direction selectivity). While these types of RGCs provide image-forming vision to the brain through axonal projections to the lateral geniculate nucleus (LGN) of the thalamus, intrinsically photosensitive RGCs enervate brain regions that entrain the circadian rhythm such as the suprachiasmatic nucleus (Hattar et al., 2002).

Each LGN receives input from both eyes and is organized into three different types of neuronal layers: magnocellular, parvocellular and koniocellular layers. The neurons of each layer convey different types of information to the primary visual cortex (V1). Neurons in the magnocellular layers transmit low-acuity, colorless motion and depth information. They respond to slight changes in luminance with fast and transient signals. Parvocellular pathway neurons convey information about color and fine details. The koniocellular layers pass on low-acuity information from photoreceptors that respond to short wavelengths of light (Carlson, 2007).

The primary visual cortex is also organized into layers similar to those found in the LGN and maintains a retinotopic organization. As visual information is integrated during transit through the visual pathways, neurons in the visual cortex become progressively specialized and can respond to more complex visual features than retinal cells (e.g., orientation or retinal disparity). V1 is an organized mosaic of modules with each module representing a small region of the visual field that is proportional to its receptive field dimensions. Although these modules, when taken together, comprise the entire visual field, they cannot individually represent objects or the totality of a scene. Such information requires further integration and is represented more holistically in the visual

association cortex (Carlson, 2007; Livingston, 2002).

Broad anatomical and functional divisions of visual association cortex were first noted by Ungerleider and Mishkin (1982) based on their electrophysiological, anatomical, and behavioral studies. They identified two main visual pathways by studying behavioral changes in monkeys with lesions to specific cortical areas. Monkeys with damage to the ventral visual pathway, which includes the infero-temporal cortex, exhibited impairments in pattern and object recognition tasks, and were only mildly impaired in "landmark" tasks. By contrast, the performance of monkeys with damage to the dorsal stream, which includes the posterior parietal cortex, was the opposite on the same tasks (Goodale & Milner, 1992). As the ventral stream contributes to conscious perception and recognition of objects, faces and color, damage to its specialized subregions can specifically impair these types of perceptions (Sacks, 1996). For example, damage to the fusiform region of the inferior temporal cortex causes prosopagnosia, the inability to recognize faces, a deficit ironically afflicting the portrait artist Chuck Close (Farley, 2011). The dorsal stream provides visuomotor guidance and contributes to perception of motion, depth, spatial organization and figure/ground segregation. Because the dorsal stream is used to recognize spatial relationships, it is also commonly referred to as the "where" system. Damage to its specialized subregions also cause peculiar visual deficits. For example, bilateral damage to visual area middle temporal (MT) in the parietal lobe causes akinetopsia (i.e., motion blindness; Zeki, 1991). Following the formation of external representations within discrete brain regions, "binding" of visual features through visual system-wide integration as well as the incorporation of information from other senses and top-down cognitive processes ultimately brings reality

together into a coherent construct. This feat would not be possible without the senses. As their lifelong reliability depends on the preservation of sensory cell/neuronal homeostasis, it is important to understand not only how the senses function normally, but also how cells within sensory systems detect and respond to internal stressors such as biomechanical strain.

1.1.2 Force-Light Synesthesia

In cognitive neuroscience the topic of polymodal sensation is strongly associated with synesthesia, a neurological condition in which the perception of a stimulus attribute in one modality causes the perception of an additional stimulus attribute in another modality (Ward, 2013). As an example, in grapheme-color synesthetes, the sight of a letter also produces the perception of color (Fig. 1.1).

Although synesthesia is considered a rare neurological condition at the systems level, we all have synesthesia, at least at the cellular level. In physiological conditions, polymodal sensation in sensory tissues is adaptive (Taylor et al., 2013), preserving homeostasis at molecular, cellular, and systems levels. By contrast, excessive polymodal sensation can be excitotoxic for neurons, causing neurodegeneration and, in the case of the visual system, blindness. The polymodal behavior of the retina was first noted more than two millennia ago and inspired early theories of vision.

1.1.3 Ancient Theories of Vision

In the fifth century B.C., Alcmaeon of Croton, a founder of Greek medicine and member of the Pythagorean sect, was the first to report that when he applied pressure to

his eye, he perceived light (Grüsser & Hagner, 1990). He concluded, “the eye obviously has a fire within, for when the eye is struck fire flashes out” (Theophrast, 1994). This observation, combined with the fact that the eyes of many vertebrates reflect light (iridescent eyeshine from the tapetum lucidum; Ollivier et al., 2004), led another Greek physician, Empedocles (419-430 B.C.), to hypothesize that light from the “fire” in the eye illuminates the external world, reflecting back from objects to the eye for visual perception to occur (Grüsser & Hagner, 1990). Plato (427-347 B.C.) and other philosophers refined this theory, including a role for external light in the formation of vision through the interaction of external and projected light (Grüsser & Hagner, 1990). An elegant experiment by Giovanni Battista Morgagni (1682-1771) disproved the idea that physical light is generated in the eye (Grüsser & Hagner, 1990). In a dark room, Morgagni indented his eye to generate perceptions of light and an assistant looked for evidence of physical light. No light was perceptible by the assistant even though pressure phosphenes were readily apparent to Morgagni. Morgagni concluded that the deformed eye does not generate light, vision is dependent on external light, and the retina is responsive to mechanical strain (Grüsser & Hagner, 1990). Although we now realize that pressure phosphenes result from the physiological responses of retinal cells to mechanical strain, very little is known about mechanosensation in retinal cells.

1.1.4 Retinal Mechanosensitivity

All cells and organisms live within mechanically active environments in which they must sense and adapt to physical changes. Cells in the retina are no exception. As a neural tissue within the eye, they are constantly exposed to shifting osmotic gradients

(Fields & Ni, 2010), IOP fluctuations/elevations (Downs et al., 2011), torsional forces of vitreal humor during saccades (Hilding, 1954), blood vessel contraction/dilation (Metea & Newman, 2006), changes in the structure and compliance of tissues surrounding the retina/optic nerve (Zatulina et al., 1989; Quigley et al., 1991; Burgoyne et al., 2005) and forces associated with tissue patterning during development (Taylor et al., 2013). In excess, biomechanical stress contributes to pathology in many retinal diseases, including ischemia, diabetic retinopathy (Suzuma et al., 2001; Pannicke et al., 2006; Wurm et al., 2008), cytotoxic retinal edema (Bringmann et al., 2004) and glaucoma (Grüsser et al., 1989; Anderson et al., 2006; Burgoyne, 2011). For example, the optic nerve head (ONH) is an important injury site during ocular hypertension. High IOP stretches laminar beams and remodels cribriform plates of the lamina cribrosa. This, combined with the outward force from IOP, causes the ONH to "cup," damaging RGC axons (Burgoyne, 2011). In addition, IOP elevations force the eye to expand/stretch and thin the sclera (Zatulina et al., 1989) and consequent physiological changes in the retina can generate osmotic gradients that cause cells to swell or shrink (Weber et al., 1998; Bringmann et al., 2004; Wurm et al., 2008; Pinar-Sueiro et al., 2011). Although the mechanisms through which excessive cell swelling and IOP compromise the viability of retinal cells are not well understood, it is clear that biomechanical strain alters retinal cell physiology through mechanosensation. For example, Grüsser et al. (1989) recorded action potentials from the optic nerve of a cat and found that when IOP is sufficiently elevated, many RGCs increase their firing rate. Because RGCs relay visual information from the retina to the brain, the increased firing rate is perceived as light, even though RGC excitation resulted from mechanosensory responses rather than light responses. Although this experiment

demonstrated that the retina responds to IOP elevations, it was not clear whether RGCs directly transduce mechanical stimuli or whether they are excited by synaptic input from other, more mechanosensitive cells. Given that an excessive responsiveness to force can cause cellular damage (Jaalouk & Lammerding, 2009), if RGCs are directly sensitive to IOP, this could explain why they, but not other cells, are killed by the effects of IOP in glaucoma.

1.1.5 Glaucoma

Glaucoma is a complex disease with a diverse set of etiologies and a common phenotype, the progressive degeneration of RGCs. These projection neurons tend to die in the peripheral retina first, causing peripheral vision loss (Kwon et al., 2009). Once dead, RCGs cannot be replaced (Crish & Calkins, 2011); consequently, glaucomatous vision loss is permanent. Glaucoma is the leading cause of irreversible blindness in the world (Giangiacomo & Coleman, 2009) and with an aging population, the global prevalence of glaucoma will rise to 80 million affected individuals by 2020 (Quigley & Broman, 2006). Eleven million of these patients will suffer from bilateral blindness (Quigley & Broman, 2006). The most common type of glaucoma is primary open-angle glaucoma (POAG), which will afflict approximately 3.4 million in the United States by 2020 (Friedman et al., 2004). Glaucoma is most frequent in Africa and Asia (Quigley & Broman, 2006). The high rates of glaucoma in these regions may reflect genetic predispositions and environmental factors such as socioeconomic status and cultural differences (e.g., access to care and treatment compliance; Takusagawa & Mansberger, 2012).

1.1.6 The Standard of Glaucoma Care

Current glaucoma treatments are limited to attempts to minimize mechanical impact by lowering IOP (Bonomi et al., 2001; Sena et al., 2010). IOP elevates when there is too much fluid production by the ciliary body (a muscle posterior to the iris that contracts the lens during accommodation) and/or too little fluid drainage, which primarily occurs by fluid outflow through the trabecular meshwork (TM) and then Schlemm's canal. IOP can be lowered by pharmacological or surgical procedures.

Pharmacological approaches commonly use eye drops to topically deliver active ingredients to targets in ciliary body and/or the TM. The typical first approach is to prescribe a once-daily treatment of prostaglandin analogues (e.g., Latanoprost or Travoprost), which promote aqueous humor drainage by reducing the outflow resistance of the uveoscleral pathway (Gaton et al., 2001). Although this approach lacks systemic side effects (other than potential headaches), it can cause conjunctival hyperemia, loss of orbital fat, eyelash elongation and darkening of eyelashes, irises and nearby skin (Weinreb et al., 2014). β-adrenergic blockers (e.g., Timolol) and α-adrenergic agonists (e.g., Brimonidine) reduce aqueous production, but cause ocular irritation and dry eyes in addition to allergic reactions and severe systemic effects (e.g., respiratory arrest in young children, kidney failure or liver failure; Weinreb et al., 2014). Carbonic anhydrase inhibitors (e.g., Dorzolamide) likewise reduce inflow and can cause ocular irritation/burning, but systemic side effects of topical treatment are minimal (Weinreb et al., 2014). Cholinergic agonists increase fluid outflow, but cause ocular irritation, myopia and ciliary muscle spasms, which can decrease vision and cause headaches (Weinreb et al., 2014). The efficacy of pharmacological treatments wanes in many patients (Shaarawy

et al., 2004). If other active ingredients do not work well or are not tolerated, sometimes combination eye drops work (Higginbotham et al., 2002). Otherwise, surgical approaches are needed to lower IOP.

Trabeculectomy is the most commonly used surgical procedure to treat glaucoma. It involves removing or lasing part of the TM and/or placing a shunt within the TM to facilitate aqueous drainage. This procedure puts patients at 43-104% risk for developing cataracts depending on surgery difficulty (Patel & Danesh-Meyer, 2013). Other potential complications include: vision loss (18%), wound leaking (14%) shallow/flat anterior chamber (13%), eyelid drooping (12%), choroidal detachment (11-14%), hyphema/bleeding in the anterior chamber (10-24%), encapsulated bleb (3-12%) and suprachoroidal hemorrhaging (0.7%; Moster & Azuara-Blanco, 2014). Given the potential lack of efficacy and/or dire complications associated with glaucoma treatment (Lichter et al., 2001), it is important to identify new therapeutic strategies. Furthermore, IOP reducing therapies cannot reverse retinal damage (Bosco et al., 2008), creating an urgent need for new approaches that prevent disease progression at an early stage.

One blatantly lacking therapeutic approach is to protect the retina directly from the effects of IOP. Unfortunately, no neuroprotective treatments are available for glaucoma (Sena et al., 2010); chiefly because the IOP transduction mechanism within RGCs remains unknown. Although some people who develop glaucoma have normal IOP (Shields, 2008), even such “normal tension” glaucoma patients benefit from IOP reduction (Heijl et al., 2002), suggesting that their RGCs might be sensitive to normal levels of pressure (Libby et al., 2005; Anderson et al., 2006; Sappington et al., 2009). What then determines retinal vulnerability to mechanical strain? The purpose of this

research project was to address this question through the identification of mechanosensitive molecules within the retina that respond to glaucomatous forces and thereby initiate biochemical cascades known to underlie the progressive degeneration of RGCs in glaucoma.

1.1.7 Genetic Contributions to Glaucoma Risk and RGC Susceptibility

Glaucoma susceptibility is primarily genetic, but its molecular basis is largely enigmatic. Several risk factors contribute to glaucoma susceptibility and they differ for distinct types of glaucoma. In primary open-angle glaucoma (POAG), the site of ocular fluid drainage (in the angle between the iris and the cornea called the iridocorneal angle, or "the angle" for short) remains open at a macroscopic level (Kwon et al., 2009). Risk factors for this type of glaucoma include elevated IOP, advanced age, African ethnicity, family history, near-sightedness, and decreased corneal thickness (Bonomi et al., 2001; Klein et al., 2004; Kwon et al., 2009). Primary acute angle closure glaucoma involves a physical blockade of fluid drainage caused by contact between either lens and iris or iris and cornea (Berkoff & Sanchez, 2005). This can happen suddenly; for example, when a patient's iris dilates in the dark (Berkoff & Sanchez, 2005). Given a liable anatomy, the structural change associated with dilation can greatly elevate IOP, making acute angle closure a medical emergency (Berkoff & Sanchez, 2005). Risk factors include Inuit and Asian ethnicity, far-sightedness, female gender, thick lenses, and certain corneal dimensions (e.g., a small corneal diameter; Giangiacomo & Coleman, 2009). In normal tension glaucoma, IOP is below 21 mmHg (Kwon et al., 2009); however, reducing

intraocular pressure can still slow disease progression (Drance et al., 2001). This suggests that the retinas and optic nerves of these patients are susceptible to normal levels of pressure (Crish & Calkins, 2011). Normal tension risk factors include IOP, advanced age, race, near-sightedness, family history, migraine, optic disk hemorrhage, and female gender (Drance et al., 2001). Pigmentary glaucoma can result from pseudoexfoliation syndrome/pigment dispersion syndrome in which the iris breaks apart, disperses, and clogs fluid drainage ducts (Takusagawa & Mansberger, 2012). Risk factors for pseudoexfoliation syndrome include lower ambient temperatures, sunlight exposure, and Caucasian ethnicity (Takusagawa & Mansberger, 2012). Trauma to the eye can cause a glaucomatous phenotype by either disrupting normal intraocular fluid dynamics or directly damaging the retina/optic nerve (Leon-Ortega & Girkin, 2002). Rare, childhood glaucomas (a.k.a. congenital glaucomas or juvenile-onset glaucomas) occur before 35 years of age, usually involve very high IOP and feature heritable risk (Kwon et al., 2009; Rao et al., 2011).

Glaucoma is a moderately to highly heritable disease, segregating in progeny as either a Mendelian trait or a complex multifactorial trait (Wiggs, 2007). There is a family history of POAG in 60% of patients and a 10 fold higher risk for first-degree relatives (Burdon, 2012). POAG heritability is around 0.81 and endophenotypes (quantitative traits contributing to disease) are also passed on at high rates (Burdon, 2012). For example, IOP and optic cup diameter (the central cup-like portion of the optic disc where the optic nerve exits the eye) have heritability estimates of 0.36 and 0.55, respectively (Klein et al., 2004). The acute angle glaucoma endophenotype of having narrow angles is 58.8% heritable in Asians (Amerasinghe et al., 2010). Because of the heritable nature of

glaucomas, linkage studies have associated several loci with POAG, acute angle closure glaucoma, normal tension glaucoma, pigmentary glaucoma, and childhood glaucoma (Weisschuh et al., 2005).

Linkage studies and genome wide association studies (GWASs) have uncovered several risk alleles and loci for glaucoma. At least 25 gene/locus variants that increase risk for POAG have been identified by linkage analysis in large affected families (Rao et al., 2011). Most notably, variations in the myocilin gene *MYOC* (a.k.a. *GLC1A*) account for 3-4% of POAG cases (Burdon, 2011). Several studies suggest that mutations in *MYOC* cause trabecular meshwork (TM) dysfunction, remodeling and/or death, limiting ocular fluid outflow (Rao et al., 2011). The first GWAS involving POAG patients found two variants at the lysyl oxidase-like 1 (*LOXL1*) locus. However, the patients with these variants had pseudoexfoliation syndrome (Burdon, 2011), highlighting the importance of accurate phenotypic distinctions. Additional studies confirmed the occurrence of *LOXL1* polymorphisms in pigmentary glaucoma patients; however, many controls (74%) also have the risk allele (compared with 92% in pseudoexfoliation patients; Takusagawa & Mansberger, 2012), indicating that additional factors determine whether *LOXL1* polymorphisms contribute to pseudoexfoliation. Possible genetic-disease associations with POAG/normal tension glaucoma include loci in or near: optineurin (*OPTN*/*GLC1E*), WD repeat domain 36 (*WD36*, *GLC1G*), neurotrophin-4 (*NTF4*, *GLC1O*), *TMCO1, ZP4*, *PLXDC2*, *DKFZp762A217* and *SRBD1* (Burdon, 2011; Rao et al., 2011). Another disease-related SNP was identified in *CDKN2B-AS1* (odds ratio of 1.5). This long, noncoding RNA regulates the expression of four genes (*TMCO1*, *CDKN2B-AS1*, *CDKN2A*, and *CDKN2B*), all of which are upregulated in RGCs by high IOP and

potentially involved in the stress response leading to apoptosis (Burdon, 2011). These and other findings emphasize the importance of relating IOP-dependent transcriptional (e.g., Miyahara et al., 2003) and posttranslational (e.g., Huang et al., 2005) alterations to pathogenic mechanisms and disease outcome. Although linkage studies and GWASs have identified many genes in the major forms of glaucoma (see also Awadalla et al., 2011 a/b; Kwon et al., 2009), less than 10% of the heritable risk for POAG can be accounted for by known genetic associations (Burdon, 2011). Although future exome and genome sequencing studies will help to identify rare alleles with large risk that can be missed by GWASs, the diversity of risk mechanisms makes it difficult to pinpoint key genes in the development of glaucoma. Thus, to understand the bulk of heritable risk and the primary pathogenic mechanisms in this complex group of polygenic diseases, there is a need for more than associative genomic studies. Further, progress in glaucoma treatment requires experimental research to elucidate how risk alleles and their interactions with other genetic, physiological and environmental factors contribute to forces that drive glaucoma and/or RGC vulnerability. Because many risk alleles remain elusive, experimental research is also needed to envision and test possible disease mechanisms that could underlie the pathogenesis or progression of neurodegeneration and visual dysfunction in glaucoma.

1.1.8 Calcium Dysregulation in Glaucoma

Calcium dysregulation in RGCs has been implicated in the pathogenesis of glaucoma, leading to calcium-mediated biochemical cascades, axonal transport deficiencies, and apoptosis (Crish & Calkins, 2011). We (Ryskamp et al., 2011) and others (Tan et al.,

2006; Crish & Calkins, 2011; Xia et al., 2012) suspect that the impinging forces of IOP open mechanosensitive ion channels, excessively elevating the concentration of cytosolic calcium ($[Ca^{2+}]_i$) in RGCs and causing apoptosis. For example, high IOP (as seen in glaucoma) triggers calcineurin activation, a calcium-dependent phosphatase that, once activated in the soma, triggers RGC apoptosis (Huang et al., 2005). Calpain activation also occurs in experimental glaucoma models and is thought to contribute to axonal transport deficiencies (Huang et al., 2008), depriving RGC cell bodies of retrograde trophic support (Quigely et al., 2000). Axonal calcium influx can also accelerate axonal degeneration (Knöferle et al., 2010). Moreover, glaucoma risk is increased by taking high doses of daily calcium supplements (Wang et al., 2012), or by not taking calcium channel blockers (Tomita, 2000). What then transduces glaucomatous forces into RGC Ca^{2+} dysregulation?

1.1.9 Retinal Mechanosensation

Cells in the eye sense impinging biomechanical strain and become stressed as they shift from their homeostatic state. This involves mechanosensation, the biological process by which mechanical forces are transduced into physiological signals such as calcium influx into brain cells (Xiong et al., 1997; Weber et al., 1999; Goforth et al., 1999; Geddes-Klein et al., 2006), driving secondary injury mechanisms (discussed below). Mechanosensitive ion channels are among the most sensitive and prevalent types of biological force sensors (Martinac, 2004; Kung, 2005). As the cell deforms, mechanosensitive ion channels open and allow ions to flow into and/or out of the cell depending on channel properties (Vogel & Sheetz, 2006; Christensen & Corey, 2007).

Among them, TRPV4 is one of the best-characterized Ca^{2+}-permeable channels (O'Neil & Heller, 2005; Suzuki & Mizuno, 2012). TRPV4 senses both physiologically relevant forces such as cell stretch and swelling (Liedtke et al., 2000; Alessandri-Haber et al., 2003; Liedtke & Friedman, 2003; Suzuki et al., 2003; Alessandri-Haber et al., 2004; Becker et al., 2005; Chen et al., 2007; Gevaert et al., 2007; Wang et al., 2007; Loukin et al., 2010; Sonkusare et al., 2012; Zaika et al., 2013) and traumatic forces (Hamanaka et al., 2007; Jian et al., 2008; Hamanaka et al., 2010). Moreover, its activation sensitizes neurons to subsequent mechanical stress, with debilitating consequences such as neuropathic pain (Alessandri-Haber et al., 2004).

Equally serious to the damage inflicted during primary mechanical strain is secondary activation of gliosis and associated inflammation, swelling/edema, oxidative stress, vascular changes, blood-brain/retina barrier breakdown, axonal atrophy, synaptic loss and cell death (Dietrich et al., 1994; Cernak et al., 2000; Okie, 2005; Büki & Povlishock, 2006; Mac Donald et al., 2011; Kamnaksh et al., 2011; Kwon et al., 2011; Cernak et al., 2011; Xiong et al., 2013). For example, traumatic brain injury (TBI) causes diffuse reactive gliosis of astrocytes and microglia, contributing to cerebral edema, inflammation and neuronal damage (Kaur et al., 1995; Pifarré et al., 2010; Readnower et al., 2010; Risling et al., 2011). Edema and glial swelling from TBI is associated with a mechanically induced influx of osmolytes, followed by water (Bourke et al., 1979; Unterberg et al., 2004; Kimbler et al., 2012). Gliosis increases almost immediately after traumatic ocular injury (TOI) and the extent of astroglial reactivity is used to assess the breadth of TBI (Agoston et al., 2009). Inhibiting gliosis (Baptiste et al., 2005; Bosco et al., 2008; Volobouéva et al., 2007) and inflammation (Arvin et al., 1996; Tezel et al.,

2001; Chen et al., 2007) is neuroprotective. Likewise, the effects of TBI-induced edema may be reversible if treatment is provided sufficiently early (Zweckberger et al., 2006). The pathological events driven by traumatic injury in many ways mimic those observed in glaucoma (Crish & Calkins, 2011; Yu-Wai-Man & Griffiths, 2013). As these secondary injury mechanisms occur on a slower time scale than the mechanosensory response to a transient insult, glaucoma and traumatic ocular injury (TOI) may be asymptomatic and unsuspected by the patient until the eye is irreversibly damaged (Cockerham et al., 2009). Current clinical interventions rely solely on limiting the mechanical impact (reducing IOP or providing physical protection from trauma), but they are unable to protect the retina directly from damage because of a largely deficient understanding of the basic biological mechanisms that transduce the traumatic impact into cellular injury and the mechanisms that mediate the subsequent injury associated with calcium dysregulation, cell swelling and glial/immune responses. Thus, **there is an *urgent need* to elucidate the molecular mechanisms that determine retinal vulnerability to biomechanical strain. Such information will guide the development of neuroprotective therapies that promote retinal resilience.**

1.2 Overview of Chapters

Chapters 2-4 provide additional background information to further contextualize my dissertation research, whereas Chapters 5-7 describe my primary research findings.

1.2.1 Chapter 2: TRPV1 and Endocannabinoids: Emerging Molecular Signals that Modulate Mammalian Vision

Although this chapter focuses on transient receptor potential vanilloid 1 (TRPV1), rather than TRPV4 (the primary molecular subject of this dissertation research), it details many important concepts regarding the study of TRP channels in the nervous system, in addition to serving as a general primer on TRP channel biology and their potential functions within the retina. It is important to keep in mind, however, that TRPV1 and TRPV4 are distinct proteins with different stimulus sensitivities, modulators, downstream calcium effectors and functions within the visual system.

1.2.2 Chapter 3: From Mechanosensitivity to Inflammatory Responses: New Players in the Pathology of Glaucoma

RGC distress and damage results from mechanical strain and a secondary inflammatory response, but the diverse molecular mechanisms involved in the initiation and propagation of RGC degeneration are poorly understood. This review provides a theoretical overview of glaucoma and emerging pathogenic mechanisms that cause degeneration of RGCs and relates intrinsic mechanosensation by RGCs via TRPV4 and other force-sensitive pathways to calcium dysregulation and activation of downstream signaling cascades that cause early dendritic and axonal remodeling and subsequent RGC death.

1.2.3 Chapter 4: Localization and Phenotype-Specific Expression of Ryanodine Calcium Release Channels in C57BL6 and DBA/2J Mouse Strains

DBA/2J (D2) and C57BL6 (B6) mice are widely used in glaucoma research. D2, but not B6, mice develop chronically elevated IOP that causes progressive degeneration of RGC axons and somata. B6 acutely develop glaucoma if their IOP is raised by obstructing fluid outflow from the eye. This chapter describes an IOP-dependent shift in the distribution and expression of an intracellular calcium release channel, ryanodine receptor 1 (RyR1), from neurons to Müller glia. Müller glial reactivity precedes RGC degeneration and may be initiated early by intrinsic mechanosensitivity to IOP or by responsiveness to RGC distress. The discovery that Müller glia respond rapidly to IOP elevations, coupled with the observation of early changes in calcium regulation mechanisms, indicated a need to study mechanosensation in Müller glia in addition to RGCs. As human Müller glia are known to express stretch-activated ion channels (Puro, 1991), both glial and neuronal mechanosensation are likely involved in the development of glaucoma.

1.2.4 Chapter 5: The Polymodal Ion Channel Transient Receptor Potential Vanilloid 4 Modulates Calcium Flux, Spiking Rate, and Apoptosis of Mouse Retinal Ganglion Cells

Elevated IOP is a primary risk factor for glaucoma, yet the mechanisms of pressure transduction in the retina are essentially unknown. In this chapter we demonstrate that the mouse retina expresses mRNA and protein for the polymodal TRPV4 channel, which is

known to mediate osmotransduction and mechanotransduction. Antibody labeling of TRPV4 revealed neuronal expression that was primarily restricted to perikarya, axons, and dendrites of RGCs. Functional TRPV4 expression in RGCs was confirmed by calcium imaging combined with pharmacological experiments. RGC responses to osmotic pressure occluded their responses to a selective TRPV4 agonist, suggesting TRPV4 as a common transduction mechanism. TRPV4-selective agonists increased the spiking frequency of RGCs within intact retinas recorded with a multielectrode array. Sustained exposure to TRPV4 agonists evoked dose-dependent apoptosis of RGCs. These results thus provided the seminal framework for considering TRPV4 as an RGC mechanosensor capable of driving a glaucomatous phenotype, in addition to suggesting its physiological role in tuning the excitability of RGCs.

1.2.5 Chapter 6: Swelling and Eicosanoid Metabolites Differentially Gate TRPV4 Channels in Retinal Neurons and Glia

This chapter discusses molecular mechanisms by which TRPV4 and glial aquaporin water channels transduce cellular volume into a calcium elevation. In it, the stretch-activated ion channel of Müller glia discovered by Puro (1991) is revealed as TRPV4. We also describe the unique discovery that the physiological properties of TRPV4 and its force-transduction mechanisms drastically differ in RGCs and Müller glia. Despite this difference, we found that calcium influx via TRPV4 exacerbated both neuronal and glial swelling in a hypoosmotic solution. For Müller glia, we further identify TRPV4 as the missing link in swelling promoted by phospholipase A2 (PLA2) and arachidonic acid (AA) signaling. We also demonstrate that aquaporin-4 (AQP4) primarily augments

TRPV4 activation by increasing the rate of hypoosmotic swelling, rather than by a direct molecular interaction as previously suggested. Our results support a model whereby swelling and proinflammatory signals differentially gate TRPV4 in retinal neurons and glia with potentially significant consequences for normal and pathological function.

1.2.6 Chapter 7: TRPV4 Signals Generate and Transduce Intraocular Pressure in Glaucoma

IOP reducing therapies are limited by side-effects, complications and efficacy that is variable across patients and time. New targets are needed for more effective and better tolerated IOP lowering. Additionally, no treatments exist that protect the retina from the mechanical effects of IOP. This is unfortunate because such treatments could complement IOP-lowering strategies to more effectively stop disease progression. This chapter describes our discovery that both of these needs are met by TRPV4 inhibition. The requirement of TRPV4 in high IOP maintenance appears to relate to its functionality in the TM, because TRPV4 inhibition reduces the extent of TM cell swelling, a morphological feature that would otherwise obstruct aqueous humor outflow. Moreover, we describe data supporting the sufficiency and necessity of TRPV4 activity in the induction of excitotoxicity by glaucomatous forces as well as its ability to potentiate NMDA receptor activity, which also contributes to RGC apoptosis in glaucoma models. The discovery of TRPV4's dual role in key pathogenic steps in glaucoma, suggest it as a lead target for future therapeutic strategies designed to prevent IOP-related neurodegeneration.

1.2.7 Chapter 8: Conclusion

Although glaucoma lacks neuroprotective treatments, we have identified TRPV4 as a promising therapeutic target to reduce the mechanosensitivity of retinal neurons and glia and to maintain IOP within a safe range. Future research directions are presented to outline potential approaches that would further advance our understanding of pathogenic roles for TRPV4 in glaucoma/TBI and of how the polymodal nature of TRPV4 might be harnessed to create a new generation of visual prostheses.

Collectively, the findings of this dissertation research provide important insights into the pathogenesis of glaucoma and explain a potential mechanism for the generation of pressure phosphenes, a polymodal sensory phenomenon that may serve as a warning of impending retinal damage and blindness.

1.3 References

Agoston DV, Gyorgy A, Eidelman O, Pollard HB (2009) Proteomic biomarkers for blast neurotrauma: targeting cerebral edema, inflammation, and neuronal death cascades. J Neurotrauma 26:901-911.

Alessandri-Haber N, Yeh JJ, Boyd AE, Parada CA, Chen X, Reichling DB, Levine JD (2003) Hypotonicity induces TRPV4-mediated nociception in rat. Neuron 39:497-511.

Alessandri-Haber N, Dina OA, Yeh JJ, Parada CA, Reichling DB, Levine JD (2004) Transient receptor potential vanilloid 4 is essential in chemotherapy-induced neuropathic pain in the rat. J Neurosci 24:4444-4452.

Amerasinghe N, Zhange J, Thalamuthu A, He M, Vithana EN, Viswanathan A, Wong TY, Foster PJ, Aung T (2010) The heritability and sibling risk of angle closure in Asians. Ophthalmol 118:480-485.

Anderson MG, Libby RT, Mao M, Cosma IM, Wilson LA, Smith RS, John SW (2006) Genetic context determines susceptibility to intraocular pressure elevation in a mouse pigmentary glaucoma. BMC Biol 4:20.

Awadalla MS, Burdon KP, Kuot A, Hewitt AW, Craig JE (2011a) Matrix

metalloproteinase-9 genetic variation and primary angle closure glaucoma in a Caucasian population. Mol Vis 17:1420-1424.

Awadalla MS, Thapa SS, Burdon KP, Hewitt AW, Craig JE (2011b) The association of hepatocyte growth factor (HGF) gene with primary angle closure glaucoma in the Nepalese population. Mol Vis 17:2248-2254.

Becker D, Blasé C, Bereiter-Hahn J, Jendrach M (2005) TRPV4 exhibits a functional role in cell-volume regulation. J Cell Sci 118:2435-2440.

Berkoff DJ, Sanchez LD (2005) An uncommon presentation of acute angle closure glaucoma. J Emerg Med 29:43-44.

Bonomi L, Marchini G, Marraffa M, Morbio R (2001) The relationship between intraocular pressure and glaucoma in a defined population. Ophthalmologica 215:34-38.

Bosco A, Inman DM, Steele MR, Wu G, Soto I, Marsh-Armstrong N, Hubbard WC, Calkins DJ, Horner PJ, Vetter ML (2008) Reduced retina microglial activation and improved optic nerve integrity with minocycline treatment in the DBA/2J mouse model of glaucoma. Invest Ophthalmol Vis Sci 49:1437-1446.

Bourke RS, Kimelberg HK, Nelson LR, Barron KD, Auen EL, Popp AJ, Waldman JB (1979) Biology of glial swelling in experimental brain edema. Advances Neurol 28:99-109.

Bringmann A, Reichenbach A, Wiedermann P (2004) Pathomechanisms of cystoid macular edema. Ophthalmic Res 36:241-249.

Büki A, Povlishock JT (2006) All roads lead to disconnection?–Traumatic axonal injury revisited. Acta Neurochirurgica 148:181-194.

Burdon KP (2012) Genome-wide association studies in the hunt for genes causing primary open-angle glaucoma: a review. Clin Exp Ophthalmol doi: 10.1111/j.1442-9071.2011.02744.x

Burgoyne CF, Downs CJ, Bellezza AJ, Francis Suh JK, Hart RT (2005) The optic nerve head as a biomechanical structure: a new paradigm for understanding the role of IOP-related stress and strain in the pathophysiology of glaucomatous optic nerve head damage. Prog Retin Eye Res 24:39-73.

Burgoyne CF (2011) A biomechanical paradigm for axonal insult within the optic nerve head in aging and glaucoma. Exp Eye Res 93:120-132.

Carlson NR (2007) Physiology of behavior. Boston: Pearson.

Cernak I, Savic VJ, Kotur J, Prokic V, Veljovic M, Grbovic D (2000) Characterization of

plasma magnesium concentration and oxidative stress following graded traumatic brain injury in humans. J Neurotrauma 17:53-68.

Cernak I, Merkle AC, Koliatsos VE, Bilik JM, Luong QT, Mahota TM, Xu L, Slack N, Windle D, Ahmed FA (2011) The pathobiology of blast injuries and blast-induced neurotrauma as identified using a new experimental model of injury in mice. Neurobiol Disease 41:538-551.

Chen G, Shi JX, Hang CH, Xie W, Liu J, Liu X (2007) Inhibitory effect on cerebral inflammatory agents that accompany traumatic brain injury in a rat model: a potential neuroprotective mechanism of recombinant human erythropoietin (rhEPO). Neurosci Lett 425:177-182.

Christensen AP, Corey DP (2007) TRP channels in mechanosensation: direct or indirect activation? Nat Rev Neurosci 8:510-521.

Cockerham GC, Goodrich GL, Weichel ED, Orcutt JC, Rizzo JF, Bower KS, Schuchard RA (2009) Eye and visual function in traumatic brain injury. J Rehabilitation Res Dev 46:811-818.

Crish SD, Calkins DJ (2011) Neurodegeneration in glaucoma: progression and calcium-dependent intracellular mechanisms. Neuroscience 176:1-11.

Dietrich WD, Alonso O, Halley M (1994) Early microvascular and neuronal consequences of traumatic brain injury: a light and electron microscopic study in rats. J Neurotrauma 11:289-301.

Downs JC, Burgoyne CF, Seigfreid WP, Reynaud JF, Strouthidis NG, Sallee V (2011) 24-hour IOP telemetry in the nonhuman primate: implant system performance and initial characterization of IOP at multiple timescales. Invest Ophthalmol Vis Sci 52:7365-7375.

Drance S, Anderson DR, Schulzer M (2001) Risk factors for progression of vision field abnormalities in normal-tension glaucoma. Am J Ophthalmol 131:699-708.

Farley T (2011) Larger than life: dyslexia, paralysis, face blindness—nothing comes between legendary artist Chuck Close and his canvas, except a brush. Neurol Now 7:14-16.

Fields RD, Ni Y (2010) Nonsynaptic communication through ATP release from volume-activated anion channels in axons. Sci Signal 3(142):ra73.

Gaton DD, Sagara T, Lindsey JD, Gabelt BT, Kaufman PL, Weinreb RN (2001) Increased matrix metalloproteinases 1, 2, and 3 in the monkey uveoscleral outflow pathway after topical prostaglandin F(2 alpha)-isopropyl ester treatment. Arch Ophthalmol 119:1165-1170.

Geddes-Klein DM, Schiffman KB, Meaney DF (2006) Mechanisms and consequences of neuronal stretch injury in vitro differ with the model of trauma. J Neurotrauma 23:193-204.

Gevaert T, Vriens J, Segal A, Everaerts W, Roskams T, Talavera K, Owsianik G, Liedtke W, Daelemans D, Dewachter I, Van Leuven F, Voets T, De Ridder D, Nilius B (2007) Deletion of the transient receptor potential cation channel TRPV4 impairs murine bladder voiding. J Clinic Invest 117:3453-3462.

Giangiacomo A, Coleman AL (2009) The epidemiology of glaucoma. In: Glaucoma: essentials in ophthalmology (Grehn F, Stamper R, ed). pp 13-21. Berlin Heidelberg: Springer-Verlag.

Goforth PB, Ellis EF, Satin LS (1999) Enhancement of AMPA-mediated current after traumatic injury in cortical neurons. J Neurosci 19:7367-7374.

Goodale MA, Milner D (1992) Separate visual pathways for perception and action. Trends Neurosci 15:20-25.

Grüsser OJ, Grüsser-Cornehis U, Kusel R, Przybyszewski AW (1989) Responses of retinal ganglion cells to eyeball deformation: a neurophysiological basis for "pressure phosphenes." Vision Res 29:181-194.

Grüsser OJ, Hagner M (1990) On the history of deformation phosphenes and the idea of internal light generated in the eye for the purpose of vision. Documenta Ophthalmol 74:57-85.

Hamanaka K, Jian MY, Weber DS, Alvarez DF, Townsley MI, Al-Mehdi AB, King JA, Liedtke W, Parker JC (2007) TRPV4 initiates the acute calcium-dependent permeability increase during ventilator-induced lung injury in isolated mouse lungs. Am J Physiol Lung Cell Mol Physiol 293:L923-L932.

Hamanaka K, Jian MY, Townsley MI, King JA, Liedtke W, Weber DS, Eyal FG, Clapp MM, Parker JC (2010) TRPV4 channels augment macrophage activation and ventilator-induced lung injury. Am J Physiol Lung Cell Mol Physiol 299(3), L353-L362.

Hattar S, Liao HW, Takao M, Berson DM, Yau KW (2002) Melanopsin-containing retinal ganglion cells: architecture, projections, and intrinsic photosensitivity. Science 295:1065-1070.

Heijl A, Leske MC, Bengtsson B, Hyman L, Bengtsson B, Hussein M (2002) Reduction of intraocular pressure and glaucoma progression: results from the Early Manifest Glaucoma Trial. Arch Ophthalmol 120:1268-1279.

Higginbotham EJ, Feldman R, Stiles M, Dubiner H (2002) Latanoprost and timolol combination therapy vs monotherapy: one-year randomized trial. Arch

Ophthalmol 120:915-922.

Hilding AC (1954) Normal vitreous, its attachments and dynamics during ocular movement. AMA Arch Ophthalmol 52:497-514.

Huang W, Fileta JB, Dobberfuhl A, Filippopolous T, Guo Y, Kwon G, Grosskreutz CL (2005) Calcineurin cleavage is triggered by elevated intraocular pressure, and calcineurin inhibition blocks retinal ganglion cell death. Proc Natl Acad Sci 102:12242-12247.

Huang W, Fileta J, Rawe I, Qu J, Grosskreutz CL (2008) Calpain activation in experimental glaucoma. Invest Ophthalmol Vis Sci 51:3049-3054.

Jaalouk DE, Lammerding J (2009) Mechanotransduction gone awry. Nature 10:63-73.

Jian MY, King JA, Al-Mehdi AB, Liedtke W, Townsley MI (2008) High vascular pressure–induced lung injury requires P450 epoxygenase–dependent activation of TRPV4. Am J Respir Cell Mol Biol 38:386.

Kamnaksh A, Kovesdi E, Kwon SK, Wingo D, Ahmed F, Grunberg NE, Long J, Agoston DV (2011) Factors affecting blast traumatic brain injury. J Neurotrauma 28:2145-2153.

Kaur C, Singh J, Lim MK, Ng BL, Yap EPH, Ling EA (1995) The response of neurons and microglia to blast injury in the rat brain. Neuropath Appl Neurobiol 21:369-377.

Kimbler DE, Shields J, Yanasak N, Vender JR, Dhandapani KM (2012) Activation of P2X7 promotes cerebral edema and neurological injury after traumatic brain injury in mice. PloS ONE 7:e41229.

Klein BEK, Klein R, Lee KE (2004) Heritability of risk factors for primary open-angle glaucoma: the beaver dam eye study. Invest Ophthalmol Vis Sci 45:59-62.

Knöferle J, Koch JC, Ostendorf T, Michel U, Planchamp V, Vutova P, Tönges L, Stadelmann C, Brück W, Bähr M, Lingor P (2010) Mechanisms of acute axonal degeneration in the optic nerve in vivo. Proc Natl Acad Sci USA 107:6064-6069.

Kung C (2005) A possible unifying principle for mechanosensation. Nature 436:647-654.

Kwon SK, Kovesdi E, Gyorgy AB, Wingo D, Kamnaksh A, Walker J, Long JB, Agoston DV (2011) Stress and traumatic brain injury: a behavioral, proteomics, and histological study. Front Neurol 2:12.

Leon-Ortega JED, Girkin CA (2002) Ocular trauma-related glaucoma. Ophthalmol Clin North Am 15:215-223.

Libby RT, Gould DB, Anderson MG, John SW (2005) Complex genetics of glaucoma susceptibility. Annu Rev Genomics Hum Genet 6:15.

Lichter PR, Musch DC, Gillespie BW, Guire KE, Janz NK, Wren PA, Mills RP, CIGTS Study Group (2001) Interim clinical outcomes in the collaborative initial glaucoma treatment study comparing initial treatment randomized to medications or surgery. Ophthalmology 108:1943-1953.

Liedtke W, Choe Y, Martí-Renom MA, Bell AM, Denis CS, Sali A, Hudspeth AJ, Friedman JM, Heller S (2000) Vanilloid receptor–related osmotically activated channel (VR-OAC), a candidate vertebrate osmoreceptor. Cell 103:525-535.

Liedtke W, Friedman JM (2003) Abnormal osmotic regulation in TRPV4 -/- mice. Proc Natl Acad Sci USA 100:13698-13703.

Livingston M (2002) Vision and art: the biology of seeing. New York: Abrams.

Loukin S, Zhou X, Su Z, Saimi Y, Kung C (2010) Wild-type and brachyolmia-causing mutant TRPV4 channels respond directly to stretch force. J Biol Chem 285:27176-27181.

Mac Donald CL, Johnson AM, Cooper D, Nelson EC, Werner NJ, Shimony JS, Snyder AZ, Raichle ME, Witherow JR, Fang R, Flaherty SF, Brody DL (2011) Detection of blast-related traumatic brain injury in US military personnel. New Engl J Med 364:2091-2100.

Martinac B (2004) Mechanosensitive ion channels: molecules of mechanotransduction. J Cell Sci, 117:2449-2460.

Metea MR, Newman EA (2006) Glial cells dilate and constrict blood vessels: a mechanism of neurovascular coupling. J Neurosci 26:2862-2870.

Mishkin M, Ungerleider LG (1982) Contribution of striate inputs to the visuospatial functions of parieto-preoccipital cortex in monkeys. Behav Brain Res 6(1), 57-77.

Miyahara T, Kikuchi T, Akimoto M, Kurokawa T, Shibuki H, Yoshimura N (2003) Gene microarray analysis of experimental glaucomatous retina from cynomologous monkey. Invest Ophthalmol Vis Sci 44:4347-4356.

Morgans CW, Zhang J, Jeffrey BG, Nelson SM, Burke NS, Duvoisin RM, Brown RL. (2009) TRPM1 is required for the depolarizing light response in retinal ON-bipolar cells. Proc Natl Acad Sci USA 106:19174-19178.

Moster MR, Azuara-Blanco A (2014) Complications of glaucoma surgery. In Clinical Glaucoma Care (pp. 609-624). Springer: New York.

O‘Neil RG, Heller S (2005) The mechanosensitive nature of TRPV channels. Pflügers Archiv 451:193-203.

Okie S (2005) Traumatic brain injury in the warzone. N Engl J Med 352:2043-2047.

Ollivier FJ, Samuelson DA, Brooks DE, Kallberg ME, Kormáromy AM (2004) Comparative morphology of the tapetum lucidum (among selected species). Veterinary Ophthalmol 7:11-22.

Pannicke T, Iandiev I, Wurm A, Uckermann O, vom Hagen F, Reichenbach A, Wiedemann P, Hammers HP, Bringmann A (2006) Diabetes alters osmotic swelling characteristics and membrane conductance of glial cells in rat retina. Diabetes. 55:633-639.

Patel HY, Danesh-Meyer HV (2013) Incidence and management of cataract after glaucoma surgery. Curr Opin Ophthalmol 24:15-20.

Pifarré P, Prado J, Giralt M, Molinero A, Hidalgo J, Garcia A (2010) Cyclic GMP phosphodiesterase inhibition alters the glial inflammatory response, reduces oxidative stress and cell death and increases angiogenesis following focal brain injury. J Neurochem 112:807-817.

Pinar Sueiro S, Urcola H, Rivas MA, Vecino E (2011) Prevention of retinal ganglion cell swelling by systemic brimonidine in a rat experimental glaucoma model. Clin Exp Ophthalmol 39:799-807.

Puro DG (1991) Stretch activated channels in human retinal Müller cells. Glia 4:456-460.

Quigley HA, Dorman-Pease ME, Brown AE (1991) Quantitative study of collagen and elastin of the optic nerve head and sclera in human and experimental monkey glaucoma. Curr Eye Res 10:877-888.

Quigley HA, McKinnon SJ, Zack DJ, Pease ME, Kerrigan-Baumrind LA, Kerrigan DF, Mitchell RS (2000) Retrograde axonal transport of BDNF in retinal ganglion cells is blocked by acute IOP elevation in rats. Invest Ophthalmol Vis Sci 41:3460-3466.

Quigley HA, Broman AT (2006) The number of people with glaucoma worldwide in 2010 and 2020. B J Ophthalmol 90:262-267.

Rao KN, Nagireddy S, Chakrabarti S (2011) Complex genetic mechanisms in glaucoma: an overview. Indian J Ophthalmol 59:S31-S42.

Readnower RD, Chavko M, Adeeb S, Conroy MD, Pauly JR, McCarron RM, Sullivan, PG (2010) Increase in blood–brain barrier permeability, oxidative stress, and activated microglia in a rat model of blast induced traumatic brain injury. J Neurosci Res 88:3530-3539.

Risling M, Plantman S, Angeria M, Rostami E, Bellander BM, Kirkegaard M, Arborelius U, Davidsson J (2011) Mechanisms of blast induced brain injuries, experimental studies in rats. Neuroimage 54:S89-S97.

Ryskamp DA, Witkovsky P, Barabas P, Huang W, Koehler C, Akimov NP, Lee SH, Chauhan S, Xing W, Rentería RC, Liedtke W, Križaj D (2011) The polymodal ion channel transient receptor potential vanilloid 4 modulates calcium flux, spiking rate, and apoptosis of mouse retinal ganglion cells. J Neurosci 31:7089-7101.

Sacks OW (1995) An anthropologist on Mars: seven paradoxical tales. New York: Knopf.

Sappington RM, Sidorova T, Long DJ, Calkins DJ (2009) TRPV1: contribution to retinal ganglion cell apoptosis and increased intracellular Ca^{2+} with exposure to hydrostatic pressure. Invest Ophthalmol Vis Sci 50:717-728.

Sena DF, Ramchand K, Lindsley K (2010) Neuroprotection for treatment of glaucoma in adults. Cochrane Database Syst Rev 17:CD006539.

Shaarawy T, Flammer J, Haefliger IO (2004) Reducing intraocular pressure: is surgery better than drugs? Eye 18:1215-1224.

Shen Y, Heimel JA, Kamermans M, Peachey NS, Gregg RG, Nawy S. (2009) A transient receptor potential-like channel mediates synaptic transmission in rod bipolar cells. J Neurosci 29:6088-6093.

Shields MB (2008) Normal-tension glaucoma: is it different from primary open-angle glaucoma? Curr Opin Ophthalmol 9:85-88.

Sonkusare SK, Bonev AD, Ledoux J, Liedtke W, Kotlikoff MI, Heppner TJ, Hill-Eubanks DC, Nelson MT (2012) Elementary Ca2+ signals through endothelial TRPV4 channels regulate vascular function. Science 336:597-601.

Suzuki M, Mizuno A, Kodaira K, Imai M (2003) Impaired pressure sensation in mice lacking TRPV4. J Cell Biol 278:22664-22668.

Suzuki M, Mizuno A (2012) The molecular mechanism of multifunctional mechano-gated channel TRPV4. In mechanically gated channels and their regulation (pp. 103-157). Springer: Netherlands.

Suzuma I, Hata Y, Clermont A, Pokras F, Rook SL, Suzuma K, Feener EP, Aiello LP (2001) Cyclic stretch and hypertension induce retinal expression of vascular endothelial growth factor and vascular endothelial growth factor receptor—2 potential mechanisms for exacerbation of diabetic retinopathy by hypertension. Diabetes 50:444-454.

Takusagawa H, Mansberger S (2012) Do ethnicity and gender influence glaucoma prevalence? Ophthalmol Management 16:24-28.

Tan JC, Kalapesi FB, Coroneo MT (2006) Mechanosensitivity and the eye: cells coping with the pressure. Br J Ophthalmol 90:383-388.

Taylor L, Moran D, Arnér K, Warrant E, Ghosh F (2013) Stretch to see: lateral tension strongly determines cell survival in long-term cultures of adult porcine retina. Invest Ophthalmol Vis Sci 54:1845-1856.

Tezel G, Li LY, Patil RV, Wax MB (2001) TNF-α and TNF-α receptor-1 in the retina of normal and glaucomatous eyes. Invest Ophthalmol Vis Sci 42:1787-1794.

Theophrast. Theophrastus and the Greek physiological psychology before Aristotole. 'De sensu' transl. by G.M. Stratton, London: G. Allen and Unwin. 1917. Reprint Amsterdam: E.J. Bonset. pp. 227. 1964.

Tomita G (2000) The optic nerve head in normal-tension glaucoma. Curr Opin Ophthalmol 11:116-120.

Unterberg AW, Stover J, Kress B, Kiening KL (2004) Edema and brain trauma. Neuroscience 129:1019-1027.

Vogel V, Sheetz M (2006) Local force and geometry sensing regulate cell functions. Nat Rev Mol Cell Biol 7:265-275.

Volobouеva LA, Suh SW, Swanson RA, Giffard RG (2007) Inhibition of mitochondrial function in astrocytes: implications for neuroprotection. J Neurochem 102:1383-1394.

Wang SY, Singh K, Lin SC (2012) The association between glaucoma prevalence and supplementation with the oxidants calcium and iron. Invest Ophthalmol Vis Sci 53:725-731.

Wang Y, Fu X, Gaiser S, Köttgen M, Kramer-Zuker A, Walz G, Wegierski T (2007) OS-9 regulates the transit and polyubiquitination of TRPV4 in the endoplasmic reticulum. J Biol Chem 282:36561-36570.

Ward J (2013) Synesthesia. Annu Rev Psychol 64:2.1-2.27.

Weber AJ, Kaufman PL, Hubbard WC (1998) Morphology of single ganglion cells in the glaucomatous primate retina. Invest Ophthalmol Vis Sci 39:2304-2320.

Weber JT, Rzigalinski BA, Willoughby KA, Moore SF, Ellis EF (1999) Alterations in calcium-mediated signal transduction after traumatic injury of cortical neurons. Cell Calcium 26:289-299.

Weinreb RN, Aung T, Medeiros FA (2014) The pathophysiology and treatment of glaucoma: a review. JAMA 311:1901-1911.

Weisschuh N, Neumann D, Wolf C, Wissinger B, Gramer E (2005) Prevalence of myocilin and optineurin sequence variants in German normal tension glaucoma patients. Mol Vis 11:284-287.

Wiggs JL (2007) Genetic etiologies of glaucoma. Arch Ophthalmol 125:30-37.

Wurm A, Iandiev I, Hollborn M, Wiedemann P, Reichenbach A, Zimmermann H, Bringmann A, Pannicke T (2008) Purinergic receptor activation inhibits osmotic glial cell swelling in the diabetic rat retina. Exp Eye Res 87:385-393.

Xia J, Lim JC, Lu W, Beckel JM, Macarak EJ, Laties AM, Mitchell CH (2012) Neurons respond directly with pannexin-mediated ATP release and autostimulation of P2X7 receptors. J Physiol 590:2285-2304.

Xiong Y, Gu Q, Peterson PL, Muizelaar JP, Lee CP (1997) Mitochondrial dysfunction and calcium perturbation induced by traumatic brain injury. J Neurotrauma 14:23-34.

Xiong Y, Mahmood A, Chopp M (2013) Animal models of traumatic brain injury. Nat Rev Neurosci 14:128-142.

Yu-Wai-Man P, Griffiths PG (2013) Surgery for traumatic optic neuropathy. Cochrane Database Syst Rev 6.

Zaika O, Mamenko M, Berrout J, Boukelmoune N, O'Neil RG, Pochynyuk O (2013) TRPV4 dysfunction promotes renal cystogenesis in autosomal recessive polycystic kidney disease. J Am Soc Nephrol 24:604-616.

Zatulina NI, Panormova NV, Sennova LG, Mal'tsev VV (1989) Quantitative biochemical shifts in the connective tissue of the rear section of the eyeball in glaucoma and atherosclerosis. Vestn Oftalmol 105:37-41.

Zeki S (1991) Cerebral akinetopsia (visual motion blindness): a review. Brain 114:811-824.

Zweckberger K, Erös C, Zimmermann R, Kim SW, Engel D, Plesnila N (2006) Effect of early and delayed decompressive craniectomy on secondary brain damage after controlled cortical impact in mice. J Neurotrauma 23:1083-1093.

Neurotypical perception

Grapheme-color synesthesia

Figure 1.1 Examples of how neurotypical persons and grapheme-color synesthetes might perceive text.

CHAPTER 2

TRPV1 AND ENDOCANNABINOIDS: EMERGING MOLECULAR SIGNALS THAT MODULATE MAMMALIAN VISION

Ryskamp DA, Redmon S, Jo AO, Križaj D (2014) TRPV1 and endocannabinoids: emerging molecular signals that modulate mammalian vision. Cells 3(3):914-38.
Reprinted with permission from Cells and MDPI.

Cells **2014**, *3*, 914-938; doi:10.3390/cells3030914

OPEN ACCESS

cells

ISSN 2073-4409

www.mdpi.com/journal/cells

Review

TRPV1 and Endocannabinoids: Emerging Molecular Signals that Modulate Mammalian Vision

Daniel A. Ryskamp [1,2,†,*], Sarah Redmon[1,2,†], Andrew O. Jo [1,†] and David Križaj [1,2,3,4,*]

[1] Department of Ophthalmology & Visual Sciences, Moran Eye Institute, University of Utah School of Medicine, Salt Lake City, UT 84132, USA; E-Mails: sarah.redmon@utah.edu (S.R.); u0751604@utah.edu (A.O.J.)

[2] Interdepartmental Program in Neuroscience, University of Utah School of Medicine, Salt Lake City, UT 84132, USA

[3] Department of Neurobiology & Anatomy, University of Utah School of Medicine, Salt Lake City, UT 84132, USA

[4] Center for Translational Medicine, University of Utah School of Medicine, Salt Lake City, UT 84132, USA

† Those authors contributed equally to this work.

* Authors to whom correspondence should be addressed; E-Mails: daniel.ryskamp@gmail.com (D.A.R.); david.krizaj@hsc.utah.edu (D.K.); Tel.: +1-801-213-2777 (D.K.); Fax: +1-801-587-8314 (D.K.).

Received: 1 July 2014; in revised form: 27 August 2014 / Accepted: 5 September 2014 / Published: 12 September 2014

Abstract: Transient Receptor Potential Vanilloid 1 (TRPV1) subunits form a polymodal cation channel responsive to capsaicin, heat, acidity and endogenous metabolites of polyunsaturated fatty acids. While originally reported to serve as a pain and heat detector in the peripheral nervous system, TRPV1 has been implicated in the modulation of blood flow and osmoregulation but also neurotransmission, postsynaptic neuronal excitability and synaptic plasticity within the central nervous system. In addition to its central role in nociception, evidence is accumulating that TRPV1 contributes to stimulus transduction and/or processing in other sensory modalities, including thermosensation, mechanotransduction and vision. For example, TRPV1, in conjunction with intrinsic cannabinoid signaling, might contribute to retinal ganglion cell (RGC) axonal transport and excitability, cytokine release from microglial cells and regulation of retinal vasculature. While excessive TRPV1 activity was proposed to induce RGC excitotoxicity,

physiological TRPV1 activity might serve a neuroprotective function within the complex context of retinal endocannabinoid signaling. In this review we evaluate the current evidence for localization and function of TRPV1 channels within the mammalian retina and explore the potential interaction of this intriguing nociceptor with endogenous agonists and modulators.

Keywords: retinal ganglion cells; TRPV1 channels; endocannabinoids; CB1 receptors

1. Introduction

Transient Receptor Potential (TRP) channels form a superfamily of non-selective cation channels that provide cells and organs within the vertebrate body with information about the external and internal environment. The channels participate in the sensory transduction of light, pain, touch, temperature, osmolarity, taste, pheromones, acidity, inflammation, oxidation, metabolic energy and polyunsaturated fatty acids [1–7], whereas loss- and gain-of-function TRP channel mutations cause diseases that range from visceral organ failure (TRPP2/polycystic kidney disease; TRPC6/focal and segmental glomerulosclerosis) to skeletomuscular dysplasias (TRPV4/Charcot-Marie-Tooth disease type 2C), locomotor dysfunction (TRPC3; cerebellar ataxia) and blindness (TRPM1; congenital stationary night blindness) [8]. Within the brain, TRP channels have increasingly been shown to play essential and supportive roles in neuronal and glial signaling [9,10] through monitoring of systemic osmo- and thermoregulation [11,12], neuro-glial-vascular coupling [13,14], initiation of neural stress responses [15], neuroprotection [16] and neurodegeneration [17]. Despite the accumulated knowledge, the primary functions for most TRP isoforms expressed in a cell type-specific manner across the vertebrate central nervous system (CNS) remain poorly understood. Functional information on TRP signaling is particularly scarce for the retina, which, however, expresses the transcripts of most, if not all, known TRP channel isoforms [18]. Localization of TRPs in the retina has been difficult given the non-specificity of most available antibodies [18–20]; however, evidence suggests that expression of some channels (e.g., TRPM1 & 3, TRPC6, TRPC7 and TRPV4) may be confined to specific subsets of retinal cells [10,17,21–23], whereas others (e.g., TRPC1, TRPC3, TRPML1, TRPM7 and TRPP2) appear to be expressed across multiple retinal layers [18,19]. The absence of functional information on TRP signaling in vertebrate retinas appears ironic given that the original dTRP channel was discovered as a light-activated photochannel in *Drosophila* photoreceptors [1,24]. Nonetheless, amongst the important discoveries from recent years is the identification of TRPM1 as the mGluR6-gated cation channel that is required for transmission of the light signal in ON bipolar cells [10,25], discovery that the *Trpm3* gene and its intronically hosted micro-RNA gene (miR-204) are localized to cells residing within the inner nuclear layer [18,26] and the demonstration of the central role of TRPC6/7 heteromers in phototransduction by melanopsin-expressing RGCs [22]. These studies showed that TRP isoforms play fundamental and irreplaceable functions in vertebrate vision. Here, we review potential roles for the vanilloid isoform 1 (TRPV1), which while arguably one of the most thoroughly studied TRP channels within the PNS and CNS, has remained understudied within the context of retinal physiology and visual signaling.

TRPV1 was first identified by Julius and coworkers when a single clone of cDNA conferred responsiveness to the spicy ingredient from hot chili peppers, capsaicin [2]. With six transmembrane domains, a pore between segments 5 and 6 and large intracellular N- and C-termini, this tetrameric ligand-gated channel shares a common structure with the other 27 mammalian TRPs as well as with the voltage-activated potassium (K_v) channel family [27]. The 6 ankyrin repeats within the N-terminus are likely to mediate protein-protein, protein-cytoskeleton and heteromeric interactions as well as trafficking, ligand binding and modulation by ATP and calmodulin [7,28–30]. The channel, at −60 mV, conducts a slowly developing nonselective cation current with a P_{Ca}/P_{Na} of 9.6 and a single channel conductance of ~−80 pS at positive and −40 pS at negative membrane potentials. TRPV1 desensitizes in response to calmodulin binding to N- and C-termini but may change its cation permeability during prolonged agonist stimulation, following exposure to protons and/or phosphorylation [2,31,32]. Indeed, Ca^{2+} entry through TRPV1 can be large enough to cause a self-impacting negative feedback on channel permeability and downregulation of voltage-operated Ca^{2+} channels [33]. The responses of the channel are additionally determined by splice variations [12], heteromultimerization with other TRP channel subunits including TRPV2-4 [34], phosphatidylinositol 4,5-biphosphate (PIP2) and other membrane-delimited lipids [35–37] and insertion/internalization [38,39]. A pivotal role for TRPV1, validated by genetic ablation, small interfering RNA knockdown and pharmacological experiments [15,40] is dynamic modulation of the neuronal response to injury that leads to nociception and hyperalgesia. The channel also contributes to pain transduction through polymodal integration of stimuli such as chemicals (capsaicin, resiniferatoxin or gingerol), pain, temperature (>42 °C), acidity, shrinking, endocannabinoids (eCBs) and eicosanoids [2,36,41,42].

TRPV1 permeability and gating are fine-tuned by a multitude of direct and indirect mechanisms. The channel is indirectly sensitized by inflammatory mediators such as bradykinin, leukotriene B4, histamines and prostaglandins that impact it in part through heteromeric G proteins and tyrosine kinase pathways, whereas certain stimuli (heat, protons, voltage) sensitize the channel to the other agonists [43,44]. TRPV1 also contains consensus sites for protein kinases A and C and src tyrosine kinases that regulate its inactivation properties through phosphorylation [45–48] and should therefore be viewed as a complex, highly modulatable sensory switch which can be flipped on or off by combinatorial action of modulators, agonists and the intra-/extracellular context [42,43,49]. Although functional data on TRPV1 obtained for any particular tissue, cell type, or condition are not automatically generalizable, it may be helpful to consider studies of TRPV1 in the brain to appreciate the state of our understanding of TRPV1 in its visual extension, the retina.

2. TRPV1 in the Brain

2.1. TRPV1 Expression in the Brain

Although TRPV1 expression is ~20-30-fold lower in the CNS compared to the dorsal root ganglion [50–52], a combination of pharmacological, genetic and biochemical data suggest widespread distribution across the neural axis from the spinal cord to brain areas that may include the hippocampus, hypothalamus, thalamus, cerebellum, cortex and limbic system [53–55]. Accordingly, functional studies have implicated the channel in drug addiction, anxiety/fear behavior and long-term

memory formation [56–58]. Injection of capsaicin induced changes in thermogenic behavior [59] and locomotion [60], presumably by acting on hypothalamic and striatal circuits. Because antibodies, radioligand binding and reverse transcription (RT)-PCR assays have provided highly variable localization evidence for TRPV1 expression across the brain, and because studies that used similar assays often reached different conclusions regarding the contribution of the channel to neuronal function [20,30,61–63], there seems to be no uniform consensus on the distribution of TRPV1 channels in the CNS. Analysis of TRPV1 distribution is further complicated by the heterogeneous expression of TRPV1 splice variants, compensatory effects in KO mice, differences in age-dependent phenotypes/expression and differential expression across mouse strains/backgrounds [12,50]. Functional studies have led to variable conclusions regarding the role of the channel in synaptic plasticity [56,57,64]. A paradigmatic example that challenges much of the previous work is the recent analysis of $Trpv1^{PLAP-nlacZ}$ reporter mice which suggests that TRPV1 expression within the brain is highly restricted, with the most pronounced reporter signals observed within the caudal hypothalamus [51], which shares with the retina the susceptibility to high doses of systemic capsaicin [65,66]. It is possible, however, that use of reporter mice might have missed alternate TRPV1 isoforms and/or resulted in an artificial decrease in endogenous TRPV1 levels [55]. Thus, although many details with respect to the cellular/regional distribution of TRPV1 remain to be resolved, it is likely that the channel has a broader distribution and range of functions within the CNS than generally thought.

3. TRPV1 in the Retina

3.1. Overview of Retinal Anatomy and Early Visual Information Processing

When light enters the eye, it is focused onto the retina by the lens and transduced by photoreceptors into electrical and chemical signals that are processed as they are passed through retinal circuits towards the brain. In a nutshell, the flow of visual signal consists of a vertical glutamatergic signals mediated by excitatory photoreceptor, bipolar and ganglion cell synapses and inhibitory/modulatory contributions from horizontal networks mediated by horizontal and amacrine cells, respectively (Figure 1).

Absorption of photons results in the reduction of tonic release of glutamate to postsynaptic horizontal cells and bipolar cells, respectively. Bipolar cells transmit this information to RGCs through two opposing yet complementary pathways. A non-inverting synapse to OFF bipolar cells mediates the excitatory response to decrements of light through ionotropic AMPA/KA receptors. Conversely, the ON pathway is based on a metabotropic mGluR6- TRPM1 mechanism whereby glutamate tonically suppresses bipolar cells and thus cells become disinhibited by light-induced suppression of glutamate release from rods and cones. As bipolar cells forward feed visual information, it is processed through parallel and serial pathways that involve feedback interactions with amacrine cells that contribute to lateral inhibition that sculpts the spatiotemporal organization of RGC receptive fields. As shown in Figure 1, RGCs represent the final output pathway that conveys the visual signal to the midbrain [67]. RGC function and output can be influenced by retinal glia that include Müller cells that span the tissue (and provide critical ionic, metabolic and modulatory of support for neurons, [68]),

protoplasmic astrocytes that line the inner limiting membrane (ILM) and (in vascularized retinas) control the permeability of the blood-retina barrier, and microglia, which represent the resident immune cells [69]. Whilst organization of retinal circuits represents a key determinant of visual information processing, the physiological state of every cell type is dynamically altered through activity-dependent and neurodegeneration-driven changes in calcium homeostasis, functional and structural connectivity across and between retinal laminae [67,69,70]. TRP channels represent new players that play increasingly visible roles in retinal neuronal and glial Ca homeostasis by transducing the RGC response to light and driving plasma membrane Ca influx as well as through interactions with intracellular Ca stores, heteromerization and activation of purinergic receptors and pannexin hemichannels [17–19,21,22,25,71–75].

Figure 1. A schematic of the retina showing overall arrangement of retinal layers and relationship to the critical vascular and pigment layers. An excitatory vertical chain (photoreceptors, bipolar cells, ganglion cells) provides a direct route for transmitting visual information to the midbrain. Lateral inputs from horizontal cells and amacrine cells provide luminance gain control and organization spatiotemporal receptive fields of retinal neurons. Müller glia provide most of the functions performed by astrocytes in the brain. Astrocytes form the blood-retina barrier together with pericytes and vascular endothelial cells. Microglia play a role in developmental pruning and the retinal immune response whereas the choroid and posterior ciliary artery feed outer and inner retinal neurons, respectively. Adapted from [70].

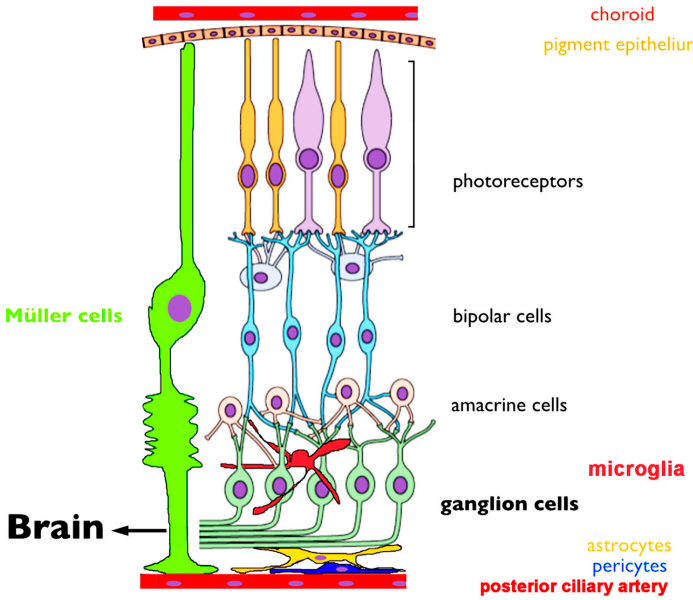

3.2. TRPV1 Channel Distribution in the Retina

The first evidence suggestive of TRPV1 expression in the retina was obtained by Ritter and Dinh [66,76], years before the seminal cloning of TRPV1 in dorsal root ganglia (DRG) [2]. The investigators used cupric silver staining to reveal capsaicin-induced neurodegeneration in the rat retina. This effect was observed in the IPL and RGCL and was also associated with impaired anterograde axonal transport [77]. Interestingly, unilateral transection of the optic nerve prior to capsaicin administration prevented contralateral spread of neurodegeneration to RGC projection sites within the midbrain [66]. In some cases, capsaicin treatment appeared to damage RGC projections without destroying the soma [76], consistent with the documented ability of capsaicin to act on axons in peripheral nerves [78]. Subsequently, Szallasi *et al.* [61], used autoradiography of whole-head cryosections to confirm the retina as a binding site for the TRPV1 agonists capsaicin and its ultrapotent analog, the *Euphorbia resinifera*-derived resiniferatoxin.

Some of these early studies may need to be re-evaluated. Similar to the limitations of approaches that exclusively rely on antibody staining, results from studies confined to the use of pharmacological agents such as capsaicin (agonist) and capsazepine (antagonist) should take into account non-specific and/or mis-targeting effects. TRPV1 was originally called the 'capsaicin receptor' based on the active ingredient in *Capsaicum* chili peppers; however, capsaicin has been subsequently shown to also affect a range of TRPV1-independent mechanisms that include activation of voltage-gated inward and outward currents, impairment of mitochondrial function, inhibition of prostaglandin E2 production and importantly, binding to the cannabinoid CB1 receptor [79–82]. The use of the agonist is particularly complex within the retinal context, as capsaicin induces large inward currents in ON-bipolar cells that mediate an excitatory, inverted, photoreceptor response towards the inner retina. Capsaicin-evoked responses within rod and cone ON bipolar cells at first appeared to be indistinguishable from the effects mediated by light and mGluR6 antagonists and therefore pointed at a "TRPV1-like" identity of the long-sought transduction channel. However, it was soon discovered that ON bipolar light responses are unaffected in Trpv1$^{-/-}$ mice, whereas they are eliminated by deletion of another TRP channel, the melastatin receptor TRPM1 [10]. While this suggested that capsaicin sensitivity is mediated through TRPM1, only partial reduction in the amplitude of capsaicin responses was observed in Trpm1$^{-/-}$ mice [25], indicating that TRPM1 might not represent the exclusive capsaicin sensor in ON bipolars. Consistent with this, Xu *et al.* [83] recently reported that the capsaicin response is eliminated in mice lacking the mGluR6 receptor, suggesting that the compound also acts on the metabotropic glutamate receptor or its downstream G_o protein heteromers. Irrespective of the precise mechanism, it is especially important to consider potential non-TRPV1-mediated effects when capsaicin is used to analyze retinal function or pathology. The results obtained by using the popular competitive antagonist capsazepine should likewise be interpreted with caution, as the drug can produce effects in Trpv1$^{-/-}$ mice. These include antagonism of voltage-activated Ca^{2+} channels [84], acetylcholine receptors [85], hyperpolarization-activated cation channels (I_h) [86] and stimulation of amiloride-sensitive ENaC channels [87].

Nonetheless, numerous studies demonstrated the presence of TRPV1 mRNA and protein in the mammalian retina as well as in teleosts, amphibians and avians [10,18,71,72,88,89], leading Zimov and Yazulla to suggest that the role of the channel in visual signaling might be conserved across

vertebrates [90,91]. A recent study, using probes and antibodies that detected TRPV1 signals in DRG, suggested that TRPV1 mRNA and protein levels in the mouse retina are unusually low [18]. The differences between studies are likely to reflect use of different antibodies and staining protocols, but also underscore the need for using Trpv1$^{-/-}$ mice as controls for semi-quantitative expression studies.

A potential role for TRPV1 in ontogeny was suggested by Leonelli *et al.* [92], who detected stable TRPV1 protein expression in embryonic and early postnatal (E19 through P14) rat retinas, followed by a marked increase in expression during the transition from eye opening to adulthood (at ~P60). Exposure of neonatal rats to capsazepine increased the prevalence of subsets of parvalbumin^{+} amacrine-like cells and increased immunoreactivity (ir) for the presynaptic amacrine marker synapsin 1b. Capsazepine also reduced the normal, developmentally driven, apoptosis in the isolated neonatal rat retina but did not affect retinal layering in the adults; thus, it was proposed that TRPV1 plays a role in the wiring of retinal circuits [93].

Similar to studies in the brain and non-excitable tissues [51,63], immunohistochemical (IHC) staining of mammalian retinas has yielded variable, antibody-specific patterns. The most commonly reported observation from studies that rely mainly on IHC is prominent TRPV1-ir in RGCs and astrocytes. In rat, TRPV1 labeling was confined to a subset of cells in the GCL and within the optic nerve head, but was weak within the optic nerve itself [92]. Further consistent with RGC localization, axotomy of the optic nerve resulted in decreased TRPV1 expression that was mirrored by an injury-induced decline in the population of TRPV1-expressing cells [88,94] and TRPV1-r was also detected within retinocollicular projections within the superior colliculus [95]. Suggestive of potential presynaptic function, TRPV1-ir puncta in the inner plexiform layer (IPL) colocalized with the synaptic vesicle marker synaptophysin. Increased density of labeled axon bundles near the optic nerve head was also observed together with the labeling of distinct cell types in the GCL that included large SMI32^{+} cell bodies, axons and dendrites and smaller Thy-1.1^{+} cells. Consistent with the labeling in retinal sections, TRPV1-ir was also observed in somata/dendrites/neurites of immunopanned and cultured RGCs [72]. Sappington *et al.* [72] reported that retinal TRPV1 expression increases with intraocular pressure (IOP) and suggested that mechanical activation of the channel induced by chronic increases in IOP may drive progressive degeneration of RGCs.

T*rpv1* mRNA signals in immunomagnetically separated postnatal and adult rat RGCs are weaker compared to the whole retina [72], indicating the transcripts are likely to be generated in other cell types in addition to RGCs. Accordingly, immunolocalization and pharmacological assays implicated photoreceptors, bipolar cells, amacrine cells and glia as potential TRPV1 expressors in rodents, teleosts and primates [92,96–98]. TRPV1-ir was observed in synaptic terminals of salamander and rat photoreceptors [92,98,99], suggesting that the channel could modulate the transmission of the response to postsynaptic bipolar and horizontal cells. However, arguing against a major role in phototransduction and neurotransmission in the outer retina, photopic and scotopic ERG a- and b-waves in Trpv1$^{-/-}$ mice are indistinguishable from field potentials in wild type animals [10]. It is possible, however, that the diffuse TRPV1-ir observed in the OPL [72,100] corresponds to Müller glial processes and/or resident microglia. Consistent with the microglial locus, TRPV1-ir is present in Iba1^{+} and OX-42^{+} cells whereas cultured retinal microglia respond to capsaicin [71,92]. TRPV1 expression in Müller cells is less clear. Leonelli *et al.* [92] did not detect TRPV1-ir in rat Müller glia whereas Martinez-Garcia *et al.* [89] reported TRPV1-ir in rabbit Müller cells. Thus, localization to

photoreceptors, Müller glia, bipolar cells and/or amacrine cells may be species-specific and the identity of TRPV1 signals in the mammalian retina remains a subject for further studies. Leonelli *et al.* [92] detected weak TRPV1-ir puncta in astrocytes that line the vasculature at the inner limiting membrane (Figure 1). This was recently confirmed in the functional study by Ho *et al.* [101] who provided evidence that the channel plays a role in guiding astrocyte migration following wound injury. Finally, TRPV1-ir was also reported in the retinal pigment epithelium in rabbits and humans [89], indicating a yet-to-be-defined role in the ion transport function of these cells that are critically important for photoreceptor function and survival.

The variable results obtained with TRPV1 antibodies and pharmacological agents suggest the need for additional functional assays as well as control experiments based on the widely available mice with the genetically ablated channel. One example of such an auxiliary method is optical imaging, which indeed shows robust, desensitizing, capsaicin-induced $[Ca^{2+}]_i$ elevations in mouse RGC somata and microglial cells, but not in Müller astroglia or photoreceptors (Figure 2). The identity of the channel was additionally confirmed by blocking capsaicin-evoked $[Ca^{2+}]_i$ elevations with capsazepine and by showing their absence in $Trpv1^{-/-}$ cells [102]. Functional expression of TRPV1 in RGCs and microglial cells, together with their absence from photoreceptors and bipolar cells suggests that the channel may play a more significant function within the inner retina.

Figure 2. An acutely isolated and dissociated mouse RGC (blue) and microglial cell (μG; green) loaded with fura-2 respond to capsaicin (40 μM) with transient $[Ca^{2+}]_i$ elevations that inactivate during stimulus application, whereas a representative photoreceptor (PR; purple) and Müller cell (MC; red) do not respond to the TRPV1 agonist (see [19,103] for methods).

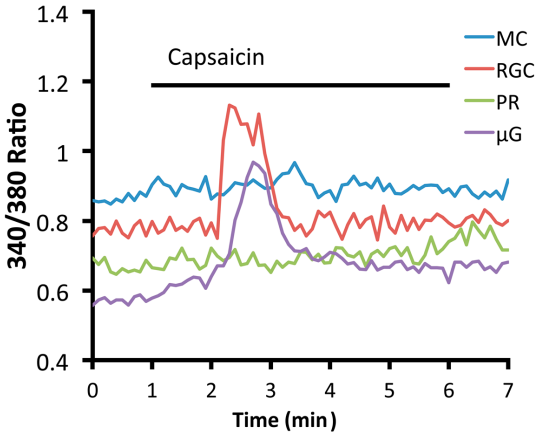

3.3. Endogenous and Synthetic TRPV1 Agonists and Retinal Signaling

Because TRPV1 receptors are unlikely to experience conspicuous nociceptive, mechanical and noxious thermal stimuli in the healthy retina, their primary activators of are likely to be endogenous polyunsaturated fatty acids. TRPV1 is gated by precursors and derivatives of arachidonic acid

commonly lumped together into the "endovanilloid/endocannabinoid" (eCB) category of signaling metabolites that are ubiquitous across all retinal layers [98]. These may include anandamide (Arachidonoyl ethanolamide; AEA), unsaturated N-acyl-dopamines (e.g., N-Arachidonoyl dopamine; NADA), 2-arachidonoglycerol (2-AG, an ester formed from arachidonic acid and glycerol) and lipoxygenase metabolites of arachidonic acid (hydroperoxyeicosatetraenoic acids; HpETEs) [36] (Figure 2).

eCBs affect TRPV1 activity directly and indirectly via activation of cannabinoid receptors (CBRs), a 2-isoform family of G protein-coupled receptors with ~44% amino acid similarity that are associated with intracellular cAMP metabolism and downstream activation of the MAPK-ERK pathway. Type I CB receptors (CB1Rs) are most abundant GPCR within the CNS and all TRPV1-expressing primary sensory neurons express CB1R *in vitro* [104]. The complexity of eCB composition translates to their biological effects. Thus, AEA activates TRPV1 and CB1Rs, whereas 2-AG is a full agonist of CB1Rs and CB2Rs but does not affect TRPV1 [105]. eCB biosynthesis from phospholipid precursors is primarily activity-dependent and follows activation of Ca^{2+}-dependent phospholipases (including phospholipases A2 and C). For example, 2-AG (which, unlike anandamide is expressed at high levels in the CNS) is primarily synthesized by phospholipase C and by diacylglycerol lipase (DAGL) acting on the second messenger diacylglycerol (DAG) [106] (Figure 3). Both AEA and 2-AG freely diffuse across the membrane but can be released into extracellular space to affect neural activity via presynaptic and/or postsynaptic binding sites. eCBs target pre- and/or postsynaptic TRPV1 channels and were reported to bind the cognate TRPV2-4 isoforms with moderate-to-high efficacy and potency (EC_{50} ~3.7 μM) [107]. The EC_{50} values for binding of cannabinoid compounds to CBs and TRPV1 are typically in the micromolar range, although some (such as NADA) can bind TRPV1 in the nanomolar range [82]. Thus, eCB release will exert a multimodal effect through separate CBR and vanilloid receptor mechanisms, but may also trigger reciprocal interactions between the two. Interestingly, coactivation of excitatory (TRPV1) and inhibitory (CB1R) eCB-dependent mechanisms can be concentration-dependent whereby CB1R-mediated effects predominate at low (nM) levels of AEA and TRPV1-mediated effects are more pronounced at higher (~μM) concentrations [104]. Alternatively, the two effectors of AEA might be activated sequentially, with stimulation of high-affinity CB1Rs preceding subsequent activation of TRPV1 [108]. Moreover, reciprocal interaction between the GPCR and the ion channel may involve CB1R-mediated sensitization or desensitization of TRPV1 through PKA/PKC-dependent regulation of its phosphorylation state [109]. With respect to the retina, CB1R transcripts were found in both plexiform layers [99,110,111], whereas DAG lipases were localized to OFF bipolar cells [112]. Given the prominent localization of TRPV1 in the inner retina, it is plausible that Ca^{2+}-dependent eCB release, associated with periods of intense ON- and OFF RGC activation results in indirect (CBR-mediated) and direct TRPV1 modulation. As if this is not complicated enough, arachidonic acid and its downstream eicosanoid metabolites also activate TRPV4, a polymodal vanilloid receptor homolog that acts as a RGC osmosensor [17]. The properties of natural stimuli (light) that lead to endocannabinoid concentrations high enough for retinal TRPV1 and/or CB1R activation remain to be identified.

Enzymatic synthesis and degradation of endovanilloid/eCBs is a likely rate-limiting step in TRPV1 activation and inhibition. AEA is degraded by the fatty acid amide hydrolase (FAAH), resulting in the production of ethanolamine and arachidonic acid (AA), whereas 2-AG can be hydrolyzed by

monoacylglycerol lipase (MAGL), α/β-hydrolase domain 6, 12 (ABHD6/ABHD12), and/or cyclooxygenase-2 (COX-2) [for retinal distributions see [112,113]. FAAH is ubiquitously expressed across the brain and the retina, with expression reported in subsets of photoreceptors, RGCs, dopaminergic and cholinergic amacrine cells and horizontal cells [98,112,114]. IHC studies in fish colocalized FAAH with CB1Rs and TRPV1 within presynaptic terminals of the IPL and OPL [90,91]. FAAH expression in photoreceptors is consistent with the observed AEA uptake [100] and localization of CB1 receptors [99]. The NMDA inhibitor MK801 reduced retinal FAAH activity [88], possibly by downregulating the Ca^{2+}-dependent modulation of the enzyme. FAAH-mediated catabolism of anandamide may be suppressed by PEA, which is present rat, cat and monkey retinas, potentiating eCB signaling *in vivo* [115]. The augmentation of eCB signaling by inhibition of FAAH can produce effects that markedly differ from those elicited by CB1 agonists [116], consistent with synergistic action on TRP channels. Likewise, the breakdown of the FAAH metabolite arachidonic acid by 12-lipoxygenase (12-LO) and 15-lipoxygenase (15-LO) generates 12(S)-HpETE and 15(S)-HpETE, which also bind and activate TRPV1 [117,118]. It would be interesting to see whether the retinas of $FAAH^{-/-}$ mice favor eCB signaling over that of endovanilloids and how this affects the responses of retinas to light/darkness.

Figure 3. Cellular activity initiates synthesis of endocannabinoids/endovanilloids, which activate (arrows) or modulate (closed circles) TRPV1 and TRPV4 activity and thereby regulate physiological responses. 2-AG (2-arachidonoylglycerol), AA (arachidonic acid), AEA (anandamide), CB1 (cannabinoid receptor type I), CB2 (cannabinoid receptor type I), DAG (diacylglycerol), FAAH (fatty acid amide hydrolase), GPCR (G protein-coupled receptor), HpETEs (hydroperoxyeicosatetraenoic acids), LO (lipoxygenase), NADA (N-arachidonoyl dopamine), NAPE (N-acylphosphatidylethanolamine), NAPE-PLD (NAPE-specific phospholipase D), PIP2 (phosphatidylinositol 4,5-bisphosphate), PKC (protein kinase C), PLA2 (phospholipase A2), PLC (phospholipase C).

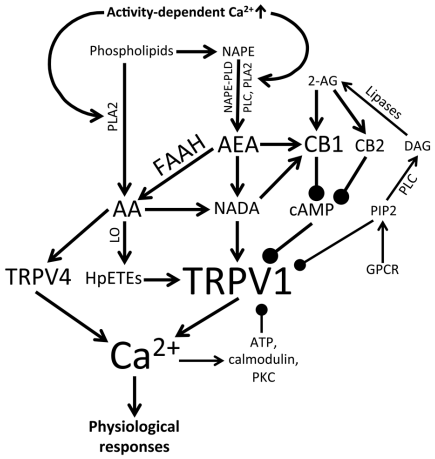

To understand TRPV1 function in the retina one must differentiate the stimulatory effects of endogenous and synthetic cannabinoids on visual signaling and their protective effects in pathological paradigms. Systemic exposure to marijuana produces a dazzling variety of visual experiences that include increased photosensitivity [119], changes in color discrimination [120] and double/blurred vision [96,121], with a mechanism of action that is likely to involve both retinal and cerebral targets. The psychoactive ingredient in marijuana, Δ^9-tetrahydrocannibinol (THC), mimics eCBs through its stimulation of CB1 receptors but does not activate TRPV1. Cannabinoid effects within the retina were also shown to be complex under experimentally tractable conditions. Amongst the observed effects are modulation of intracellular signaling in most retinal cell types including potassium and calcium currents in amphibian and fish photoreceptors [96,122], voltage-operated currents in rodent RGCs [123] and transmitter release from amacrine and bipolar processes in teleosts and mice [97,124].

Data from exogenous CB1 agonists, eCB measurements, and FAAH inhibition has suggested an important role for eCB signaling in neuroprotection. THC lowers IOP and protects the retina from excitotoxic damage [96,125,126]. Analogously, synthetic cannabinoids evinced remarkable protection for photoreceptors and bipolar cells in a rat model of retinitis pigmentosa [127] and were suggested to reduce retinal pigment epithelium (RPE) and RGC damage in models of ischemia, glaucoma, diabetic retinopathy, oxidative damage and/or traumatic ocular injury. Suggestive of lost protection, decreased levels of 2-AG have been reported in ocular tissues from glaucoma patients [128]. FAAH inhibition elevates AEA in young, but not old, rat retinas, an effect that was associated with CB1-dependent RGC neuroprotection following axotomy [129]. In a study of ischemic-reperfusion (I-R), Nucci *et al.* [88] used high IOP (~120 mmHg) to block blood flow within and induce RGC loss in the rat retina. The cytotoxic effect of I-R was antagonized by systemic FAAH inhibition or intravitreal injection of MetAEA, a stable analogue of anandamide. MetAEA-mediated neuroprotection was blocked by inhibition of either CB1 or TRPV1, indicating that both receptors might be involved in neuroprotective effects of anandamide. Other studies showed that cells exposed to excitotoxic conditions can be rescued with eCBs, possibly by suppressing excessive release of glutamate, depolarization-mediated Ca^{2+} overloads and/or excessive firing within the retina [123,124,130]. It is unclear if TRPV1 and CB1Rs regulate the same neuroprotective pathway [but see 102]. Moreover, it remains to be seen whether CB1 and/or TRPV1 inhibition or genetic deletion exacerbate RGC loss in I-R. While eCBs act via CB1Rs [98], the consequences of parallel activation of TRPV1 were not assessed. Thus, it is not known whether CB1R activation protects retinal neurons synergistically with TRPV1 and/or CB1Rs provide protection by antagonizing Ca^{2+} overloads mediated by TPRV1. In either case, CB1Rs and TRPV1 represent novel potential targets that might confer neuroprotection within the retina without causing excitotoxicity. A bottleneck in investigating these potentially ubiquitous signaling pathways in the retina has been that, in contrast to the effects of synthetic cannabinoids applied to (isolated, cultured) retinal cells, the biological functions of eCBs, TRPV1 and their interactions across retinal circuits remain almost entirely unknown.

3.4. Is TRPV1 Neurodegenerative or Neuroprotective?

The expression of TRPV1 in the IPL and GCL [66,72,92] implies a potential role for pathological enhancement of RGC excitability, post-synaptic voltage-operated Ca^{2+} influx and glutamate

receptor-mediated currents that lead to cell injury via Ca^{2+} overload. Consistent with this, maximal TRPV1 activation has been shown to cause neuronal and glial excitotoxicity in other areas of the brain [131–134]. Expanding the results from early studies in the retina [66,77], a recent study reported that capsaicin exposure is sufficient to induce apoptosis in cultured RGCs [72]. Intravitreal injection of capsaicin likewise caused retinal thinning and increased the number of Fluoro-Jade B positive cells in the GCL and INL, particularly in axotomized retinas, an effect that was blocked by capsazepine [94]. Because TRPV1 channels contribute to mechanosensation in some cell types [42,135], but see [136], exposure to hydrostatic pressure was employed to test whether TRPV1 might represent the intrinsic pressure-sensitive pathway through which RGCs respond to elevated IOP. Cultured RGCs and microglia were placed into a pressure chamber and the authors reported increased $[Ca^{2+}]_i$ when the pressure was raised by 70 mm Hg [71,72]. The observation that excessive TRPV1 activity is excitotoxic for RGCs, potentially due to Ca^{2+} overload [72,137], is a valuable step forward in our understanding of TRPV1 pathophysiology within the retina. By providing evidence that the channel might be intrinsically sensitive to pressure, these data provide an attractive model for mechanically-induced Ca^{2+} dysregulation and RGC remodeling/apoptosis in IOP-induced retinal disease. However, the experimental paradigm has recently been questioned within the context of glaucoma [138], as intended pressure application within the standard laboratory incubator may not have reached the intended pressure differential across the plasma membrane due to non-compressibility of water. Moreover, loss of TRPV1 channels is not protective in mouse glaucoma models [17]. Nonetheless, the mechanobiology of IOP and distribution of mechanical forces across retinal tissue under pathological conditions remains a key challenge in retinal research. This includes characterization of the pressure gradient between the inner and outer eye, which might result in the expansion of the orbit [73] and the optic nerve head [139]. TRPV1, which may sense mechanical stress under certain conditions (such as mechanical hyperalgesia or cell shrinking) [42] might therefore play an accentuated role in retinal pathology.

While TRPV1 activation might be deleterious under some conditions, it has been associated with neuroprotection in other contexts [140]. Recent findings [16], which show that IOP-induced damage to RGCs is augmented in $Trpv1^{-/-}$ animals, suggest that a novel neuroprotective function for TRPV1 channels. RGC injury in $Trpv1^{-/-}$ mice and capsazepine-treated rats was associated with inhibited anterograde axonal transport of a fluorescently tagged marker, axonal loss and astrogliosis in the microbead occlusion glaucoma model. TRPV1 ablation also suppressed a post-IOP exposure-dependent increase in RGC firing and increased the amount of depolarizing current needed to reach the RGC firing threshold. The authors suggest that TRPV1 activity rescues RGCs by promoting their excitability during retinal stress. Another protective mechanism might involve TRPV1-dependent release of the protective interleukin 6 (IL-6) from activated microglia [141], as TRPV1 inhibition by iodo-resiniferatoxin (specific) and Ruthenium Red (non-specific) prevented hydrostatic pressure-induced release of IL-6 and NFκB translocation into the nucleus of microglia [71]. A recent *in vivo* study by Sakamoto *et al.* [142] showed that TRPV1 agonists (capsaicin or SA13353) might evince a paradoxical suppression of NMDA-mediated excitotoxicity of rat RGCs. This effect was prevented by capsazepine, CGRP (8–37) (calcitonin gene-related peptide receptor antagonist) or RP67580 (tachykinin NK_1 receptor antagonist). CGRP and substance P, which are increased by electrical stimulation of the retina [143] and metabolic stress [144],

were protective [142]. Low levels of systemic capsaicin were reported to elevate the CGRP concentration and reduce apoptosis in the GCL of rats with STZ-induced diabetic retinopathy [144]. Taken together, the results from capsaicin exposure studies appear contradictory and unresolved. It appears that TRPV1 activity can be beneficial or detrimental to RGCs depending on the disease model, the extent of TRPV1 activation and activation of auxiliary calcium effectors, however, there is also the serious concern of concomitant overstimulation of capsaicin-sensitive mechanisms such as TRPM1 that needs to be addressed in future work.

3.5. TRPV1 and Retinal Vasoregulation

TRPV1 is expressed in vascular endothelial cells and arteriolar smooth muscle cells [20,51,145,146] and may modulate vascular tone and permeability by serving as a source of Ca^{2+} for NO synthesis. Donnerer and Lembeck [147] first showed that capsaicin evokes vascular responses that are independent of sensory innervation. TRPV1's contribution to the regulation of blood distribution appears to be tissue-specific, as TRPV1 agonists can cause neurogenic vasodilation (in the skin) and vasoconstriction (in skeletal muscle) [148–150]. In the retina, TRPV1-ir colocalized with vascular endothelial cells at the inner limiting membrane [92], suggesting that the channel might also modulate vascular flow and/or permeability in this tissue, possibly via Ca^{2+}-dependent upregulation of inducible and endothelial NO synthase isoforms [151] and/or production of CGRP [145,152]. eCB analogs reduced proliferation of human retinal vascular endothelial cells [153], suggesting additional roles in the regulation of vascular leakage and integrity of the blood-retina-barrier.

TRPV1 expression in astrocytes lining blood vessels within the inner retina is also likely to modulate glial control of vascular tone and/or Ca^{2+}-dependent astrogliosis [101]. Inflammation that accompanies reactive gliosis of protoplasmic astrocytes and Müller glia can itself affect blood-retina-barrier permeability, vascular leakage and oxidative damage [73]. As these events are particularly hazardous to RGCs, both pathological and neuroprotective aspects of TRPV1 and eCB activity may offer potential benefits for treating traumatic, inflammatory and ischemic optic neuropathies in diabetic retinopathy, ischemia, optic neuritis and glaucoma.

4. Conclusions

Although TRPV1 expression has been documented across many cell types and in species across phyla ranging from fish to nonhuman primates, at present remarkably little definitive information is available about what the channel is doing in visual processing, retinal development and homeostatic functions of retinal neurons, glia and vasculature. At the very least, it seems that the network comprised of TRPV1 channels, CB1 receptors, eCBs /eicosanoids, kinases and phosphatases (Figure 3) represents a novel neuromodulatory system that could tune the excitability of retinal neurons through amplification or dampening of retinal output and/or contribute to activity-dependent refinement and retinal patterning of visual circuits. The polymodal properties of the TRPV1 channel suggest that, similar to its sibling TRPV4 [17,73], eCB-dependent modulation of Ca^{2+} entry could drive numerous Ca^{2+}-dependent processes associated with normal and pathological retinal physiology. The prominent functional expression of TRPV1 channels in RGCs and microglia (Figure 2) and the stupendous complexity of endovanilloid/endocannabinoid signaling (Figure 3) suggest that the

channels could modulate the diverse presynaptic inputs to RGCs as well as participate in nonretrograde, light-dependent, modulation of retinal output. It will be important to determine how TRPV1 activators and modulators orchestrate channel properties and its interactions with voltage and calcium effectors such as voltage-operated Ca^{2+} channels, NMDA receptors and Ca^{2+}-dependent transcription factors (e.g., NFAT, NFkB, c-fos and DREAM). A particularly interesting area of research will be to evaluate the role of CB1R–TRPV1 interactions, especially under pathological conditions where cannabinoids can provide significant neuroprotection [98]. Given that TRPV1 was identified as a potential intracellular Ca^{2+} release channel [154] studies are also needed to evaluate its relationship to Ca^{2+} release from intracellular stores and activation of store-operated currents, which have been shown to play an increasingly prominent function in retinal Ca^{2+} homeostasis [74,103,155,156]. Because light-dependent changes in $[Ca^{2+}]_i$ levels are the main driver of tonic neurotransmission that characterizes retinal signaling in light and darkness [157], Ca^{2+} influx and clearance in retinal neurons are under tight control. A clear example of such exquisite control are photoreceptors where μV changes in presynaptic membrane potential translate into discernable differences in $[Ca^{2+}]_i$ within photoreceptor terminals and visual perception [158,159]. Thus, even modest $[Ca^{2+}]_i$ elevations mediated by physiological TRPV1 activation could have significant repercussion for downstream visual signaling. Finally, taking into account the reported roles for TRPV1 in hypertonic transduction and mechanosensation [160], it will be of interest whether the channel also contributes to retinal osmoregulation and intrinsic responsiveness to IOP and/or mechanical trauma. This would implicate this polymodal channel in key aspects of retinal homeostasis and response to stress. In summary, the determination of the role that TRP channels play in invertebrate vision together with the elucidation of TRPV1 function in acute and chronic pain represent two of the pinnacles of modern neuroscience. In comparison, TRPV1 research in the mammalian visual system is in its infancy and more studies are needed to better define the involvement of this channel in sensory transduction at the single cell level within the retina, function of visual circuits and the pathogenesis/etiology of blinding diseases.

Acknowledgments

This work was supported by the (University of Utah) Undergraduate Research Opportunity Program (A.J.), HHMI Med into Grad scholarship (D.R.), NIH (T32DC008553, D.R.; RO1EY13870, RO1EY022076, P30EY014800 Vision Core grant), Department of Defense W81XWH-12-1-0244, State of Utah TCIP, Glaucoma Research Foundation and unrestricted grants from Research to Prevent Blindness to the Moran Eye Institute.

Author Contributions

D.A.R., S.R., A.O.J. and D.K. wrote the review. D.A.R., S.R. and A.O.J. collected and analyzed the data.

Conflicts of Interest

The authors declare no conflict of interest.

References

1. Minke, B. Light-induced reduction in excitation efficiency in the *trp* mutant of Drosophila. *J. Gen. Physiol.* **1982**, *79*, 361–385.
2. Caterina, M.J.; Schumacher, M.A.; Tominaga, M.; Rosen, T.A.; Levine, J.D.; Julius, D. The capsaicin receptor: A heat-activated ion channel in the pain pathway. *Nature* **1997**, *389*, 816–824.
3. Clapham, D.E. TRP channels as cellular sensors. *Nature* **2003**, *426*, 517–524.
4. Suzuki, M.; Mizuno, A.; Kodaira, K.; Imai, M. Impaired pressure sensation in mice lacking TRPV4. *J. Biol. Chem.* **2003**, *278*, 22664–22668.
5. Watanabe, H.; Vriens, J.; Prenen, J.; Droogmans, G.; Voets, T.; Nilius, B. Anandamide and arachidonic acid use epoxyeicosatrienoic acid to activate TRPV4 channels. *Nature* **2003**, *424*, 434–438.
6. Kraft, R.; Harteneck, C. The mammalian melastatin-related transient receptor potential cation channels: An overview. *Pflugers Arch.* **2005**, *451*, 204–211.
7. Phelps, C.B.; Wang, R.R.; Choo, S.S.; Gaudet, R. Differential regulation of TRPV1, TRPV3, and TRPV4 sensitivity through a conserved binding site on the ankyrin repeat domain. *J. Biol. Chem.* **2010**, *285*, 731–740.
8. Nilius, B.; Owsianik, G. Transient receptor potential channelopathies. *Pflugers Arch.* **2010**, *460*, 437–450.
9. Kraft, R.; Grimm, C.; Grosse, K.; Hoffmann, A.; Sauerbruch, S.; Kettenmann, H.; Schultz, G.; Harteneck, C. Hydrogen peroxide and ADP-ribose induce TRPM2-mediated calcium influx and cation currents in microglia. *Am. J. Physiol. Cell Physiol.* **2004**, *286*, 129–137.
10. Shen, Y.; Heimel, J.A.; Kamermans, M.; Peachey, N.S.; Gregg, R.G.; Nawy, S. A transient receptor potential-like channel mediates synaptic transmission in rod bipolar cells. *J. Neurosci.* **2009**, *29*, 6088–6093.
11. Gavva, N.R.; Bannon, A.W.; Surapaneni, S.; Hovland, D.N.; Lehto, S.G.; Gore, A.; Juan, T.; Deng, H.; Han, B.; Klionsky, L.; *et al.* The vanilloid receptor TRPV1 is tonically activated *in vivo* and involved in body temperature regulation. *J. Neurosci.* **2007**, *27*, 3366–3374.
12. Sudbury, J.R.; Ciura, S.; Sharif-Naeini, R.; Bourque, C.W. Osmotic and thermal control of magnocellular neurosecretory neurons-role of an N-terminal variant of TRPV1. *Eur. J. Neurosci.* **2010**, *32*, 2022–2030.
13. Dunn, K.M.; Hill-Eubanks, D.C.; Liedtke, W.B.; Nelson, M.T. TRPV4 channels stimulate Ca^{2+}-induced Ca^{2+} release in astrocytic endfeet and amplify neurovascular coupling responses. *Proc. Natl. Acad. Sci. U.S.A.* **2013**, *110*, 6157–6162.
14. Filosa, J.A.; Yao, X.; Rath, G. TRPV4 and the regulation of vascular tone. *J. Cardiovasc. Pharmacol.* **2013**, *61*, 113–119.
15. Caterina, M.J.; Leffler, A.; Malmberg, A.B.; Martin, W.J.; Trafton, J.; Petersen-Zeitz, K.R.; Koltzenburg, M.; Basbaum, A.I.; Julius, D. Impaired nociception and pain sensation in mice lacking the capsaicin receptor. *Sci.* **2000**, *288*, 306–313.

16. Ward, N.J.; Ho, K.W.; Lambert, W.S.; Weitlauf, C.; Calkins, D.J. Absence of transient receptor potential vanilloid-1 accelerates stress-induced axonopathy in the optic projection. *J. Neurosci.* **2014**, *34*, 3161–3170.
17. Ryskamp, D.A.; Witkovsky, P.; Barabas, P.; Huang, W.; Koehler, C.; Akimov, N.P.; Lee, S.H.; Chauhan, S.; Xing, W.; Renteria, R.C.; *et al.* The polymodal ion channel transient receptor potential vanilloid 4 modulates calcium flux, spiking rate, and apoptosis of mouse retinal ganglion cells. *J. Neurosci.* **2011**, *31*, 7089–7101.
18. Gilliam, J.C.; Wensel, T.G. TRP channel gene expression in the mouse retina. *Vis. Res.* **2011**, *51*, 2440–2452.
19. Molnar, T.; Barabas, P.; Birnbaumer, L.; Punzo, C.; Kefalov, V.; Križaj, D. Store-operated channels regulate intracellular calcium in mammalian rods. *J. Physiol.* **2012**, *590*, 3465–3481.
20. Tóth, A.; Czikora, Á.; Pásztor, E.T.; Dienes, B.; Bai, P.; Csernoch, L.; Rutkai, I.; Csató, V.; Mányiné, I.S.; Pórszász, R.; *et al.* Vanilloid receptor-1 (TRPV1) expression and function in the vasculature of the rat. *J. Histochem. Cytochem.* **2014**, *62*, 129–144.
21. Sekaran, S.; Lall, G.S.; Ralphs, K.L.; Wolstenholme, A.J.; Lucas, R.J.; Foster, R.G.; Hankins, M.W. 2-Aminoethoxydiphenylborane is an acute inhibitor of directly photosensitive retinal ganglion cell activity *in vitro* and *in vivo*. *J. Neurosci.* **2007**, *27*, 3981–3986.
22. Xue, T.; Do, M.T.H.; Riccio, A.; Jiang, Z.; Hsieh, J.; Wang, H.C.; Merbs, S.L.; Welsbie, D.S.; Yoshioka, T.; Weissgerber, P.; *et al.* Melanopsin signaling in mammalian iris and retina. *Nature* **2011**, *479*, 67–73.
23. Albert, E.S.; Bec, J.M.; Desmadryl, G.; Chekroud, K.; Travo, C.; Gaboyard, S.; Bardin, F.; Marc, I.; Dumas, M.; Lenaers, G.; *et al.* TRPV4 channels mediate the infared laser-evoked response in sensory neurons. *J. Neurophysiol.* **2012**, *107*, 3227–3234.
24. Montell, C.; Jones, K.; Hafen, E.; Rubin, G. Rescue of the *Drosophila* phototransduction mutation *trp* by germline transformation. *Science* **1985**, *230*, 1040–1043.
25. Morgans, C.W.; Zhang, J.; Jeffrey, B.G.; Nelson, S.M.; Burke, N.S.; Duvoisin, R.M.; Brown, R.L. TRPM1 is required for the depolarizing light response in retinal ON-bipolar cells. *Proc. Natl. Acad. Sci. U.S.A.* **2009**, *106*, 19174–19178.
26. Krol, J.; Busskamp, V.; Markiewicz, I.; Stadler, M.B.; Ribi, S.; Richter, J.; Duebel, J.; Bicker, S.; Fehling, H.J.; Schübeler, D.; *et al.* Characterizing light-regulated retinal microRNAs reveals rapid turnover as a common property of neuronal microRNAs. *Cell* **2010**, *141*, 618–631
27. Moiseenkova-Bell, V.Y.; Stanciu, L.A.; Serysheva, I.I.; Tobe, B.J.; Wensel, T.G. Structure of TRPV1 channel revealed by electron cryomicroscopy. *Proc. Natl. Acad. Sci. U.S.A.* **2008**, *105*, 7451–7455.
28. Arniges, M.; Fernández-Fernández, J.M.; Albrecht, N.; Schaefer, M.; Valverde, M.A. Human TRPV4 channel splice variants revealed a key role of ankyrin domains in multimerization and trafficking. *J. Biol. Chem.* **2006**, *281*, 1580–1586.
29. Lishko, P.V.; Procko, E.; Jin, X.; Phelps, C.B.; Gaudet, R. The ankyrin repeats of TRPV1 bind multiple ligands and modulate channel sensitivity. *Neuron* **2007**, *54*, 905–918.
30. Everaerts, W.; Nilius, B.; Owsianik, G. The vanilloid transient receptor potential channel TRPV4: From structure to disease. *Prog. Biophys. Mol. Biol.* **2010**, *103*, 2–17.

31. Tominaga, M.; Caterina, M.J.; Malmberg, A.B.; Rosen, T.A.; Gilbert, H.; Skinner, K.; Raumann, B.E.; Basbaum, A.I.; Julius, D. The cloned capsaicin receptor integrates multiple pain-producing stimuli. *Neuron* **1998**, *21*, 531–543.
32. Numazaki, M.; Tominaga, T.; Takeuchi, K.; Murayama, N.; Toyooka, H.; Tominaga, M. Structural determinant of TRPV1 desensitization interacts with calmodulin. *Proc. Natl. Acad. Sci. U.S.A.* **2003**, *100*, 8002–8006.
33. Wu, Z.Z.; Chen, S.R.; Pan, H.L. Transient receptor potential vanilloid type 1 activation down-regulates voltage-gated calcium channels through calcium-dependent calcineurin in sensory neurons. *J. Biol. Chem.* **2005**, *280*, 18142–18151.
34. Hellwig, N.; Albrecht, N.; Harteneck, C.; Schultz, G.; Schaefer, M. Homo- and heteromeric assembly of TRPV channel subunits. *J. Cell Sci.* **2005**, *118*, 917–928.
35. Prescott, E.D.; Julius, D. A modular PIP2 binding site as a determinant of capsaicin receptor. *Science* **2003**, *300*, 1284–1288.
36. Van der Stelt, M.; Di Marzo, V. Endovanilloids. *Eur. J. Biochem.* **2004**, *271*, 1827–1834.
37. Woo, D.H.; Jung, S.J.; Zhu, M.H.; Park, C.K.; Kim, Y.H.; Oh, S.B.; Lee, C.J. Direct activation of transient receptor potential vanilloid 1 (TRPV1) by diacylglycerol (DAG). *Mol. Pain* **2008**, *4*, 1744–8069.
38. Zhang, X.; Huang, J.; McNaughton, P.A. NGF rapidly increases membrane expression of TRPV1 heat-gated ion channels. *Neuromol. Med.* **2005**, *24*, 4211–4223.
39. Sanz-Salvador, L.; Andrés-Borderia, A.; Ferrer-Montiel, A.; Planells-Cases, R. Agonist- and Ca^{2+}-dependent desensitization of TRPV1 channel targets the receptor to lysosomes for degradation. *J. Biol. Chem.* **2012**, *287*, 19462–19471.
40. Christoph, T.; Grünweller, A.; Mika, J.; Schäfer, M.K.; Wade, E.J.; Weihe, E.; Erdmann, V.A.; Frank, R.; Gillen, C.; Kurreck, J. Silencing of vanilloid receptor TRPV1 by RNAi reduces neuropathic and visceral pain *in vivo*. *Biochem. Biophys. Res. Commun.* **2006**, *350*, 238–243.
41. McNamara, F.N.; Randall, A.; Gunthorpe, M.J. Effects of piperine, the pungent component of black pepper, at the human vanilloid receptor (TRPV1). *Br. J. Pharmacol.* **2005**, *144*, 781–790.
42. Prager-Khoutorsky, M.; Khoutorsky, A.; Bourque, C.W. Unique Interweaved Microtubule Scaffold Mediates Osmosensory Transduction via Physical Interaction with TRPV1. *Neuron* **2014**, *83*, 866–878.
43. Immke, D.C.; Gavva, N.R. The TRPV1 receptor and nociception. *Semin. Cell Dev. Biol.* **2006**, *17*, 582–591.
44. Vigna, S.R.; Shahid, R.A.; Nathan, J.D.; McVey, D.C.; Liddle, R.A. Leukotriene B4 mediates inflammation via TRPV1 in duct obstruction-induced pancreatitis in rats. *Pancreas* **2011**, *40*, 708–714.
45. Bhave, G.; Hu, H.J.; Glauner, K.S.; Zhu, W.; Wang, H.; Brasier, D.J.; Oxford, G.S.; Gereau, R.W. Protein kinase C phosphorylation sensitizes but does not activate the capsaicin receptor transient receptor potential vanilloid 1 (TRPV1). *Proc. Natl. Acad. Sci. U.S.A.* **2003**, *100*, 12480–12485.
46. Mandadi, S.; Tominaga, T.; Numazaki, M.; Murayama, N.; Saito, N.; Armati, P.J.; Roufogalis, B.D.; Tominaga, M. Increased sensitivity of desensitized TRPV1 by PMA occurs through PKCε-mediated phosphorylation at S800. *Pain* **2006**, *123*, 106–116.

47. Tominaga, M.; Wada, M.; Masu, M. Potentiation of capsaicin receptor activity by metabotropic ATP receptors as a possible mechanism for ATP-evoked pain and hyperalgesia. *Proc. Natl. Acad. Sci. U.S.A.* **2001**, *98*, 6951–6956.
48. Puntambekar, P.; Van Buren, J.; Raisinghani, M.; Premkumar, L.S.; Ramkumar, V. Direct interaction of adenosine with the TRPV1 channel protein. *J. Neurosci.* **2004**, *29*, 153–158.
49. Nagy, I.; Sántha, P.; Jancsó, G.; Urbán, L. The role of the vanilloid (capsaicin) receptor (TRPV1) in physiology and pathology. *Eur. J. Pharmacol.* **2004**, *500*, 351–369.
50. Sanchez, J.F.; Krause, J.E.; Cortright, D.N. The distribution and regulation of vanilloid receptor VR1 and VR1 5' splice variant RNA expression in rat. *Neurosci.* **2001**, *107*, 373–381.
51. Cavanaugh, D.J.; Chesler, A.T.; Jackson, A.C.; Sigal, Y.M.; Yamanaka, H.; Grant, R.; O'Donnell, D.; Nicoll, R.A.; Shah, N.M.; Julius, D.; *et al.* TRPV1 reporter mice reveal highly restricted brain distribution and functional expression in arteriolar smooth muscle cells. *J. Neurosci.* **2011**, *31*, 5067–5077.
52. Han, L.; Ma, C.; Liu, Q.; Weng, H.-J.; Cui, Y.; Tang, Z.; Kim, Y.; Nie, H.; Qu, L.; Patel, K.N.; *et al.* A subpopulation of nociceptors specifically linked to itch. *Nat. Neurosci.* **2013**, *16*, 174–182.
53. Di Marzo, V. Targeting the endocannabinoid system: To enhance or reduce? *Nat. Rev.* **2008**, *7*, 438–455.
54. Kauer, J.A.; Gibson, H.E. Body-temperature maintenance as the predominant function of the vanilloid receptor TRPV1. *Trends in Neurosci.* **2009**, *32*, 215–224.
55. Martins, D.; Tavares, I.; Morgado, C. "Hotheaded": The role of TRPV1 in brain functions. *Neuropharmacol.* **2014**, *85*, 151–157.
56. Marsch, R.; Foeller, E.; Rammes, G.; Bunck, M.; Kössl, M.; Holsboer, F.; Zieglgänsberger, W.; Landgraf, R.; Lutz, B.; Wotjak, C.T. Reduced anxiety, conditioned fear, and hippocampal long-term potentiation in transient receptor potential vanilloid type 1 receptor-deficient mice. *J. Neurosci.* **2007**, *27*, 832–839.
57. Gibson, H.E.; Edwards, J.G.; Page, R.S.; Van Hook, M.J.; Kauer, J.A. TRPV1 channels mediate long-term depression at synapses on hippocampal interneurons. *Neuron* **2008**, *57*, 746–759.
58. Adamczyk, P.; Miszkiel, J.; McCreary, A.C.; Filip, M.; Papp, M.; Przegaliński, E. The effects of cannabinoid CB1, CB2 and vanilloid TRPV1 receptor antagonists on cocaine addictive behavior in rats. *Brain Res.* **2012**, *1444*, 45–54.
59. Osaka, T.; Kobayashi, A.; Lee, T.H.; Namba, Y.; Inoue, S.; Kimura, S. Lack of integrative control of heat production and heat loss after capsaicin administration. *Pflugers Arch.* **2000**, *440*, 440–445.
60. Dawbarn, D.; Harmar, A.J.; Pycock, C.J. Intranigral injection of capsaicin enhances motor activity and depletes nigral 5-hydroxytrptamine but not substance P. *Neuropharmacol.* **1981**, *20*, 341–346.
61. Szallasi, A.; Nilsson, S.; Farkas-Szallasi, T.; Blumberg, P.M.; Hökfelt, T.; Lundberg, J.M. Vanilloid (capsaicin) receptors in the rat: Distribution in the brain, regional differences in the spinal cord, axonal transport to the periphery, and depletion by systemic vanilloid treatment. *Brain Res.* **1995**, *703*, 175–183.
62. Benninger, F.; Freund, T.F.; Hájos, N. Control of excitatory synaptic transmission by capsaicin is unaltered in TRPV1 vanilloid receptor knockout mice. *Neurochem. Int.* **2008**, *52*, 89–94.

63. Everaerts, W.; Sepúlveda, M.R.; Gevaert, T.; Roskams, T.; Nilius, B.; De Ridder, D. Where is TRPV1 expressed in the bladder, do we see the real channel? *Naunyn Schmiedebergs Arch Pharmacol.* **2009**, *379*, 421–425.
64. Brown, T.E.; Chirila, A.M.; Schrank, B.R.; Kauer, J.A. Loss of interneuron LTD and attenuated pyramidal cell LTP in TRPV1 and TRPV3 KO mice. *Hippocampus* **2013**, *23*, 662–671.
65. Ritter, S.; Dinh, T.T. Capsaicin-induced neuronal degeneration: Silver impregnation of cell bodies, axons, and terminals in the central nervous system of the adult rat. *J. Comp. Neurol.* **1988**, *271*, 79–90.
66. Ritter, S.; Dinh, T. Capsaicin-induced neuronal degeneration in the brain and retina of preweanling rats. *J. Comp. Neurol.* **1990**, *296*, 447–461.
67. Marc, R.E.; Jones, B.W.; Watt, C.B.; Anderson, J.R.; Sigulinsky, C.; Lauritzen, S. Retinal connectomics: Towards complete, accurate networks. *Prog. Retin. Eye Res.* **2013**, *37*, 141–162.
68. Bringmann, A.; Iandiev, I.; Pannicke, T.; Wurm, A.; Hollborn, M.; Wiedemann, P.; Osborne, N.N.; Reichenbach, A. Cellular signaling and factors involved in Müller cell gliosis: Neuroprotective and detrimental effects. *Prog. Retin. Eye Res.* **2009**, *28*,423–451.
69. Cuenca, N.; Fernández-Sánchez, L.; Campello, L.; Maneu, V.; De la Villa, P.; Lax, P.; Pinilla, I. Cellular responses following retinal injuries and therapeutic approaches for neurodegenerative diseases. *Prog. Retin. Eye Res.* 2014, in press.
70. Chalupa, L.M.; Werner, J.S. *The Visual Neurosciences*; MIT Press: Cambridge, MA, USA, 2003.
71. Sappington, R.M.; Calkins, D.J. Contribution of TRPV1 to microglia-derived IL-6 and NFκB translocation with elevated hydrostatic pressure. *Investig. Ophthalmol. Vis. Sci.* **2008**, *49*, 3004–3017.
72. Sappington, R.M.; Sidorova, T.; Long, D.J.; Calkins, D.J. TRPV1: Contribution to retinal ganglion cell apoptosis and increased intracellular Ca^{2+} with exposure to hydrostatic pressure. *Investig. Ophthalmol. Vis. Sci.* **2009**, *50*, 717–728.
73. Križaj, D.; Ryskamp, D.A.; Tian, N.; Tezel, G.; Mitchell, C.H.; Slepak, V.Z.; Shestopalov, V.I. From mechanosensitivity to inflammatory responses: New players in the pathology of glaucoma. *Curr. Eye Res.* **2014**, *39*, 105–119.
74. Szikra, T.; Cusato, K.; Thoreson, W.B.; Barabas, P.; Bartoletti, T.M.; Križaj, D. Depletion of calcium stores regulates calcium influx and signal transmission in rod photoreceptors. *J. Physiol.* **2008**, *586*, 4859–4875.
75. Beckel, J.M.; Argall, A.J.; Lim, J.C.; Xia, J.; Lu, W.; Coffey, E.E.; Macarak, E.J.; Shahidullah, M.; Delamere, N.A.; Zode, G.S.; *et al.* Mechanosensitive release of adenosine 5'-triphosphate through pannexin channels and mechanosensitive upregulation of pannexin channels in optic nerve head astrocytes: A mechanism for purinergic involvement in chronic strain. *Glia* **2014**, *62*, 1486–1501
76. Ritter, S.; Dinh, T. Age-related changes in capsaicin-induced degeneration in rat brain. *J. Comp. Neurol.* **1992**, *318*, 103–116.
77. Ritter, S.; Dinh, T.T. Prior optic nerve transection reduces capsaicin-induced degeneration in rat subcortical visual structures. *J. Comp. Neurol.* **1991**, *308*, 79–90.
78. Jancsó, G.; Király, E.; Jancsó-Gábor, A. Direct evidence for an axonal site of action of capsaicin. *Naunyn Schmiedebergs Arch. Pharmacol.* **1980**, *313*, 91–94.

79. Kim, C.S.; Kawada, T.; Kim, B.S.; Han, I.S.; Choe, S.Y.; Kurata, T.; Yu, R. Capsaicin exhibits anti-inflammatory property by inhibiting IκB-a degradation in LPS-stimulated peritoneal macrophages. *Cell Signal.* **2003**, *15*, 299–306.
80. Costa, R.M.; Liu, L.; Nicolelis, M.A.L.; Simon, S.A. Gustatory effects of capsaicin that are independent of TRPV1 receptors. *Chem. Senses* **2005**, *30*, i198–i200.
81. Athanasiou, A.; Smith, P.A.; Vakilpour, S.; Kumaran, N.M.; Turner, A.E.; Bagiokou, D.; Layfield, R.; Ray, D.E.; Westwell, A.D.; Alexander, S.P.; *et al.* Vanilloid receptor agonists and antagonists are mitochondrial inhibitors: How vanilloids cause non-vanilloid receptor mediated cell death. *Biochem. Biophys. Res. Commun.* **2007**, *354*, 50–55.
82. Di Marzo, V.; De Petrocellis, L.; Fezza, F.; Ligresti, A.; Bisogno, T. Anandamide receptors. *Prostaglandins Leukot. Essent. Fat. Acids* **2002**, *66*, 377–391.
83. Xu, Y.; Dhingra, A.; Fina, M.E.; Koike, C.; Furukawa, T.; Vardi, N. mGluR6 deletion renders the TRPM1 channel in retina inactive. *J. Neurophysiol.* **2012**, *107*, 948–957.
84. Docherty, R.J.; Yeat, J.C.; Piper, A.S. Capsazepine block of voltage-activated calcium channels in adult rat dorsal root ganglion neurones in culture. *Br. J. Pharmacol.* **1997**, *121*, 1461–1467.
85. Liu, L.; Simon, S.A. Capsazepine, a vanilloid receptor antagonist, inhibits nicotinic acetylcholine receptors in rat trigeminal ganglia. *Neurosci. Lett.* **1997**, *228*, 29–32.
86. Ray, A.M.; Benham, C.D.; Roberts, J.C.; Gill, C.H.; Lanneau, C.; Gitterman, D.P.; Harries, M.; Davis, J.B.; Davies, C.H. Capsazepine protects against neuronal injury caused by oxygen glucose deprivation by inhibition I(h). *J. Neurosci.* **2003**, *23*, 10146–10153.
87. Yamamura, H.; Ugawa, S.; Ueda, T.; Nagao, M.; Shimada, S. Capsazepine is a novel activator of the δ subunit of the human epithelial Na^+ channel. *J. Biol. Chem.* **2004**, *279*, 44483–44489.
88. Nucci, C.; Gasperi, V.; Tartaglione, R.; Cerulli, A.; Terrinoni, A.; Bari, M.; De Simone, C.; Agrò, A.F.; Morrone, L.A.; Corasaniti, M.T.; *et al.* Involvement of the endocannabinoid system in retinal damage after high intraocular pressure-induced ischemia in rats. *Investig. Ophthalmol. Vis. Sci.* **2007**, *48*, 2997–3004.
89. Martinez-Garcia, M.C.; Martinez, T.; Pañeda, C.; Gallego, P.; Jimenez, A.I.; Merayo, J. Differential expression and localization of transient receptor potential vanilloid 1 in rabbit and human eyes. *Histol. Histopathol.* **2013**, *28*, 1507–1516.
90. Zimov, S.; Yazulla, S. Localization of vanilloid receptor 1 (TRPV1/VR1)-like immunoreactivity in goldfish and zebrafish retinas: Restriction to photoreceptor synaptic ribbons. *J. Neurocytol.* **2004**, *33*, 441–452.
91. Zimov, S.; Yazulla, S. Vanilloid receptor 1 (TRPV1/VR1) co-localizes with fatty acid amide hydrolase (FAAH) in retinal amacrine cells. *Vis. Neurosci.* **2007**, *24*, 581–591.
92. Leonelli, M.; Martins, D.O.; Kihara, A.H.; Britto, L.R. Ontogenetic expression of the vanilloid receptors TRPV1 and TRPV2 in the rat retina. *Int. J. Dev. Neurosci.* **2009**, *27*, 709–718.
93. Leonelli, M.; Martins, D.O.; Britto, L.R. TRPV1 receptors modulate retinal development. *Int. J. Dev. Neurosci.* **2011**, *29*, 405–413.
94. Leonelli, M.; Martins, D.O.; Britto, L.R. TRPV1 receptors are involved in protein nitration and Müller cell reaction in the acutely axotomized rat retina. *Exp. Eye Res.* **2010**, *91*, 755–768.

95. Maione, S.; Cristino, L.; Migliozzi, A.L.; Georgiou, A.L.; Starowicz, K.; Salt, T.E.; Di Marzo, V. TRPV1 channels control synaptic plasticity in the developing superior colliculus. *J. Physiol.* **2009**, *587*, 2521–2535.
96. Fan, S.F.; Yazulla, S. Biphasic modulation of voltage-dependent currents of retinal cones by cannabinoid CB1 receptor agonist WIN 55212-2. *Vis. Neurosci.* **2003**, *20*, 177–188.
97. Warrier, A.; Wilson, M. Endocannabinoid signaling regulates spontaneous transmitter release from embryonic retinal amacrine cells. *Vis. Neurosci.* **2007**, *24*, 25–35.
98. Yazulla, S. Endocannabinoids in the retina: From marijuana to neuroprotection. *Prog. Retin. Eye Res.* **2008**, *27*, 501–526.
99. Straiker, A.; Stella, N.; Piomelli, D.; Mackie, K.; Karten, H.J.; Maguire, G. Cannabinoid CB1 receptors and ligands in vertebrate retina: Localization and function of an endogenous signaling system. *Proc. natl. Acad. Sci. U.S.A.* **1999**, *96*, 14565–14570.
100. Glaser, S.T.; Deutsch, D.G.; Studholme, K.M.; Zimov, S.; Yazulla, S. Endocannabinoids in the intact retina: 3 H-anandamide uptake, fatty acid amide hydrolase immunoreactivity and hydrolysis of anandamide. *Vis. Neurosci.* **2005**, *22*, 693–705.
101. Ho, K.W.; Lambert, W.S.; Calkins, D.J. Activation of TRPV1 cation channel contributes to stress-induced astrocyte migration. *Glia* **2014**, Epub ahead of print.
102. Jo, A.O.; Ryskamp, D.A.; Redmon, S.; Barabas, P.; Križaj, D. Nonretrograde endocannabinoid signaling modulates retinal ganglion cell calcium homeostasis through the TRPV1cation channel. *Investig. Ophtalmol. Vis. Sci.* **2014**, *55*, E-Abstract 3021.
103. Szikra, T.; Barabas, P.; Bartoletti, T.M.; Huang, W.; Akopian, A.; Thoreson, W.B.; Križaj, D. Calcium homeostasis and cone signaling are regulated by interactions between calcium stores and plasma membrane ion channels. *PLoS One* **2009**, *4*, e6723.
104. Ahluwalia, J.; Urban, L.; Bevan, S.; Nagy, I. Anandamide regulates neuropeptide release from capsaicin-sensitive primary sensory neurons by activating both the cannabinoid 1 receptor and the vanilloid receptor 1 *in vitro*. *Eur. J. Neurosci.* **2003**, *12*, 2611–2618.
105. Kishimoto, Y.; Kano, M. Endogenous cannabinoid signaling through the CB1 receptor is essential for cerebellum-dependent discrete motor learning. *J. Neurosci.* **2006**, *26*, 8829–8837.
106. Cadas, H.; Gaillet, S.; Beltramo, M.; Venance, L.; Piomelli, D. Biosynthesis of an endogenous cannabinoid precursor in neurons and its control by calcium and cAMP. *J. Neurosci.* **1996**, *16*, 3934–3942.
107. De Petrocellis, L.; Schiano, M.A.; Imperatore, R.; Cristino, L.; Starowicz, K.; Di Marzo, V. A re-evaluation of 9-HODE activity at TRPV1 channels in comparison with anandamide: Enantioselectivity and effects at other TRP channels and in sensory neurons. *Br. J. Pharmacol.* **2012**, *167*, 1643–1651.
108. Tóth, B.I.; Dobrosi, N.; Dajnoki, A.; Czifra, G.; Oláh, A.; Szöllosi, A.G.; Juhász, I.; Sugawara, K.; Paus, R.; Bíró, T. Endocannabinoids modulate human epidermal keratinocyte proliferation and survival via the sequential engagement of cannabinoid receptor-1 and transient receptor potential vanilloid-1. *J. Invest. Dermatol.* **2011**, *131*, 1095–1104
109. Jeske, N.A.; Patwardhan, A.M.; Gamper, N.; Price, T.J.; Akopian, A.N.; Hargreaves, K.M. Cannabinoid WIN 55,212–2 regulates TRPV1 phosphorylation in sensory neurons. *J. Biol. Chem.* **2006**, *281*, 32789–32890.

110. Buckley, N.E.; Hansson, S.; Harta, G.; Mezey, E. Expression of the CB1 and CB2 receptor messenger RNAs during embryonic development in the rat. *Neuroscience* **1998**, *82*, 1131–1149.
111. Porcella, A.; Maxia, C.; Gessa, G.L.; Pani, L. The human eye expresses high levels of CB1 cannabinoid receptor mRNA and protein. *Eur. J. Neurosci.* **2000**, *12*, 1123–1127.
112. Hu, S.S.J.; Arnold, A.; Hutchens, J.M.; Radicke, J.; Cravatt, B.F.; Wager-Miller, J.; Mackie, K.; Straiker, A. Architecture of cannabinoid signaling in mouse retina. *J. Comp. Neurol.* **2010**, *518*, 3848–3866.
113. Wilkinson-Berka, J.L.; Alousis, N.S.; Kelly, D.J.; Gilbert, R.E. COX-2 inhibition and retinal angiogenesis in a mouse model of retinopathy of prematurity. *Invest. Ophthalmol. Vis. Sci*. **2003**, *44*, 974–979.
114. Struik, M.L.; Yazulla, S.; Kamermans, M. Cannabinoid agonist WIN 55212-2 speeds up the cone response to light offset in goldfish retina. *Vis. Neurosci.* **2006**, *23*, 285–293.
115. Matias, I.; Wang, J.W.; Moriello, A.S.; Nieves, A.; Woodward, D.F.; Di Marzo, V. Changes in endocannabinoid and palmitoylethanolamide levels in eye tissues of patients with diabetic retinopathy and age-related macular degeneration. *Prostaglandins Leukot. Essent. Fat. Acids* **2006**, *75*, 413–418.
116. Kumar, R.N.; Chambers, W.A.; Pertwee, R.G. Pharmacological actions and therapeutic uses of cannabis and cannabinoids. *Anaesthesia* **2001**, *56*, 1059–1068.
117. Hwang, S.W.; Cho, H.; Kwak, J.; Lee, S.Y.; Kang, C.J.; Jung, J.; Cho, S.; Min, K.H.; Suh, Y.G.; Kim, D.; *et al.* Direct activation of capsaicin receptors by products of lipoxygenases: Endogenous capsaicin-like substances. *Proc. Natl. Acad. Sci. U.S.A.* **2000**, *97*, 6155–6160.
118. Piomelli, D. The ligand that came from within. *Trends in Pharmacol. Sci.* **2001**, *22*, 17–19.
119. Russo, E.B.; Merzouki, A.; Mesa, J.M.; Frey, K.A.; Bach, P.J. Cannabis improves night vision: A case study of dark adaptometry and scotopic sensitivity in kif smokers of the Rif mountains of northern Morocco. *J. Ethnopharmacol.* **2004**, *93*, 99–104.
120. Adams, A.J.; Brown, B.; Haegerstrom-Portnoy, G.; Flom, M.C.; Jones, R.T. Evidence for acute effects of alcohol and marijuana on color discrimination. *Percept. Psychophys.* **1976**, *20*, 119–124.
121. Dawson, W.W.; Jimenez-Antillon, C.F.; Perez, J.M.; Zeskind, J.A. Marijuana and vision—after ten years' use in Costa Rica. *Investig. Ophtalmol. Vis. Sci.* **1977**, *16*, 689–699.
122. Straiker, A.; Sullivan, J.M. Cannabinoid receptor activation differentially modulates ion channels in photoreceptors of the tiger salamander. *J. Neurophysiol.* **2003**, *89*, 2647–2654.
123. Lalonde, M.R.; Jollimore, C.A.B.; Stevens, K.; Barnes, S.; Kelly, M.E.M. Cannabinoid receptor-mediated inhibition of calcium signaling in rat retinal ganglion cells. *Mol. Vis.* **2006**, *12*, 1160–1166.
124. Middleton, T.P.; Protti, D.A. Cannabinoids modulate spontaneous synaptic activity in retinal ganglion cells. *Vis. Neurosci.* **2011**, *28*, 393–402.
125. El-Remessy, A.B.; Khalil, I.E.; Matragoon, S.; Abou-Mohamed, G.; Tsai, N.J.; Roon, P.; Caldwell, R.B.; Caldwell, R.W.; Green, K.; Liou, G.I. Neuroprotective effect of (-)Δ^9-tetrahydrocannabinol and cannabidiol in *N*-Methyl-D-Aspartate-induced retinal neurotoxicity. *Am. J. Pathol.* **2003**, *163*, 1997–2008.

126. Opere, C.A.; Zheng, W.D.; Zhao, M.; Lee, J.S.; Kulkarni, K.H.; Ohia, S.E. Inhibition of potassium- and ischemia-evoked [3H] D-aspartate release from isolated bovine retina by cannabinoids. *Curr. Eye Res.* **2006**, *31*, 645–653.
127. Lax, P.; Esquiva, G.; Altavilla, C.; Cuenca, N. Neuroprotective effect of the cannabinoid agonist HU210 on retinal degeneration. *Exp. Eye Res.* **2014**, *120*, 175–185.
128. Chen, J.; Matias, I.; Dinh, T.; Lu, T.; Venezia, S.; Nieves, A.; Woodward, D.F.; Di Marzo, V. Finding of endocannabinoids in human eye tissues: Implications for glaucoma. *Biochem. Biophys. Res. Commun.* **2005**, *330*, 1062–1067.
129. Slusar, J.E.; Cairns, E.A.; Szczesniak, A.M.; Bradshaw, H.B.; Di Polo, A.; Kelly, M.E. The fatty acid amide hydrolase inhibitor, URB597, promotes retinal ganglion cell neuroprotection in a rat model of optic nerve axotomy. *Neuropharmacology* **2013**, *72*, 116–125.
130. Millns, P.J.; Chimenti, M.; Ali, N.; Ryland, E.; de Lago, E.; Fernandez-Ruiz, J.; Chapman, V.; Kendall, D.A. Effects of inhibition of fatty acid amide hydrolase vs the anandamide membrane transporter on TRPV1-mediated calcium responses in adult DRG neurons; the role of CB receptors. *Eur. J. Neurosci.* **2006**, *24*, 3489–3495.
131. Shin, C.Y.; Shin, J.; Kim, B.M.; Wang, M.H.; Jang, J.H.; Surh, Y.J.; Oh, U. Essential role of mitochondrial permeability transition in vanilloid receptor 1-dependent cell death of sensory neurons. *Mol. Cell Neurosci.* **2003**, *24*, 57–68.
132. Kim, S.R.; Lee, D.Y.; Chung, E.S.; Oh, U.; Kim, S.U.; Jin, B.K. Transient receptor potential vanilloid subtype 1 mediates cell death of mesencephalic dopaminergic neurons *in vivo* and *in vitro*. *J. Neurosci.* **2005**, *25*, 662–671.
133. Kim, S.R.; Kim, S.U.; Oh, U.; Jin, B.K. Transient receptor potential vanilloid subtype 1 mediates microglial cell death *in vivo* and *in vitro* via Ca^{2+}-mediated mitochondrial damage and cytochrome c release. *J. Immunol.* **2006**, *177*, 4322–4329.
134. Shirakawa, H.; Yamaoka, T.; Sanpei, K.; Sasaoka, H.; Nakagawa, T.; Kaneko, S. TRPV1 stimulation triggers apoptotic cell death of rat cortical neurons. *Biochem. Biophys. Res. Commun.* **2008**, *377*, 1211–1215.
135. Birder, L.A.; Nakamura, N.Y.; Kiss, S.; Nealen, M.L.; Barrick, S.; Kanai, A.J.; Wang, E.; Ruiz, G.; de Groat, W.C.; Apodaca, G.; *et al.* Altered urinary bladder function in mice lacking the vanilloid receptor TRPV1. *Nat. Neurosci.* **2002**, *5*, 856–860.
136. Eijkelkamp, N.; Quick, K.; Wood, J.N. Transient receptor potential channels and mechanosensation. *Neurosci.* **2013**, *36*, 519–546.
137. Ho, K.W.; Ward, N.J.; Calkins, D.J. TRPV1: A stress response protein in the central nervous system. *Am. J. Neurodegener. Dis.* **2012**, *1*, 1–14.
138. Sanderson, J.; Rhodes, J.; Osborne, A.; Broadway, D. Increased hydrostatic pressure does not cause loss of retinal ganglion cell viability in human organotypic retinal cultures. *Acta Ophthalmol.* **2011**, *89*, doi:10.1111/j.1755–3768.2011.1255.x.
139. Burgoyne, C.F. A biomechanical paradigm for axonal insult within the optic nerve head in aging and glaucoma. *Exp. Eye Res.* **2011**, *93*, 120–132.

140. Veldhuis, W.B.; van der Stelt, M.; Wadman, M.W.; van Zadelhoff, G.; Maccarrone, M.; Fezza, F.; Veldink, G.A.; Vliegenthart, J.F.G.; Bär, P.R.; Nicolay, K.; *et al.* Neuroprotection by the endogenous cannabinoid anandamide and arvanil against *in vivo* excitotoxicity in the rat: Role of vanilloid receptors and lipoxygenases. *J. Neurosci.* **2003**, *23*, 4127–4133.
141. Sappington, R.M.; Chan, M.; Calkins, D.J. Interleukin-6 protects retinal ganglion cells from pressure-induced death. *Investig. Ophthalmol. Vis. Sci.* **2006**, *47*, 2932–2942.
142. Sakamoto, K.; Kuroki, T.; Okuno, Y.; Sekiya, H.; Watanabe, A.; Sagawa, T.; Ito, H.; Mizuta, A.; Mori, A.; Nakahara, T.; *et al.* Activation of the TRPV1 channel attenuates N-methyl-D-aspartic acid-induced neuronal injury in the rat retina. *Eur. J. Pharmacol.* **2014**, *733*, 13–22.
143. Bronzetti, E.; Artico, M.; Koyacs, I.; Felici, L.M.; Magliulo, G.; Vignone, D.; D'Ambrosio, A.; Forte, F.; De Liddo, R.; Feher, J. Expression of neurotransmitters and neurotrophins in neurogenic inflammation of the rat retina. *Eur. J. Histochem.* **2007**, *51*, 251–260.
144. Yang, J.H.; Guo, Z.; Zhang, T.; Meng, X.X.; Sun, T.; Wu, J. STZ treatment induced apoptosis of retinal cells and effect of up-regulation of calcitonin gene related peptide in rats. *J. Diabetes Complicat.* **2013**, *27*, 531–537.
145. Ching, L.C.; Kou, Y.R.; Shyue, S.K.; Su, K.H.; Wei, J.; Cheng, L.C.; Yu, Y.B.; Pan, C.C.; Lee, T.S. Molecular mechanisms of activation of endothelial nitric oxide synthase mediated by transient receptor potential vanilloid type 1. *Cardiovasc. Res.* **2011**, *91*, 492–501.
146. Martin, E.; Dahan, D.; Cardouat, G.; Gillibert-Duplantier, J.; Marthan, R.; Savineau, J.P.; Ducret, T. Involvement of TRPV1 and TRPV4 channels in migration of rat pulmonary arterial smooth muscle cells. *Pflugers Arch.* **2012**, *464*, 261–272.
147. Donnerer, J.; Lembeck, F. Analysis of the effects of intravenously injected capsaicin in the rat. *Naunyn Schmiedebergs Arch. Pharmacol.* **1982**, *320*, 54–57.
148. Wang, L.; Wang, D.H. TRPV1 gene knockout impairs post ischemic recovery in isolated perfused heart in mice. *Circ.* **2005**, *112*, 3617–3623.
149. Kark, T.; Bagi, Z.; Lizanecz, E.; Pásztor, E.T.; Erdei, N.; Czikora, A.; Papp, Z.; Edes, I.; Pórszász, R.; Tóth, A. Tissue-specific regulation of microvascular diameter: Opposite functional roles of neuronal and smooth muscle located vanilloid receptor-1. *Mol. Pharmacol.* **2008**, *73*, 1405–1412.
150. Guarini, G.; Ohanyan, V.A.; Kmetz, J.G.; DelloStritto, D.J.; Thoppil, R.J.; Thodeti, C.K.; Meszaros, J.G.; Damron, D.S.; Bratz, I.N. Disruption of TRPV1-mediated coupling of coronary blood flow to cardiac metabolism in diabetic mice: Role of nitric oxide and BK channels. *Am. J. Physiol. Heart Circ. Physiol.* **2012**, *303*, H216-H223.
151. Leonelli, M.; Martins, D.O.; Britto, L.R. Retinal cell death induced by TRPV1 activation involves NMDA signaling and upregulation of nitric oxide synthases. *Cell Mol. Neurobiol.* **2013**, *33*, 379–392.
152. Prieto, D.; Benedito, S.; Nielsen, P.J.; Nyborg, N.C.B. Calcitonin gene-related peptide is a potent vasodilator of bovine retinal arteries *in vitro*. *Exp. Eye Res.* **1991**, *53*, 399–405.
153. Samudre, S.S.; Nicholls, M.; Williams, P.B.; Lattanzio, F.A. Endocannabinoid analogs reduce human retinal vascular endothelial cell proliferation. *FASEB J.* **2009**, *23*, E-Abstract LB404.

154. Turner, H.; Fleig, A.; Stokes, A.; Kinet, J.P.; Penner, R. Discrimination of intracellular calcium store subcompartments using TRPV1 (transient receptor potential channel, vanilloid subfamily member 1) release channel activity. *Biochem. J.* **2003**, *371*, 341–350.
155. Križaj, D.; Bao, J.X.; Schmitz, Y.; Witkovsky, P.; Copenhagen, D.R. Caffeine-sensitive calcium stores regulate synaptic transmission from retinal rod photoreceptors. *J. Neurosci.* **1999**, *19*, 7249–7261.
156. Chen, M.; Križaj, D.; Thoreson, W.B. Intracellular calcium stores drive slow non-ribbon vesicle release from rod photoreceptors. *Front. Cell. Neurosci.* **2014**, *8*, doi:10.3389/fncel.2014.00020.
157. Križaj, D.; Copenhagen, D.R. Calcium regulation in photoreceptors. *Front. Biosci.* **2002**, *7*, d2023–d2044.
158. Fain, G.L.; Granda, A.M.; Maxwell, J.M. Voltage signal of photoreceptors at visual threshold. *Nature* **1977**, *265*, 181–183.
159. Thoreson, W.B.; Rabi, K.; Townes-Anderson, E.; Heidelberger, R. A highly Ca^{2+}-sensitive pool of vesicles contributes to linearity at the rod photoreceptor ribbon synapse. *Neuron* **2004**, *42*, 595–605.
160. Ciura, S.; Liedtke, W.; Bourque, C.W. Hypertonicity sensing in organum vasculosum lamina terminalis neurons: A mechanical process involving TRPV1 but not TRPV4. *J. Neurosci.* **2011**, *31*, 14669–14676.

CHAPTER 3

FROM MECHANOSENSITIVITY TO INFLAMMATORY RESPONSES: NEW PLAYERS IN THE PATHOLOGY OF GLAUCOMA

David Krizaj was the first author of this review and organized both the theme and the collaborative authorship of this review. My role in this publication was to write a first draft of the background and sections pertaining to research in David's lab. I also helped to create all three figures and to revise each version of the manuscript.

Krizaj D, Ryskamp DA, Tian N, Tezel G, Mitchell CH, Slepak VZ, Shestopalov VI (2013) From mechanosensitivity to inflammatory responses: new players in the pathology of glaucoma. Current Eye Research 39(2):105-119. Reprinted with permission from Current Eye Research and Informa Healthcare.

Current Eye Research, Early Online, 1–15, 2013

ISSN: 0271-3683 print / 1460-2202 online
DOI: 10.3109/02713683.2013.836541

informa
healthcare

REVIEW ARTICLE

From Mechanosensitivity to Inflammatory Responses: New Players in the Pathology of Glaucoma

David Križaj[1,2,3], Daniel A. Ryskamp[1,3], Ning Tian[1,3], Gülgün Tezel[4], Claire H. Mitchell[5,6], Vladlen Z. Slepak[7] and Valery I. Shestopalov[8,9,10]

[1]Department of Ophthalmology and Visual Sciences, [2]Department of Physiology, [3]Program in Neuroscience, University of Utah School of Medicine, Salt Lake City, UT, USA, [4]Department of Ophthalmology & Visual Sciences, University of Louisville, Louisville, KY, USA, [5]Department of Anatomy and Cell Biology, [6]Department of Physiology, University of Pennsylvania, Philadelphia, PA, USA, [7]Department of Molecular Pharmacology, [8]Department of Ophthalmology, Bascom Palmer Eye Institute, [9]Department of Ophthalmology, Cell Biology and Anatomy, University of Miami Miller School of Medicine, Miami, FL, USA, and [10]Vavilov Institute for General Genetics, Moscow, Russia

ABSTRACT

Purpose of the study: Many blinding diseases of the inner retina are associated with degeneration and loss of retinal ganglion cells (RGCs). Recent evidence implicates several new signaling mechanisms as causal agents associated with RGC injury and remodeling of the optic nerve head. Ion channels such as Transient receptor potential vanilloid isoform 4 (TRPV4), pannexin-1 (Panx1) and P2X7 receptor are localized to RGCs and act as potential sensors and effectors of mechanical strain, ischemia and inflammatory responses. Under normal conditions, TRPV4 may function as an osmosensor and a polymodal molecular integrator of diverse mechanical and chemical stimuli, whereas P2X7R and Panx1 respond to stretch- and/or swelling-induced adenosine triphosphate release from neurons and glia. Ca^{2+} influx, induced by stimulation of mechanosensitive ion channels in glaucoma, is proposed to influence dendritic and axonal remodeling that may lead to RGC death while (at least initially) sparing other classes of retinal neuron. The secondary phase of the retinal glaucoma response is associated with microglial activation and an inflammatory response involving Toll-like receptors (TLRs), cluster of differentiation 3 (CD3) immune recognition molecules associated with the T-cell antigen receptor, complement molecules and cell type-specific release of neuroactive cytokines such as tumor necrosis factor-α (TNF-α) and interleukin-1β (IL-1β). The retinal response to mechanical stress thus involves a diversity of signaling pathways that sense and transduce mechanical strain and orchestrate both protective and destructive secondary responses.

Conclusions: Mechanistic understanding of the interaction between pressure-dependent and independent pathways is only beginning to emerge. This review focuses on the molecular basis of mechanical strain transduction as a primary mechanism that can damage RGCs. The damage occurs through Ca^{2+}-dependent cellular remodeling and is associated with parallel activation of secondary ischemic and inflammatory signaling pathways. Molecules that mediate these mechanosensory and immune responses represent plausible targets for protecting ganglion cells in glaucoma, optic neuritis and retinal ischemia.

Keywords: ATP, calcium, cytokines, glaucoma, glia, inflammation, mechanosensation, retinal ganglion cells

INTRODUCTION

The spatiotemporal properties of retinal ganglion cell (RGC) action potentials within the axons of the optic nerve represent the entire visual output projected from the eye to the brain. Loss of RGCs therefore culminates in vision loss in debilitating blinding diseases such as ischemia, diabetic retinopathy

Received 26 December 2012; revised 8 August 2013; accepted 12 August 2013; published online 21 October 2013

Correspondence: David Krizaj, Department of Ophthalmology & Visual Sciences, Moran Eye Center, University of Utah School of Medicine, Salt Lake City, UT 84132, USA. E-mail: david.krizaj@hsc.utah.edu

and glaucoma.[1] While the biological mechanisms that compromise RGC viability in retinal disease are currently under intense experimental scrutiny, potentially useful insights into the disease etiology might be obtained from the observation that RGC degeneration may, at least initially, occur without injury to other classes of retinal neurons.[1,2] Many studies have investigated the anatomical and molecular mechanisms that could account for the selective vulnerability of RGCs in glaucoma and diabetes. It has been suggested that RGCs are uniquely vulnerable to disruptions in energy supply[3] mitochondrial function[4] and axonal transport[5] due to the need to support metabolically expensive long-distance axons. This need is tended through continuous supply of glucose, oxygen and signaling molecules across the blood–retina barrier (BRB), which in turn requires intact function of pericytes, astroglia, microglia and Müller cell endfeet that interface between the vascular endothelium and RGC somata/axons. Astroglia contribute to the metabolic homeostasis of RGCs through glucose/lactate transport mediated by monocarboxylate transporters (MCTs), glucose transporters (SLC2A), glutamate transporters, Gamma-aminobutyric acid (GABA) transporters and the proposed glutamate-glutamine shuttle driven by the bidirectional System N (SN1) transporter.[6–8] While blood vessels and glia maintain the ocular immune privilege by shielding the retina from systemic inflammation, glaucomatous RGC dysfunction might also involve the breakdown of the glial-vascular-immune interface, resulting in increased vascular permeability, hypoxia/ischemia, release of free radicals, cytokines, eicosanoids and growth factors and access of auto-immune molecules.[5,9] Importantly, RGCs are uniquely susceptible to trauma and biomechanical strain, leading to their selective loss in several debilitating blinding diseases.[9,10]

Excessive mechanical stress compromises the viability of many sensory systems, including hearing, somatosensation and vision.[11,12] Glaucoma, the blinding disease most commonly associated with pathological mechanical stress in the eye, is a designation that covers many distinct eye diseases unified by anterior chamber dysfunction, optic neuropathy and glial activation. Its etiology is linked to many known risk factors that include mechanical, genetic (monogenic or polygenic), epigenetic and environmental factors, and possibly combinations thereof.[13] A major risk factor for developing primary open angle glaucoma (which accounts for the majority of glaucoma patients) is ocular hypertension[9,14] caused by increased production or decreased outflow of aqueous humor within the anterior chamber.[15] Positive correlations between intraocular pressure (IOP) levels and RGC loss, and between duration of elevated IOP and RGC axon loss, have been reported for glaucomatous mice, rats, primates and humans.[9,14,16,17] Currently, pharmacological targeting of increased IOP represents by far the most common clinical treatment of glaucoma. Because the disease is too often identified by the time when axonal atrophy and somatic degeneration reach the irreversible terminal stage, there is an increasing interest in early diagnosis and neuroprotective strategies that will complement IOP reduction within the anterior eye.[18] Both require us to understand the mechanotransduction mechanism at the target (RGCs). As discussed below, application of pressure/stretch triggers influx of calcium ions into RGCs through several classes of putative mechanosensitive ion channels. Given that excessive calcium entry overloads cells with calcium and drives neuronal death in many neurodegenerative diseases in the retina and the brain,[19–21] mechanosensitive channels represent obvious neuroprotection targets in glaucoma.

Although pharmacological targeting of IOP-elevations represents by far the most common clinical treatment of glaucoma, recent studies suggest that the disease also involves pressure-independent mechanisms mediated by vascular, glial and immune cells. Reactive astroglia and microglia appear to regulate RGC survival through parallel and intersecting pathways that encompass elevated levels of the vasoconstrictor endothelin-1, inflammatory chemokines and cytokines (e.g. TNF-α, IL-1β and IL-18), ATP, eicosanoids and/or damage-associated molecular patterns (DAMPs) released by injured and dying RGCs, which in turn activate multiple RGC targets, including TNF-α, TGF-β, IL receptors, the inflammasome and T-cell antigen receptor (TCR)/major histocompatibility complex (MHC) immune complexes.[22–27] Secondary insults, triggered by molecules released from injured RGCs, together with cytokines released from reactive glia and immune molecules arriving from leaky blood vessels may further disrupt the blood retina barrier and facilitate additional infiltration of circulating immune cells,[28,29] thereby fueling RGC damage inflicted by the primary mechanical stress.[22,30,31] Obviously, diagnosis and treatment of glaucoma will need to simultaneously address the primary (pressure-related) and secondary (inflammatory and ischemic) symptoms as well as consider the possibility that glaucomatous injury is exacerbated through feedback interactions between primary and secondary pathways.

The aim of this mini-review is to describe recent developments in glaucoma research, focusing on genetic, physiological and pharmacological studies, many from the authors' laboratories. We introduce molecular mechanisms that underlie intrinsic RGC mechanosensation, showcase the intimate relationship between immune and inflammatory pathways in glaucoma and conclude by identifying a novel retinal immune recognition mechanism that might contribute to glaucomatous remodeling in the inner retina.

INTRAOCULAR PRESSURE AND GLAUCOMA

All cells and organisms live within mechanically active environments in which they must sense and adapt to physical forces such as hydrostatic pressure, osmotic swelling/shrinkage, shear flow and developmentally driven tissue stretch.[32,33] Cells in the eye are additionally exposed to intraocular pressure, the magnitude of which reflects the elasticity of ocular tissues and the balance between production and drainage of aqueous humor within the anterior chamber. Biomechanical strain, exerted by the IOP, was suggested to play a central role in the normal development of the vertebrate retina through scleral expansion and continuous stretching of the eye. Consistent with this view, IOP dissipation blocked ocular expansion even as the neural retina continued to grow.[34,35] Furthermore, Coulombre showed that IOP-deprived chick retinas are forced to increase their thickness, suggesting that mechanical stress is required for proper establishment of retinal circuits. Thus, as observed in other tissues,[33,36] morphogenesis, migration, adhesion, osmoregulation and contractility of developing ocular cells are likely to be influenced by mechanical forces that include IOP.

Given that vision loss in animal glaucoma models and humans reflects the magnitude and time course of IOP elevations,[9,14,16,17,37] it would appear that the identification of mechanosensitive mechanisms within RGCs, retinal vasculature and glia should represent a priority target in glaucoma research. Potential candidate mechanisms might include pressure- and/or stretch-sensitive ion channels, enzymes, cytoskeletal proteins, extracellular matrix proteins or combinations thereof. Force-induced stretching of focal adhesion junctions could, for example, reveal intracellular binding sites for cytoskeletal proteins and influence activation of mechanosensitive ion channels.[38,39] Another possibility is that the pressure gradient across axons within the optic nerve mechanically and/or biochemically impairs axonal transport between the cell body and midbrain synapses, depriving RGCs of critical ''neurotrophic factors''.[40–44] The perfusion pressure difference between arm-measured blood pressure and IOP is a strong risk factor for incidence and progression of open angle glaucoma.[18] Variants of the ''vascular hypothesis''[45,46] suggest that the primary defect in glaucoma is due to vasoconstriction and insufficient blood supply, caused by compromised arterial flow through the capillaries connected to the peripapillary choroid and the circle of Zinn–Haller. There is, however, little clear evidence that chronic IOP increases observed in most ocular hypertensive patients directly affect ocular blood flow. The biomechanics of this process, especially with respect to the late remodeling of the optic nerve head, has been reviewed elsewhere.[24,47]

The observations that some of the earliest actions of increased IOP target the dendritic field size, the number of synapses as well as light-evoked responses of RGCs[48–53] suggested that the primary retinal pressure sensors may be RGCs themselves. Consistent with this view, pressure-induced reductions in axon thickness and deformation of the optic nerve head in primate glaucoma models appear later than abnormalities in the dendritic arbors.[54] How do RGCs sense mechanical stress? Ocular hypertension could affect the cells through compressive forces (force/cross sectional area) and/or tensile strain (local stretch of the tissue). A major role for compression is doubtful given that the neural retina is entirely enclosed within the eye. However, even in healthy eyes IOP-driven increases in ocular volume could exacerbate tensile forces that impinge on pre-stressed extracellular matrix, cytoskeleton and plasma membrane structures. The pressure–volume relationship described by Friedenwald's ocular rigidity coefficient (''resistance exerted against distending forces'') is between 0.0126 mm Hg/μL and 0.0224 mm Hg/μL.[55,56] According to Pallikaris et al.,[57], 20 mm Hg increase in IOP ought to increase the volume of the human eye by ~30 microliters whereas tonometric measurements from living eyes give a larger volume increment of ~45 microliters,[58] which leads to the prediction that a 20 mm Hg increase in IOP would expand the ocular volume by ~1%. Showing that retinal cells respond to 1% stretch would confirm that they are directly sensitive to the tensile forces driven by IOP changes that are commonly observed in glaucoma. Ocular rigidity is lower in glaucoma compared to healthy subjects.[59] Thus, an increase in IOP will provoke larger tensile stretch forces across membrane/matrix proteins in glaucomatous RGCs compared to healthy cells and should be more efficacious in crossing the thresholds of intrinsic mechanosensitive mechanisms. Mechanical forces and submicrometer displacements generated by IOP elevations are comparable to the measured free energies of known mechanosensitive channels.[60,61]

MECHANOSENSATION, TRPV4 SIGNALING AND RGC NEURODEGENERATION

The long-standing question in glaucoma research has been whether RGCs are themselves capable of transducing mechanical stimuli generated by physiological changes in IOP amplitude. *In vitro*, *in vivo* and preclinical evidence published in recent years shows that RGCs are themselves highly sensitive to mechanical forces.[9,62–67] RGC viability has been shown to be affected by physical compression, tensile stretch, prolonged swelling and IOP elevations, which, in intact preparations, were able to induce changes in the

molecular composition and synaptic organization within hours to weeks.[63,68–70]

The recently identified Transient Receptor Potential (TRP) and Piezo channels represent obvious candidates for retinal IOP transducers. While little is known about the Piezo family, the seven subfamilies of the TRP superfamily – so named after their *Drosophila* homolog, which plays a key role in phototransduction – are crucial for the perception of sensory information in vertebrates and invertebrates.[11] Most TRP isoforms are nonselective cation channels that are permeable to Ca^{2+}, therefore their activation serves as suitable trigger for many different types of intracellular signaling events. Members of four TRP subfamilies, specifically of the vanilloid (TRPV), ankyrin (TRPA), polycystin (TRPP), and canonical (TRPC) families are relevant to mechanosensation. These channels are only weakly sensitive to depolarization but open in response to a wide variety of mechanical, osmotic, chemical and thermal stimuli.[22] RGCs express mechanosensitive TRPC1, 3-, 6-, 7- and TRPV1- and 4-channel isoforms.[66,71–73] TRPV4 is a particularly attractive candidate as a glaucoma mechanosensor because, while strongly expressed in RGCs, it is excluded from other types of retinal neuron.[66] Selective TRPV4 agonists, such as 4α-PDD and GSK1016790A, induce calcium influx into RGCs and increase the rate of spontaneous RGC firing, whereas excessive TRPV4 stimulation induces RGC apoptosis but spares other retinal neurons.[66,74] Mechanosensitive TRPV4-mediated responses could account for the increased excitability and reduced RGC survival induced by experimental elevation of IOP or membrane stretch.[66] The precise mechanism through which membrane tension activates RGC TRPV4 channels is unclear. The mutually not incompatible mechanisms include direct activation by lipid stretch,[75] phospholipase A2 or through mechanochemical feedback involving β1 integrins and/or focal adhesion kinases.[76,77]

It remains to be determined whether excessive calcium influx through TRPV4 channels contributes to calcium dysregulation that has been linked to the pathogenesis of glaucoma in animal studies and clinical trials.[23,78,79] Interestingly, the risk for developing the disease in humans is increased by taking high daily doses of calcium supplements[80] or by not taking calcium channel blockers.[78] At the very least, calcium ions are going to play a central role in cytoskeletal reorganization that underpins dendritic/axonal remodeling in glaucoma. According to the model shown in Figure 1, local Ca^{2+} influx driven by excessive TRPV4 activation contributes to increased baseline $[Ca^{2+}]_i$ levels and RGC hyperexcitability. This leads to activation of Ca^{2+}-dependent genes belonging to NFAT (nuclear factor of activated T-cells), c-fos, DREAM (*DRE antagonistic modulator protein*) and/or CREB (cAMP response element-binding protein) families and triggers Ca^{2+}-dependent catabolic enzymes such as calcineurin and calpains, as well as the cytoskeletal remodeling pathways involving actin and/or microtubular assemblies.[8,23,81–86] Calcium levels also modulate the opening probability of purinergic channels and pannexin hemichannels and could affect their responsiveness to mechanical stimuli. Consistent with this, TRPV4-mediated Ca^{2+} entry was shown to regulate ATP release, which, *via* P2X7 receptors, could exacerbate mechanically-induced cell injury and facilitate release cytoactive molecules such as endothelin and/or TNF-α.[87,88]

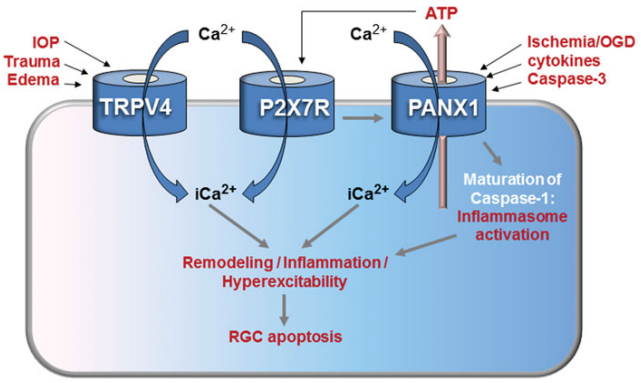

FIGURE 1. Proposed model for RGC mechanotransduction. Pressure-induced membrane stretch activates plasma membrane TRPV4 channels leading to calcium entry, activation of Panx1 and ATP release. This leads to secondary activation of P2X channels and P2Y receptors on neurons and glial cells. Calcium dysregulation may then trigger dendritic and axonal remodeling, inflammation, glial reactivity, RGC hyperexcitability, and eventually, apoptosis.

The emergence of new models of mechanical gating[33,89] suggests that force transduction cannot be disentangled from intracellular biochemistry. Hence, while the direct mechanosensory function of TRPV4 figures most prominently, the polymodal features of TRPV4 activation, such as sensitivity to swelling and inflammatory agents[75,76] place the channel squarely within the crossroads of mechanosensing, inflammatory signaling and anatomical remodeling. Inflammatory mediators would exacerbate RGC injury, induced by mechanically generated TRP-mediated Ca^{2+} overload (Figures 1 and 2). According to this view, TRPV4 signaling represents an epicenter that links primary, pressure-induced RGC damage to secondary pathophysiological mechanisms mediated by glial-vascular inputs (delineated below). Pannexin channels link the mechanosensitive release of ATP to P2X7 receptor-mediated death of RGCs.

MECHANOSENSITIVE RELEASE OF ATP VIA PANNEXINS AND AUTOSTIMULATION OF P2X7R RECEPTORS ON RGCs

In the eye, the mechanical strains resulting from increased IOP are also associated with ATP release. This ATP can mediate physiological and pathological responses through binding to purinergic P2 receptors, the ligand-gated ion channels activated by ATP.[90–92] Several isoforms of ionotropic P2X receptors, including P2X3-5 and P2X7 were reported to be expressed in RGCs.[93] Increased concentrations of extracellular ATP are present in the aqueous humor of human patients with acute[94] or chronic[95] glaucoma. Extracellular ATP is also elevated in the retina following acute elevations in IOP from rat and bovine retina,[68,96] and preliminary data suggest a prolonged increase in retinal ATP occurs in primate and rat models of chronic glaucoma.[97,98] Because extracellular ATP is rapidly degraded in the central nervous system (CNS) by ecto-ATPases, such sustained increase is the evidence of a prolonged release from stressed neural cells. While the ATP released in response to mechanical strain can act at multiple receptors, the P2X7 receptor is of particular interest given its ability to initiate both inflammatory responses and neuronal death.[99,100] Since RGCs express P2X7Rs, stimulation with its agonist, 2′(3′)-O-(4-Benzoylbenzoyl) adenosine-5′-triphosphate (BzATP), elevates intracellular Ca^{2+} and kills RGCS *in vitro*.[101] BzATP also kills RGCs *in vivo*; this death is inhibited by P2X7R blockers MRS 2540 and Brilliant blue G.[102] This suggests that the mechanosensitive release of ATP accompanying elevation of IOP may influence ganglion cell health in acute and chronic glaucoma.[103,104]

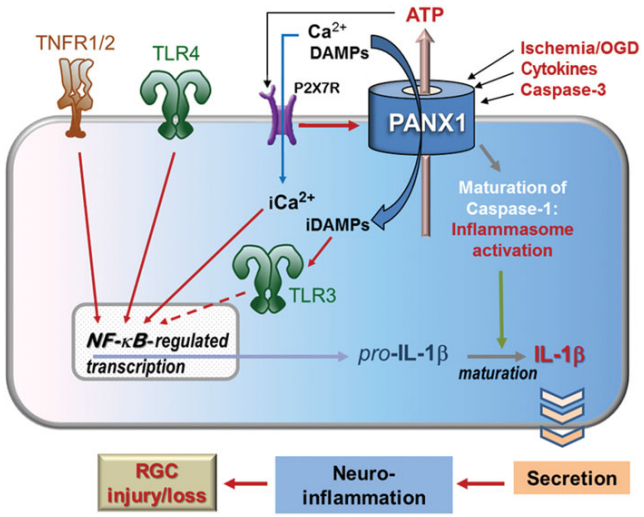

FIGURE 2. Schematic diagram of signaling mediated by surface receptors and Panx1 in the injured retina. Although signaling by TNFRs, TLR4 (signals through MyD88 and/or TRIF) and Ca^{2+} can feed directly into NF-κB activation, TLR3 signaling *via* TRIF first results in the transcription of type 1 interferon genes. These can also promote NF-κB-regulated transcription (dashed arrow). Ultimately, the maturation of pro-IL-1β into IL-1β ***via*** inflammasome pathways perpeturates inflammation and worsens the glaucomatous damage.

Given the pathological effects of excess extracellular ATP on ganglion cells, the cellular source of this released ATP and the signaling pathways leading to this release are of interest. Although Müller cells release ATP into the region surrounding RGCs upon mechanical stimulation, its rapid dephosphorylation into adenosine may limit the concentrations reaching RGC membranes.[105,106] In a healthy retina with little mechanically-evoked ATP release, ATP dephosphorylation regulates P2X7 receptor activity, because P2X7R requires relatively high concentrations of ATP for activation.[107] In disease, sufficient ATP to activate the P2X7 receptors may come from the efflux of ATP through channels in close proximity to the P2X7 receptor on the membrane, with local concentrations high enough to autostimulate the receptors. The pannexin-1 (Panx1) channel, which can be recruited and directly activated by P2X7R, has been recently implicated in this role.[67,108–110]

Pannexins are membrane channels with a high single channel conductance of 500 pS that are permeable to molecules over 1 kDa.[111] Unlike connexin gap junction proteins, pannexin channels are not coupled to partners in adjacent cells but instead act as pores connecting the cell interior to extracellular space; opening of the pore is tightly regulated to maintain cellular integrity.[109] Pannexins are widely distributed and have important implications for inflammation, as discussed below. However, pannexins have two characteristics essential to the current context; they are highly permeable to ATP and open upon application of mechanical strain to the membrane.[67] Whether pannexins are themselves the primary mechanosensor or activated by other upstream mechanosensitive sensors through Rho kinase,[112] their ability to release ATP in proximity to P2X7 receptors upon stretch of the membrane implicates them in connecting elevated IOP with activation of the p2X7 receptors.

This pannexin/P2X7R system was recently found to translate mechanical strain into receptor activation in ganglion cells.[113] RGCs strained by stretching on a silicone substrate, or swollen with hypotonic solution, released ATP. This release was inhibited by pannexin blockers carbenoxolone, probenecid and inhibitory peptide, ^{10}Panx, implicating the pannexin channel in the efflux. Importantly, this mechanosensitive release came from isolated immunopanned cells, identifying RGCs themselves as a cellular source of releasable ATP. Whole cell ion currents activated by swelling were reduced by pannexin channel blockers by removal of extracellular ATP with apyrase or by P2X7R blockers A438079, AZ10606120 and zinc. Together, these observations strongly support a model whereby the mechanosensitive release of ATP through pannexin channels on RGCs autostimulates P2X7 receptors on the cells.

The consequences of this mechanosensitive autostimulation are likely to be more complex than originally thought. Although stimulation of the P2X7R is widely associated with cell death, the expression of pannexins[114] and P2X7 receptors[115,116] in healthy adult RGCs suggests that death is not a necessarily consequence of receptor stimulation. However, the massive ATP release that accompanies excessive mechanical strain may push the system into a pathological state. The location of the pannexin/P2X7 receptors may also influence the function of this mechanosensitive ATP release and autostimulation. According to immunohistochemical analysis, Panx1 and P2X7 proteins are expressed on both the soma and neurites of isolated ganglion cells.[113] As much of the mechanical strain in glaucoma occurs at or near the optic nerve head,[117] expression of this mechanosensitive signaling pair along neurites suggests the system may translate strain in the optic nerve head to local damage in ganglion cell axons.

THE ROLE OF PANNEXIN1-ACTIVATED PATHWAYS IN RGC INJURY

The Panx1 protein forms large non-selective membrane channels and is implicated in paracrine signaling and regulation of the inflammasome. Compared to connexin hemichannels, Panx1 channels are less sensitive to extracellular Ca^{2+}, and open when intracellular Ca^{2+} increases, suggesting them to serve as an additional pathway for Ca^{2+} influx across membrane in pathological conditions.[118–120] Importantly, Panx1 membrane channels have superior permeability to ATP, which prompted referring to them as "the ATP channels" suitable for paracrine signaling in astrocytes, neurons and other cell types.[88] As described above, pannexins are implicated in massive ATP release by glial and blood endothelial cells is typically observed in various pathologies.[89–92] Moreover, Panx1 channels were shown to regulate the inflammasome.[121,122] The Panx1-mediated pathway activates faster in pathogenic conditions, i.e. after stress, injury and cytokine exposure, when cells were shown to decrease the number of gap junctions in the plasma membrane in favor of hemichannels made of either connexins or pannexins.[123–125] Mechanistically, the abnormal opening of Panx1 channels is facilitated by a combination of pathogenic stimuli typically released after stress or injuries, including mechanical stress, extracellular K+, ATP, glutamate, cytokines and Zn^{2+} and proteolysis by active caspase-3.[109,126–129]

Recent studies utilizing gene knockdown and knockout mouse models suggested that Panx1 plays a key role in ischemic death of multiple types of neurons.[130,131] Several reports showed that overstimulation of the Panx1 channels facilitate neuronal loss in models of stroke, glaucoma, retinal ischemia, spreading depression and enteric colitis.[99,130–135]

Because RGCs express high levels of Panx1 and are extremely susceptible to ischemic injury, we tested the hypothesis that activation of Panx1 directly facilitates rapid and selective loss of RGC neurons in ischemia. Our data generated using the Panx1 knockout mice, which are significantly protected from ischemic injury, showed that two distinct neurotoxic processes are mediated by these channels in ischemic conditions.[130]

As revealed by dye transfer and calcium imaging assays, one mechanism involves permeation of RGC plasma membranes. This causes an imbalance of small molecules, and, in particular, an influx of Ca^{2+} and the efflux of ATP.[130,132,136] Ca^{2+} overload, which activates Ca^{2+}-dependent proteases and facilitates apoptosis, can occur directly *via* Ca^{2+}-insensitive Panx1 channels (Figures 1 and 2). In addition, an opening of Panx1 channels can occur *via* the P2X7R-dependent mechanism in response to several external and internal stimuli of physiological or pathological nature, which prompted researchers to name P2X7R-Panx1 a ''death complex''.[99,120,137–139] It is plausible that prolonged opening of Panx1 can be triggered by a combination of pathological factors such as increases in extracellular concentration of known agonists including ATP, K^+, Zn^{2+}, glutamate and pro-inflammatory cytokines.[67,109,124,128,140] Such a combination is common in retinal or brain ischemia (stroke) and other CNS injuries.[99,130,131]

The second process that is interrupted in the Panx1 knockout is the activation of caspase-1 and inflammasome-mediated production of IL-1β and IL-18.[84–86] The inflammasome is a macromolecular complex, first characterized in macrophages[108,141] and, more recently, in glia and neurons.[122] The well-known pathway for transcriptional activation of IL-1β and IL-18 genes involves stimulation of TNF and Toll-like receptors (TLRs),[28,142–146] which causes the activation of NF-κB (nuclear factor kappa-light-chain-enhancer of activated B cells)-dependent gene transcription (Figures 2 and 3). Thus, production of these ILs depends on two independent pathways: (1) transcriptional activation *via* the NF-κB pathway and (2) proteolytic processing of IL precursors by the inflammasome.

How does Panx1 contribute to inflammasome activation? One feasible mechanism is a direct interaction with the inflammasome complex that facilitates proteolytic processing of caspase-1 and results in Il-1β release, as reported by Pelegrin and Surprenant.[141] The second mechanism of Panx1-mediated inflammasome activation involves transcriptional activation of IL-1β, since the large pore of the Panx1 channel can provide a gateway for the entry of pro-inflammatory molecules into the cell, leading to stimulation of intracellular membrane receptors such as TLR3.[86,108,141] TLR3, as well as surface receptors TLR4 and TNFR, cause transcriptional activation of NF-κB (Figure 2) and have been recently implicated in several neurodegenerations, including glaucoma.[147–149] In a similar fashion, the activation Panx1 and, subsequently, the inflammasome can be triggered *via* stimulation of P2X7 receptors by extracellular ATP.[150,151] It was demonstrated that Panx1 is essential for P2X7R-induced proteolytic cleavage of caspase-1 and subsequent IL-1β maturation/release, which can be blocked by pharmacological blockade of the Panx1 channels with small interfering RNA, mimetic peptide or carbenoxolone.[108,121,151,152] Likewise, genetic ablation of Panx1 resulted in a robust neuroprotection in mouse models of enteric colitis and traumatic brain injury.[39,43] Importantly, a study of neuron-specific Panx1 knockout mice demonstrated that Panx1-mediated neurotoxicity is facilitated by the endogenous, neuronal inflammasome.[84,122] Neuronal types expressing high levels of Panx1, such as RGCs, are vulnerable to Panx1-mediated death in response to certain pathological and pro-inflammatory stimuli. Opening of Panx1 channels was shown to be independent of TLR activation.[86] Combined with our own results,[130] this finding allowed us to propose a model where Panx1 acts in parallel, not downstream of TLRs. This model implies synergy between the MyD88-NF-κB pathway and Panx1-mediated processes for IL-1β processing and secretion. Indeed, cytokine maturation appears to be a crucial step in the neurotoxic pro-inflammatory program that is activated in injured CNS *via* the MyD88-NF-κB pathway.[122,130,153] Consistent with our hypothesis, the extent of neuroprotection in Panx1 knockout mice is similar to that observed in the knockouts of caspase-1, P2X7 receptor, TNF receptors 1/2, TLR3/4 and conditional knockouts of NF-κB.[130,142,154–158] In a similar fashion, pharmacological blockade of P2X7R, NALP1/3 or ASC subunits of inflammasome showed robust neuroprotection in various CNS injuries,[84,85,151,159] a strong evidence for neurotoxic effects of inflammasome activation.

TNFR and TLR Signaling Promote Inflammation through NF-κB, Driving RGC Degeneration

Increased glial production of TNF-α in the glaucomatous human retina and optic nerve has been implicated in RGC death and inflammatory processes through the TNFR signaling.[28,160–162] High-throughput characterization of the retinal proteome has recently indicated a prominent up-regulation of TNFR-mediated apoptosis pathway and inflammation signaling in human glaucoma.[161] Retinal proteins exhibiting increased expression in glaucoma have included TNF-α, TNFR1 and various downstream adaptor/interacting proteins, such as TNFR1-associated death domain protein (TRADD) and the members of the TNFR-associated factor (TRAF) family, and protein

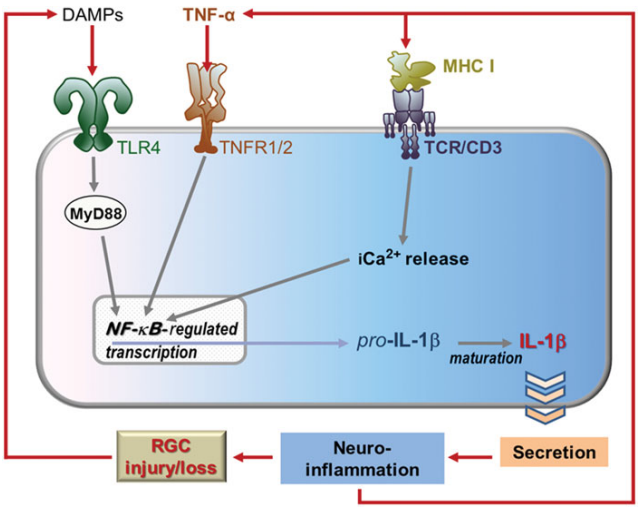

FIGURE 3 Retinal signaling and cellular remodeling mediated by TLR, TNF and immune molecules involves neuronal-glial circuits. The activation of TLR4, TNFRs and TCRs can promote NF-κB-regulated transcription, generating pro-IL-1β, which is then processed into IL-1β and secreted. This drives glial reactivity and furthers inflammation (e.g. the release of more TNF-α), thus perpetuating the inflammatory cycle. As RGCs are damaged and killed, they may release DAMPS (e.g. certain HSPs) that activate innate immune receptors such as TLR4 and thereby worsen glaucoma. The activation of TCR/CD3 may be involved in glaucomatous dendritic remodeling, which may disturb normal circuit functions and degrade the fidelity of visual processing.

kinases involved in TNF-α/TNFR1 signaling. Proteomics data support that a complex crosstalk relationship between multiple signaling pathways determines diverse bioactivities of TNF-α.[28] Besides the proteolytic caspase cascade, co-activation of calpain-mediated pathways, mitochondrial dysfunction and endoplasmic reticulum stress may reinforce each other during RGC apoptosis in glaucoma. Regarding TNFR-mediated inflammation signaling, proteomics analysis of the glaucomatous human retina has produced data supporting NF-κB activation, JAK/STAT signaling and inflammasome assembly.[161] Proteomics analysis of RGC and astrocyte samples has also showed cell-specific regulation of TNF-α signaling in experimental glaucoma, such as caspase activation leading to apoptosis in RGCs, but NF-κB activation promoting cell survival and inflammation in astrocytes.[162] In addition, the type of receptor preferentially used is important in determining the outcomes of TNF-α signaling. This multifunctional cytokine can bind two different receptors of the TNFR superfamily, TNFR1 (p55) and TNFR2 (p75). TNFR1 appears to be the primary receptor for both neurodegenerative and inflammatory consequences of TNF-α signaling in glaucoma.[161] This is because a death domain present on the intracellular region of TNFR1, but not present in TNFR2, leads to apoptotic cell death, while signaling through TNFR2 leads primarily to cell proliferation. TNFR1 is also the primary signaling receptor responsible for the majority of TNF-α-mediated inflammatory responses, particularly those mediated by the soluble TNF-α required for inflammation.[28,163]

The glaucomatous human retina also exhibits upregulation of TLR signaling[149] (Figures 2 and 3). Innate immune activity in the CNS can be triggered by numerous pathways after recognition of invading pathogens or tissue stress/injury by pattern recognition receptors,[164] which include TLRs and nucleotide-binding oligomerization domain-like receptors (NLRs). Although TLRs are membrane-spanning receptors, NLRs are cytoplasmic sensors that form a platform for the assembly of the inflammasome, a multiprotein complex that processes pro-ILs into their mature forms *via* proteolytic cleavage by caspase-1,[165] as is evident in glaucoma.[161,162] TLRs recognize a wide variety of pathogen-associated molecular patterns and also the DAMPs expressed during tissue stress or injury.[166] Recent proteomics studies of human glaucoma and animal models have revealed that glial cells, including both microglia and astroglia, are the main cell types that express a repertoire of TLRs, as well as several inflammasome-related molecules.[149,162] In addition, there is *in vitro* evidence

indicating that glaucomatous stress-related intrinsic ligands, such as heat shock proteins (HSPs) and oxidation products, can activate glial TLRs and stimulate T cells.[149] After recognizing specific molecular patterns, TLRs recruit adaptor proteins, such as MyD88, and activate NF-κB (Figure 2), a major transcription factor for the expression of pro-inflammatory cytokines.[167] Proteomic data from human glaucoma and animal models, along with the findings of *in vitro* treatment experiments, support the notion that the glial TLR signaling initiated by glaucomatous stress-related ligands includes MyD88-dependent pathways.[149]

NF-κB activation after binding TNFRs and TLRs triggers the transcriptional activation of pro-ILs that are processed into their active forms by the inflammasome.[165] Glaucomatous retinal proteome exhibits increased glial expression of specific kinases involved in the NF-κB activation pathway, such as receptor-interacting serine-threonine kinase (RIPK), NF-κB-inducing kinase (NIK), and inhibitory kappa B (IκB) kinases (IκKs), including a master regulator, IκKgamma (NF-κB essential modulator), and phosphorylation of NF-κB subunits, NF-κB1-p105/p50 and p65.[161,162] Although NF-κB regulates neuronal survival programs, including in the retina and optic nerve,[168] this transcription factor is a master regulator of the inflammatory responses leading to secondary neurodegenerative processes.[167,169] The NF-κB pathway may similarly play a major role in regulation of glia-driven pro-inflammatory processes during glaucomatous neurodegeneration.[162] As implicated in other neurodegenerative diseases,[170] TNF-α/TNFR signaling, TLR signaling and the inflammasome together exhibit the potent inflammatory capacity with beneficial and detrimental outcomes in glaucoma. NF-κB, as being a common player of inflammation through TNFR or TLR signaling, appears to be a promising treatment target to provide immunomodulation in glaucoma[171] and deserves further studies.

Function and Possible Mechanisms of Activation of Immune Molecules in the Retina

Recent studies demonstrated that genes typically associated with the immune system, such as those in the MHC and complements, are expressed by neurons in various regions of the CNS, including retina, and may play important roles in synapse formation during normal development and pathogenesis in CNS diseases.[25,172–177] Consistent with this notion, genetic deletion or mutation of a number of MHC class I genes (such as a MHCI co-subunit β2-microglobulin or a key component of MHCI receptor complex CD3ζ), complements or complement receptors result in the failure of development of the eye-specific segregation of RGC axonal projections to the dLGN.[25,174,178,179] On the other hand, over-expression of MHCI molecules caused effects on the retinogeniculate projections opposite to that of MHCI or complement mutations.[180] Furthermore, the expression of complements is up-regulated in glaucomatous retinas,[181] and over-expression of MHCI molecules significantly enhanced the recovery of locomotor abilities after spinal cord injury.[181]

The precise molecular mechanisms of how MHCI molecules and complement cascade expressed by CNS neurons are activated, and how they regulate the normal development and pathogenesis of CNS diseases are unclear. It was suggested that the expression and activity of MHCI molecules and complement cascade are regulated by neuronal activity. Consistently, retinal activity was found to regulate the level of mRNA of MHCI molecules in the dorsal lateral geniculate nucleus (dLGN).[173] In retina, the effects of CD3ζ seem to be cell-type and neurotransmitter-specific. Xu et al.,[25] reported that CD3ζ is specifically expressed by RGCs and mice with genetic mutation of CD3ζ exhibited a selective reduction of glutamate receptor-mediated synaptic transmission of RGCs. It was also postulated that activation of immune molecules in neurons could produce similar intracellular signals as those generated in immune cells but with different ultimate effects, such as altering synaptic development, strength, neuronal morphology or circuit properties downstream of synaptic activity[25,182,183] (Figure 3). In the immune system, activation of CD3ζ triggers several downstream cascades, including a Ras-MAPK pathway and actin-based cytoskeleton reorganization, which regulates immune cell polarization, migration and dendritic growth.[184–186] It has been shown that most components of these cascades are expressed in the CNS and implicated in activity-dependent synaptic plasticity.[182,187] In addition, direct activation of CD3ζ on hippocampal neurons affects cell morphology by promoting dendritic pruning through a tyrosine-based phosphorylation signaling motif common to the immune system.[172] Furthermore, neuronal activity in the retina is also suggested to regulate the complement-dependent activation of the resident immune cells in retina, microglia, which in turn regulates the developmental remodeling of RGC axonal projection during normal development through a process similar to "phagocytosis".[178] Recent studies also implied that retinal microglia might play an important role in RGC death in glaucomatous retinal degeneration.[188–190] These observations strongly support the possibility that the immune molecules and cells could regulate the neuronal structure and function through mechanisms similar to those in the immune system.

CONCLUDING REMARKS

Analysis of signaling pathways associated with RGC injury points at intracellular involvement of ubiquitous messenger molecules such as Ca^{2+} and ATP, which could participate in intrinsic mechanosensation and drive feedback pathways associated with secondary glial and vascular mechanisms. Because $[Ca^{2+}]_i$ maintenance is critically important for the regulation of excitability, cytoskeletal integrity, metabolism and synaptic function, disruption of Ca^{2+} homeostasis would ultimately lead to anatomical and physiological remodeling observed in glaucoma. Recent evidence suggests that such Ca^{2+} overloads in RGCs could be mediated by TRPV4, P2X7R and/or pannexin channels. The effect of mechanical stress on resident mechanosensitive channels has to be placed within the larger context encompassing secondary inflammatory and immune responses driven by feedback loops between injured RGCs, astrocytes, microglia and the vascular endothelium. Inflammatory cytokines and complement molecules released from glial and endothelial cells could drive the plasma membrane P2X7R-Panx1 complex as well as complex arrays of immune/inflammatory signaling molecules that might include TNF-α, IL-1β, Toll-like and T-cell receptors. The ensuing reconfiguration of intracellular signals is proposed to involve the NF-κB pathway and activation of the inflammasome complex.

Current glaucoma treatments are limited to minimization of mechanical impact mediated by elevated IOP and lack tools that would protect RGCs by targeting the mechanosensing mechanisms and/or secondary inflammatory/immune pathways within the retina. Thus, development of novel neuroprotective treatments depends on our ability to characterize the force transduction mechanisms that mediate retinal IOP sensing (TRPV4, Panx1 and P2X7R discussed here) together with the role of secondary interactions between RGCs and the surrounding vascular endothelial cells, pericytes, astrocytes, Müller cells and microglia.

ACKNOWLEDGEMENTS

Supported by NIH grants T32DC008553 (DAR), EY14232, EY021517 (VIS), EY013434, EY015537 (CHM), EY13870, EY022076 (DK), EY018666 and GM060019 (VZS), EY013813 and EY017131 (GT), Center Grants P30 EY014801 (VIS) and P30 EY14800 (DK), Department of Defense (VIS, DK), Russian Federal Special Program Grant 2012-1.5-12-000-1002-018 (V.I.S.), University of Utah Translational Seed grant (DK), State of Utah TCIP (DK), Foundation Fighting Blindness (DK) and unrestricted grants from RPB to Bascom Palmer Eye Institute (Miami) and Moran Eye Institute (Salt Lake City). The authors would like to thank Dr. Harilaos Ginis (University of Crete, Greece) for helpful comments.

DECLARATION OF INTEREST

The authors report no conflicts of interest. The authors alone are responsible for the content and writing of this article.

REFERENCES

1. Harwerth RS, Crawford ML, Frishman LJ, Viswanathan S, Smith 3rd EL, Carter-Dawson L. Visual field defects and neural losses from experimental glaucoma. Prog Retin Eye Res 2002;21:91–125.
2. Jakobs TC, Libby RT, Ben Y, John SW, Masland RH. Retinal ganglion cell degeneration is topological but not cell type specific in DBA/2J mice. J Cell Biol 2005;171:313–325.
3. Baltan S, Inman DM, Danilov CA, Morrison RS, Calkins DJ, Horner PJ. Metabolic vulnerability disposes retinal ganglion cell axons to dysfunction in a model of glaucomatous degeneration. J Neurosci 2010;30:5644–5652.
4. Tezel G. Oxidative stress in glaucomatous neurodegeneration: mechanisms and consequences. Prog Retin Eye Res 2006;25:490–513.
5. Quigley HA, Addicks EM. Chronic experimental glaucoma in primates. I. Production of elevated intraocular pressure by anterior chamber injection of autologous ghost red blood cells. Invest Ophthalmol Vis Sci 1980;19:126–136.
6. Umapathy NS, Li W, Mysona BA, Smith SB, Ganapathy V. Expression and function of glutamine transporters SN1 (SNAT3) and SN2 (SNAT5) in retinal Muller cells. Invest Ophthalmol Vis Sci 2005;46:3980–3987.
7. Sullivan RK, Woldemussie E, Macnab L, Ruiz G, Pow DV. Evoked expression of the glutamate transporter GLT-1c in retinal ganglion cells in human glaucoma and in a rat model. Invest Ophthalmol Vis Sci 2006;47:3853–3859.
8. Reichenbach A, Bringmann A. Müller cells in the healthy and diseased retina. New York: Springer; 2010. pp xiv, 417.
9. Bonomi L, Marchini G, Marraffa M, Morbio R. The relationship between intraocular pressure and glaucoma in a defined population. Data from the Egna-Neumarkt Glaucoma Study. Ophthalmologica 2001;215:34–38.
10. Blanch RJ, Ahmed Z, Berry M, Scott RA, Logan A. Animal models of retinal injury. Invest Ophthalmol Vis Sci 2012;53:2913–2920.
11. Nilius B, Owsianik G. Transient receptor potential channelopathies. Pflugers Arch 2010;460:437–450.
12. Christensen AP, Corey DP. TRP channels in mechanosensation: direct or indirect activation? Nat Rev Neurosci 2007;8:510–521.
13. Wiggs JL. The cell and molecular biology of complex forms of glaucoma: updates on genetic, environmental, and epigenetic risk factors. Invest Ophthalmol Vis Sci 2012;53:2467–2469.
14. Sommer A, Tielsch JM, Katz J, Quigley HA, Gottsch JD, Javitt J, et al. Relationship between intraocular pressure and primary open angle glaucoma among white and black Americans. The Baltimore Eye Survey. Arch Ophthalmol 1991;109:1090–1095.

15. Stamer WD, Acott TS. Current understanding of conventional outflow dysfunction in glaucoma. Curr Opin Ophthalmol 2012;23:135–143.
16. John SW, Smith RS, Savinova OV, Hawes NL, Chang B, Turnbull D, et al. Essential iris atrophy, pigment dispersion, and glaucoma in DBA/2J mice. Invest Ophthalmol Vis Sci 1998;39:951–962.
17. Chauhan BC, Pan J, Archibald ML, LeVatte TL, Kelly ME, Tremblay F. Effect of intraocular pressure on optic disc topography, electroretinography, and axonal loss in a chronic pressure-induced rat model of optic nerve damage. Invest Ophthalmol Vis Sci 2002;43:2969–2976.
18. Quigley HA. Clinical trials for glaucoma neuroprotection are not impossible. Curr Opin Ophthalmol 2012;23:144–154.
19. Sharma AK, Rohrer B. Sustained elevation of intracellular cGMP causes oxidative stress triggering calpain-mediated apoptosis in photoreceptor degeneration. Curr Eye Res 2007;32:259–269.
20. Vallazza-Deschamps G, Fuchs C, Cia D, Tessier LH, Sahel JA, Dreyfus H, et al. Diltiazem-induced neuroprotection in glutamate excitotoxicity and ischemic insult of retinal neurons. Doc Ophthalmol 2005;110:25–35.
21. Bezprozvanny I, Hayden MR. Deranged neuronal calcium signaling and Huntington disease. Biochem Biophys Res Commun 2004;322:1310–1317.
22. Wax MB, Tezel G. Immunoregulation of retinal ganglion cell fate in glaucoma. Exp Eye Res 2009;88:825–830.
23. Crish SD, Calkins DJ. Neurodegeneration in glaucoma: progression and calcium-dependent intracellular mechanisms. Neuroscience 2011;176:1–11.
24. Burgoyne CF. A biomechanical paradigm for axonal insult within the optic nerve head in aging and glaucoma. Exp Eye Res 2011;93:120–132.
25. Xu HP, Chen H, Ding Q, Xie ZH, Chen L, Diao L, et al. The immune protein CD3zeta is required for normal development of neural circuits in the retina. Neuron 2010;65:503–515.
26. Steele MR, Inman DM, Calkins DJ, Horner PJ, Vetter ML. Microarray analysis of retinal gene expression in the DBA/2J model of glaucoma. Invest Ophthalmol Vis Sci 2006;47:977–985.
27. Stasi K, Nagel D, Yang X, Wang RF, Ren L, Podos SM, et al. Complement component 1Q (C1Q) upregulation in retina of murine, primate, and human glaucomatous eyes. Invest Ophthalmol Vis Sci 2006;47:1024–1029.
28. Tezel G. TNF-alpha signaling in glaucomatous neurodegeneration. Prog Brain Res 2008;173:409–421.
29. Huang W, Xing W, Ryskamp DA, Punzo C, Krizaj D. Localization and phenotype-specific expression of ryanodine calcium release channels in C57BL6 and DBA/2J mouse strains. Exp Eye Res 2011;93:700–709.
30. Lebrun-Julien F, Duplan L, Pernet V, Osswald I, Sapieha P, Bourgeois P, et al. Excitotoxic death of retinal neurons in vivo occurs via a non-cell-autonomous mechanism. J Neurosci 2009;29:5536–5545.
31. Tezel G. The immune response in glaucoma: a perspective on the roles of oxidative stress. Exp Eye Res 2011;93:178–186.
32. Delmas P. Polycystins: from mechanosensation to gene regulation. Cell 2004;118:145–148.
33. Eyckmans J, Boudou T, Yu X, Chen CS. A hitchhiker's guide to mechanobiology. Dev Cell 2011;21:35–47.
34. Coulombre AJ, Coulombre JL. The role of intraocular pressure in the development of the chick eye. IV. Corneal curvature. AMA Arch Ophthalmol 1958;59:502–506.
35. Coulombre AJ, Coulombre JL. Lens development. I. Role of the lens in eye growth. J Exp Zool 1964;156:39–47.
36. Vogel V, Sheetz M. Local force and geometry sensing regulate cell functions. Nat Rev Mol Cell Biol 2006;7:265–275.
37. Morrison JC, Moore CG, Deppmeier LM, Gold BG, Meshul CK, Johnson EC. A rat model of chronic pressure-induced optic nerve damage. Exp Eye Res 1997;64:85–96.
38. del Rio A, Perez-Jimenez R, Liu R, Roca-Cusachs P, Fernandez JM, Sheetz MP. Stretching single talin rod molecules activates vinculin binding. Science 2009;323:638–641.
39. Stewart AP, Smith GD, Sandford RN, Edwardson JM. Atomic force microscopy reveals the alternating subunit arrangement of the TRPP2-TRPV4 heterotetramer. Biophys J 2010;99:790–797.
40. Quigley HA, Green WR. The histology of human glaucoma cupping and optic nerve damage: clinicopathologic correlation in 21 eyes. Ophthalmology 1979;86:1803–1830.
41. Danias J, Lee KC, Zamora MF, Chen B, Shen F, Filippopoulos T, et al. Quantitative analysis of retinal ganglion cell (RGC) loss in aging DBA/2NNia glaucomatous mice: comparison with RGC loss in aging C57/BL6 mice. Invest Ophthalmol Vis Sci 2003;44:5151–5162.
42. Schlamp CL, Li Y, Dietz JA, Janssen KT, Nickells RW. Progressive ganglion cell loss and optic nerve degeneration in DBA/2J mice is variable and asymmetric. BMC Neurosci 2006;7:66.
43. Adalbert R, Coleman MP. Axon pathology in age-related neurodegenerative disorders. Neuropathol Appl Neurobiol 2013;39:90–108.
44. Crish SD, Sappington RM, Inman DM, Horner PJ, Calkins DJ. Distal axonopathy with structural persistence in glaucomatous neurodegeneration. Proc Natl Acad Sci USA 2010;107:5196–5201.
45. Begg IS, Drance SM. Progress of the glaucomatous process related to recurrent ischaemic changes at the optic disc. Exp Eye Res 1971;11:141.
46. Fechtner RD, Weinreb RN. Mechanisms of optic nerve damage in primary open angle glaucoma. Surv Ophthalmol 1994;39:23–42.
47. Fortune B, Burgoyne CF, Cull GA, Reynaud J, Wang L. Structural and functional abnormalities of retinal ganglion cells measured in vivo at the onset of optic nerve head surface change in experimental glaucoma. Invest Ophthalmol Vis Sci 2012;53:3939–3950.
48. Weber AJ, Harman CD, Viswanathan S. Effects of optic nerve injury, glaucoma, and neuroprotection on the survival, structure, and function of ganglion cells in the mammalian retina. J Physiol 2008;586:4393–4400.
49. Stevens SL, Ciesielski TM, Marsh BJ, Yang T, Homen DS, Boule JL, et al. Toll-like receptor 9: a new target of ischemic preconditioning in the brain. J Cereb Blood Flow Metab 2008;28:1040–1047.
50. Porciatti V, Nagaraju M. Head-up tilt lowers IOP and improves RGC dysfunction in glaucomatous DBA/2J mice. Exp Eye Res 2010;90:452–460.
51. Kong YX, van Bergen N, Bui BV, Chrysostomou V, Vingrys AJ, Trounce IA, et al. Impact of aging and diet restriction on retinal function during and after acute intraocular pressure injury. Neurobiol Aging 2012;33:1126 e15–25.
52. Bui BV, He Z, Vingrys AJ, Nguyen CT, Wong VH, Fortune B. Using the electroretinogram to understand how intraocular pressure elevation affects the rat retina. J Ophthalmol 2013;2013:262467.
53. Banitt MR, Ventura LM, Feuer WJ, Savatovsky E, Luna G, Shif O, et al. Progressive loss of retinal ganglion cell function precedes structural loss by several years in glaucoma suspects. Invest Ophthalmol Vis Sci 2013;54:2346–2352.

54. Weber AJ, Kaufman PL, Hubbard WC. Morphology of single ganglion cells in the glaucomatous primate retina. Invest Ophthalmol Vis Sci 1998;39:2304–2320.
55. Eisenlohr JE, Langham ME, Maumenee AE. Manometric studies of the pressure-volume relationship in living and enucleated eyes of individual human subjects. Br J Ophthalmol 1962;46:536–548.
56. Dastiridou AI, Ginis HS, De Brouwere D, Tsilimbaris MK, Pallikaris IG. Ocular rigidity, ocular pulse amplitude, and pulsatile ocular blood flow: the effect of intraocular pressure. Invest Ophthalmol Vis Sci 2009;50:5718–5722.
57. Pallikaris IG, Kymionis GD, Ginis HS, Kounis GA, Tsilimbaris MK. Ocular rigidity in living human eyes. Invest Ophthalmol Vis Sci 2005;46:409–414.
58. Silver DM, Geyer O. Pressure-volume relation for the living human eye. Curr Eye Res 2000;20:115–120.
59. Wang J, Freeman EE, Descovich D, Harasymowycz PJ, Kamdeu Fansi A, Li G, et al. Estimation of ocular rigidity in glaucoma using ocular pulse amplitude and pulsatile choroidal blood flow. Invest Ophthalmol Vis Sci 2013;54: 1706–1711.
60. Markin VS, Sachs F. Thermodynamics of mechanosensitivity. Phys Biol 2004;1:110–124.
61. Wiggins P, Phillips R. Membrane-protein interactions in mechanosensitive channels. Biophys J 2005;88:880–902.
62. Niittykoski M, Kalesnykas G, Larsson KP, Kaarniranta K, Akerman KE, Uusitalo H. Altered calcium signaling in an experimental model of glaucoma. Invest Ophthalmol Vis Sci 2010;51:6387–6393.
63. Agar A, Li S, Agarwal N, Coroneo MT, Hill MA. Retinal ganglion cell line apoptosis induced by hydrostatic pressure. Brain Res 2006;1086:191–200.
64. Sappington RM, Carlson BJ, Crish SD, Calkins DJ. The microbead occlusion model: a paradigm for induced ocular hypertension in rats and mice. Invest Ophthalmol Vis Sci. 2010;51:207–216.
65. Pang IH, Clark AF. Rodent models for glaucoma retinopathy and optic neuropathy. J Glaucoma 2007;16:483–505.
66. Ryskamp DA, Witkovsky P, Barabas P, Huang W, Koehler C, Akimov NP, et al. The polymodal ion channel transient receptor potential vanilloid 4 modulates calcium flux, spiking rate, and apoptosis of mouse retinal ganglion cells. J Neurosci 2011;31:7089–7101.
67. Xia J, Lim JC, Lu W, Beckel JM, Macarak EJ, Laties AM, et al. Neurons respond directly to mechanical deformation with pannexin-mediated ATP release and autostimulation of P2X7 receptors. J Physiol 2012;590:2285–2304.
68. Resta V, Novelli E, Vozzi G, Scarpa C, Caleo M, Ahluwalia A, et al. Acute retinal ganglion cell injury caused by intraocular pressure spikes is mediated by endogenous extracellular ATP. Eur J Neurosci 2007;25:2741–2754.
69. Balaratnasingam C, Morgan WH, Bass L, Ye L, McKnight C, Cringle SJ, et al. Elevated pressure induced astrocyte damage in the optic nerve. Brain Res 2008;1244:142–154.
70. Fu CT, Tran T, Sretavan D. Axonal/glial upregulation of EphB/ephrin-B signaling in mouse experimental ocular hypertension. Invest Ophthalmol Vis Sci 2010;51:991–1001.
71. Molnar T, Barabas P, Birnbaumer L, Punzo C, Kefalov V, Krizaj D. Store-operated channels regulate intracellular calcium in mammalian rods. J Physiol 2012;590:3465–3481.
72. Xue T, Do MT, Riccio A, Jiang Z, Hsieh J, Wang HC, et al. Melanopsin signalling in mammalian iris and retina. Nature 2011;479:67–73.
73. Sappington RM, Sidorova T, Long DJ, Calkins DJ. TRPV1: contribution to retinal ganglion cell apoptosis and increased intracellular Ca2+ with exposure to hydrostatic pressure. Invest Ophthalmol Vis Sci 2009;50:717–728.
74. Frye A, Ryskamp D, Križaj D. Overstimulation of TRPV4 *in vivo* induces selective apoptosis of retinal ganglion cells. An acute *in vivo* experimental model for glaucoma. IOVS Abstr. 2012:Ft. Lauderdale, FL.
75. Loukin S, Zhou X, Su Z, Saimi Y, Kung C. Wild-type and brachyolmia-causing mutant TRPV4 channels respond directly to stretch force. J Biol Chem 2010;285: 27176–27181.
76. Watanabe H, Vriens J, Prenen J, Droogmans G, Voets T, Nilius B. Anandamide and arachidonic acid use epoxyeicosatrienoic acids to activate TRPV4 channels. Nature 2003; 424:434–438.
77. Matthews BD, Thodeti CK, Tytell JD, Mammoto A, Overby DR, Ingber DE. Ultra-rapid activation of TRPV4 ion channels by mechanical forces applied to cell surface beta1 integrins. Integr Biol (Camb) 2010;2:435–442.
78. Tomita G. The optic nerve head in normal-tension glaucoma. Curr Opin Ophthalmol 2000;11:116–120.
79. Nickells RW, Howell GR, Soto I, John SW. Under pressure: cellular and molecular responses during glaucoma, a common neurodegeneration with axonopathy. Annu Rev Neurosci 2012;35:153–179.
80. Wang SY, Singh K, Lin SC. The association between glaucoma prevalence and supplementation with the oxidants calcium and iron. Invest Ophthalmol Vis Sci 2012;53: 725–731.
81. Huang W, Fileta J, Rawe I, Qu J, Grosskreutz CL. Calpain activation in experimental glaucoma. Invest Ophthalmol Vis Sci 2010;51:3049–3054.
82. Garcia-Valenzuela E, Shareef S, Walsh J, Sharma SC. Programmed cell death of retinal ganglion cells during experimental glaucoma. Exp Eye Res 1995;61:33–44.
83. Nakagawa T, Yuan J. Cross-talk between two cysteine protease families. Activation of caspase-12 by calpain in apoptosis. J Cell Biol 2000;150:887–894.
84. de Rivero Vaccari JP, Lotocki G, Alonso OF, Bramlett HM, Dietrich WD, Keane RW. Therapeutic neutralization of the NLRP1 inflammasome reduces the innate immune response and improves histopathology after traumatic brain injury. J Cereb Blood Flow Metab 2009;29:1251–1261.
85. Abulafia DP, de Rivero Vaccari JP, Lozano JD, Lotocki G, Keane RW, Dietrich WD. Inhibition of the inflammasome complex reduces the inflammatory response after thromboembolic stroke in mice. J Cereb Blood Flow Metab 2009;29:534–544.
86. Kanneganti TD, Lamkanfi M, Kim YG, Chen G, Park JH, Franchi L, et al. Pannexin-1-mediated recognition of bacterial molecules activates the cryopyrin inflammasome independent of Toll-like receptor signaling. Immunity 2007;26:433–443.
87. Clarke TC, Williams OJ, Martin PE, Evans WH. ATP release by cardiac myocytes in a simulated ischaemia model: inhibition by a connexin mimetic and enhancement by an antiarrhythmic peptide. Eur J Pharmacol 2009;605: 9–14.
88. Seminario-Vidal L, Kreda S, Jones L, O'Neal W, Trejo J, Boucher RC, et al. Thrombin promotes release of ATP from lung epithelial cells through coordinated activation of rho- and Ca2+-dependent signaling pathways. J Biol Chem 2009;284:20638–20648.
89. Ingber DE. From cellular mechanotransduction to biologically inspired engineering: 2009 Pritzker Award Lecture, BMES Annual Meeting October 10, 2009. Ann Biomed Eng 2010;38:1148–1161.
90. Burnstock G. Release of vasoactive substances from endothelial cells by shear stress and purinergic mechanosensory transduction. J Anat 1999;194:335–342.
91. Sadananda P, Shang F, Liu L, Mansfield KJ, Burcher E. Release of ATP from rat urinary bladder mucosa: role of acid, vanilloids and stretch. Br J Pharmacol 2009;158: 1655–1662.

92. Winters SL, Davis CW, Boucher RC. Mechanosensitivity of mouse tracheal ciliary beat frequency: roles for Ca2+, purinergic signaling, tonicity, and viscosity. Am J Physiol Cell Physiol 2007;292:L614–L624.
93. Wheeler-Schilling TH, Marquordt K, Kohler K, Guenther E, Jabs R. Identification of purinergic receptors in retinal ganglion cells. Brain Res Mol Brain Res 2001;92:177–180.
94. Zhang X, Li A, Ge J, Reigada D, Laties AM, Mitchell CH. Acute increase of intraocular pressure releases ATP into the anterior chamber. Exp Eye Res 2007;85:637–643.
95. Li A, Zhang X, Zheng D, Ge J, Laties AM, Mitchell CH. Sustained elevation of extracellular ATP in aqueous humor from humans with primary chronic angle-closure glaucoma. Exp Eye Res 2011;93:528–533.
96. Reigada D, Lu W, Zhang M, Mitchell CH. Elevated pressure triggers a physiological release of ATP from the retina: possible role for pannexin hemichannels. Neurosci 2008;157:396–404.
97. Lu W, Rasmussen C, Gabelt B, Hennes B, Kaufman P, Laties AM, et al. Upregulation of NTPDase 1 in an experimental monkey glaucoma model. Invest Ophthalmol Vis Sci 2007;48:4804 (Abstract).
98. Lu W, Hu H, Laties AM, Sevigney J, Mitchell CH. Upregulation of Retinal NTPDase 1 and vitreal ATP levels in an experimental rat glaucoma model. Invest Ophthalmol Vis Sci 2008;49:ARVO E abstract:869.
99. Gulbransen BD, Bashashati M, Hirota SA, Gui X, Roberts JA, MacDonald JA, et al. Activation of neuronal P2X7 receptor-pannexin-1 mediates death of enteric neurons during colitis. Nat Med 2012;18:600–604.
100. Clark AK, Staniland AA, Marchand F, Kaan TK, McMahon SB, Malcangio M. P2X7-dependent release of interleukin-1beta and nociception in the spinal cord following lipopolysaccharide. J Neurosci 2010;30: 573–582.
101. Zhang X, Zhang M, Laties AM, Mitchell CH. Stimulation of P2X7 receptors elevates Ca2+ and kills retinal ganglion cells. Invest Ophthalmol Vis Sci 2005;46:2183–2191.
102. Hu H, Lu W, Zhang M, Zhang X, Argall AJ, Patel S, et al. Stimulation of the P2X7 receptor kills rat retinal ganglion cells in vivo. Exp Eye Res 2010;91:425–432.
103. Mitchell CH, Lu W. Retinal ganglion cells and glaucoma: traditional patterns and new possibilities. Curr Topics Membr 2008;62:301–322.
104. Mitchell CH, Lu W, Hu H, Zhang X, Reigada D, Zhang M. The P2X(7) receptor in retinal ganglion cells: a neuronal model of pressure-induced damage and protection by a shifting purinergic balance. Purinergic Signal 2009;5: 241–249.
105. Newman EA. Propagation of intercellular calcium waves in retinal astrocytes and Muller cells. J Neurosci 2001;21: 2215–2223.
106. Newman EA. Glial cell inhibition of neurons by release of ATP. J Neurosci 2003;23:1659–1666.
107. North RA. Molecular physiology of P2X receptors. Physiol Rev 2002;82:1013–1067.
108. Pelegrin P, Surprenant A. Pannexin-1 mediates large pore formation and interleukin-1beta release by the ATP-gated P2X7 receptor. EMBO J 2006;25:5071–5082.
109. Bunse S, Locovei S, Schmidt M, Qiu F, Zoidl G, Dahl G, et al. The potassium channel subunit Kvbeta3 interacts with pannexin 1 and attenuates its sensitivity to changes in redox potentials. Febs J 2009;276:6258–6270.
110. Dubyak GR. Both sides now: multiple interactions of ATP with pannexin-1 hemichannels. Focus on ''A permeant regulating its permeation pore: inhibition of pannexin 1 channels by ATP''. Am J Physiol Cell Physiol 2009;296: C235–C241.
111. Bao L, Locovei S, Dahl G. Pannexin membrane channels are mechanosensitive conduits for ATP. FEBS Letts 2004; 572:65–68.
112. Seminario-Vidal L, Okada SF, Sesma JI, Kreda SM, van Heusden CA, Zhu Y, et al. Rho signaling regulates pannexin 1-mediated ATP release from airway epithelia. J Biol Chem 2011;286:26277–26286.
113. Xia J, Lim JC, Lu W, Beckel JM, Macarak EJ, Laties AM, et al. Neurons respond directly to mechanical deformation with pannexin-mediated ATP release and autostimulation of P2X7 receptors. J Physiol 2012;590.10: 2285–2304.
114. Dvoriantchikova G, Ivanov D, Panchin Y, Shestopalov VI. Expression of pannexin family of proteins in the retina. FEBS Letts 2006;580:2178–2182.
115. Franke H, Klimke K, Brinckmann U, Grosche J, Francke M, Sperlagh B, et al. P2X(7) receptor-mRNA and -protein in the mouse retina; changes during retinal degeneration in BALBCrds mice. Neurochem Int 2005;47:235–242.
116. Vessey KA, Fletcher EL. Rod and cone pathway signalling is altered in the P2X7 receptor knock out mouse. Plos One 2012;7:290–305.
117. Yang H, Thompson H, Roberts MD, Sigal IA, Downs JC, Burgoyne CF. Deformation of the early glaucomatous monkey optic nerve head connective tissue after acute IOP elevation in 3-D histomorphometric reconstructions. Invest Ophthalmol Vis Sci 2011;52:345–363.
118. Vanden Abeele F, Bidaux G, Gordienko D, Beck B, Panchin YV, Baranova AV, et al. Functional implications of calcium permeability of the channel formed by pannexin 1. J Cell Biol 2006;174:535–546.
119. Locovei S, Wang J, Dahl G. Activation of pannexin 1 channels by ATP through P2Y receptors and by cytoplasmic calcium. FEBS Lett 2006;580:239–244.
120. Poornima V, Madhupriya M, Kootar S, Sujatha G, Kumar A, Bera AK. P2X7 receptor-pannexin 1 hemichannel association: effect of extracellular calcium on membrane permeabilization. J Mol Neurosci 2012;46:585–594.
121. Pelegrin P, Barroso-Gutierrez C, Surprenant A. P2X7 receptor differentially couples to distinct release pathways for IL-1beta in mouse macrophage. J Immunol 2008; 180:7147–7157.
122. Silverman WR, de Rivero Vaccari JP, Locovei S, Qiu F, Carlsson SK, Scemes E, et al. The pannexin 1 channel activates the inflammasome in neurons and astrocytes. J Biol Chem 2009;284:18143–18151.
123. Striedinger K, Petrasch-Parwez E, Zoidl G, Napirei M, Meier C, Eysel UT, et al. Loss of connexin36 increases retinal cell vulnerability to secondary cell loss. Eur J Neurosci 2005;22:605–616.
124. Orellana JA, Saez PJ, Shoji KF, Schalper KA, Palacios-Prado N, Velarde V, et al. Modulation of brain hemichannels and gap junction channels by pro-inflammatory agents and their possible role in neurodegeneration. Antioxid Redox Signal 2009;11:369–399.
125. Contreras JE, Sanchez HA, Eugenin EA, Speidel D, Theis M, Willecke K, et al. Metabolic inhibition induces opening of unapposed connexin 43 gap junction hemichannels and reduces gap junctional communication in cortical astrocytes in culture. Proc Natl Acad Sci USA 2002;99:495–500.
126. Bao L, Locovei S, Dahl G. Pannexin membrane channels are mechanosensitive conduits for ATP. FEBS Lett 2004; 572:65–68.
127. Barbe MT, Monyer H, Bruzzone R. Cell-cell communication beyond connexins: the pannexin channels. Physiology (Bethesda) 2006;21:103–114.
128. Brough D, Pelegrin P, Rothwell NJ. Pannexin-1-dependent caspase-1 activation and secretion of IL-1beta is regulated by zinc. Eur J Immunol 2009;39:352–358.

129. Scemes E, Spray DC. Extracellular K(+) and astrocyte signaling via connexin and pannexin channels. Neurochem Res 2012;37:2310–2316.
130. Dvoriantchikova G, Ivanov D, Barakat D, Grinberg A, Wen R, Slepak VZ, Shestopalov VI. Genetic ablation of Pannexin1 protects retinal neurons from ischemic injury. PlosOne 2012;7:e31991.
131. Bargiotas P, Krenz A, Hormuzdi SG, Ridder DA, Herb A, Barakat W, et al. Pannexins in ischemia-induced neurodegeneration. Proc Natl Acad Sci USA 2011;108: 20772–20777.
132. Zhang L, Deng T, Sun Y, Liu K, Yang Y, Zheng X. Role for nitric oxide in permeability of hippocampal neuronal hemichannels during oxygen glucose deprivation. J Neurosci Res 2008;86:2281–2291.
133. Orellana JA, Hernandez DE, Ezan P, Velarde V, Bennett MV, Giaume C, et al. Hypoxia in high glucose followed by reoxygenation in normal glucose reduces the viability of cortical astrocytes through increased permeability of connexin 43 hemichannels. Glia 2010;58:329–343.
134. Domercq M, Perez-Samartin A, Aparicio D, Alberdi E, Pampliega O, Matute C. P2X7 receptors mediate ischemic damage to oligodendrocytes. Glia 2009;58:730–740.
135. Bargiotas P, Monyer H, Schwaninger M. Hemichannels in cerebral ischemia. Curr Mol Med 2009;9:186–194.
136. Thompson RJ, Zhou N, MacVicar BA. Ischemia opens neuronal gap junction hemichannels. Science 2006;312: 924–927.
137. Pelegrin P, Surprenant A. The P2X(7) receptor-pannexin connection to dye uptake and IL-1beta release. Purinergic Signal 2009;5:129–137.
138. Locovei S, Scemes E, Qiu F, Spray DC, Dahl G. Pannexin1 is part of the pore forming unit of the P2X(7) receptor death complex. FEBS Lett 2007;581:483–488.
139. Iglesias R, Locovei S, Roque A, Alberto AP, Dahl G, Spray DC, et al. P2X7 receptor-Pannexin1 complex: pharmacology and signaling. Am J Physiol Cell Physiol 2008;295: C752–C760.
140. Orellana JA, Froger N, Ezan P, Jiang JX, Bennett MV, Naus CC, et al. ATP and glutamate released via astroglial connexin43 hemichannels mediate neuronal death through activation of pannexin 1 hemichannels. J Neurochem 2011;118:826–840.
141. Pelegrin P, Surprenant A. Pannexin-1 couples to maitotoxin- and nigericin-induced interleukin-1beta release through a dye uptake-independent pathway. J Biol Chem 2007;282:2386–2394.
142. Ziegler G, Harhausen D, Schepers C, Hoffmann O, Rohr C, Prinz V, et al. TLR2 has a detrimental role in mouse transient focal cerebral ischemia. Biochem Biophys Res Commun 2007;359:574–579.
143. Tang SC, Arumugam TV, Xu X, Cheng A, Mughal MR, Jo DG, et al. Pivotal role for neuronal Toll-like receptors in ischemic brain injury and functional deficits. Proc Natl Acad Sci USA 2007;104:13798–13803.
144. Shibuya E, Meguro A, Ota M, Kashiwagi K, Mabuchi F, Iijima H, et al. Association of Toll-like receptor 4 gene polymorphisms with normal tension glaucoma. Invest Ophthalmol Vis Sci 2008;49:4453–4457.
145. Beg AA, Baltimore D. An essential role for NF-kappaB in preventing TNF-alpha-induced cell death. Science 1996; 274:782–784.
146. Micheau O, Tschopp J. Induction of TNF receptor I-mediated apoptosis via two sequential signaling complexes. Cell 2003;114:181–190.
147. Zhang Z, Trautmann K, Schluesener HJ. Microglia activation in rat spinal cord by systemic injection of TLR3 and TLR7/8 agonists. J Neuroimmunol 2005;164: 154–160.
148. Shiose S, Chen Y, Okano K, Roy S, Kohno H, Tang J, et al. Toll-like receptor 3 is required for development of retinopathy caused by impaired all-trans-retinal clearance in mice. J Biol Chem 2011;286:15543–15555.
149. Luo C, Yang X, Kain AD, Powell DW, Kuehn MH, Tezel G. Glaucomatous tissue stress and the regulation of immune response through glial Toll-like receptor signaling. Invest Ophthalmol Vis Sci 2010;51:5697–5707.
150. Ayna G, Krysko DV, Kaczmarek A, Petrovski G, Vandenabeele P, Fesus L. ATP release from dying autophagic cells and their phagocytosis are crucial for inflammasome activation in macrophages. PLoS One 2012;7:e40069.
151. Riteau N, Gasse P, Fauconnier L, Gombault A, Couegnat M, Fick L, et al. Extracellular ATP is a danger signal activating P2X7 receptor in lung inflammation and fibrosis. Am J Respir Crit Care Med 2010;182:774–783.
152. Pelegrin P. Targeting interleukin-1 signaling in chronic inflammation: focus on P2X(7) receptor and Pannexin-1. Drug News Perspect. 2008;21:424–433.
153. de Rivero Vaccari JP, Lotocki G, Marcillo AE, Dietrich WD, Keane RW. A molecular platform in neurons regulates inflammation after spinal cord injury. J Neurosci 2008;28:3404–3414.
154. Tezel G, Yang X, Yang J, Wax MB. Role of tumor necrosis factor receptor-1 in the death of retinal ganglion cells following optic nerve crush injury in mice. Brain Res 2004;996:202–212.
155. Nakazawa T, Nakazawa C, Matsubara A, Noda K, Hisatomi T, She H, et al. Tumor necrosis factor-alpha mediates oligodendrocyte death and delayed retinal ganglion cell loss in a mouse model of glaucoma. J Neurosci 2006;26:12633–12641.
156. Hyakkoku K, Hamanaka J, Tsuruma K, Shimazawa M, Tanaka H, Uematsu S, et al. Toll-like receptor 4 (TLR4), but not TLR3 or TLR9, knock-out mice have neuroprotective effects against focal cerebral ischemia. Neuroscience 2010;171:258–267.
157. Dvoriantchikova G, Barakat DJ, Hernandez E, Shestopalov VI, Ivanov D. Toll-like receptor 4 contributes to retinal ischemia/reperfusion injury. Mol Vis 2010;16: 1907–1912.
158. Barakat DJ, Dvoriantchikova G, Ivanov D, Shestopalov VI. Astroglial NF-kappaB mediates oxidative stress by regulation of NADPH oxidase in a model of retinal ischemia reperfusion injury. J Neurochem 2012;120: 586–597.
159. Murphy N, Cowley TR, Richardson JC, Virley D, Upton N, Walter D, Lynch MA. The Neuroprotective effect of a specific P2X(7) receptor antagonist derives from its ability to inhibit assembly of the NLRP3 inflammasome in glial cells. Brain Pathol 2011;22:295–306.
160. Tezel G, Wax MB. Increased production of tumor necrosis factor-alpha by glial cells exposed to simulated ischemia or elevated hydrostatic pressure induces apoptosis in cocultured retinal ganglion cells. J Neurosci 2000;20: 8693–8700.
161. Yang X, Luo C, Cai J, Powell DW, Yu D, Kuehn MH, et al. Neurodegenerative and inflammatory pathway components linked to TNF-alpha/TNFR1 signaling in the glaucomatous human retina. Invest Ophthalmol Vis Sci 2011;52:8442–8454.
162. Tezel G, Yang X, Luo C, Cai J, Powell DW. An astrocyte-specific proteomic approach to inflammatory responses in experimental rat glaucoma. Invest Ophthalmol Vis Sci 2012;53:4220–4233.
163. Cabal-Hierro L, Lazo PS. Signal transduction by tumor necrosis factor receptors. Cell Signal 2012;24:1297–1305.

164. Blander JM, Sander LE. Beyond pattern recognition: five immune checkpoints for scaling the microbial threat. Nat Rev Immunol 2012;12:215–225.
165. Ogura Y, Sutterwala FS, Flavell RA. The inflammasome: first line of the immune response to cell stress. Cell 2006; 126:659–662.
166. Creagh EM, O'Neill LA. TLRs, NLRs and RLRs: a trinity of pathogen sensors that co-operate in innate immunity. Trends Immunol 2006;27:352–357.
167. Harari OA, Liao JK. NF-kappaB and innate immunity in ischemic stroke. Ann N Y Acad Sci 2010;1207:32–40.
168. Takahashi Y, Katai N, Murata T, Taniguchi SI, Hayashi T. Development of spontaneous optic neuropathy in NF-kappaBetap50-deficient mice: requirement for NF-kappaBetap50 in ganglion cell survival. Neuropathol Appl Neurobiol 2007;33:692–705.
169. Hayden MS, Ghosh S. Shared principles in NF-kappaB signaling. Cell 2008;132:344–362.
170. Hanamsagar R, Hanke ML, Kielian T. Toll-like receptor (TLR) and inflammasome actions in the central nervous system. Trends Immunol 2012;33:333–342.
171. Tezel G. Immune regulation toward immunomodulation for neuroprotection in glaucoma. Curr Opin Pharmacol. 2013;13:23–31.
172. Baudouin SJ, Angibaud J, Loussouarn G, Bonnamain V, Matsuura A, Kinebuchi M, et al. The signaling adaptor protein CD3zeta is a negative regulator of dendrite development in young neurons. Mol Biol Cell 2008;19: 2444–2456.
173. Corriveau RA, Huh GS, Shatz CJ. Regulation of class I MHC gene expression in the developing and mature CNS by neural activity. Neuron 1998;21:505–520.
174. Huh GS, Boulanger LM, Du H, Riquelme PA, Brotz TM, Shatz CJ. Functional requirement for class I MHC in CNS development and plasticity. Science 2000;290: 2155–2159.
175. Ishii T, Hirota J, Mombaerts P. Combinatorial coexpression of neural and immune multigene families in mouse vomeronasal sensory neurons. Curr Biol 2003; 13:394–400.
176. Syken J, Shatz CJ. Expression of T cell receptor beta locus in central nervous system neurons. Proc Natl Acad Sci USA 2003;100:13048–13053.
177. Syken J, Grandpre T, Kanold PO, Shatz CJ. PirB restricts ocular-dominance plasticity in visual cortex. Science 2006; 313:1795–1800.
178. Schafer DP, Lehrman EK, Kautzman AG, Koyama R, Mardinly AR, Yamasaki R, et al. Microglia sculpt postnatal neural circuits in an activity and complement-dependent manner. Neuron 2012;74:691–705.
179. Stevens B, Allen NJ, Vazquez LE, Howell GR, Christopherson KS, Nouri N, et al. The classical complement cascade mediates CNS synapse elimination. Cell 2007;131:1164–1178.
180. Wu ZP, Washburn L, Bilousova TV, Boudzinskaia M, Escande-Beillard N, Querubin J, et al. Enhanced neuronal expression of major histocompatibility complex class I leads to aberrations in neurodevelopment and neuror-epair. J Neuroimmunol 2011;232:8–16.
181. Joseph MS, Bilousova T, Zdunowski S, Wu ZP, Middleton B, Boudzinskaia M, et al. Transgenic mice with enhanced neuronal major histocompatibility complex class I expression recover locomotor function better after spinal cord injury. J Neurosci Res 2011;89:365–372.
182. Boulanger LM, Huh GS, Shatz CJ. Neuronal plasticity and cellular immunity: shared molecular mechanisms. Curr Opin Neurobiol 2001;11:568–578.
183. Fourgeaud L, Boulanger LM. Synapse remodeling, compliments of the complement system. Cell 2007;131: 1034–1036.
184. Smith-Garvin JE, Koretzky GA, Jordan MS. T cell activation. Annu Rev Immunol 2009;27:591–619.
185. Kiefer F, Vogel WF, Arnold R. Signal transduction and co-stimulatory pathways. Transpl Immunol 2002;9:69–82.
186. Baniyash M. TCR zeta-chain downregulation: curtailing an excessive inflammatory immune response. Nat Rev Immunol 2004;4:675–687.
187. Shatz CJ. MHC class I: an unexpected role in neuronal plasticity. Neuron 2009;64:40–45.
188. Bosco A, Crish SD, Steele MR, Romero CO, Inman DM, Horner PJ, et al. Early reduction of microglia activation by irradiation in a model of chronic glaucoma. Plos One 2012;7:e43602.
189. Bosco A, Inman DM, Steele MR, Wu G, Soto I, Marsh-Armstrong N, et al. Reduced retina microglial activation and improved optic nerve integrity with minocycline treatment in the DBA/2J mouse model of glaucoma. Invest Ophthalmol Vis Sci 2008;49:1437–1446.
190. Bosco A, Steele MR, Vetter ML. Early microglia activation in a mouse model of chronic glaucoma. J Comp Neurol 2011;519:599–620.

CHAPTER 4

LOCALIZATION AND PHENOTYPE-SPECIFIC EXPRESSION OF RYANODINE CALCIUM RELEASE CHANNELS IN C57BL6 AND DBA/2J MOUSE STRAINS

Wei Huang was the first author of this publication and David Krizaj designed the study. My role in this article involved inducing acute glaucoma in C57BL6 mice with microbead injections, IOP measurement, immunohistochemistry, confocal imaging and contributions to writing the results and methods for Figure 6.

Huang W, Xing W, Ryskamp DA, Punzo C, Križaj D (2011) Localization and phenotype-specific expression of ryanodine calcium release channels in C57BL6 and DBA/2J mouse strains. Experimental Eye Research 93(5):700-709. Reprinted with permission from Experimental Eye Research and Elsevier.

Experimental Eye Research 93 (2011) 700–709

Contents lists available at SciVerse ScienceDirect

Experimental Eye Research

journal homepage: www.elsevier.com/locate/yexer

Localization and phenotype-specific expression of ryanodine calcium release channels in C57BL6 and DBA/2J mouse strains

Wei Huang[a], Wei Xing[a], Daniel A. Ryskamp[a], Claudio Punzo[b], David Križaj[a,c,*]

[a] Department of Ophthalmology & Visual Sciences, John A. Moran Eye Center, University of Utah School of Medicine, Salt Lake City, UT 84132, USA
[b] Department of Ophthalmology, University of Massachusetts Medical School, Worcester, MA 01605, USA
[c] Department of Physiology, University of Utah School of Medicine, Salt Lake City, UT 84132, USA

ARTICLE INFO

Article history:
Received 21 June 2011
Accepted in revised form 4 September 2011
Available online 14 September 2011

Keywords:
calcium
ryanodine receptor
retina
mueller glia
glaucoma
C57BL6
DBA/2J-*Gpnmb*$^{+}$ strain

ABSTRACT

The DBA/2J (D2) and C57BL6 (B6) mouse strains are widely used in research as models for anxiety, addiction and chronic glaucoma. D2, but not B6, animals develop elevated intraocular pressure (IOP) that leads to progressive degeneration of retinal ganglion cell (RGC) axons and perikarya. Here we compare the expression and localization of intracellular ryanodine receptor (RyR) Ca^{2+} store mechanisms in retinas from D2 and B6 animals. A subset of experiments included retinas from D2-*Gpnmb*$^{+}$ mice as strain-specific controls for D2s. RT-PCR analysis showed 6–8 -fold upregulation RyR1, but not RyR2 or RyR3 transcripts, in D2 retinas. The upregulation was more pronounced in D2 retinas categorized as exhibiting moderate or severe glaucoma eyes compared to eyes with no/little glaucoma. In B6 retinas, RyR1 was expressed in neuronal perikarya/processes across all three retinal layers whereas little labeling was observed in astrocyte, microglial or Müller cell processes. In contrast, RyR1 antibodies strongly labeled radial processes of in D2 Müller glia, in which the staining colocalized with the activated glial stress marker GFAP. RyR1 staining in 1 month-old D2-*Gpnmb*$^{+}$ strain resembled expression in B6 retinas whereas moderate RyR1, but not GFAP, localization to Müller glia was observed in 10–12 months – old D2-*Gpnmb*$^{+}$ eyes. Both RyR1-ir and GFAP-ir were augmented in the microbead injection model of acute experimental glaucoma. We conclude that RyR1 exhibits differential expression and localization in two ubiquitously used mouse lines. While RyR1 signals can be regulated in a strain-specific manner, our data also suggest that RyR1 transcription is induced by early glial activation and/or elevation in intraocular pressure.

1. Introduction

It is increasingly evident that glaucoma is a multifactorial disease involving complex interactions between multiple genes, vascular factors, innate and adaptive immune system and environmental factors (Gordon et al., 2002). Many features of the human disease have been replicated in mouse models of chronic glaucoma. The most widely used DBA/2J (D2) strain is characterized by recessive mutations in *Gpnmb* (GpnmbR150X) and *Tyrp1* (*Tyrp1*^{b}) genes which cause an increase in IOP at >6 months (John et al., 1998; Libby et al., 2005). D2 animals consequently express a phenotype that is similar to the chronic age-related glaucoma in humans with increased intraocular pressure (IOP), progressive degeneration of retinal axons, loss of RGC perikarya, glial activation, retinal remodeling and excavation of the optic nerve head (Anderson et al., 2002; Danias et al., 2003; Libby et al., 2005; Soto et al., 2008).

The D2 phenotype includes multiple contributions from genes that are distinct from the two mutations that regulate aqueous outflow in the anterior chamber. For example, the D2 strain varies from the B6 strain that is commonly used as a "wild-type" strain in terms of anxiety, locomotor behavior, visual behavior, hippocampus-dependent learning performance, addiction, water consumption, life span and susceptibilities to a wide variety of stresses (Belzung and Griebel, 2001; Lucki et al., 2001; Puk et al., 2008; Barabas et al., 2011). At least 77 genes and ESTs show >1.5-fold mean increase in brains of adult B6 compared to D2 mice, with particular changes in genes that regulate signaling pathways, gene regulation and metabolism (Misra et al., 2007; Singh et al., 2007). With respect to calcium regulation, B6 and D2 tissues differ in expression of several Ca^{2+}-associated proteins that include ionotropic glutamate receptors (NMDA2B), voltage-operated Ca^{2+}

* Corresponding author. Tel.: +1 801 213 2777; fax: +1 801 587 8314.
E-mail address: david.krizaj@hsc.utah.edu (D. Križaj).

0014-4835/$ – see front matter © 2011 Elsevier Ltd. All rights reserved.
doi:10.1016/j.exer.2011.09.001

channels, calcium/calmodulin-dependent protein kinase II (CamKII), calcineurin phosphatases, inositol triphosphate receptors and a MAP kinase (Esplin et al., 1994; Grice et al., 2007). We focused on ryanodine receptors (RyRs) which play a crucial role in neuronal function as well as in the etiology of neurodegenerative diseases such as Alzheimer, Parkinson's, Huntingdon's diseases and spinocerebellar ataxia (Guo et al., 2011; Kasumu and Bezprozvanny, in press). Ca^{2+} release from ryanodine stores amplifies Ca^{2+}-dependent signals induced by voltage-operated, glutamatergic and purinergic signals resulting in increased excitability of neuronal/glial cells (Nedergaard et al., 2010). Given that ryanodine signaling in optic astrocytes is directly activated by hydrostatic pressure (Mandal et al., 2010) and that D2 animals develop glaucoma following persistent elevation in IOP (John et al., 1998; Libby et al., 2005; Soto et al., 2008), it would seem important to determine whether RyR expression and cellular localization are affected in D2 mice. Because the expression and localization of ryanodine receptor isoforms in the mouse retina are not known, we first compared the abundance of RyR transcripts in B6 and D2 retinas and determined the localization of the two main retinal RyR isoforms in the mouse retina. We also tested the hypothesis that the dramatic phenotype observed in D2 animals derives, in part, from elevation in IOP.

Our data show that the two strains exhibit marked differences in the expression of genes coding for RyR1, but not RyR2 or RyR3, isoforms. The D2 phenotype was associated with a shift in RyR1 expression to activated Müller astroglia. Similar shifts were observed following experimental elevation of IOP, suggesting that RyR signaling might be associated with glial activation in mechanically stressed retinas.

2. Methods

2.1. Animals

Animals were maintained in a pathogen-free facility under a 12-hour light–dark cycle (Utah) and 14 h light/10 h dark cycle (Jackson) with standard rodent chow available *ad libitum*. D2 and D2-*Gpnmb*$^{+}$ mice were obtained from The Jackson Laboratory and/or from Dr. Simon John's (JAX) colony. The D2-*Gpnmb*$^{+}$ mice are homozygous for a wild-type allele of *Gpnmb* on a D2 genetic background. The strain develops iris disease similar to that in D2s but does not develop increased IOP or axonal degeneration (Howell et al., 2007). In contrast, aging D2 animals show progressive loss of RGC markers and loss of RGCs (John et al., 1998; Howell et al., 2007; Barabas et al., 2011). All experiments adhered to the NIH Guide for the Care and Use of Laboratory Animals and the ARVO Statement for the Use of Animals in Ophthalmic and Vision Research and were approved by the Institutional Animal Care and Use Committee at the University of Utah.

2.2. Semiquantitative RT-PCR

Total RNA from retina was extracted with Trizol and total RNA was converted to cDNA using the SuperScript III First-Strand Synthesis kit from Invitrogen. Real-time PCR was performed on a thermocycler (GeneAmp 5700; ABI, Foster City, CA) using Power SYBR Green PCR Master Mix (Applied Biosystems, Foster City, CA) reagents according to the manufacturer's instructions. Table 1 lists the primers used. Two sets of primers were used for identification of the RyR1 isoform. After amplification, the ratio of gene-of-interest mRNA to glyceraldehyde-3-phosphate dehydrogenase (*Gapdh*) reference gene was calculated for each sample. A random sample at in the 1-month cohort was assigned a value of 1 and other values calculated relative to the sample. Every experiment consisted of samples from at least 5 animals, each gene was studied in 3–5 separate experiments.

Table 1
List of forward and reverse primers used for RT-PCR analysis. The RyR1 gene was tested with two separate sets of primers.

Gene	Forward	Reverse
Gapdh	ACT TCA ACA GCA ACT CCC ACT CTT C	GGG TGG TCC AGG GTT TCT TAC TC
RyR1-A	AGT CAA GAC GCT CCG CAC CAT C	GGC TCG TCC TCA TCT TCG CTC TT
RyR1-B	TAC TTC GAC ACA ACC CCA CA	ACA GTC TCC AGC AGG GAA GA
RyR2	CTA CCC GAA CCT CCA GCG ATA CT	GCA AAA GAA GGA GAT GAT GGT GTG
RyR3	ATG AGC CGG ATA TGA AGT GTG ACG A	TGA ATG ATG GCC AGC AAG ATG AC
Brn3a	AGA GAC AGA AGC AGA AGC GGA TGA	GCC CCC AAA TGA GAG CAG AAA CTT
Gfap	GGA CAT CGA GAT CGC CAC CTA CAG	TGA CCT CAC CAT CCCGCA TCT C

2.3. In situ hybridization

In situ hybridization and probe synthesis were performed as described previously (Punzo and Cepko, 2007). Sp6 RNA polymerase was used to generate the probes by sub-cloning part of the coding sequence into pGEMT-Easy (Promega). The forward primer for *RyR1* was: AGAGGGCGATGAAGATGAGAA; reverse primer: AAGATGTCCCCGTGTTTGTC. The forward primer for *RyR2* was AAACACCAGCCTTCGGAGTA; the reverse primer was TAGCCAAA GATGGGAAGGTG (Table 1). For cryosections, the eyes were dissected in PBS (0.1 M Phosphate Buffer solution), fixed in 4% PFA (Paraformaldehyde)/PBS at RT, washed with PBS and equilibrated in 10 min steps of increasing concentrations of sucrose (5–30%). The tissue was embedded in 1:1 mixture of OCT and 30% sucrose in PBS for 15 min and freeze dryed in dry ice/ethanol. For paraffin sections, retinas were fixed for 30 min in 4% PF/PBS at RT, washed with PBS and dehydrated to 100% ethanol using a ladder of increased EtOH concentrations before embedding in 50/50 xylene/paraffin (60 °C; 15 min) and 100% paraffin (4 × 30 min at 60 °C).

2.4. Tonometer measurements

IOP was measured in mice between 10:00 AM and 1:00 PM with the TonoLab rebound tonometer (Colonial Medical Supply, Franconia, NH/Tyolat, Helsinki, Finland). Mice were sedated with intraperitoneal injection of Avertin with final amount calculated by weight (e.g., 0.5 ml for 21–24 g animals). Animals were placed on a jack stand platform and the tonolab was clamped on a ring stand and centered onto the mid-cornea. During measurements animals were neither restrained nor touched. Each eye was measured twenty consecutive times, the highest and lowest values were discarded and the values were averaged. At 1 month, the pooled mean IOP for D2 eyes was not significantly different from B6 eyes (12.80 ± 0.55 vs. 12.08 ± 0.64 mm Hg). At 9 months, IOP levels in D2 eyes were significantly increased with respect to B6 eyes (21.50 ± 1.58 vs. 11.0 ± 0.66 mm Hg, $N = 15$; $P < 0.001$; Mann–Whitney unpaired test).

2.5. Immunohistochemistry

Immunostaining followed previously described protocols (Rentería et al., 2005; Ryskamp et al., 2011). Fixed transverse sections of the retina were washed in PBS for 15 min before permeabilization and blocking with 0.5% Triton X-100 and 10% goat

serum. The slides were incubated with primary antibodies in the blocking solution for 4 h at RT, washed twice in PBS and subsequently incubated for 4 h with secondary antibodies. The primary antibodies utilized in the study were anti-RyR1 (rabbit polyclonal; 1:100, Millipore/Chemicon AB9078, Temecula, CA) raised against a peptide from human RyR1; as per manufacturers datasheet, in Western blots the antibody produces a band at the appropriate M.W. (also, see Medina-Ortiz et al., 2007). The anti-RyR2 (rabbit polyclonal; Millipore/Chemicon AB9080) antibody was derived from a synthetic peptide based on human protein and has been characterized previously (García-Pérez et al., 2008). The anti-GFAP (mouse monoclonal; 1:500; Sigma); anti-glutamine synthetase (mouse monoclonal; 1:1000; BD Biosciences) and anti-Brn3a (mouse monoclonal; 1:100; Santa Cruz Biotechnology) have been well characterized. The secondary antibodies were goat anti-mouse or goat anti-rabbit IgG (H + L) conjugated to fluorophores (Alexa 488 and Alexa 594; Invitrogen), diluted 1:500 or 1:1000, goat anti-mouse Cy3 from Jackson ImmunoResearch at 1:1000 or Mac1-CD11b-AlexaFluor 488 from BD Pharmingen at 1:200. After incubation, sections on slides were washed in PBS and mounted using Vectashield (Vector, Burlingame, CA). Negative controls without a primary antibody showed no staining. Immunofluorescent and differential interference contrast (DIC) images were acquired at depths of 12 bits on a confocal microscope (Zeiss LSM 510) using 488 nm Ar (10%) and 594 nm He/Ne (100%) lines for fluorophore excitation, suitable band-pass or long-pass filters for emission detection and 40×/1.2 NA oil objectives. The analysis was performed in sections obtained from at least 3 animals at each age examined.

2.6. Microbead injection

The injection protocol roughly followed the procedure described in Chen et al. (2011). During the week prior to microbead injection, IOP was measured two or three times to establish a baseline. In preparation for the microbead injection procedure, pupils were dilated with 1% tropicamide (Bausch & Lomb, Rochester, NY) and mice were deeply sedated with an intraperitoneal injection of Ketamine/Xylazine (90 mg/10 mg per kg body weight). Heat pads were used to maintain body temperature. 0.5% proparacaine (Bausch & Lomb) was applied to the eyes for topical analgesia. The cornea was punctured with a sharp needle and some of the aqueous humor was gently drained. Using a 5.0 μl syringe (Hamilton; Reno, NV), 2 μl of a microbead solution (polystyrene FluoSpheres with diameter of 15 μm at a concentration of 1×10^7 beads/ml in PBS; Invitrogen) was slowly injected into the anterior chamber of a randomly selected eye. 2 μl of PBS was injected into the other eye of each mouse as an internal control. Injected eyes were treated with 0.5% erythromycin (Bausch & Lomb) and mice were closely monitored until consciousness was regained. Mice were allowed to recover for 72 h before biweekly IOP measurements resumed. Of 10 eyes injected with microbeads, 3 showed a persistent elevation in IOP compared to PBS-injected contralateral controls. These three were used for data shown in Fig. 7.

2.7. Axon damage assessment

The severity of glaucoma was assessed in PPD-labeled nerves using an established grading scheme (Howell et al., 2007). Eyes were classified with no or early (no detectable axon damage/loss compared to B6), moderate (10–50% damage) or severe (>50% damage) glaucoma. The total number of examined retinas was No/Early glaucoma (9 months, $N = 8$; 12–15 months, $N = 3$); Moderate (9 months, $N = 3$; 12–15 months, $N = 3$), Severe glaucoma (9 months, $N = 2$; 12 months, $N = 4$; 15 months, $N = 4$).

3. Results

In this study, we employed two strategies to gain deeper insight into the expression and distribution of intracellular transport mechanisms in the D2 retina. Semi-quantitative reverse transcription (RT)-PCR was used to compare total retinal mRNA content of transcripts coding for ryanodine receptor Ca^{2+} release channels in B6 and D2 mice. In the second approach, *in situ* hybridization and immunohistochemistry were used to identify the retinal localization of RyR1, the intracellular Ca^{2+} release channel that exhibited the most prominent upregulation of transcription in D2 retinas.

3.1. RyR1 signals in the B6 retina

Real-time PCR on cDNAs isolated from intact tissue showed that mRNA for RyR isoform 1 is transcribed in the B6 strain (Fig. 1A). The *RyR1* antisense probe showed prominent signals within the inner nuclear (INL) and ganglion cell layers (RGCL) (Fig. 1B).

Broadly consistent with *in situ* hybridization results, RyR1 protein was localized across all retinal strata, along neuronal cell bodies in INL and RGCL and in dendrites and axons within the IPL and NFL (Fig. 1C). While RyR1 signals were never observed in outer segments (OSs) of rods or cones, RyR1 immunoreactivity (ir) was more pronounced in the ellipsoid/inner segment region (Fig. 1C, arrowheads) and was also observed in the ONL. RyR1-ir was stronger in the IPL sublamina a compared to sublamina b, suggesting that RyR1-mediated Ca^{2+} release could be disproportionately associated with OFF retinal signaling. RyR1 staining colocalized with the RGC marker Brn3a (Fig. 1D). Consistent with previous observations in spinal motoneurons (Ouardouz et al., 2003), RyR1 signals were observed in the nerve fiber layer proximal to RGC somata and in unmyelinated axonal projections entering the ONH (Fig. 1C and D). Staining of the astrocyte-rich lamina that represents the transition zone from the ONH to the optic nerve was lower compared to the NFL, the proximal ONH and the myelinated portion of the nerve vitread from the retina (Figs. 1C and 2A). Axonal staining in B6 retinas was distinct from glutamine synthetase (GS)- and Glial Fibrillary Acidic Protein (GFAP) signals localized to Müller cell and astrocyte processes at the ILM (Fig. 1E–G). Given the recent demonstration of the protective role of complement inhibition in glaucomatous degeneration (Howell et al., 2011) we also tested whether RyR1s are localized to retinal microglial cells. However, no colocalization was observed between RyR1 and Mac-1:AlexaFluor-488 immunolabeled cells residing in the IPL (Fig. 1H).

B6 sections almost never evinced GFAP-ir in the IPL/INL or the ONH whereas the RyR1 antibody strongly labeled the NFL entering the optic cup (arrowheads in 2A) and fibers within the optic nerve. Accordingly, little colocalization with glutamine synthetase or GFAP was observed in the ONH (Fig. 2B). RyR1 labeling of the astrocyte-rich prelaminar region was always weak.

3.2. RyR1 signals in D2 and D2-Gpnmb$^+$ retinas

D2 retinas expressed RyR1 mRNA (Fig. 3A) which was localized mainly to the INL (Fig. 3B). Retinas with severe glaucoma exhibited a trend towards higher RyR1 mRNA content compared to retinas with no or early glaucoma, almost reaching significance with respect to Severe vs. No/Early glaucoma (Fig. 3C).

In contrast to the highly uniform and reproducible immunostaining pattern in B6 retinas, RyR1 signals in D2 retinas were variable in terms of neuronal vs. glial expression. The anti-RyR1

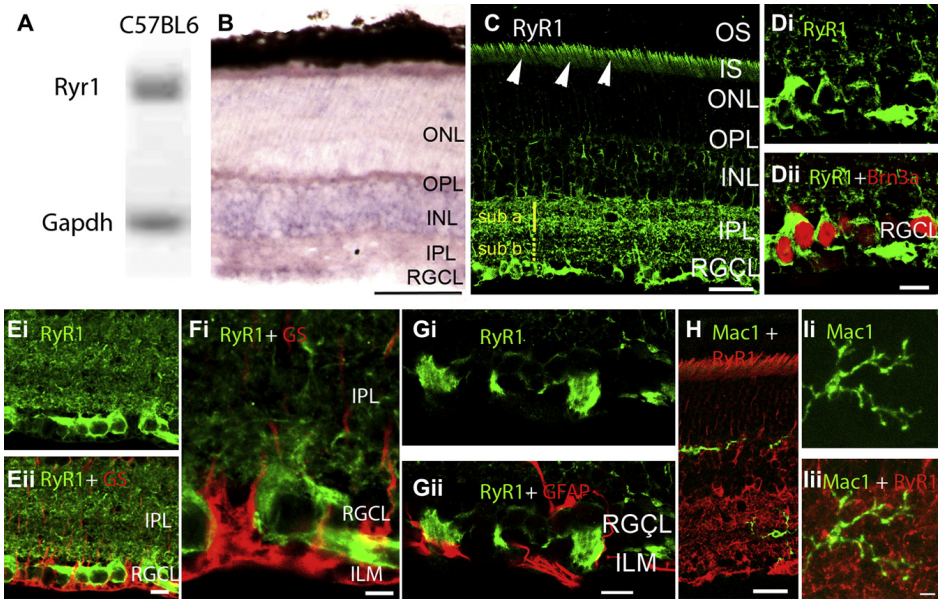

Fig. 1. RyR1 gene expression, mRNA and protein distribution in the B6 retina. (A) Amplicons for *RyR1* and glyceraldehyde-3-phosphate dehydrogenase (*Gapdh*) isolated from the total retinal pool and separated on a 20% agarose gel. (B) In situ hybridization analysis of 12 month-old B6 retinas exposed to *RyR1* antisense probes. The reaction product is localized to perikarya in INL and RGC layers. Weak labeling is seen in the ONL, with the labeling of rod inner segments by the antisense probe. Radial processes spanning the retina are weakly labeled. Scale bar = 50 μm (C) RyR1 localization in an adult (9 month-old) B6 retina. The RyR1 antibody labels rod ellipsoids and inner segments (arrowheads), perikarya within the INL, RGCL and the IPL; RyR1-ir in the sublamina a is more pronounced compared to sublamina b. Scale bar = 20 μm (D) 12 months-old retina. RyR1 signal in the RGCL colocalizes with the RGC marker Brn3a. (E–G) 15 months-old retina. RyR1 signal in the RGCL and ILM shows little colocalization with glutamine synthetase (GS) or GFAP. Scale bar = 10 μm (H & I) RyR1-ir does not colocalize with the microglial marker Mac-1. Scale bar = 20 μm in H, 10 μm in I.

antibody labeled thin radial processes in the inner retina of 9 month-old D2 animals with no detectable axonal loss ("no or early glaucoma") (arrowheads; Fig. 3Di). Such RyR1-ir processes, which were rarely labeled in B6 retinas, extended from the ILM towards the OPL. These signals colocalized with glutamine synthetase (Fig. 3H) and GFAP (Fig. 3D and F), an intermediate filament which represents an early glial marker for retinal stress and is upregulated in Müller cells following acute or chronic elevation in IOP (Lam et al., 2003; Xue et al., 2006). The intensity of RyR1-ir and GFAP-ir in radial processes appeared to be accentuated in retinas

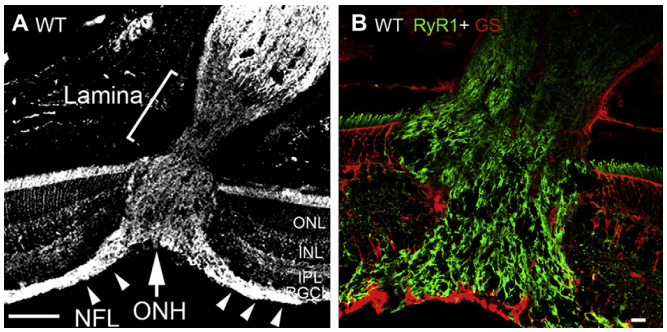

Fig. 2. B6 retinas, RyR1 expression in the optic nerve head. (A) The RyR1 antibody labels the retinal nerve fiber layer (NFL; arrowheads), the ONH (arrow) and the myelinated portion of the optic nerve whereas RyR1 expression in the astrocyte lamina is modest. Scale bar = 100 μm. (B) Double labeling for RyR1 and GS shows little GS signal within the ONH of the B6 retina. Scale bar = 10 μm.

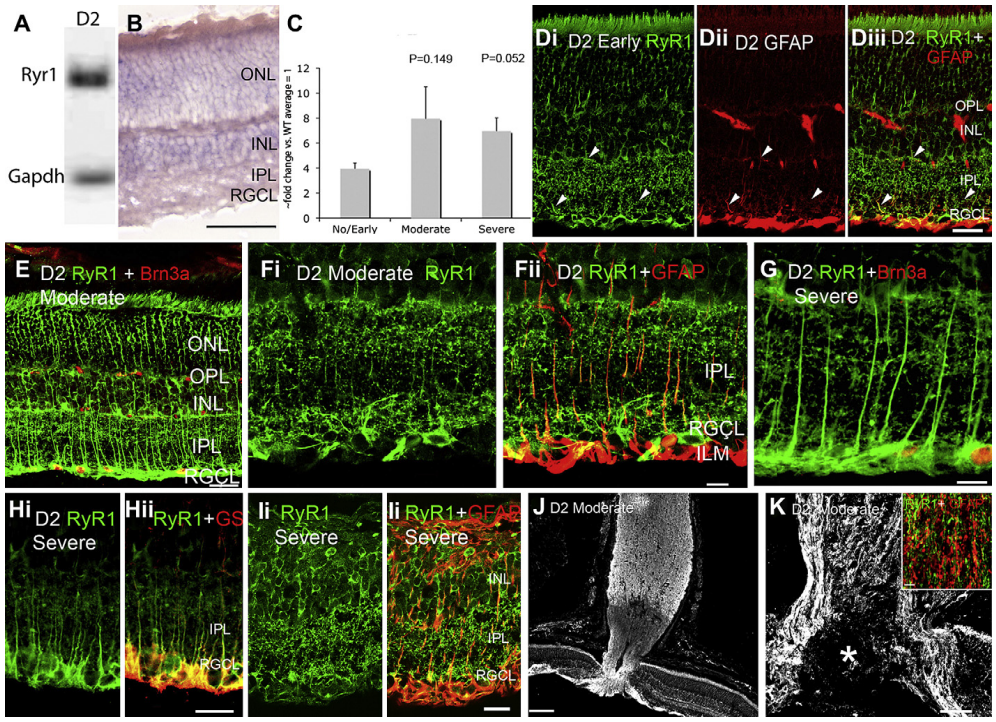

Fig. 3. RyR1 expression in D2 retina. (A) PCR products for *RyR1* and *Gapdh* mRNA from the total retinal pool. (B) D2 retinas labeled by the *RyR1* antisense probe. The reaction product is localized to perikarya in INL and RGC layers. The antisense probe weakly labels the ONL, rod inner segments and radial processes spanning the retina. Scale bar = 50 μm (C) RT-PCR for *RyR1*, expressed as ~fold change with respect to age-matched B6 retinas. (D) RyR1 and GFAP localization in No/Early glaucoma D2 retina. Some, but not all, radial RyR1-ir processes expressed GFAP (arrowheads). (E) Moderate glaucoma retina, double labeled for RyR1 and BRN3a, a Z-stack from 12 consecutive sections. Scale bar = 20 μm. (F) Moderate glaucoma. There is an upregulation and partial colocalization of RyR1- and GFAP-ir processes in the IPL and the ILM/RGCL. Scale bar = 20 μm. (G) Severe glaucoma, double labeled for RyR1 and Brn3a. Scale bar = 10 μm. (H) Severe glaucoma, retina labeled for RyR1 and glutamine synthetase. Scale bar = 20 μm. (J) Severe glaucoma in a 15 month-old D2 retina exhibiting glial hypertrophy and retinal remodeling. Scale bar = 10 μm (J & K) ONH regions from two moderate glaucoma eyes. (J) The RyR1 antibody labels the NFL, ONH and the myelinated region of the optic nerve. Scale bar = 100 μm. (K) Moderate glaucoma. RyR1 signal surrounds the excavated region within the ONH (asterisk). *Inset:* Severe glaucoma. Double labeling of the glial laminar region in the optic nerve shows modest colocalization between RyR1 and GFAP signals. Scale bar = 10 μm.

classified into 'moderate' (N = 6) and 'severe' (N = 12) axonal degeneration categories (Fig. 3E–I). In extreme cases of severe glaucoma, retinas exhibited characteristics typical of Phase 3 'remodeling' (Marc et al., 2003) with disappearance of RGC/displaced amacrine perikarya, depletion of the INL and hypertrophy of glial processes which encased the remaining neuronal perikarya and reinforced both retinal laminas (OLM & ILM; Fig. 3I). In such remodeled retinas, glial processes appeared to lose the RyR1 signal (Fig. 3Ii and ii), however, the sample size was limited (N = 2 animals at 15 months of age with severe glial hypertrophy). Intensity of RyR1-ir in radial processes varied between individual retinas within each category; panels E and F display retinal sections from two eyes with moderate glaucoma that exhibited different amounts of RyR1 signal.

RyR1 staining in D2 eyes was emphasized in the ONH tissue surrounding the 'excavated' area in moderate and severe glaucomatous eyes (asterisk in Fig. 3K). We also investigated whether RyR1 signals in glaucomatous eyes are upregulated in astrocytes in addition to Müller glia. As shown in the inset of Fig. 3K, little colocalization was observed between the astrocyte marker and RyR1-immunopositive nerve processes within the optic lamina.

The appropriate control strain for D2 animals are D2-*Gpnmb*$^+$ mice which are homozygous for a wild-type allele of *Gpnmb* on the D2 genetic background. Similar to D2s, D2-*Gpnmb*$^+$ mice develop iris disease but do not exhibit increased IOP or axonal degeneration (Howell et al., 2007). Localization of RyR1 mRNA in D2-*Gpnmb*$^+$ retinas was similar to signals observed in B6 and D2 retinas (Fig. 4B). Likewise, the pattern of RyR1-ir and GFAP-ir in 1 month-old (N = 3) and a subset of 10–12 month-old D2 -*Gpnmb*$^+$ retinas resembled the staining observed in B6 retinas (N = 4/10) (Fig. 4C and D). However, the majority of 10–12 month-old D2 -*Gpnmb*$^+$ retinal samples (6/10 animals) exhibited RyR1-ir within processes that traversed the INL. These processes were GFAP-immunonegative (data not shown) but colocalized with the Müller glial marker glutamine synthetase (Fig. 4E–F). The intensity of RyR1-ir in such D2-*Gpnmb*$^+$ retinas was similar to signals seen in No/Early glaucoma D2 retinas (Fig. 3D). In contrast to D2 tissue, however, GFAP expression mirrored B6 signals in the majority of 10–12 month-old

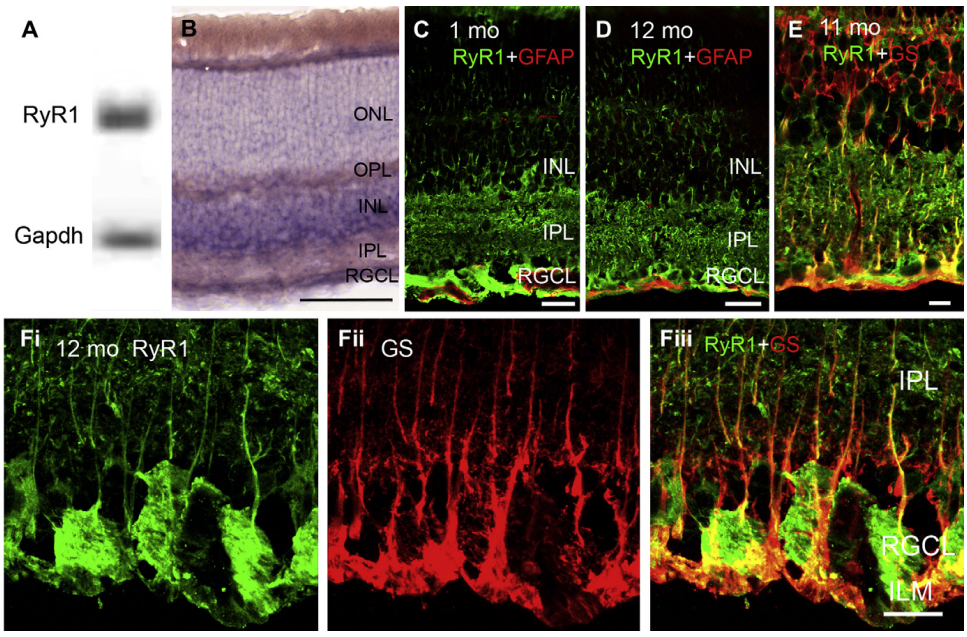

Fig. 4. RyR1 expression in D2-*Gpnmb*$^{+}$ retinas. (A) PCR products for *RyR1* and *Gapdh* mRNA from the total retinal pool. (B) In situ hybridization signals in D2-*Gpnmb*$^{+}$ retinas show similar localization to B6 and D2 retinas. Scale bar = 50 μm (C & D) 1 month and 12 months-old retinas, double labeled for RyR1 and GFAP show little colocalization. Scale bars = 20 μm (E–F) A subset of 11–12 months-old D2-*Gpnmb*$^{+}$ retinas showed RyR1-ir signals within the ILM and IPL regions. These processes colocalized with glutamine synthetase. Scale bars = 10 μm.

D2-*Gpnmb*$^{+}$ eyes ($N = 8/10$; Fig. 4D) whereas GFAP-ir processes extending into the INL were observed within circumscribed patches of two D2-*Gpnmb*$^{+}$ retinas (data not shown). With respect to RyR1 staining, differences between RyR1 staining in 10–12 months-old D2-*Gpnmb*$^{+}$ animals could reflect different animal subpopulations and/or differential responses to the loss of *Tyrp1*^{b}. Consistent with the latter hypothesis that suggests aging-dependent stress associated with iris disease, RyR1-ir was more pronounced in Müller cells from adult D2-*Gpnmb*$^{+}$ samples compared to 1 month-old eyes.

3.3. *RyR1 mRNA is upregulated in D2 retinas*

The RyR family is comprised of 3 isoforms (RyR1-3) that are ubiquitously expressed across neurons and glia. Real-time PCR on cDNAs isolated from intact B6 and D2 tissue showed that mRNAs for all 3 RyR isoforms are transcribed in both strains. *RyR1* mRNA levels in D2 retinas were consistently higher compared to B6 control retinas (Fig. 1). The upregulation was observed at 1 month after birth (6.94 ± 1.07 −fold increase over WT; $P < 0.01$; Mann–Whitney unpaired test) and persisted up to 15 months, the most advanced age studied (5.33 ± 1.01-fold increase; $P < 0.01$, Mann–Whitney unpaired test) (Fig. 1A). To determine whether *RyR1* upregulation was a strain-specific, was associated with elevated IOP or loss of the *Tyrp1*^{b} gene, we analyzed two time points in retinas from D2-*Gpnmb*$^{+}$ mice. RyR1 expression in D2-*Gpnmb*$^{+}$ retinas ($N = 4$) was not significantly different from B6 retinas at 1 month, but showed an increase at 5 months that was significant compared to B6 ($N = 8$) and D2 ($N = 6$) eyes ($P = 0.0003$; one-way ANOVA). Thus, at least in 1 month-old animals, transcription of *RyR1* is not affected by general strain-specific features and the differences must lie downstream of the mutant *Gpnmb* gene whereas RyR1 mRNA levels may be elevated in older animals, possibly reflecting a strain-dependent or *Tyrp1*^{b}-dependent phenotype.

3.4. *RyR1 is localized to glia in an acute glaucoma model*

We next tested whether upregulation of RyR1 signals within glial cells was an IOP-dependent process. IOP in B6 eyes was elevated by injection of Alexa488 nm-conjugated microbeads (Chen et al., 2011). Fourteen days following injection, the IOP was elevated in injected eyes from 3/10 animals. In these eyes, the IOP was 23.57 ± 2.96 mm Hg compared to 12.93 ± 1.40 mm Hg in PBS-injected contralateral eyes ($N = 3$; $P = 0.0047$). GFAP immunoreactivity in Müller cells was enhanced in all microbead-injected eyes that exhibited elevated IOP (Fig. 6B), consistent with increased resistance to mechanical stress (Bringmann et al., 2009). In contrast to GFAP signals in D2 retinas which often showed patches of strong GFAP-ir interspersed with weaker staining, GFAP-ir in eyes exposed to experimentally-induced IOP elevations appeared to be uniform across the retina. Colocalization between GFAP and RyR1 signals was observed in the proximal retina (Fig. 6B), suggesting that glial activation in this glaucoma model is also associated with increased expression of RyR1. Taken together, this data shows that development of glaucoma is associated with isoform-specific changes in expression of intracellular Ca^{2+} release channels.

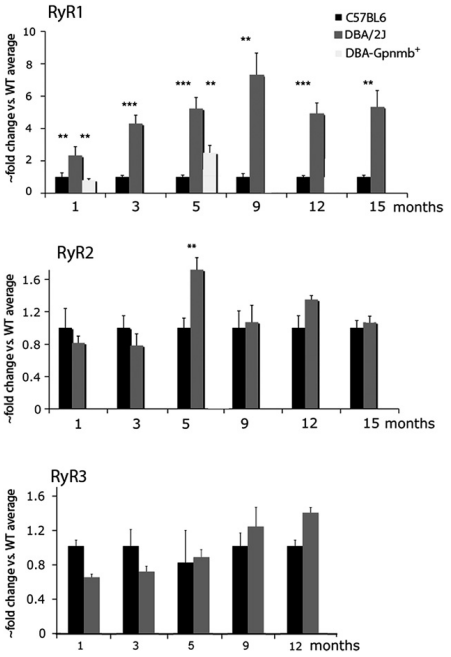

Fig. 5. RyR gene expression in B6 and D2 retinas. (A) RT-PCR. RyR1 transcripts are strongly upregulated in D2 compared to B6 retinas. Analysis of D2-*Gpnmb*$^{+}$ samples shows no difference from B6 expression at 1 month but a significant upregulation at 5 months. (B & C) RyR2 and RyR3 mRNA levels show no consistent differences between B6 and D2 retinas.

3.5. Expression and localization of the RyR2 isoform is unchanged in the D2 retina

The antisense riboprobe localized RyR2 transcripts to INL, RGCL and ONL regions (Fig. 7B). Similar to previously reported staining in the rabbit (Shoshan-Barmatz et al., 2007), RyR2 signals in the mouse were observed across all retinal layers with a predominant labeling of Brn3a-immunopositive perikarya in the RGCL and the nerve fiber layer (Fig. 7C and H). Localization of RyR2 in D2 retinas was similar to the localization observed in B6 eyes (Fig. 7E–I). RyR2 staining in D2 retinas did not overlap with glutamine synthetase-ir processes in the ONL (Fig. 7F) or GFAP-ir in the IPL (Fig. 7E), indicating low levels of RyR2 expression in activated Müller glia. At high confocal gains, weakly labeled RyR2-ir signals that were difficult to distinguish from background labeling were occasionally observed in the IPL (Fig. 7I). This data suggests that RyR2 in the mouse retina is a predominantly neuronal isoform.

In contrast to *RyR1*, expression of the *RyR2* and RyR3 genes was relatively unchanged between 1 month and 15 month-old retinas of B6 and D2 eyes (Fig. 5B & C) excepting a transient increase that was measured for RyR2 at 5 months (1.72 ± 0.15 -fold; $N = 3$; $P < 0.001$; Kruskal–Wallis nonparametric ANOVA). We also compared expression of RyR2 and RyR2 genes in 5 month-old D2-*Gpnmb*$^{+}$ retinas ($N = 4$ for each strain) and observed no significant differences in expression for RyR2 ($P = 0.3418$, one-way ANOVA) or RyR3 ($P = 0.7816$; one-way ANOVA).

4. Discussion

In this paper we determined the localization of RyR1 and RyR2 channels in the mouse retina and compared their expression between widely used “wild-type” B6 and “glaucoma model” D2 mouse strains. We show that expression and localization of RyR1, but not RyR2, isoforms exhibit both strain-specific and IOP-dependent features, suggesting that RyRs contribute to pathological remodeling of neuronal-glial interfaces in chronic glaucoma.

RyR1 riboprobes and anti-RyR1 antibodies labeled neuronal perikarya together with cellular processes. This pattern of RyR1 immunoreactivity in the B6 mouse was largely consistent with previously reported data from the rabbit retina (Shoshan-Barmatz et al., 2007). In contrast to the rabbit in which the RyR1 antibody labeled the outer segment, RyR1 and RyR2 signals in mouse photoreceptors were mainly confined to the ER-rich inner segment and cell body regions. Thus, these channels are likely to participate in the well-known feedback between voltage-operated channels, ER and mitochondria (Križaj et al., 2003). Another interesting feature of RyR1 immunoreactivity in the B6 mouse retina was the consistently stronger staining of the IPL sublamina b compared to the sublamina a, possibly suggesting a more prominent role for Ca^{2+}-induced Ca^{2+} release (CICR) in the retinal OFF pathway.

Retinal RyR1 mRNA content was increased ~2.5-fold in 1 month-old D2 compared to B6 retinas, preceding the onset of iridocorneal angle closure, IOP elevation and degeneration of RGC axons (John et al., 1998; Danias et al., 2003; Libby et al., 2005; Inman and Horner, 2007). This effect was not observed in previous microarray studies of retinal gene expression, most likely because RT-PCR is more sensitive for detecting changes in gene expression (Steele et al., 2006; Guo et al., 1999); however, at least one study identified several genes associated with voltage-operated Ca^{2+} entry and ER signaling which could participate in CICR (Panagis et al., 2010). RyR1 upregulation in D2 retinas coincided with increased levels of GFAP and early glial activation, which precede the onset of increased IOP by several months (Inman and Horner, 2007; Bosco et al., 2011). Several pieces of evidence suggest that RyR1 expression could play a role in the pathogenesis of glaucoma: (1) There was a consistent trend towards higher RyR1 mRNA transcript content in retinas categorized as expressing moderate/severe glaucoma compared to no/early glaucoma; (2) The abundance of RyR1 mRNA in D2 retinas was higher than in D2-*Gpnmb*$^{+}$ retinas; (3) The intensity of RyR1 signals in Müller glia coincided with the severity of glaucoma; and (4) The phenotype of retinas with experimentally-induced IOP elevations retinas was similar to the moderate/severe glaucoma phenotype in D2 retinas.

Given that the onset of RyR1 upregulation in D2 eyes coincided with appearance of GFAP signals in Müller glia, the regulation of the RyR1 gene is likely to be associated with activation of Muller glia rather than RGC death. Müller cells are in a good topographic position to be the first retinal cell type to sense and respond to changes in IOP through ER-rich endfeet which transduce mechanical stimulation through regenerative [Ca^{2+}] increases (Keirstead and Miller, 1995; Newman, 2001; Li et al., 2001). It is unclear whether Müller glial RyR channels are directly activated by hydrostatic pressure as reported for optic nerve astrocytes (e.g., Mandal et al., 2010) or by Ca^{2+} influx through stretch- and pressure-sensitive plasma membrane channels (Puro, 1991; Lindqvist et al., 2010; Ryskamp et al., 2011). In either case, the astroglial response to mechanical and neurochemical stress is likely to include augmented CICR. Intracellular Ca^{2+} release channels tend to malfunction at early stages of neurodegeneration (Nedergaard et al., 2010) and it is therefore not inconceivable that suppression of RyR-mediated amplification of intracellular Ca^{2+} signals will be protective with respect to glial activation and gliotic

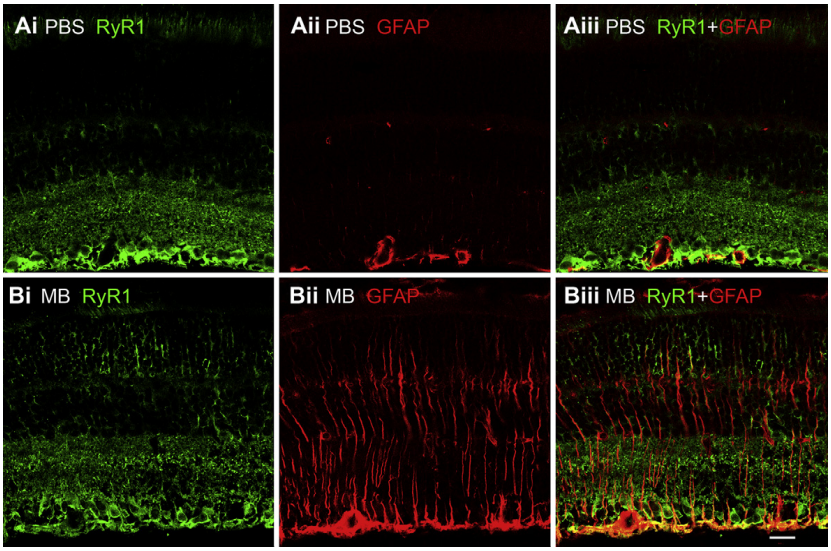

Fig. 6. Acute glaucoma model. B6 eyes were injected with PBS (A) or microbeads (B) and colabeled with RyR1 and GFAP antibodies. Microbead-injected eyes exhibited prominent GFAP-ir which showed partial colocalization with RyR1. In contrast, no colocalization was observed in sham controls.

remodeling observed in retinal ischemia, diabetic retinopathy and/or glaucoma (Marc et al., 2003; see also Frandsen and Schousboe, 1991; Niebauer and Gruenthal, 1999; Popescu et al., 2002; Stirling and Stys, 2010; Kasumu and Bezprozvanny, in press).

The increase in the expression of Müller cell RyRs fits the general context of upregulated Ca^{2+}-dependent signal transduction pathways in D2 retinas (reviewed in Whitmore et al., 2005; Crish and Calkins, 2011), early Müller cell activation in D2 retinas

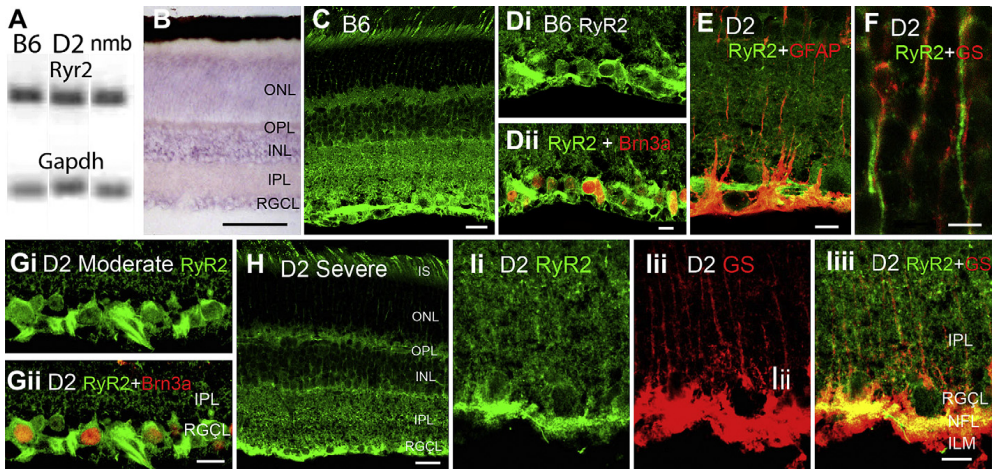

Fig. 7. RyR1 expression and localization in B6m D2 and D2-*Gpnmb*$^{+}$ retinas. (A) PCR amplicons for *RyR2* and *Gapdh*. (B) ISH for *RyR2*. The reaction product is localized to perikarya in INL, RGCL and distal ONL. Scale bar = 50 μm (C & D) RyR2 immunolocalization in the adult B6 retina. The RyR2 antibody labels all retinal layers, with a prominent signal in the RGCL. (E–I) D2 retinas. (E) Inner retina. Double labeling for RyR2 and GFAP shows little colocalization. Scale bar = 10 μm. (F) Outer retina. Double labeling for RyR2 and glutamine synthetase in the ONL. RyR2-ir photoreceptor processes do not colocalize with radial processes of GS-ir Müller cells. Scale bar = 5 μm (Gi & ii) Moderate glaucoma, double labeling for RyR2 and Brn3a. The RyR2 antibody labels cell bodies of RGCs (arrowheads) and axonal processes in the NFL (arrow). Scale bar = 10 μm. (H) Severe glaucoma. Scale bar = 20 μm (Ii-iii) Severe glaucoma. Double labeling for RyR2 and GS shows little colocalization in the IPL. Scale bar = 10 μm.

(Inman and Horner, 2007), augmented neuronal excitability and susceptibility to stress in D2 animals (Esplin et al., 1994) and the increasingly recognized role of glial RyRs in axonal injury (Stirling and Stys, 2010). B6 and D2 mouse strains exhibit numerous differences in biochemistry, physiology and behavior, including higher levels of angiotensin AT1 receptors, GABA receptor/channels, endothelin and complement signaling in D2 animals (DuBois et al., 2006; Golding et al., 2011; Howell et al., 2011), lower levels of protein kinase C and COMT (Bowers et al., 1995; Grice et al., 2007) and differential expression of NMDA receptors, voltage-operated Ca^{2+} channels and calcineurin (Esplin et al., 1994; Grice et al., 2007).

However, our data argue against a simple glaucoma vs. non-glaucoma dichotomy of retinal RyR1 and GFAP expression. The early upregulation of RyR1, *Gfap* and microglial markers in D2 retinas (Inman and Horner, 2007) suggests that at least part of the RyR1 expression phenotype might be derived from *Gpnmb* loss of function rather than glaucoma per se. This conjecture is supported by the observation that RyR1 mRNA levels were elevated in D2 animals that had not (yet) exhibited glaucomatous RGC degeneration. Furthermore, the expression pattern of RyR1 signals in a subset of adult D2-*Gpnmb*$^{+}$ mice suggests that their retinas differ from both B6 and D2 animals. In particular, RyR1 signals that were observed in some GFAP-immunonegative D2-*Gpnmb*$^{+}$ Müller cells indicate that the RyR1 gene may be expressed in the absence of glial activation. Consistent with our observations, Porciatti et al. (2010) have recently shown that B6 and D2-*Gpnmb*$^{+}$ eyes differentially respond to spatial contrast, manifesting differential strain-specific organization of inner retinal circuits. As expected, contrast gain control mechanisms also differed between B6 vs. D2, and D2 vs. D2-*Gpnmb*$^{+}$ eyes (Porciatti et al., 2010). It remains to be determined whether moderate RyR1 expression in Müller cells is associated with the D2 phenotype or whether the RyR1 gene is regulated by the mild IOP increase and iris disease observed in D2-*Gpnmb*$^{+}$ animals (Howell et al., 2007).

In contrast to consistent upregulation of RyR1, expression or localization of RyR2, the main neuronal and retinal isoform, did not change in D2 retinas. Likewise, RyR3, typically considered an embryonic/neonatal isoform expressed at low levels in non-neuronal tissues or co-expressed with RyR2 (Bertocchini et al., 1997), showed no changes in mRNA transcript levels in D2 animals (Fig. 7). We conclude that retinal intracellular Ca^{2+} release channels express plasticity in terms of isoform-specificity, transcription and localization. RyR1 expression and localization is highly sensitive to genetic and environmental influences that include the strain, iris disease, retinal gliosis and acute or chronic changes in IOP.

Acknowledgements

The work was supported by the National Institutes of Health (RO1EY13870, T32DC008553, P30EY014800), The Foundation Fighting Blindness, Knights Templar Eye Foundation, Moran TIGER award and by the unrestricted grant from Research to Prevent Blindness to the Moran Eye Center at the University of Utah. We thank Drs. Gareth Howell and Simon John (Jackson Labs and HHMI) for generously providing D2 and D2-*Gpnmb*$^{+}$ founder mice, for help in classification of D2 eyes and for illuminating discussions. We also thank Dr. Jessica Li (University of Utah) for teaching us to perform retinal microinjections.

References

Anderson, M.G., Smith, R.S., Hawes, N.L., Zabaleta, A., Chang, B., Wiggs, J.L., John, S.W., 2002. Mutations in genes encoding melanosomal proteins cause pigmentary glaucoma in D2 mice. Nat. Genet. 30 (1), 81–85.

Barabas, P., Huang, W., Chen, H., Koehler, C.L., Howell, G., John, S.W., Tian, N., Rentería, R.C., Križaj, D., 2011. Missing optomotor head-turning reflex in the DBA/2J mouse. Invest. Ophthalmol. Vis. Sci. 52, 6766–6773.

Belzung, C., Griebel, G., 2001. Measuring normal and pathological anxiety-like behaviour in mice: a review. Behav. Brain Res. 125 (1–2), 141–149.

Bertocchini, F., Ovitt, C.E., Conti, A., Barone, V., Schöler, H.R., Bottinelli, R., Reggiani, C., Sorrentino, V., 1997. Requirement for the ryanodine receptor type 3 for efficient contraction in neonatal skeletal muscles. EMBO J. 16, 6956–6963.

Bosco, A., Steele, M.R., Vetter, M.L., 2011. Early microglia activation in a mouse model of chronic glaucoma. J. Comp. Neurol. 519, 599–620.

Bowers, B.J., Christensen, S.C., Pauley, J.R., Paylor, R., Yuva, L., Dunbar, S.E., Wehner, J.M., 1995. Protein and molecular characterization of hippocampal protein kinase C in C57BL/6 and DBA/2 mice. J. Neurochem. 64, 2737–2746.

Bringmann, A., Iandiev, I., Pannicke, T., Wurm, A., Hollborn, M., Wiedemann, P., Osborne, N.N., Reichenbach, A., 2009. Cellular signaling and factors involved in Müller cell gliosis: neuroprotective and detrimental effects. Prog. Retin Eye Res. 28, 423–451.

Chen, H., Wei, X., Cho, K.S., Chen, G., Sappington, R., Calkins, D.J., Chen, D.F., 2011. Optic neuropathy due to microbead-induced elevated intraocular pressure in the mouse. Invest. Ophthalmol. Vis Sci. 52, 36–44.

Crish, S.D., Calkins, D.J., 2011. Neurodegeneration in glaucoma: progression and calcium-dependent intracellular mechanisms. Neuroscience 176, 1–11.

Danias, J., Lee, K.C., Zamora, M.F., Chen, B., Shen, F., Filippopoulos, T., Su, Y., Goldblum, D., Podos, S.M., Mittag, T., 2003. Quantitative analysis of retinal ganglion cell (RGC) loss in aging DBA/2NNia glaucomatous mice: comparison with RGC loss in aging C57/BL6 mice. Invest. Ophthalmol. Vis. Sci. 44, 5151–5162.

DuBois, D.W., Perlegas, A., Floyd, D.W., Weiner, J.L., McCool, B.A., 2006. Distinct functional characteristics of the lateral/basolateral amygdala GABAergic system in C57BL/6J and DBA/2J mice. J. Pharmacol. Exp. Ther. 318, 629–640.

Esplin, M.S., Abbott, J.R., Smart, M.L., Burroughs, A.F., Frandsen, T.C., Litzinger, M.J., 1994. Voltage-sensitive calcium channel development in epileptic DBA/2J mice suggests altered presynaptic function. Epilepsia 35, 911–914.

Frandsen, A., Schousboe, A., 1991. Dantrolene prevents glutamate cytotoxicity and Ca^{2+} release from intracellular stores in cultured cerebral cortical neurons. J. Neurochem. 56, 1075–1078.

García-Pérez, C., Hajnóczky, G., Csordás, G., 2008. Physical coupling supports the local Ca^{2+} transfer between sarcoplasmic reticulum subdomains and the mitochondria in heart muscle. J. Biol. Chem. 283, 32771–32780.

Golding, B.J., Overall, A.D., Gard, P.R., 2011. Strain differences and the role of AT(1) receptor expression in anxiety. Int. J. Mol. Epidemiol. Genet. 2, 51–55.

Gordon, M.O., Beiser, J.A., Brandt, J.D., Heuer, D.K., Higginbotham, E.J., Johnson, C.A., Keltner, J.L., Miller, J.P., Parrish, R.K., Wilson, M.R., Kass, M.A., 2002. The ocular hypertension treatment study: baseline factors that predict the onset of primary open-angle glaucoma. Arch. Ophthalmol. 20, 714–720.

Grice, D.E., Reenilä, I., Männistö, P.T., Brooks, A.I., Smith, G.G., Golden, G.T., Buxbaum, J.D., Berrettini, W.H., 2007. Transcriptional profiling of C57 and DBA strains of mice in the absence and presence of morphine. BMC Genomics 8, 76.

Guo, Q., Fu, W., Sopher, B.L., Miller, M.W., Ware, C.B., Martin, G.M., Mattson, M.P., 1999. Increased vulnerability of hippocampal neurons to excitotoxic necrosis in presenilin-1 mutant knock-in mice. Nat. Med. 5, 101–106.

Guo, Y., Johnson, E.C., Cepurna, W.O., Dyck, J.A., Doser, T., Morrison, J.C., 2011. Early gene expression changes in the retinal ganglion cell layer of a rat glaucoma model. Invest. Ophthalmol. Vis. Sci. 52, 1460–1473.

Howell, G.R., Libby, R.T., Marchant, J.K., Wilson, L.A., Cosma, I.M., Smith, R.S., Anderson, M.G., John, S.W., 2007. Absence of glaucoma in D2 mice homozygous for wild-type versions of Gpnmb and Tyrp1. BMC Genet. 8, 45.

Howell, G.R., Macalinao, D.G., Sousa, G.L., Walden, M., Soto, I., Kneeland, S.C., Barbay, J.M., King, B.L., Marchant, J.K., Hibbs, M., Stevens, B., Barres, B.A., Clark, A.F., Libby, R.T., John, S.W., 2011. Molecular clustering identifies complement and endothelin induction as early events in a mouse model of glaucoma. J. Clin. Invest. 121, 1429–1444.

Inman, D.M., Horner, P.J., 2007. Reactive nonproliferative gliosis predominates in a chronic mouse model of glaucoma. Glia 55, 942–953.

John, S.W., Smith, R.S., Savinova, O.V., Hawes, N.L., Chang, B., Turnbull, D., Davisson, M., Roderick, T.H., Heckenlively, J.R., 1998. Essential iris atrophy, pigment dispersion, and glaucoma in D2 mice. Invest. Ophthalmol. Vis Sci. 39, 951–962.

Kasumu, A., Bezprozvanny, I. Deranged calcium signaling in Purkinje cells and pathogenesis in spinocerebellar ataxia 2 (SCA2) and other Ataxias. Cerebellum, in press 2010 May 18 [Epub ahead of print].

Keirstead, S.A., Miller, R.F., 1995. Calcium waves in dissociated retinal glial (Müller) cells are evoked by release of calcium from intracellular stores. Glia 14, 14–22.

Križaj, D., Lai, F.A., Copenhagen, D.R., 2003. Ryanodine stores and calcium regulation in the inner segments of salamander rods and cones. J. Physiol. 547, 761–774.

Lam, T.T., Kwong, J.M., Tso, M.O., 2003. Early glial responses after acute elevated intraocular pressure in rats. Invest. Ophthalmol. Vis. Sci. 44, 638–645.

Li, Y., Holtzclaw, L.A., Russell, J.T., 2001. Müller cell Ca^{2+} waves evoked by purinergic receptor agonists in slices of rat retina. J. Neurophysiol. 85, 986–994.

Libby, R.T., Anderson, M.G., Pang, I.H., Robinson, Z.H., Savinova, O.V., Cosma, I.M., Snow, A., Wilson, L.A., Smith, R.S., Clark, A.F., John, S.W., 2005. Inherited glaucoma in DBA/2J mice: pertinent disease features for studying the neurodegeneration. Vis. Neurosci. 22, 637–648.

Lindqvist, N., Liu, Q., Zajadacz, J., Franze, K., Reichenbach, A., 2010. Retinal glial (Müller) cells: sensing and responding to tissue stretch. Invest. Ophthalmol. Vis. Sci. 51, 1683–1690.

Lucki, I., Dalvi, A., Mayorga, A.J., 2001. Sensitivity to the effects of pharmacologically selective antidepressants in different strains of mice. Psychopharmacology (Berl) 155, 315–322.
Mandal, A., Shahidullah, M., Delamere, N.A., 2010. Hydrostatic pressure-induced release of stored calcium in cultured rat optic nerve head astrocytes. Invest. Ophthalmol. Vis. Sci. 51, 3129–3138.
Marc, R.E., Jones, B.W., Watt, C.B., Strettoi, E., 2003. Neural remodeling in retinal degeneration. Prog. Retin Eye Res. 22, 607–655.
Medina-Ortiz, W.E., Gregg, E.V., Brun-Zinkernagel, A.M., Koulen, P., 2007. Identification and functional distribution of intracellular Ca channels in mouse lacrimal gland acinar cells. Open Ophthalmol. 1, 8–16.
Misra, V., Lee, H., Singh, A., Huang, K., Thimmulappa, R.K., Mitzner, W., Biswal, S., Tankersley, C.G., 2007. Global expression profiles from C57BL/6J and DBA/2J mouse lungs to determine aging-related genes. Physiol. Genomics 31, 429–440.
Nedergaard, M., Rodríguez, J.J., Verkhratsky, A., 2010. Glial calcium and diseases of the nervous system. Cell Calcium 47, 140–149.
Newman, E.A., 2001. Propagation of intercellular calcium waves in retinal astrocytes and Müller cells. J. Neurosci. 21, 2215–2223.
Niebauer, M., Gruenthal, M., 1999. Neuroprotective effects of early vs. late administration of dantrolene in experimental status epilepticus. Neuropharmacology 38, 1343–1348.
Ouardouz, M., Nikolaeva, M.A., Coderre, E., Zamponi, G.W., McRory, J.E., Trapp, B.D., Yin, X., Wang, W., Woulfe, J., Stys, P.K., 2003. Depolarization-induced Ca^{2+} release in ischemic spinal cord white matter involves L-type Ca^{2+} channel activation of ryanodine receptors. Neuron 40, 53–63.
Panagis, L., Zhao, X., Ge, Y., Ren, L., Mittag, T.W., Danias, J., 2010. Gene expression changes in areas of focal loss of retinal ganglion cells in the retina of DBA/2J mice. Invest. Ophthalmol. Vis Sci. 51, 2024–2034.
Popescu, B.O., Oprica, M., Sajin, M., Stanciu, C.L., Bajenaru, O., Predescu, A., Vidulescu, C., Popescu, L.M., 2002. Dantrolene protects neurons against kainic acid induced apoptosis in vitro and in vivo. J. Cell. Mol. Med. 6, 555–569.
Porciatti, V., Chou, T.H., Feuer, W.J., 2010. C57BL/6J, DBA/2J, and DBA/2J.Gpnmb mice have different visual signal processing in the inner retina. Mol. Vis. 16, 2939–2947.
Puk, O., Dalke, C., Hrabé de Angelis, M., Graw, J., 2008. Variation of the response to the optokinetic drum among various strains of mice. Front Biosci. 13, 6269–6275.
Punzo, C., Cepko, C., 2007. Cellular responses to photoreceptor death in the rd1 mouse model of retinal degeneration. Invest. Ophthalmol. Vis. Sci. 48, 849–857.
Puro, D.G., 1991. Stretch-activated channels in human retinal Muller cells. Glia 4, 456–460.
Rentería, R.C., Strehler, E.E., Copenhagen, D.R., Krizaj, D., 2005. Ontogeny of plasma membrane Ca2+ ATPase isoforms in the neural retina of the postnatal rat. Vis. Neurosci. 22, 263–274.
Ryskamp, D.A., Witkovsky, P., Barabas, P., Huang, W., Koehler, C., Akimov, N.P., Lee, S.H., Chauhan, S., Xing, W., Rentería, R.C., Liedtke, W., Krizaj, D., 2011. The polymodal ion channel transient receptor potential vanilloid 4 modulates calcium flux, spiking rate, and apoptosis of mouse retinal ganglion cells. J. Neurosci. 31, 7089–7101.
Shoshan-Barmatz, V., Zakar, M., Shmuelivich, F., Nahon, E., Vardi, N., 2007. Retina expresses a novel variant of the ryanodine receptor. Eur. J. Neurosci. 26, 3113–3125.
Singh, S.M., Treadwell, J., Kleiber, M.L., Harrison, M., Uddin, R.K., 2007. Analysis of behavior using genetical genomics in mice as a model: from alcohol preferences to gene expression differences. Genome 50, 877–897.
Soto, I., Oglesby, E., Buckingham, B.P., Son, J.L., Roberson, E.D., Steele, M.R., Inman, D.M., Vetter, M.L., Horner, P.J., Marsh-Armstrong, N., 2008. Retinal ganglion cells downregulate gene expression and lose their axons within the optic nerve head in a mouse glaucoma model. J. Neurosci. 28, 548–561.
Steele, M.R., Inman, D.M., Calkins, D.J., Horner, P.J., Vetter, M.L., 2006. Microarray analysis of retinal gene expression in the DBA/2J model of glaucoma. Invest. Ophthalmol. Vis. Sci. 47, 977–985.
Stirling, D.P., Stys, P.K., 2010. Mechanisms of axonal injury: internodal nanocomplexes and calcium deregulation. Trends. Mol. Med. 16, 160–170.
Whitmore, A.V., Libby, R.T., John, S.W., 2005. Glaucoma: thinking in new ways-a rôle for autonomous axonal self-destruction and other compartmentalised processes? Prog. Retin Eye Res. 24, 639–662.
Xue, L.P., Lu, J., Cao, Q., Hu, S., Ding, P., Ling, E.A., 2006. Muller glial cells express nestin coupled with glial fibrillary acidic protein in experimentally induced glaucoma in the rat retina. Neuroscience 139, 723–732.

CHAPTER 5

THE POLYMODAL ION CHANNEL TRANSIENT RECEPTOR POTENTIAL VANILLOID 4 MODULATES CALCIUM FLUX, SPIKING RATE, AND APOPTOSIS OF MOUSE RETINAL GANGLION CELLS

Ryskamp DA, Witkovsky P, Barabas P, Huang W, Koehler C, Akimov NP, Lee SH, Chauhan S, Xing W, Rentería RC, Liedtke W, Križaj D (2011) The polymodal ion channel transient receptor potential vanilloid 4 modulates calcium flux, spiking rate, and apoptosis of mouse retinal ganglion cells. The Journal of Neuroscience 31(19):7089-7101. Reprinted with permission from The Journal of Neuroscience.

The Journal of Neuroscience, May 11, 2011 • 31(19):7089–7101 • 7089

Cellular/Molecular

The Polymodal Ion Channel Transient Receptor Potential Vanilloid 4 Modulates Calcium Flux, Spiking Rate, and Apoptosis of Mouse Retinal Ganglion Cells

Daniel A. Ryskamp,[1,2]* Paul Witkovsky,[4]* Peter Barabas,[1]* Wei Huang,[1] Christopher Koehler,[5] Nikolay P. Akimov,[5] Suk Hee Lee,[6] Shiwani Chauhan,[1] Wei Xing,[1] René C. Rentería,[5] Wolfgang Liedtke,[6] and David Križaj[1,2,3]

[1]Department of Ophthalmology & Visual Sciences, John A. Moran Eye Center, [2]Interdepartmental Program in Neuroscience, and [3]Department of Physiology, University of Utah School of Medicine, Salt Lake City, Utah 84132, [4]Department of Ophthalmology, New York University School of Medicine, New York, New York 10016, [5]Department of Physiology and Center for Biomedical Neuroscience, University of Texas Health Science Center at San Antonio, San Antonio, Texas, and [6]Department of Medicine and Neurobiology, and Center for Translational Neuroscience, Duke University Medical Center, Durham, North Carolina 27710

Sustained increase in intraocular pressure represents a major risk factor for eye disease, yet the cellular mechanisms of pressure transduction in the posterior eye are essentially unknown. Here we show that the mouse retina expresses mRNA and protein for the polymodal transient receptor potential vanilloid 4 (TRPV4) cation channel known to mediate osmotransduction and mechanotransduction. TRPV4 antibodies labeled perikarya, axons, and dendrites of retinal ganglion cells (RGCs) and intensely immunostained the optic nerve head. Müller glial cells, but not retinal astrocytes or microglia, also expressed TRPV4 immunoreactivity. The selective TRPV4 agonists 4α-PDD and GSK1016790A elevated $[Ca^{2+}]_i$ in dissociated RGCs in a dose-dependent manner, whereas the TRPV1 agonist capsaicin had no effect on $[Ca^{2+}]_{RGC}$. Exposure to hypotonic stimulation evoked robust increases in $[Ca^{2+}]_{RGC}$. RGC responses to TRPV4-selective agonists and hypotonic stimulation were absent in Ca^{2+}-free saline and were antagonized by the nonselective TRP channel antagonists Ruthenium Red and gadolinium, but were unaffected by the TRPV1 antagonist capsazepine. TRPV4-selective agonists increased the spiking frequency recorded from intact retinas recorded with multielectrode arrays. Sustained exposure to TRPV4 agonists evoked dose-dependent apoptosis of RGCs. Our results demonstrate functional TRPV4 expression in RGCs and suggest that its activation mediates response to membrane stretch leading to elevated $[Ca^{2+}]_i$ and augmented excitability. Excessive Ca^{2+} influx through TRPV4 predisposes RGCs to activation of Ca^{2+}-dependent proapoptotic signaling pathways, indicating that TRPV4 is a component of the response mechanism to pathological elevations of intraocular pressure.

Introduction

Cells of multicellular organisms experience mechanical stimuli that range from the direct mechanical impact of pulling and stretching to changes in osmotic and hydrostatic pressure (Wang and Thampatty, 2006; Bourque, 2008). Mechanical stretch or pressure activates ion channels in the plasma membrane (Loukin et al., 2010a,b), resulting in depolarization, increased intracellular Ca^{2+} concentration ($[Ca^{2+}]_i$) (Zabel et al., 1996; Wu and Davis, 2001), and changes in gene expression, cell shape, and cytoskeletal organization (Naruse et al., 1998; Thodeti et al., 2009).

Recent studies have established that members of the transient receptor potential (TRP) superfamily transduce visual, chemical, thermal, mechanical, painful, and osmotic stimuli into Ca^{2+} fluxes (for review, see Liedtke and Kim, 2005; Kung, 2005; Christensen and Corey, 2007; Sharif-Naeini et al., 2008). We are particularly interested in the possibility that the vertebrate retina, which is exposed to systemic blood pressure, hydrostatic pressure from the CSF, and intrinsic intraocular pressure (IOP), contains one or more pressure-sensitive TRP channels. Pathological elevations in IOP or systemic pressure represent primary risk factors for glaucoma, a group of inherited optic neuropathies characterized by apoptotic loss of retinal ganglion cells (RGCs), degeneration of the optic nerve, and progressive loss of visual fields (Quigley, 2005; Whitmore et al., 2005). The cellular pathophysiology of glaucoma is not well understood, in part because the mechanisms that couple the mechanical stimulus (ΔIOP) to cellular signal transduction remain to be characterized.

Received Jan. 20, 2011; revised March 10, 2011; accepted March 26, 2011.

Author contributions: D.A.R. and D.K. designed research; D.A.R., P.W., P.B., W.H., C.K., N.P.A., S.H.L., S.C., W.X., R.C.R., and D.K. performed research; W.L. contributed unpublished reagents/analytic tools; D.A.R., P.W., P.B., R.C.R., W.L., and D.K. analyzed data; D.K. wrote the paper.

The work was supported by the National Institutes of Health (Grants T32DC008553, R01EY13870, and P30EY014800), the International Retina Research Foundation, the Richard H. Chartrand Foundation, The Foundation Fighting Blindness, the Neuroscience Program at the University of Utah, and the Moran TIGER award. The research was also supported by unrestricted grants from Research to Prevent Blindness to the Moran Eye Institute at the University of Utah. We thank Dr. Ning Tian (University of Utah) for the gift of Thy1:CFP mice and Thy1:GFP sections; and Dr. Tünde Molnar and Ms. Carolyn Groves for help with data analysis.

*D.A.R., P.W., and P.B. contributed equally to this work.

Correspondence should be addressed to David Križaj, Department of Ophthalmology & Visual Sciences, John A. Moran Eye Center, University of Utah School of Medicine, Salt Lake City, UT 84132. E-mail: david.krizaj@hsc.utah.edu.

DOI:10.1523/JNEUROSCI.0359-11.2011

 0270-6474/11/317089-13$15.00/0

In eukaryotic cells, the TRP vanilloid 4 (TRPV4) channel (GenBank accession number NM_022017) represents a polymodal mechanism that transduces osmotic pressure, shear force stimuli, mechanical stretch, and moderate warmth (~27–37°C) into cation influx with a preference for Ca^{2+} (P_{Ca}/P_{Na} ~6) (Liedtke et al., 2000; Güler et al., 2002; O'Neil and Heller, 2005). The channel may be activated by intracellular mediators such as arachidonic acid and cytochrome P450-dependent formation of 5,6-epoxyeicosatrienoic acid (Vriens et al., 2004, but see Loukin et al., 2009). In neural tissues, TRPV4 expression has been localized to sensory neurons in dorsal root and trigeminal ganglia, inner ear hair cells, Merkel cells, hippocampal and hypothalamic neurons, and astrocytes (Liedtke et al., 2000; Reiter et al., 2006; Benfenati et al., 2007; Shibasaki et al., 2007; Alessandri-Haber et al., 2009). Mice lacking TRPV4 have defects in noxious mechanosensation and pressure sensation (Liedtke and Friedman, 2003; Suzuki et al., 2003), whereas the functional ortholog of TRPV4 in the worm *Caenorhabditis elegans*, OSM-9, mediates osmotic, mechanical, and chemical avoidance (Liedtke et al., 2003). Together, these findings suggest that TRPV4 represents an evolutionarily conserved element of the neural response to mechanical stimulation.

We report here that TRPV4 is expressed in RGC somata and optic axon fibers. Transient activation of TRPV4 induced Ca^{2+} influx and increased the excitability of ganglion cells, whereas sustained activation resulted in RGC apoptosis. The prominent expression of TRPV4-immunoreactivity (IR) at the optic nerve head (ONH), and the role of TRPV4 in gating Ca^{2+} entry and RGC firing, implicate this channel in the retinal remodeling that occurs during chronic increases in IOP.

Materials and Methods

Animals

C57BL/6J mice of either sex were obtained from commercial suppliers, whereas B6.Cg-Tg(*Thy1*-CFP)23Jrs/J (hereafter, Thy1:CFP) animals or retinal sections were a kind gift from Dr. Ning Tian (University of Utah, Salt Lake City, UT). The animals were maintained in the University animal quarters on a 12 h light/dark cycle. Mice were fed lab chow and water *ad libitum*. Mice were killed before isolation and dissociation of retinas (Duncan et al., 2006). Animal handling and anesthetic procedures were approved by University Institutional Animal Care committees and conform to National Institutes of Health guidelines.

Histology

Eyes were enucleated, and their corneas and lenses dissected away. The remaining posterior pole of the eye was fixed by immersion for 1 h at room temperature in freshly prepared 4% paraformaldehyde in 0.1 M phosphate buffer, pH 7.2, then washed 3 × 10 min in pH 7.2 PBS. Fixed eye tissue was then immersed for 12–16 h in 30% sucrose at 4°C, embedded in OCT (Ted Pella), cryostat sectioned at 16 μm, and mounted on Superfrost slides (Fisher Scientific). After drying for 1 h at 37°C, slides were stored frozen (−80°C) until used. Dissociated cells were isolated with papain (7 U/ml; Worthington), plated on concanavalin A-coated coverslips, fixed in 4% paraformaldehyde in 0.1 M phosphate buffer, pH 7.2, for 30 min, washed 3 × 10 min in pH 7.2 PBS, and stored at 4°C.

Immunohistochemistry. For fluorescence immunocytochemistry, cryostat sections were thawed and washed in PBS, then placed for 30 min to 1 h in blocking solution (10 ml of PBS, 30 μl of Triton X-100, 100 mg of bovine serum albumin, 100 μl of 10% w/v Na azide solution). Primary and secondary antibodies were diluted in blocking solution and applied for 2 and 1 h, respectively, at room temperature, with three intervening washes in PBS. After a final set of washes in PBS, the sections were covered in VectaShield (Vector Laboratories).

Terminal deoxynucleotidyl transferase-mediated dUTP-biotin nick end labeling assay. Retinas were embedded, cryosectioned, and processed for terminal deoxynucleotidyl transferase-mediated biotinylated UTP nick end labeling (TUNEL) following the protocol by Gavrieli et al. (1992). After 30 min rehydration in 70% ethanol, 2× 5 min rinses in PBS and 1% Triton-X in 1% citrate buffer, pH 7.3, the slides were subjected to a final rinse in PBS. Slides were then incubated for 30 min in the reaction buffer (30 mM Trizma-HCl, 140 mM Na^+ cacodylate, 1.0 mM $CaCl_2$, 0.2% Triton X-100, pH 7.2). Positive controls were treated with DNase I (Roche Diagnostics) (10 U/ml) in the reaction buffer. Next, slides were treated for 1 h with 0.03 U/μl terminal transferase and 4 μM biotin-16-dUTP (Roche Diagnostics). The reaction was terminated in 30 mM Na^+ citrate, 300 mM NaCl, and 0.2% Triton X-100 in PBS (5 min), and rinsed in PBS (2×5 min), exposed to 1% bovine serum albumin in PBS for 20 min, and rinsed. As a negative control, the retinal sections were processed omitting the incubation step with terminal deoxynucleotidyl transferase during DNA labeling. Apoptotic cells were visualized with a confocal microscope (LSM510; Zeiss) and categorized by size. We found that our fixation protocol resulted in ~1 μm shrinkage in the diameter of dissociated Brn3a-IR cells in retinal sections. Therefore, the TUNEL analysis compared cells with a diameter of >6 μm (presumed RGCs) to photoreceptor cells with diameters of 3–5 μm (the identity of photoreceptors was confirmed by immunostaining for mouse cone arrestin (a gift from Dr. Wolfgang Baehr, University of Utah, Salt Lake City, UT) and rhodopsin (Santa Cruz Biotechnology). A cell was deemed to be TUNEL positive if the fluorescent signal completely filled the cell body.

Table 1. Primary antibodies and their sources and dilutions

Target	Company	Catalog number
TRPV4	Alomone Labs	ACC-034 rabbit 1:500–1:1000
TRPV4	MBL International Corporation	LS-A8583 rabbit 1:200–1:1000
TRPV4	Affinity Bioreagents/Thermo Scientific Pierce/OSenses	OSR00136W rabbit 1:200–1:1000
TRPV4	Abcam	Ab63003 rabbit 1:200–1:1000
TRPV4	Lifespan Biosciences	LS-C94498 rabbit 1:200–1:1000
Brn3a	Santa Cruz Biotechnology	sc-8429 mouse 1:100
Cone arrestin	Gift from Dr. Wolfgang Baehr (University of Utah)	Mouse 1:100–1:500
Rhodopsin	Santa Cruz Biotechnology	sc-57433 mouse 1:100
ChAT	Chemicon	AB144-P goat 1:200
GAD-65	Developmental Studies Hybridoma Bank	GAD-6 mouse 1:1000
GFAP	Sigma	G3893 mouse 1:500
GFP	Santa Cruz Biotechnology	sc-9996 mouse 1:100–1:500

Image acquisition and processing

Sections were examined by confocal microscopy (LSM 510, Zeiss; or PM 800, Nikon). Digital images were acquired separately from each laser channel, then recombined. Files were further processed with deconvolution software (AutoQuant Imaging). Adjustments of contrast and intensity were made in Photoshop (Adobe); any such adjustments were made uniformly to the entire image.

Western blot

We essentially followed the procedure outlined in previous publications (Liedtke and Friedman, 2003; Phan et al., 2009). In brief, homogenized retinal tissue was subjected to protein preparation and denaturation, and proteins (10 μg per lane) were separated on an SDS gel, then immunoblotted to polyvinylidene difluoride membranes. After blocking with milk powder, TRPV4 was immunodetected using the above antibody (Phan et al., 2009) and peroxidase-based chemoluminescence.

Primary and secondary antibodies

Table 1 shows the primary and secondary antibodies used in this study. Multiple commercially available anti-TRPV4 antibodies (ACC-034, Alomone Labs; LS-A8583, MBL International Corporation; OSR00136W, Affinity Bioreagents; and ab63003, Abcam) were tested by immunostaining and Western blots in wild-type and TRPV4-null mice. However, the only antibody that proved completely satisfactory was LS-C94498 (Lifespan Biosciences), based on the following criteria: (1) The antibody stained Western blot bands of 85 and 106 kDa from retinal tissue har-

vested from wild-type mice but not from TRPV4-null mice (see Fig. 1); (2) it colocalized with green fluorescent protein (GFP) in RGCs from transgenic animals in which GFP was driven by the *Trpv4* gene promoter (see Fig. 2*C*); and (3) it detected protein bands of appropriate molecular mass from HEK293 cells transfected with *Trpv4* cDNA, whereas the bands were missing in immunoblots from nonexpressing cells (Fig. 1). All TRPV4-IR data reported in the present study were obtained with the anti-TRPV4 antibody LS-C94498. No immunostaining was observed when the primary antibody was omitted.

Semiquantitative RT-PCR

Total RNA from retina was extracted with Trizol, and total RNA (2 μg of total RNA used for first-strand synthesis with oligo-dT and primers) was converted to cDNA using the SuperScript III First-Strand Synthesis kit from Invitrogen. PCR products were amplified in a thermocycler (Veriti, ABI) with nucleic acid stain (SYBR Green, ABI) reagents according to the manufacturer's instructions. Amplification of PCR products was measured by fluorescence associated with binding of double-stranded DNA to SYBR Green in the reaction mixture. After an initial denaturation step of 50°C for 2 min and 95°C for 10 min, PCR was repeated for 40 cycles at 95°C for 15 s, 58°C for 30 s, and 72°C for 30 s. After amplification, the ratio of gene-of-interest mRNA to a housekeeping gene, glyceraldehyde-3-phosphate dehydrogenase (*Gapdh*), was calculated for each sample. Five to 10 independent biological replicates (retinas) were used at each age.

Generation of a bacterial artificial chromosome transgenic mouse line with a fluorescent reporter driven by the Trpv4 *promoter*

A mouse bacterial artificial chromosome (BAC) harboring the *Trpv4* gene was modeled by "recombineering" (Copeland et al., 2001), so that the copepod-GFP coding region was placed directly after the ATG start codon of mouse *Trpv4*. In addition, this BAC was engineered to not harbor exons 10–14, so that a functional ion channel could not arise from the transgene. Engineered DNA served as a transgenesis template, which was constructed following standard procedures (Zhao et al., 2008). Of four resulting transgenic lines, the one used revealed robust fluorescence in trigeminal ganglion sensory neurons (not illustrated), both in acute sections and acute dissociations, colocalizing with TRPV4 immunolabeling. This line was outcrossed for five or more generations before analysis of retinas.

Calcium imaging

Calcium imaging was performed on acutely isolated retinal cells, as described previously (Szikra et al., 2009). In brief, dissociated retinal cells were plated on concanavalin A-coated (0.2 mg/ml; Sigma) coverslips, loaded with fura-2 AM (1–5 μM; Invitrogen) for 15–30 min and washed for 10 min in dye-free L-15 medium. Cells were viewed with Nikon Ti inverted or 600EF upright microscopes using 20× 0.95 numerical aperture (NA), 40× 0.85 NA, or 40× 1.25 NA objective lenses. Excitation for 340 and 380 nm filters (Chroma and Semrock) was provided by a 150 W Xenon arc lamp (DG4, Sutter Instruments). Fluorescence emission was high-pass filtered at 510 nm and captured with cooled digital CCD cameras (HQ2, Photometrics). Data acquisition and F_{340}/F_{380} ratio calculations were performed by NIS Elements software. Fluorescence imaging was performed on regions of interest (ROIs) encompassing the RGC perikaryon, typically at 3 × 3 binning. Background fluorescence was measured in similarly sized ROIs in neighboring areas devoid of cells. After sequential image acquisition (0.167–0.5 Hz) of cell fluorescence at 340/380 nm, the background was subtracted. Calibration of free $[Ca^{2+}]_i$ was performed *in vivo* using 10 μM ionomycin and 10 mM Ca^{2+} or 0 Ca^{2+}/3 mM EGTA. The apparent free $[Ca^{2+}]_i$ was determined from the equation $[Ca^{2+}]_i = ((R - R_{min})/(R_{max} - R)) \times (F^{380}{}_{max}/F^{380}{}_{min}) \times K_d$, where R is the ratio of emission intensity at 510 nm evoked by 340 nm excitation versus emission intensity at 510 nm evoked by 380 nm excitation, R_{min} is the ratio at zero free Ca^{2+}, R_{max} is the ratio at saturating Ca^{2+}, and the dissociation constant K_d for Ca^{2+}-fura 2 at room temperature was taken to be 224 nM (Neher, 1995). Glutamate (100 μM) was added at the beginning of each experiment to control for neuronal health, type, and responsiveness. DMSO, the solvent for the indicator dye, did not induce any responses in RGCs (data not shown). Previous studies using Mn^{2+} quenching showed that 95% of the fura-2 fluorescence emanates from the cytosol in the cells (Szikra et al., 2009). Experiments were conducted at room temperature, and encompassed stimulation with glutamate, TRPV4, and TRPV1 agonists and antagonists.

Cell identification

RGCs in short-term culture were identified initially by morphology and perikaryal size (7–15 μm). In a subset of experiments, RGCs isolated from Thy1:CFP retinas were used and identified by intrinsic fluorescence (Raymond et al., 2009). Alternatively, test neurons isolated from wild-type retinas were confirmed as RGCs by immunocytochemistry. In each experiment, a 100 μM glutamate stimulus was used to confirm that the visually identified putative RGCs expressed ionotropic glutamate receptors. Presumed RGCs responded to 30 mM KCl with rapid high-amplitude increases in $[Ca^{2+}]_i$, indicating that the cells were healthy and maintained their excitability. In a subset of experiments, cells recorded during stimulation with hypotonic saline or TRPV4 agonists were fixed and immunostained with TRPV4 and Brn3a antibodies.

Solutions and reagents

The isotonic superfusing saline contained the following (in mM): 133 NaCl, 2.5 KCl, 2 $CaCl_2$, 1.5 $MgCl_2$, 1.25 NaH_2PO_4, 10 HEPES hemisodium salt, 10 glucose, 1 pyruvic acid, 1 lactic acid, and 0.5 glutathione. In Ca^{2+}-free solutions, no external Ca^{2+} was added, and the saline was supplemented with 1 mM EGTA. The osmolarity and pH of each external solution was measured before each experiment. pH was adjusted to 7.4 with NaOH. Osmolarity was measured with a vapor-pressure osmometer (VAPRO); for control saline, osmolarity was 280 mOsm. For experiments involving hypotonic stimulation, the isotonic ringer contained 132 mM mannitol and the NaCl concentration was reduced to 57.5 mM. Hypoosmotic solutions were prepared by reducing the final concentration of mannitol to 44.5 mM without changing the ionic composition. In a subset of experiments using hypotonic stimulation, cells were coloaded with fura-2 AM + calcein AM (1 μM; Invitrogen). Calcein fluorescence was elicited using 490 nm excitation filters. Because calcein fluorescence is Ca^{2+} independent and volume dependent, it was used as a measure of changes in the cell volume.

Unless otherwise indicated, the salts and reagents were purchased from Sigma. Ruthenium Red and capsaicin were purchased from Ascent Scientific. Capsaicin and capsazepine were also purchased from Tocris. 4α-PDD was obtained from LC Laboratories.

Multielectrode array recordings and data analysis

Multielectrode array (MEA) recordings were performed using multielectrode, extracellular recording chambers (MEA1060 system, MultiChannel Systems) consisting of an array of 60 planar electrodes, each 10 μm in diameter, spaced 100 μm apart for a total array size of 700 μm^2, as described previously (Rentería et al., 2006). Briefly, young adult C57BL6J mice were killed after 1 h of dark adaptation, and an eye was removed under dim red illumination. The retina was dissected and placed with the ganglion cell side against the recording electrodes using a piece of nitrocellulose paper as support. The retina was typically placed on the array within a millimeter of the optic nerve head, and a manipulator (Cell Micro Controls) was used to hold the tissue down with slight pressure. Retinas were perfused at room temperature for 30 min and at 30°C for another 30 min before recordings were started, the temperature was maintained at 30°C thereafter, and spontaneous spiking in the dark was recorded. The perfusion saline was either Ames' medium or Ringer's modified solution as follows (in mM): 124 NaCl, 2.5 KCl, 2 $CaCl_2$, 2 $MgCl_2$, 1.25 NaH_2PO_4, 26 $NaHCO_3$, and 22.2 glucose; the pH was maintained at 7.3–7.4 by bubbling with 95% O_2/5% CO_2 mixed gas. Voltage signals sampled at 50 kHz were bandpass filtered at 100 Hz to 3 kHz, and waveforms that crossed a negative voltage threshold (set at −5.5 SDs of the mean noise) were recorded to disk for off-line analysis. Under these conditions, nearly all recorded cells are likely to be RGCs (Rentería et al., 2006).

Spike trains for each RGC were determined by spike sorting based on clustering in principal component space using software (Offline Sorter, Plexon). Not every detected waveform was assigned to a unit; obvious automatic sorting errors were corrected for each cluster manually (Rentería et al.,

2006). Time stamps of the action potentials of each sorted unit were used to generate peristimulus time histograms (30 s bins). The average spike rates during the 3 min period before and after drug application were determined for every recorded cell and expressed as the percentage change in firing in the presence of drug. This normalization allowed for comparison of cells with varied initial spike rates. The very few cells that had zero rates before application and spiking during drug application were considered to have increased by 100%.

Statistical analysis

Data are expressed as the mean ± SEM, with the number of cells, slides, or animals indicated by *N*. Cell diameter data are expressed as the mean ± SD. Statistical comparisons between two treatments in the same cell were determined using the *t* test; unless indicated otherwise, comparisons between different groups were evaluated by the Mann–Whitney test or the Wilcoxon signed rank test. Data obtained in multielectrode array studies were analyzed with the Wilcoxon signed rank test. A value of $p < 0.05$ was considered statistically significant.

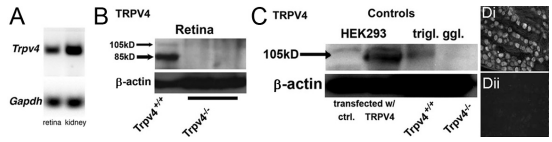

Figure 1. Expression of TRPV4 at the mRNA and protein levels in mouse retina. ***A***, PCR amplicons for *Trpv4* and glyceraldehyde-3-phosphate dehydrogenase (*Gapdh*) isolated from total retinal RNA pool and separated on a 2% agarose gel. ***B***, TRPV4 antibody recognizes a primary band of 85 kDa and a secondary band at 105 kDa in wild-type adult mouse retina. No signal is detected in TRPV4$^{-/-}$ retinas. ***C***, TRPV4 antibody recognized a major 105 kDa band in TRPV4-expressing HEK293 cell cultures and trigeminal ganglion tissue; no signal was apparent in a TRPV4 nonexpressor line. ***D***, Nodose ganglion. TRPV4-IR is observed in wild-type (***Di***) but not TRPV4$^{-/-}$ (***Dii***) tissue.

Results

TRPV4 mRNA and protein in the mouse retina

RT-PCR was performed using total RNA extracted from adult (postnatal day 90) mouse retinas. Gel analysis revealed PCR products at the appropriate size of 174 bp. The same transcript was amplified in kidney tissue, known to express *Trpv4* (Strotmann et al., 2000, Liedtke et al., 2000; Güler et al., 2002) (Fig. 1*A*).

We next compared TRPV4 protein expression in tissues derived from wild-type and TRPV4-null mice (see Materials and Methods). Consistent with RT-PCR, immunoblots from wild-type mouse retinas showed a primary band of 85 kDa and a secondary band at 105 kDa, which probably correspond to unglycosylated and *N*-glycosylated forms of TRPV4, respectively, which is in keeping with previous reports (Fig. 1*B*) (Liedtke and Friedman, 2003; Benfenati et al., 2007; Hartmannsgruber et al., 2007). Both bands were absent in retinal tissue derived from TRPV4-null mice (Fig. 1*B*). The TRPV4 antibody was validated in Western blots from HEK293 cells transfected with *Trpv4* cDNA (Fig. 1*C*) and in trigeminal ganglion tissue known to robustly express *Trpv4* (Liedtke et al., 2000; Liedtke and Friedman, 2003). As an additional test of the TRPV4 antibody, we immunostained the kidney, choroid plexus, and nodose ganglion tissues in which TRPV4 is expressed (Liedtke et al., 2000; Strotmann et al., 2000; Brierley et al., 2008). The patterns of TRPV4 expression in these tissues were identical to those identified in previous reports (data not shown). For example, the somata of neurons within the nodose ganglion (Fig. 1*Di*) were strongly TRPV4 immunoreactive, whereas the nodose tissue from a TRPV4-null mouse was unlabeled by the TRPV4 antibody (Fig. 1*Dii*).

TRPV4 immunoreactivity in the mouse retina

TRPV4-IR in retinal ganglion cells

In wild-type mouse retinas, TRPV4-IR was punctate and distributed throughout the inner retina (Fig. 2*A*). A dense array of TRPV4-IR puncta was seen within cell bodies located in the ganglion cell layer (gcl). TRPV4-IR was distributed at a lower density throughout the inner plexiform layer (ipl), but only very sparse TRPV4-IR was located within the inner nuclear layer (inl). This immunostaining pattern was absent in retinas of TRPV4-null mice (Fig. 2*B*). The apparent immunostaining of the outer plexiform layer (opl) is nonspecific since it was identical in wild-type and TRPV4-null retinas (Fig. 2*A*,*B*). Within the outer nuclear layer (onl) consisting primarily of photoreceptor nuclei, TRPV4-IR was seen in vertical processes of Müller glial cells (see also Fig. 2*M* for Müller cell signals in the ipl).

We also analyzed a transgenic mouse in which GFP was driven by the entire promoter of the mouse *Trpv4* gene. The 50 kDa *Trpv4* gene was centered within the 200 kDa GFP insert present in a BAC (see Materials and Methods). Using an antibody against GFP, retinal immunostaining was confined to cell bodies within the ganglion cell layer, although additional staining was noted in retinal blood vessels, in keeping with well established vascular-endothelial TRPV4 expression (Hartmannsgruber et al., 2007; Mendoza et al., 2010). When the retina was stained with anti-GFP, the marker was detected in cell bodies of the ganglion cell layer (Fig. 2*C*). Confirming that reporter gene expression was faithful to the targeted gene, *Trpv4*, GFP-IR was absent in wild-type mouse retina (not illustrated).

To probe whether TRPV4-IR is associated primarily or exclusively with ganglion cells, we immunostained the retina for Brn3a (also called POU4f1), a transcription factor found almost exclusively in developing (Liu et al., 2000) and mature ganglion cells (Nadal-Nicolás et al., 2009). We found that TRPV4-IR colocalized with that of Brn3a in ganglion cell perikarya and dendrites (Fig. 2*D*, arrow). Prominent additional TRPV4-IR was found within ganglion cell axon bundles in the optic fiber layer (ofl) (Fig. 2*D*), and also was abundant within the optic nerve head (Fig. 2*H*) and the laminar region of the optic nerve (Fig. 2*I*). The nearly universal distribution of Brn3a-IR in mouse retinal ganglion cells, together with the finding that Brn3a-IR and TRPV4-IR almost invariably colocalize, indicates that TRPV4 protein is distributed among a large fraction of mouse retinal ganglion cells.

A second marker for ganglion cells was provided by a construct in which GFP was linked to the promoter of Thy1, a ganglion cell-specific protein (see Materials and Methods). GFP-IR and TRPV4-IR colocalize in perikarya and dendrites of RGCs (Fig. 2*E*) and in displaced ganglion cell perikarya (Fig. 2*L*). Finally, immunostaining with an SMI-32 antibody that labels intermediate filaments in somata and axonal processes of wide-field αRGCs colocalized with TRPV4-IR processes in the ofl entering the optic nerve head (Fig. 2*K*).

TRPV4-IR is weak or absent in retinal amacrine cells

Approximately 50% of the cells within the ganglion cell layer in rodent retinas are displaced amacrine neurons rather than ganglion cells, whereas a subset of cells in the proximal inl belong to displaced RGCs (Perry and Walker, 1980; Jeon et al., 1998). To probe possible colocalization of TRPV4-IR with amacrine cells, we immunostained the retina with an antibody against choline acetyltransferase, a marker for starburst amacrine cells (Fig. 2*G*), and with glutamic acid decarboxylase 65 (GAD-65), a marker for

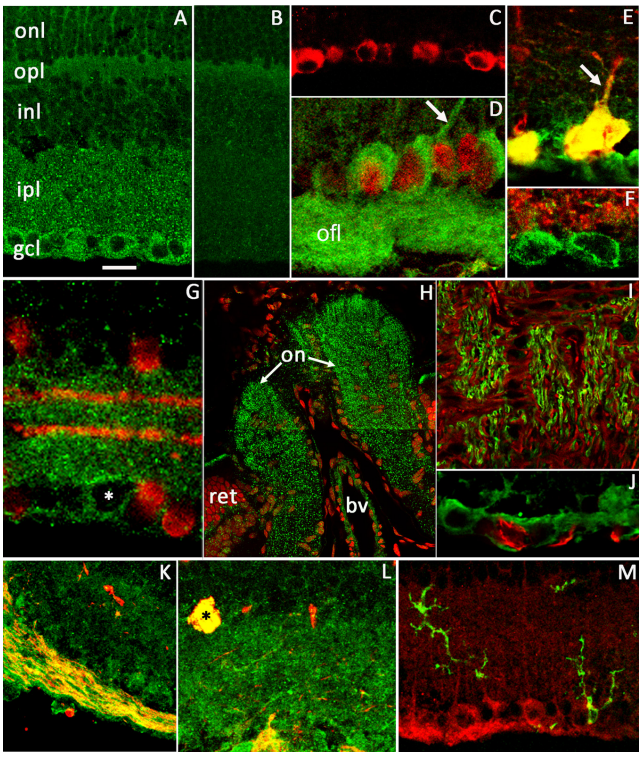

Figure 2. TRPV4 immunoreactivity in the mouse retina. ***A***, Vertical section of mouse retina. TRPV4-IR is expressed in ganglion cell somata and throughout the ipl. TRPV-IR in the onl is expressed in vertical fibers of Müller glial cells which run through this layer. Scale bars: (in ***A***) ***A–C***, ***I–M***, 20 μm; (in ***A***) ***D–G***, 15 μm; (in ***A***) ***H***, 40 μm. ***B***, Absence of specific TRPV4 immunostaining in the retina of a TRPV4-null mouse. ***C***, Transgenic retina produced by recombineering with copGFP sequence inserted *cis*- to the *Trpv4* promoter (see Materials and Methods). GFP (red) is localized to cytosol of retinal ganglion cells. ***D***, Colocalization of TRPV4-IR (green) and Brn3a-IR (red), a ganglion cell-specific protein in ganglion cell somata. Additional TRPV4-IR is seen in a ganglion cell dendrite (arrow) and in the ofl, which contains ganglion cell axons en route to the optic nerve. ***E***, Colocalization of TRPV4-IR (green) and GFP-IR (red) in a mouse line in which CFP was coupled to the promoter of Thy-1, a ganglion cell specific protein. Colocalization is seen both in the ganglion cell bodies (yellow) and in a ganglion cell dendrite (arrow). ***F***, TRPV4-IR in ganglion cell bodies (green) does not colocalize with GAD-65-IR (red). ***G***, TRPV4-IR (green) does not colocalize with ChAT-IR (red) seen in cell bodies of starburst amacrine cells (red) and in two discrete horizontal bands in the ipl. A labeled ganglion cell body is indicated by an asterisk. ***H***, Montage of the optic nerve (on) showing immunolabeling of optic nerve fibers with TRPV4 (green). Cell nuclei are stained with Sytox Orange. bv, Blood vessel; ret, retina. ***I***, Higher-magnification view of the optic nerve, illustrating that TRPV4-IR (green) is confined to optic nerve axons, whereas astrocytes labeled with a GFAP antibody (red) do not colocalize with TRPV4-IR. ***J***, Vertical section of retina illustrating ganglion cells labeled with the TRPV4 antibody. GFAP-IR-labeled astrocytes in the ofl (red) do not colocalize with TRPV4. ***K***, Vertical section of retina illustrating boundary between ofl and on. TRPV4-IR (green) is seen within these layers, and it colocalizes with intermediate filament immunoreactivity (SMI-32; red). The merged portions appear yellow. ***L***, Vertical section of retina illustrating a displaced ganglion cell (asterisk) at the inl/ipl border that colocalizes with TRPV4-ir (green) and GFP-IR in mice in which GFP is coupled to the Thy-1 promoter. Amacrine cell bodies at this same interface do not label with either antibody. A labeled ganglion cell (yellow profile) in the gcl is seen at bottom. ***M***, Vertical section of retina labeled with antibodies against TRPV4 (red) and Alexa Fluor-conjugated rat anti-mouse CD11B (green), a microglial-specific antibody. TRPV4-IR is seen in ganglion cell bodies and Müller glial cell processes. Two labeled microglial cells do not colocalize with TRPV4-IR.

GABAergic amacrine cells (Figs. 2*F*, 3*A*) that constitute a substantial fraction of displaced amacrine cells in the RGC layer (May et al., 2007). These tests revealed no colocalization of TRPV4-IR with ChAT-IR cells. Moreover, no colocalization with the dopaminergic amacrine cell marker tyrosine hydroxylase was observed (data not shown). A total of 4.6% of cells that labeled with the GABAergic marker GAD-65 stained with the TRPV4 antibody; however, the intensity of TRPV4-IR signals in this subset of cells was always significantly weaker compared with Brn3a-IR cells. Occasionally, a Brn3a-IR or SMI-32-IR cell body was detected in the inl. These perikarya were always TRPV4 immunopositive (Fig. 2*L*). Collectively, these data indicate that TRPV4-IR is associated with mouse retinal ganglion cells and may be localized to a small subset of GABAergic amacrine cells. Within the mouse ganglion cell, TRPV4-IR is associated principally with the perikaryon and the axon, but at least some ganglion cell dendrites also express TRPV4 (Fig. 2*D*,*F*, arrow).

TRPV4-IR in retinal glial cells

Detailed inspection of TRPV4-IR in the inner and outer retina revealed radial immunopositive processes that correspond to Müller macroglia (Fig. 2*M*). To assess TRPV4 expression in astrocytes, sections from the retina and at the glial lamina at the optic nerve head were colabeled with the glial fibrillar acidic protein (GFAP) antibody. No colocalization was observed, as TRPV4 and GFAP signals in the retina and the glial lamina appeared to label two distinct populations (Fig. 2*I*,*J*). Likewise, costaining with the microglia-specific Mac-1/CD11b antibody showed no overlap with TRPV4 (Fig. 2*M*) but showed staining in the radial processes emanating from the inner limiting membrane that may correspond to Müller macroglia. These data indicate that in the wild-type mouse retina TRPV4 is excluded from astrocytes and microglia but is expressed in Müller cells.

Physiological tests of TRPV4 function in mouse retina

Identification of RGCs in short-term culture

In retinal neurons isolated into short-term culture (see Materials and Methods) GABAergic neurons, identified by GAD65-IR, were invariably distinct from cells showing TRPV4-IR (Fig. 3*Ai–iii*). It was also apparent that TRPV4-IR cells were larger than those immunostained by GAD-65 (Fig. 3*Aiii*,*B*). Another test of ganglion cell identity in cultured neurons was immunoreactivity to an anti-Brn3a antibody (Fig. 4*Ai*). Brn3a-IR cells were invariably immunopositive for TRPV4, whereas photoreceptor and presumed amacrine perikarya were not (Figs. 2–4).

We extended measures of cell diameters to Brna3a-IR and Thy1:CFP neurons in culture and compared their dimensions to those of Brna3a-IR neurons in retinal slices; the data are summarized in Figure 3*B*. Diameters of dissociated Brn3a-IR cells were 9.1 ± 1.5 μm ($N = 74$; mean ± SD), not significantly different from 10.2 ± 1.8 μm ($N = 58$) in dissociated Thy1:CFP cells and 10.3 ± 2.0 μm in Brn3a-IR cells in

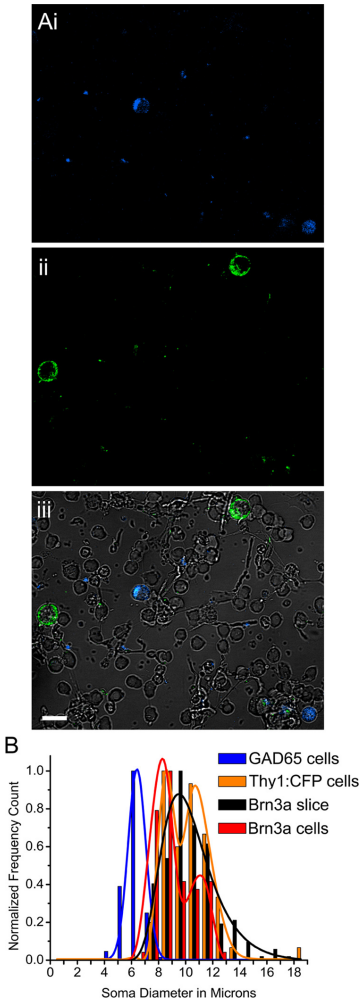

Figure 3. TRPV4 is not expressed in amacrine cells. ***A***, Double labeling for GAD-65-IR (***Ai***; blue), TRPV-IR (***Aii***; green), and superimposed transmitted image (***Aiii***) shows that TRPV4 signals are expressed in a population of cells that is distinct from GABAergic amacrine cells. Scale bar, 10 μm. ***B***, The distribution of cell diameters from dissociated RGCs that were (Brn3a) or were not (Thy1:CFP+) fixed, overlaps with Brn3a-IR somata from retinal sections. Little overlap in diameter distributions is seen between the RGC cohorts and GABAergic cells.

retinal sections ($N = 201$) ($p > 0.05$, Dunn's multiple-comparisons test) (Fig. 3*B*). The distribution of cell diameters confirms that the vast majority of ganglion cells have diameters ≥ 8 μm, whereas GABAergic amacrines are almost invariably <8 μm. Moreover, the size distributions of ganglion cell diameters based on the different criteria illustrated in Figure 3*B* are coextensive. Thus, our selection of a neuron for physiological study initially was made on the basis of cell diameter. In a few cases, we recorded Ca^{2+} signals from cyan fluorescent protein (CFP)-positive RGCs isolated from Thy1:CFP retinas, and in other experiments we confirmed the identity of TRPV4 agonist-responding cells by immunostaining the test cells for TRPV4-IR and Brn3a-IR following drug exposure.

TRPV4 agonists induce an increase in $[Ca^{2+}]_{RGC}$

Once a putative RGC was selected for experimentation, we first tested the ability of glutamate to evoke an increase in $[Ca^{2+}]_i$. RGCs have ionotropic glutamate receptors that result in ganglion cell depolarization and calcium entry, so a vigorous response to glutamate is a good initial test of RGC viability. To evaluate functional expression of TRPV4 channels in the retina, we measured calcium concentrations in dissociated RGCs before and after TRPV4 agonist application, using ratiometric Ca^{2+} imaging of RGCs loaded with Fura-2 AM.

On average, glutamate (100 μM) evoked a $[Ca^{2+}]_{RGC}$ increase of 490 ± 25 nM (mean ± SE) over a baseline of 45 ± 2 nM ($N = 216$; $p < 0.0001$, Wilcoxon matched-pairs signed ranks test). Endogenous TRPV4 channels in dissociated neurons were activated with the following two selective TRPV4 activators: the synthetic phorbol ester 4α-phorbol 12-myristate13-acetate (didecanoate; 4α-PDD), which directly binds to the transmembrane region of the protein (Watanabe et al., 2002; Vriens et al., 2007; Loukin et al., 2010a); and the recently characterized high-affinity agonist GSK1016790A (hereafter GSK; EC_{50} ~1–10 nM) (Thorneloe et al., 2008; Willette et al., 2008). Figure 4*B* illustrates a simultaneous recording from two putative RGCs that responded to glutamate and the two TRPV4 agonists (GSK, 25 nM; 4α-PDD, 30 μM). At 25 and 100 nM, GSK elicited robust $[Ca^{2+}]_i$ increases in 40.5 and 47.2% of glutamate-responding cells ($N = 10$ and 4 experiments), respectively (Figs. 4, 5, 6). In the continued presence of TRPV4 activators, $[Ca^{2+}]_i$ levels typically exhibited a decline, consistent with desensitization of the channel (Fig. 4*B*).

Mean $[Ca^{2+}]_{RGC}$ elevation induced by 25 nM GSK was 381 ± 41 nM over the $[Ca^{2+}]_{RGC}$ baseline (Fig. 4*G*) ($N = 23$; $p < 0.0001$, Wilcoxon matched-pairs signed-ranks test), whereas 100 nM GSK elevated $[Ca^{2+}]_i$ by 600 ± 210 nM ($N = 9$; $p < 0.004$, Wilcoxon matched-pairs signed-ranks test). In 15 putative RGCs, 4α-PDD (30 μM) increased the 340/380 ratio from 0.464 ± 0.029 to 1.430 ± 0.097 ($p < 0.0001$, paired *t* test) (Fig. 4*B*,*E*). When cells that had been stimulated with TRPV4 activators were subsequently immunostained for TRPV4 and Brn3a, the two markers labeled responding cells (Fig. 4*D*, arrowhead) but not GSK-insensitive cells. The average diameter of cells that responded to TRPV4 agonists was 8.9 ± 1.0 μm, not significantly different from diameters of Thy1:CFP and Brn3a-IR dissociated cells ($p > 0.05$) (Figs. 3*B*, 4*H*). The very substantial overlap of these two populations, responders and immunoreactive cells, provides more evidence that at least the great majority of cells selected for physiological study were retinal ganglion cells. Our data would also suggest that a subset of large-diameter RGCs may not express TRPV4 (Fig. 3*B*) or respond to TRPV4 agonists (Fig. 4*G*).

Ruthenium Red and lanthanides are nonselective TRP channel blockers that also antagonize activation of TRPV4 channels (Liedtke et al., 2000; Strotmann et al., 2000; Watanabe et al., 2002). $[Ca^{2+}]_i$ responses to GSK and 4α-PDD were suppressed by Ruthenium Red (10 μM; $N = 85$) (Fig. 4*D*,*E*,*G*). The antagonist decreased the amplitude of GSK-evoked $[Ca^{2+}]_i$ responses from 341 ± 41 nM ($N = 23$) to 139 ± 22 nM (Fig. 4*G*) ($N = 16$; $p = 0.0001$, Mann–Whitney test) and reduced the percentage of cells responding to GSK from 40.5 ± 6.7 ($N = 10$) to 16.9 ± 4.2% ($N = 4$; $p = 0.026$, unpaired *t* test). In the phorbol ester-

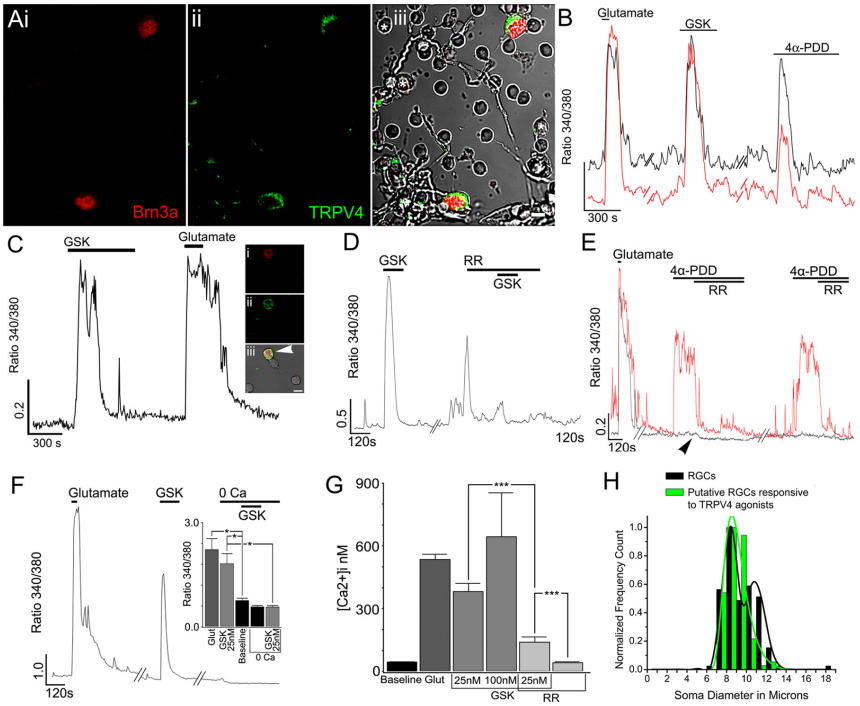

Figure 4. TRPV4 agonists selectively elevate $[Ca^{2+}]_i$ in mouse RGCs. ***A***, Brn3a-IR (***Ai***) and TRPV4 (***Aii***) colocalize in two RGCs (***Aiii***). TRPV4-IR is absent from putative amacrine somata (asterisks). Scale bar, 5 μm. ***B***, Application of GSK1016790A or 4α-PDD induces Ca^{2+} influx into two simultaneously recorded RGCs. ***C***, Four retinal cells immunostained for Brn3a and TRPV4. The cell that responded to GSK with $[Ca^{2+}]_i$ increase, but not nonresponders, exhibited colocalization of Brn3a (***i***) and TRPV4 (***ii***) immunoreactivity after fixation and immunolabeling. ***iii***, Transmitted image with superimposed TRPV4 and Brn3a signals. Scale bar, 5 μm. ***D***, GSK-induced $[Ca^{2+}]_i$ responses are antagonized by Ruthenium Red (RR). ***E***, Simultaneous recording from a putative RGC (red trace) and a putative amacrine cell (black trace) stimulated with 4α-PDD. Ruthenium Red antagonizes TRPV4 agonist responses evoked in the RGC. The amacrine cell is unresponsive to 4α-PDD; however, Ruthenium Red slightly reduced baseline $[Ca^{2+}]_i$ in this cell (arrowhead). ***F***, Putative RGC, stimulated with GSK in the presence and absence of extracellular Ca^{2+}. Extracellular calcium is required for agonist-evoked $[Ca^{2+}]_i$ elevations. Inset, Comparison of $[Ca^{2+}]_i$ for glutamate, GSK, baseline levels in Ca^{2+}-free saline and in 0 Ca^{2+} + 25 nM GSK. ***G***, Cumulative $[Ca^{2+}]_i$ for calibrated RGC baseline and responses to glutamate (100 μM), GSK (25 and 100 nM), GSK (25 nM) + Ruthenium Red (10 μM) and Ruthenium Red alone. $^*p < 0.05$; $^{**}p < 0.001$; $^{***}p < 0.0001$. ***H***, Distribution of cell diameters for dissociated RGCs (Thy1:CFP and Brn3-IR cells; black trace) and putative RGCs that responded to TRPV4 agonists (green trace).

insensitive cell depicted in Figure 4*E*, Ruthenium Red by itself lowered baseline $[Ca^{2+}]_i$ (arrowhead), indicating suppression of tonic Ca^{2+} influx through TRP-like channels. On average, Ruthenium Red decreased baseline $[Ca^{2+}]_i$ from 50 ± 3 nM to 47 ± 4 nM ($N = 133$; $p = 0.0003$, Wilcoxon matched-pairs signed-ranks test).

The rise in intracellular Ca^{2+} induced by exposure to GSK depends on extracellular Ca^{2+}. Figure 4*F* illustrates that a test cell shows normal increases in $[Ca^{2+}]_i$ in responses to GSK in 2 mM $[Ca^{2+}]_o$, but this increase was abolished in zero extracellular $[Ca^{2+}]_o$ ($N = 8$; $p = 0.78$, paired t test). The mean fluorescence changes induced by glutamate or GSK in normal versus zero extracellular Ca^{2+} are summarized in the inset to Figure 4*F*.

Ligand-evoked $[Ca^{2+}]_i$ increases in mouse RGCs can be augmented by secondary contributions from voltage-operated Ca^{2+} channels (Hartwick et al., 2008). We therefore investigated whether the response to 25 nM GSK was affected by suppression of voltage-operated Ca^{2+} entry. In the presence of the nonselective voltage-gated calcium channel antagonist cadmium (Cd^{2+}; 100 μM), high KCl (30 mM)-evoked $[Ca^{2+}]_i$ increases were blocked ($N = 5$; data not shown). Nonetheless, GSK elevated $[Ca^{2+}]_i$ to 355 ± 110 nM in Cd^{2+}-containing saline ($N = 6$), a value not significantly different from responses to the agonist alone ($p > 0.89$, Mann–Whitney test). Cd^{2+} had no significant effect on the percentage of GSK-responding cells (31.3 ± 5.2%; $p > 0.36$, unpaired t test).

A representation of glutamate- and GSK-evoked $[Ca^{2+}]_i$ elevations in a presumed RGC is represented graphically in Figure 5. This cell was proximal to a perikaryon from a presumed rod photoreceptor (Fig. 5*A*). A 60 s exposure to a saturating concentration of the neurotransmitter (100 μM) and sustained (5 min) exposure to GSK (25 nM) evoked an increase in global free $[Ca^{2+}]_i$ across the RGC cytosol, with superimposed local $[Ca^{2+}]_i$ elevations. The response to the TRPV4 agonist desensitized during continued exposure (Fig. 5*J*,*K*) in contrast to responses to sustained $[Ca^{2+}]_i$ elevations that were observed during 3–5 min exposures to glutamate. No changes in $[Ca^{2+}]_i$ were observed in the simultaneously recorded rod perikaryon.

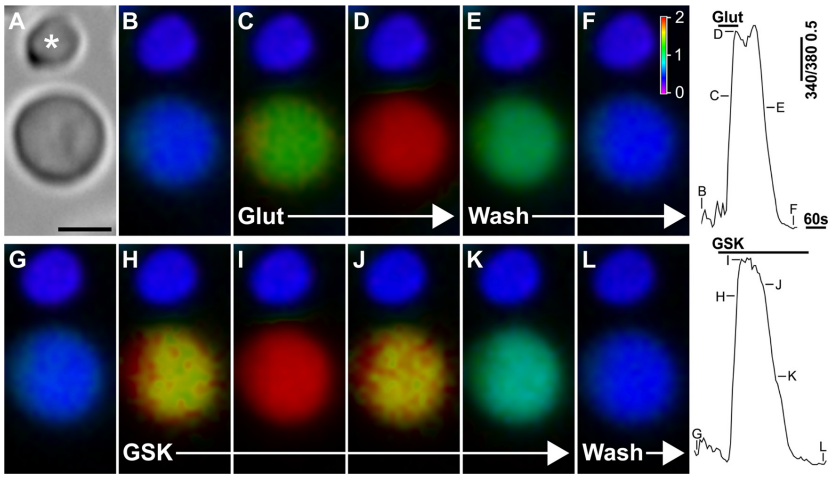

Figure 5. GSK-induced $[Ca^{2+}]_i$ dynamics in an RGC. ***A***, Transmitted image of a putative RGC and rod photoreceptor. Scale bar, 5 μm. The temporal progression of upper and lower image sequences is illustrated by the adjacent traces. ***B***, ***G***, Unstimulated cells perfused with control saline. ***C***, ***D***, The RGC responds to the bath application of glutamate with a large increase in $[Ca^{2+}]_i$. ***E***, ***F***, Washout. Scale bar: ***F***, 340/380 ratio level. ***H–K***, Application of GSK transiently elevates $[Ca^{2+}]_i$ in the RGC but not the rod. ***J***, ***K***, $[Ca^{2+}]_i$ levels decline in the continued presence of GSK. ***L***, Washout.

Hypotonic stimuli evoke changes in cytosolic $[Ca^{2+}]_i$

TRPV4 was originally identified as a plasma membrane channel activated by hypotonic cell swelling (Liedtke et al., 2000; Strotmann et al., 2000; Watanabe et al., 2002; Vriens et al., 2004; Loukin et al., 2010a). A decrease in extracellular osmolarity induces Ca^{2+} influx through TRPV4 channels (Güler et al., 2002; Liedtke and Friedman, 2003; Raoux et al., 2007; Phan et al., 2009). To determine whether hypotonicity modulates $[Ca^{2+}]_{RGCs}$, cells were exposed to saline solutions with osmolarity reduced from 280 to 190 mOsm. As illustrated in Figure 6*A* for an RGC loaded with the Ca^{2+}-insensitive cell-volume indicator dye calcein AM, a reduction in osmolarity of the superfusing saline from 280 to 192 mOsm saline evoked sustained swelling of the cell. The resulting increase in cell volume was detected as a decrease in the intensity of calcein fluorescence (Fig. 6*A*, green trace). In contrast to hypotonic stimuli, no change in intracellular volume was observed during exposure to 100 μM glutamate.

Cell swelling was accompanied by tonicity-dependent elevations in $[Ca^{2+}]_i$. The 190–195 mOsm saline evoked an average $[Ca^{2+}]_i$ increase of 439 ± 59 nM ($N = 48$; $p < 0.0001$) (Fig. 6) in 72 ± 7% of putative RGCs. During continued stretch, $[Ca^{2+}]_i$ levels gradually returned to control levels, indicating desensitization of the mechanosensing mechanism (Fig. 6). The diameters of cells that responded to hypotonic stimulation with $[Ca^{2+}]_i$ increases (8.7 ± 1 μm; $N = 126$) were not significantly different from diameters of dissociated Brn3a-immunopositive cells (9.1 ± 1.5 μm; $p > 0.05$; $N = 74$) (Fig. 6*E*). Swelling-mediated $[Ca^{2+}]_i$ signals also were measured in the presence of gadolinium (Gd^{3+}), a universal antagonist of Ca^{2+}-permeable TRP channels (including TRPV4) (Gustin et al., 1988; Becker et al., 2005). Gd^{3+} (100 μM) reduced, from 72.1 ± 6.7% ($N = 10$) to 26.0 ± 9.5% ($N = 3$ slides), the percentage of RGCs that responded to hypotonic stimulation with a $[Ca^{2+}]_i$ increase ($p < 0.02$, unpaired *t* test, Welch corrected) but had no effect on cell swelling, as indicated by unchanged calcein responses (Fig. 6*A*). Overall, the amplitude of hypotonic stretch-induced $[Ca^{2+}]_i$ increases was reduced by Gd^{3+} to 261 ± 42 nM ($N = 17$; $p < 0.05$, Mann–Whitney test). Hypotonicity-induced $[Ca^{2+}]_i$ responses were suppressed by Ruthenium Red to 206 ± 21 nM ($N = 22$; $p < 0.0001$, Mann–Whitney test) (Fig. 6*C*,*D*), and the percentage of RGCs responding to hypotonic stimulation in the presence of the antagonist decreased from 72.1 ± 6.7% ($N = 10$) to 16.9 ± 4.2% ($N = 3$ slides; $p < 0.005$, unpaired *t* test, Welch corrected).

We asked whether hypotonically induced $[Ca^{2+}]_i$ elevations are mediated by TRPV4. $[Ca^{2+}]_i$ increases induced by TRPV4 agonists and membrane stretch typically desensitized with a time constant of several tens of seconds. Stimulation with GSK at the asymptotic end of the desensitized response elicited little or no change in $[Ca^{2+}]_i$ (169.9 ± 66.2 nM), whereas significant $[Ca^{2+}]_i$ increases (524.0 ± 63.8 nM) were measured following washout with isotonic saline (Fig. 6*G*) ($N = 14$; $p < 0.002$, Wilcoxon matched-pairs signed-ranks test). Of 84.4 ± 4.6% putative RGCs that responded to hypotonic stimuli in this experiment, 2.0 ± 0.7% exhibited a response to GSK during membrane stretch, significantly less than the 51.7 ± 7% that responded to GSK alone ($N = 3$ slides, 14 cells; $p < 0.05$, paired *t* test). To confirm that hypotonic cell swelling evoked Ca^{2+} influx from the extracellular space, cells were challenged with Ca^{2+}-free saline. RGCs responding to hypotonic stimulation in 2 mM Ca^{2+}-containing saline with $[Ca^{2+}]_i$ elevations displayed no change in $[Ca^{2+}]_i$ in Ca^{2+}-free hypotonic saline ($N = 0/14$) (Fig. 6*D*). Thus, stretch-induced $[Ca^{2+}]_i$ elevations in RGCs primarily depend on entry of extracellular Ca^{2+} rather than on release from intracellular stores. Together, these data indicate that RGCs express an osmosensitive channel that exhibits the pharmacological profile of TRPV4.

GSK-responding RGCs constituted a subset of the total hypotonicity-sensitive cell cohort, possibly indicating the expression of other volume increase-sensitive channels within RGCs. We therefore tested for functional expression of TRPV1, another vanilloid TRP channel that has been associated with pressure-sensitive $[Ca^{2+}]_i$ responses in RGCs (Sappington et al., 2009). Under our experimental conditions, the TRPV1 agonist capsai-

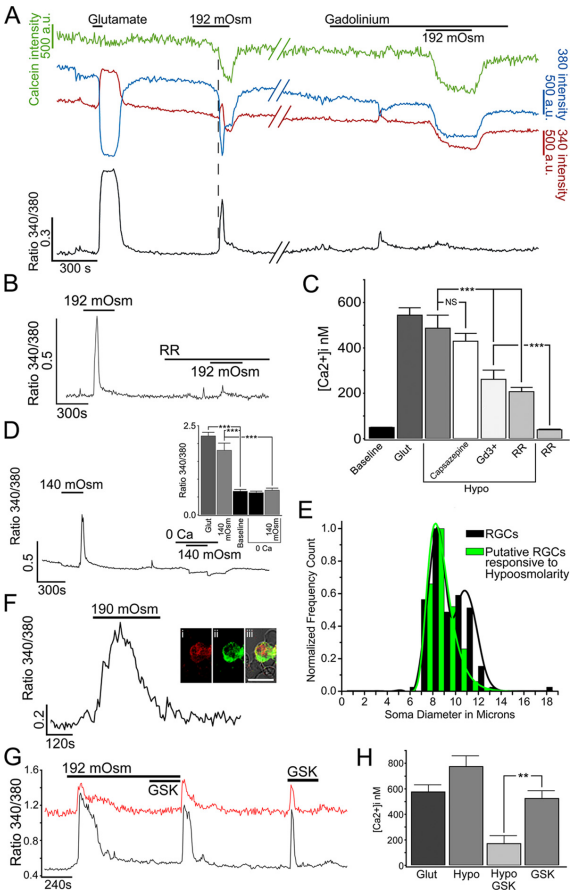

Figure 6. Cell stretch elevates $[Ca^{2+}]_{RGC}$. ***A***, Simultaneous recording of RGC volume (calcein, green trace), 340 nm (red trace), 380 nm (blue trace) intensities, and $[Ca^{2+}]_i$ (fura-2 ratio, black trace). An increase in RGC volume was indicated by a drop in calcein fluorescence intensity during hypotonic stimulation (decreased osmolarity in superfusing saline from 280 to 192 mOsm). Glutamate stimulation increased $[Ca^{2+}]_i$ but evoked no change in the calcein signal. The increase in $[Ca^{2+}]_i$ induced by hypotonic stimulation was antagonized by Gd^{3+}. ***B***, Hypotonically induced $[Ca^{2+}]_i$ elevations are antagonized by Ruthenium Red. ***C***, Cumulative total for calibrated RGC $[Ca^{2+}]_i$ responses to glutamate (100 μM), hypotonic stimulation (192 mOsm), and hypotonic stimulation in the presence of capsazepine, Ruthenium Red (10 μM) or Gd^{3+} (100 μM). NS, $p > 0.05$; *$p < 0.05$; **$p < 0.001$; ***$p < 0.0001$. ***D***, $[Ca^{2+}]_i$ trace from a GSK-sensitive RGC. Hypotonically evoked $[Ca^{2+}]_i$ increase requires Ca^{2+} influx from the extracellular space. Inset, Relative $[Ca^{2+}]_i$ totals for control and hypotonically stimulated RGCs with and without the presence of extracellular calcium. ***E***, Distribution of cell diameters from dissociated RGCs (Thy1:CFP and Brn3-IR cells; black trace) and the hypotonicity-responding cohort (green trace). ***F***, Hypotonicity-responding cell, labeled with TRPV4 and Brn3a antibodies. Scale bar, 10 μm. ***G***, Hypotonicity-induced membrane stretch occludes the response to GSK. The volume decrease following the hypotonic step was associated with a transient increase in $[Ca^{2+}]_i$. ***H***, Cumulative calibrated responses to glutamate (100 μM), hypotonic stimulation (190–195 mOsm), GSK (25 nM) and GSK in the presence of hypotonic stretch shows a marked reduction in the amplitude of the TRPV4 agonist-evoked response during mechanical stimulation.

cin (5–100 μM) did not induce a rise in $[Ca^{2+}]_i$ in acutely isolated mouse RGCs ($N > 110$). Moreover, the selective TRPV1 antagonist capsazepine (5 μM) had no effect on the amplitude of hypotonic stretch-evoked increases (487 ± 59 nM in controls; $N = 48$ vs 429 ± 48 in the presence of capsazepine; $N = 29$; $p = 0.39$, Mann–Whitney test) (Fig. 6*C*) or the percentage of cells responding to hypotonic stimulation ($N = 2$; 62.0 ± 14.9%; $p = 0.62$, unpaired t test). These results argue against a significant role for TRPV1 signals in stretch-evoked Ca^{2+} signaling in mouse RGCs.

TRPV4 agonists modulate RGC firing

Given that TRPV4 activation elevates $[Ca^{2+}]$ in RGCs, we asked whether the depolarizing cation influx through the TRPV4 channel modulates RGC excitability. Intact retinas were isolated from the eye and positioned on MEAs, which allow recording of spontaneous spikes from many RGCs simultaneously (Rentería et al., 2006). Perfusion with the TRPV4 agonists 4α-PDD (5 μM) or GSK (100 or 300 nM) evoked a transient increase in the frequency of spontaneous firing in a subset of recorded RGCs. The spike rates of three RGCs, in which typical increases in spiking after GSK application occurred, are shown in Figure 7*A*. For all recorded cells, the average firing rate during the first 3 min after drug application was compared with the preapplication frequency (4α-PDD: $N = 160$ RGCs from three retinas; GSK: $N = 115$ RGCs from 4 retinas). Figure 7, *B* and *C*, shows the changes in cell firing evoked by each TRPV4 agonist as a percentage of the preapplication firing frequency. Each agonist evoked increased spike rates of twofold or more in a large percentage of the recorded RGCs (Fig. 7*B*,*C*, arrows) ($p < 0.00001$ for 4α-PDD; $p < 0.02$ for GSK; Wilcoxon signed-rank test). The increase in spike rate during drug application was transient, exhibiting significant adaptation in the continued presence of drug (Fig. 7*A*). Displaced amacrine cells either do not spike (Zhou and Fain, 1996) or express few action potentials in response to depolarizing current injection (Ozaita et al., 2004). This suggests that the majority of cells responding to TRPV4 agonists were RGCs, although some nonresponders (5–10%/retina) may have been displaced amacrine cells. These experiments indicate that TRPV4 activation transiently increased RGC excitability and augmented RGC output from the retina.

Sustained activation of TRPV4 channels is cytotoxic for RGCs

We next considered whether extended stimulation with a TRPV4 agonist impacts the survival of acutely isolated RGCs. As shown previously (Otori et al., 1998; Hartwick et al., 2008), 1 h incubation with the AMPA/KA receptor agonist kainate (10 μM) increased the number of TUNEL-positive cells by 68 ± 7% ($N = 305$; $p < 0.0001$, Mann–Whitney) (Fig. 8*B*,*D*), whereas RGCs exposed only to control saline supplemented with L15 showed little TUNEL signal (Fig. 8*A*,*D*). Exposure

to GSK1016790A induced significant cell death, which was confined to cells with large somata (>6 μm, arrowheads). The 25 nM GSK induced TUNEL-positive signals in 33 ± 7% ($N = 1523$; $p = 0.0002$), and 100 nM GSK induced TUNEL labeling in 67 ± 13% of presumed RGCs ($N = 917$; $p < 0.0005$). GSK had relatively little effect on signals in presumed photoreceptor perikarya (cell diameters, 3–5 μm; arrows).

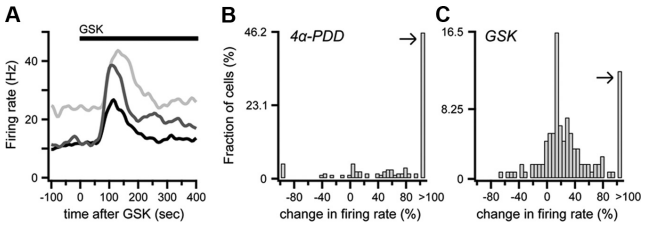

Figure 7. TRPV4 agonists transiently increase spontaneous firing rate of RGCs. ***A***, The spontaneous firing rates of three RGCs recorded on a multielectrode array are shown during the application of GSK at time 0 (300 nM; black bar). The rate increased for 2–3 min before returning to the initial baseline level during the continued presence of the drug for nearly all responsive cells. ***B***, A histogram of the change in firing rates of individual RGCs during the 3 min after 4α-PDD (5 μM) application compared with the pretreatment firing rate is shown for all cells recorded from three treated retinas. Cells with a rate double or higher in drug are combined in the rightmost bin (>100; arrow); nearly half of the cells were in this category, and most cells increased their firing. As with GSK, the increase was transient (not illustrated). ***C***, Histogram as in ***B***, but here the applied drug was GSK (100 or 300 nM; $N = 4$ retinas). As in ***B***, cells with a spike rate double or higher during the initial period of drug exposure are combined in the rightmost bin (>100; arrow), constituting >12% of the recorded cells. The bias in the distribution to positive values reveals that most cells increased firing in response to GSK application.

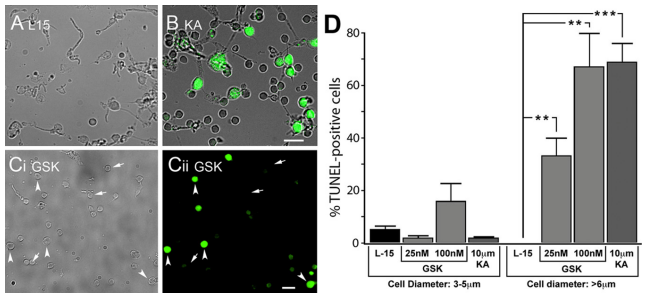

Figure 8. Exposure to TRPV4 agonist induces RGC apoptosis. ***A***, TUNEL (FITC) + transmitted image in control dissociated mouse retinal cells. No TUNEL staining is observed under control conditions. ***B***, TUNEL staining + transmitted image. Cells were exposed to kainate (KA; 10 μM) for 1 h. ***Ci***, ***Cii***, Transmitted image and TUNEL staining in cells exposed for 1 h to 25 nM GSK. Arrowheads point at putative RGCs; arrows point at putative photoreceptors. Scale bars, 10 μm. ***D***, Cumulative data for putative photoreceptors (cell diameters 3–5 μm) and putative RGCs (cell diameters >6 μm) in L15 medium, 25 nM GSK, 100 nM GSK, and KA in all experiments. $^{**}p < 0.001$; $^{***}p < 0.0001$.

Discussion

This study provides anatomical, molecular, and physiological evidence that the polymodal pressure-sensitive TRPV4 ion channel participates in the transduction of hypotonic stimuli and contributes to Ca^{2+}-dependent intracellular signaling and membrane excitability of mammalian RGCs. First, we have shown that the wild-type mouse retina expresses TRPV4 mRNA and protein. Second, we show that the TRPV4 protein is localized primarily in RGC somata and axons. Third, using Ca^{2+} imaging and MEA recording, we directly demonstrate that TRPV4 channels contribute to transmembrane Ca^{2+} flux and spike firing rates of RGCs. Finally, we show that pharmacological characteristics of hypotonicity-induced $[Ca^{2+}]_i$ increases in RGCs match the known pharmacology of TRPV4 and that sustained activation of this subtype of TRPV channels initiates cell death pathways in RGCs.

In the mouse retina, almost every cell identified with RGC-specific markers (Thy1:CFP; Thy1:GFP; Brn3a; SMI-32) was immunopositive for TRPV4, indicating that all identified RGC perikarya express TRPV4. TRPV4-IR was particularly prominent within RGC axons in the nerve fiber layer and the optic nerve head, both of which represent initial targets for deleterious effects of increased IOP. TRPV4 staining was excluded from amacrine, astrocytic, and microglial processes in the retina but was apparent in Müller cell processes. Our demonstration of the localization of the channels to RGCs suggests that retinal output neurons are capable of transducing mechanical, thermal, and/or osmotic stimuli.

Functional role for TRPV4 in the retina

Cell stretch induced by hypotonic swelling caused a marked increase in $[Ca^{2+}]_i$ of RGCs. Because the resting membrane potential of RGCs is within the operational range for inactivating and persistent Na^+ conductances (~ −60 mV) (Kim and Rieke, 2003; Hayashida and Ishida, 2004; Margolis et al., 2010), we postulate that sustained depolarization through stretch-sensitive cation-permeable channels will contribute to the excitability and dynamic range of RGC responses (Shibasaki et al., 2007) by countering, in a significant subset of RGCs, the tonic inhibition mediated by GABAergic and glycinergic amacrines. Consistent with this hypothesis, TRPV4 activators 4α-PDD and GSK1016790A elevated $[Ca^{2+}]_i$ and caused a >100-fold increase in the frequency of spontaneous RGC spiking. While TRPV4 activation may also have influenced the increase in spiking through reciprocal neuroglial interactions (Newman, 2001), the comparable time courses of agonist-evoked $[Ca^{2+}]_i$ signals and spike firing argues for a predominant action on RGCs themselves. This finding may be relevant to entoptic physiology as it implicates TRPV4 channels in the perception of "pressure phosphenes" believed to originate in RGCs (Grüsser et al., 1989).

The effects of pharmacological and hypotonic stimulation observed in RGCs are consistent with properties of heterologously expressed and endogenous TRPV4 channels (Liedtke et al., 2000; Strotmann et al., 2000; Becker et al., 2005; Hartmannsgruber et al., 2007). Plasma membrane ion channels activated by an increase in cell volume were reported to be identical to TRPV4 agonist-sensitive channels with respect to Ca^{2+} permeability, rectification behavior, and permeability sequence of monovalent cations (Watanabe et al., 2002; Phan et al., 2009). While all Brn3a-IR and Thy1:CFP-positive cells labeled with TRPV4 antibodies, only a subset of dissociated putative RGCs was activated by hypotonic stimulation (~72%) or TRPV4 agonists (~16.7–

95.8%). We attribute the variability in stretch- and agonist-induced responses to the mechanical trauma associated with the dissociation protocol, which may have compromised a necessary step in TRPV4 activation. It is possible that, as suggested for other tissues (Raoux et al., 2007; Sharif-Naeini et al., 2008; Alessandri-Haber et al., 2009), RGC plasma membranes have other volume increase-sensitive channels such as TRPC1, TRPV1, TRPV2, TREK-1, 2, or TRAAK (TWIK-related arachidonic acid-stimulated potassium channel) (Maingret et al., 1999; Reyes et al., 2000; Križaj, 2005; Leonelli et al., 2009). In particular, TRPV1 was recently implicated in mediating $[Ca^{2+}]_i$ increases and pressure-induced apoptotic cell death in cultured rat RGCs (Sappington et al., 2009). While no isoforms of TRPV1 are known to be affected by hypotonic stimulation (Liedtke et al., 2000; Strotmann et al., 2000; Loukin et al., 2009) and stimulation with specific TRPV1 agonists/antagonists failed to induce changes in $[Ca^{2+}]_i$ in acutely dissociated mouse RGCs under isotonic or hypotonic conditions, the difference between our study and that of Sappington et al. (2009) can be attributed in part to the dramatic upregulation of *Trpv1* gene expression in cultured RGCs. We propose that TRPV4 is a necessary sensing/transducer protein that participates in the RGC response to volume increase, whereas TRPV1 may contribute to RGC excitability as well, once upregulated under certain culture conditions.

Consistent with a role in sensory transduction, TRPV4 is expressed in sensory neurons of dorsal root ganglia, in the trigeminal ganglion, and in hair cells (Liedtke et al., 2000; Alessandri-Haber et al., 2009). A major TRPV4 role in healthy RGCs may be to function as an osmoreceptor (Liedtke et al., 2003; Liedtke and Kim, 2005). The RGC cytosolic volume should be susceptible to local changes in tonicity that occur during the light response or retinal waves (Huang and Karwoski, 1992; Dmitriev et al., 1999). Swelling-induced increases in $[Ca^{2+}]_i$, but not swelling itself, were suppressed by Gd^{3+} and Ruthenium Red, two compounds that inhibit osmosensory transduction (Liedtke et al., 2003; Bourque, 2008). Activation of endogenous TRPV4 channels has been implicated in other mechanotransduction events including shear stress in vascular endothelia (Hartmannsgruber et al., 2007), stretch-induced integrin signaling (Thodeti et al., 2009), shear stress-mediated relaxation of endothelial cells (Mendoza et al., 2010), and viscous load-coupled ciliary activity in epithelial cells (Andrade et al., 2005).

Implications for glaucoma

TRPV4 localization to the NFL, ONH and the proximal optic nerve together with proapoptotic effects of sustained TRPV4 channel stimulation appear to implicate this channel in the initiation and progression of glaucomatous remodeling. The pressure-induced activation range of TRPV4 (10–30 mmHg) (Loukin et al., 2010b) matches the sustained IOP elevations in chronic glaucoma that can span a range of 10 to several tens of mmHg over the control value of 10–15 mmHg (Bonomi et al., 2001; Quigley, 2005; Whitmore et al., 2005). Increases in hydrostatic or intraocular pressure are correlated with RGC death in cell cultures (Tezel and Wax, 2000; Agar et al., 2006), isolated retinas (Resta et al., 2007), the acute rat glaucoma model (Morrison et al., 1997), the chronic DBA/2J mouse model (John et al., 1998; Libby et al., 2005b), and human glaucoma patients (Bonomi et al., 2001; Gordon et al., 2002), whereas lowering of the IOP slows the progression of axonal loss at all stages of glaucomatous degeneration (Quigley, 2005). Rapid and severe IOP rises (such as occur in acute angle closure glaucoma) (Saw et al., 2003) may cause RGC loss within hours (Naskar et al., 2002) by compromising RGC function at their axons (Quigley, 1983) and their cell bodies (Libby et al., 2005a; Agar et al., 2006; Liu et al., 2007).

Our calcium imaging and immunolocalization experiments suggest that RGC perikarya and axons could be targeted by changes in mechanical and osmotic pressure. At the level of the perikaryon, $[Ca^{2+}]_{RGC}$ increases induced by membrane stretch and TRPV4 agonists had maximal amplitudes comparable to levels evoked by intense stimulation of ionotropic glutamate receptors. Consistent with the hypothesis that RGCs represent the first responder to an acute increase in IOP is the finding that the cornea-positive arm of the scotopic threshold response, the component of the visual ERG response that is the most sensitive to increased IOP, has a significant contribution from RGCs (Bui and Fortune, 2004; Kong et al., 2009). While retinal astrocytes and microglia were not immunolabeled by the TRPV4 antibody, it remains to be determined whether retinal glial TRPV4 expression is affected by sustained IOP increases, a possibility based on TRPV4 expression in cortical astrocytes (Benfenati et al., 2007) and the sensitivity of astrocyte Ca^{2+} homeostasis to increases in hydrostatic pressure (Mandal et al., 2010).

While the *Trpv4* gene plays a critical function in regulation of systemic tonicity in mammals (Liedtke et al., 2000; Bourque, 2008; McHugh et al., 2010), inappropriate activation of TRPV4 in rodents and canines produces an acute circulatory collapse associated with edema, pulmonary hypertension, endothelial injury, ischemia, and/or cell death (Willette et al., 2008). We report that sustained exposure to TRPV4 agonists compromises the viability of mouse RGCs by triggering the apoptotic process, consistent with the observation that even low levels of elevated $[Ca^{2+}]_i$ are toxic for RGCs if sustained over an extended period of time (Hartwick et al., 2008). RGCs express the PAR-2 receptor that has been implicated in sensitization of TRPV4 to mechanical stimuli (Luo et al., 2005; Grant et al., 2007). Moreover, gain-of-function TRPV4 mutations cause a range of cellular problems that include axonal neuropathy and suppression of growth (Camacho et al., 2010; Loukin et al., 2010b; Zimoń et al., 2010). Thus, antagonizing excessive TRPV4 activation may be protective against apoptosis in RGCs stressed by sustained mechanical and/or osmotic stimulation.

Together, our data indicate the presence, in mammalian RGCs, of a novel background cation-permeable channel that confers mechanical/pressure sensitivity to cells that convey light-evoked signals to visual centers in the brain. The TRPV4 mechanism in RGCs represents a prime molecular target for severe blinding diseases such as diabetic retinopathy and glaucoma.

References

Agar A, Li S, Agarwal N, Coroneo MT, Hill MA (2006) Retinal ganglion cell line apoptosis induced by hydrostatic pressure. Brain Res 1086:191–200.

Alessandri-Haber N, Dina OA, Chen X, Levine JD (2009) TRPC1 and TRPC6 channels cooperate with TRPV4 to mediate mechanical hyperalgesia and nociceptor sensitization. J Neurosci 29:6217–6228.

Andrade YN, Fernandes J, Vázquez E, Fernández-Fernández JM, Arniges M, Sánchez TM, Villalón M, Valverde MA (2005) TRPV4 channel is involved in the coupling of fluid viscosity changes to epithelial ciliary activity. J Cell Biol 168:869–874.

Becker D, Blase C, Bereiter-Hahn J, Jendrach M (2005) TRPV4 exhibits a functional role in cell-volume regulation. J Cell Sci 118:2435–2440.

Benfenati V, Amiry-Moghaddam M, Caprini M, Mylonakou MN, Rapisarda C, Ottersen OP, Ferroni S (2007) Expression and functional characterization of transient receptor potential vanilloid-related channel 4 (TRPV4) in rat cortical astrocytes. Neuroscience 148:876–892.

Bonomi L, Marchini G, Marraffa M, Morbio R (2001) The relationship be-

tween intraocular pressure and glaucoma in a defined population: data from the Egna-Neumark glaucoma study. Ophthalmologica 215:34–38.
Bourque CW (2008) Central mechanisms of osmosenstation and systemic osmoregulation. Nat Rev Neurosci 9:519–531.
Brierley SM, Page AJ, Hughes PA, Adam B, Liebregts T, Cooper NJ, Holtmann G, Liedtke W, Blackshaw LA (2008) Selective role for TRPV4 ion channels in visceral sensory pathways. Gastroenterology 134:2059–2069.
Bui BV, Fortune B (2004) Ganglion cell contributions to the rat full-field electroretinogram. J Physiol 555:153–173.
Camacho N, Krakow D, Johnykutty S, Katzman PJ, Pepkowitz S, Vriens J, Nilius B, Boyce BF, Cohn DH (2010) Dominant TRPV4 mutations in nonlethal and lethal metatropic dysplasia. Am J Med Genet A 152A: 1169–1177.
Christensen AP, Corey DP (2007) TRP channels in mechanosensation: direct of indirect activation? Nat Rev Neurosci 8:510–521.
Copeland NG, Jenkins NA, Court DL (2001) Recombineering: a powerful new tool for mouse functional genomics. Nat Rev Genet 2:769–779.
Dmitriev AV, Govardovskii VI, Schwahn HN, Steinberg RH (1999) Light-induced changes of extracellular ions and volume in the isolated chick retina-pigment epithelium preparation. Vis Neurosci 16:1157–1167.
Duncan JL, Yang H, Doan T, Silverstein RS, Murphy GJ, Nune G, Liu X, Copenhagen D, Tempel BL, Rieke F, Križaj D (2006) Scotopic visual signaling in the mouse retina is modulated by high-affinity plasma membrane calcium extrusion. J Neurosci 26:7201–7211.
Gavrieli Y, Sherman Y, Ben-Sasson SA (1992) Identification of programmed cell death in situ via specific labeling of nuclear DNA fragmentation. J Cell Biol 119:493–501.
Gordon MO, Beiser JA, Brandt JD, Heuer DK, Higginbotham EJ, Johnson CA, Keltner JL, Miller JP, Parrish RK 2nd, Wilson MR, Kass MA (2002) The ocular hypertension treatment study. Arch Ophthalmol 120:714–720.
Grant AD, Cottrell GS, Amadesi S, Trevisani M, Nicoletti P, Materazzi S, Altier C, Cenac N, Zamponi GW, Bautista-Cruz F, Lopez CB, Joseph EK, Levine JD, Liedtke W, Vanner S, Vergnolle N, Geppetti P, Bunnett NW (2007) Protease-activated receptor 2 sensitizes the transient receptor potential vanilloid 4 ion channel to cause mechanical hyperalgesia in mice. J Physiol 578:715–733.
Grüsser OJ, Grüsser-Cornehls U, Kusel R, Przybyszewski AW (1989) Responses of retinal ganglion cells to eyeball deformation: a neurophysiological basis for "pressure phosphenes." Vision Res 29:181–194.
Güler AD, Lee H, Iida T, Shimizu I, Tominaga M, Caterina M (2002) Heat-evoked activation of the ion channel, TRPV4. J Neurosci 22:6408–6414.
Gustin MC, Zhou XL, Martinac B, Kung C (1988) A mechanosensitive ion channel in the yeast plasma membrane. Science 242:762–765.
Hartmannsgruber V, Heyken WT, Kacik M, Kaistha A, Grgic I, Harteneck C, Liedtke W, Hoyer J, Köhler R (2007) Arterial response to shear stress critically depends on endothelial TRPV4 expression. PLoS ONE 2:e827.
Hartwick AT, Hamilton CM, Baldridge WH (2008) Glutamatergic calcium dynamics and deregulation of rat retinal ganglion cells. J Physiol 586:3425–3446.
Hayashida Y, Ishida AT (2004) Dopamine receptor activation can reduce voltage-gated Na^+ current by modulating both entry into and recovery from inactivation. J Neurophysiol 92:3134–3141.
Huang B, Karwoski CJ (1992) Light-evoked expansion of subretinal space volume in the retina of the frog. J Neurosci 12:4243–4252.
Jeon CJ, Strettoi E, Masland RH (1998) The major cell populations of the mouse retina. J Neurosci 18:8936–8946.
John SW, Smith RS, Savinova OV, Hawes NL, Chang B, Turnbull D, Davisson M, Roderick TH, Heckenlively JR (1998) Essential iris atrophy, pigment dispersion, and glaucoma in DBA/2j mice. Invest Ophthalmol Vis Sci 39:951–962.
Kim KJ, Rieke F (2003) Slow Na^+ inactivation and variance adaptation in salamander retinal ganglion cells. J Neurosci 23:1506–1516.
Kong YX, Crowston JG, Vingrys AJ, Trounce IA, Bui VB (2009) Functional changes in the retina during and after acute intraocular pressure elevation in mice. Invest Ophthalmol Vis Sci 50:5732–5740.
Križaj D (2005) Compartmentalization of calcium entry pathways in mouse rods. Eur J Neurosci 22:3292–3296.
Kung C (2005) A possible unifying principle for mechanosensation. Nature 436:647–654.
Leonelli M, Martins DO, Kihara AH, Britto LR (2009) Ontogenetic expression of the vanilloid receptors TRPV1 and TRPV2 in the rat retina. Int J Dev Neurosci 27:709–718.
Libby RT, Li Y, Savinova OV, Barter J, Smith RS, Nickells RW, John SW (2005a) Susceptibility to neurodegeneration in a glaucoma is modified by Bax gene dosage. PLoS Genet 1:17–26.
Libby RT, Gould DB, Anderson MG, John SW (2005b) Complex genetics of glaucoma susceptibility. Annu Rev Genomics Hum Genet 6:15–44.
Liedtke W, Friedman JM (2003) Abnormal osmotic regulation in $trpv4^{-/-}$ mice. Proc Natl Acad Sci U S A 100:13698–13703.
Liedtke W, Kim C (2005) Functionality of the TRPV subfamily of TRP ion channels: add mechano-TRP and osmo-TRP to the lexicon! Cell Mol Life Sci 62:2985–3001.
Liedtke W, Choe Y, Martí-Renom MA, Bell AM, Denis CS, Sali A, Hudspeth AJ, Friedman JM, Heller S (2000) Vanilloid receptor-related osmotically activated channel (VR-OAC), a candidate vertebrate osmoreceptor. Cell 103:525–535.
Liedtke W, Tobin DM, Bargmann CI, Friedman JM (2003) Mammalian TRPV4 (VR-OAC) directs behavioral responses to osmotic and mechanical stimuli in Caenorhabditis elegans. Proc Natl Acad Sci U S A 100:14531–14536.
Liu Q, Ju WK, Crowston JG, Xie F, Perry G, Smith MA, Lindsey JD, Weinreb RN (2007) Oxidative stress is an early event in hydrostatic pressure-induced retinal ganglion cell damage. Invest Ophthalmol Vis Sci 48:4580–4589.
Liu W, Khare SL, Liang X, Peters MA, Liu X, Cepko CL, Xiang M (2000) All Brn3 genes can promote retinal ganglion cell differentiation in the chick. Development 127:3237–3247.
Loukin SH, Su Z, Kung C (2009) Hypotonic shocks activate rat TRPV4 in yeast in the absence of polyunsaturated fatty acids. FEBS Lett 583:754–758.
Loukin S, Su Z, Zhou X, Kung C (2010a) Forward genetic analysis reveals multiple gating mechanisms of TRPV4. J Biol Chem 285:19884–19890.
Loukin S, Zhou X, Su Z, Saimi Y, Kung C (2010b) Wild-type and brachyolmia-causing mutant TRPV4 channels respond directly to stretch force. J Biol Chem 285:27176–27181.
Luo W, Wang Y, Reiser G (2005) Two types of protease-activated receptors (PAR-1 and PAR-2) mediate calcium signaling in rat retinal ganglion cells RGC-5. Brain Res 1047:159–167.
Maingret F, Fosset M, Lesage F, Lazdunski M, Honoré E (1999) TRAAK is a mammalian neuronal mechano-gated K+ channel. J Biol Chem 274:1381–1387.
Mandal A, Shahidullah M, Delamere NA (2010) Hydrostatic pressure-induced release of stored calcium in cultured rat optic nerve head astrocytes. Invest Ophthalmol Vis Sci 51:3129–3138.
Margolis DJ, Gartland AJ, Euler T, Detwiler PB (2010) Dendritic calcium signaling in ON and OFF mouse retinal ganglion cells. J Neurosci 30:7127–7138.
May CA, Nakamura K, Fujiyama F, Komatsu Y, Yanagawa Y (2007) Homozygous GAD65 and heterozygous GAD67 knock-out mice reveal normal retinal development and maintenance despite reduced amounts of GABA. Acta Neuropathol 113:101–103.
McHugh J, Keller NR, Appalsamy M, Thomas SA, Raj SR, Diedrich A, Biaggioni I, Jordan J, Robertson D (2010) Portal osmopressor mechanism linked to transient receptor potential vanilloid 4 and blood pressure control. Hypertension 55:1438–1443.
Mendoza SA, Fang J, Gutterman DD, Wilcox DA, Bubolz AH, Li R, Suzuki M, Zhang DX (2010) TRPV4-mediated endothelial Ca^{2+} influx and vasodilation in response to shear stress. Am J Physiol Heart Circ Physiol 298:H466–H476.
Morrison JC, Moore CG, Deppmeier LM, Gold BG, Meshul CK, Johnson EC (1997) A rat model of chronic pressure-induced optic nerve damage. Exp Eye Res 64:85–96.
Nadal-Nicolás FM, Jiménez-López M, Sobrado-Calvo P, Nieto-López L, Cánovas-Martínez I, Salinas-Navarro M, Vidal-Sanz M, Agudo M (2009) Brn3a as a marker of retinal ganglion cells: qualitative and quantitative time course studies in naïve and optic nerve-injured retinas. Invest Ophthalmol Vis Sci 50:3860–3868.
Naruse K, Yamada T, Sokabe M (1998) Involvement of SA channels in orienting response of cultured endothelial cells to cyclic stretch. Am J Physiol 274:H1532–H1538.
Naskar R, Wissing M, Thanos S (2002) Detection of early neuron degener-

ation and accompanying microglial responses in the retina of a rat model of glaucoma. Invest Ophthalmol Vis Sci 43:2962–2968.
Neher E (1995) The use of fura-2 for estimating Ca buffers and Ca fluxes. Neuropharmacology 34:1423–1442.
Newman EA (2001) Calcium signaling in retinal glial cells and its effect on neuronal activity. Prog Brain Res 132:241–254.
O'Neil RG, Heller S (2005) The mechanosensitive nature of TRPV channels. Pflugers Arch 451:193–203.
Otori Y, Wei JY, Barnstable CJ (1998) Neurotoxic effects of low doses of glutamate on purified rat retinal ganglion cells. Invest Ophthalmol Vis Sci 39:972–981.
Ozaita A, Petit-Jacques J, Völgyi B, Ho CS, Joho RH, Bloomfield SA, Rudy B (2004) A unique role for Kv3 voltage-gated potassium channels in starburst amacrine cell. J Neurosci 24:7335–7343.
Perry VH, Walker M (1980) Amacrine cells, displaced amacrine cells and interplexiform cells in the retina of the rat. Proc R Soc Lond B Biol Sci 208:415–431.
Phan MN, Leddy HA, Votta BJ, Kumar S, Levy DS, Lipshutz DB, Lee SH, Liedtke W, Guilak F (2009) Functional characterization of TRPV4 as an osmotically sensitive ion channel in porcine articular chondrocytes. Arthritis Rheum 60:3028–3037.
Quigley HA (1983) Experimental glaucoma damage mechanism. Arch Ophthalmol 101:1301–1302.
Quigley HA (2005) Glaucoma: macrocosm to microcosm the Friedenwald Lecture. Invest Ophthalmol Vis Sci 26:2662–2670.
Raoux M, Rodat-Despoix L, Azorin N, Giamarchi A, Hao J, Maingret F, Crest M, Coste B, Delmas P (2007) Mechanosensor channels in mammalian somatosensory neurons. Sensors 7:1667–1682.
Raymond ID, Pool AL, Vila A, Brecha NC (2009) A thy1-CFP DBA/2J mouse line with cyan fluorescent protein expression in retinal ganglion cells. Vis Neurosci 26:453–465.
Reiter B, Kraft R, Günzel D, Zeissig S, Schulzke JD, Fromm M, Harteneck C (2006) TRPV4-mediated regulation of epithelial permeability. FASEB J 20:1802–1812.
Rentería RC, Tian N, Cang J, Nakanishi S, Stryker MP, Copenhagen DR (2006) Intrinsic ON responses of the retinal OFF pathway are suppressed by the ON pathway. J Neurosci 26:11857–11869.
Resta V, Novelli E, Vozzi G, Scarpa C, Caleo M, Ahluwalia A, Solini A, Santini E, Parisi V, Di Virgilio F, Galli-Resta L (2007) Acute retinal ganglion cell injury caused by intraocular pressure spikes is mediated by endogenous extracellular ATP. Eur J Neurosci 25:2741–2754.
Reyes R, Lauritzen I, Lesage F, Ettaiche M, Fosset M, Lazdunski M (2000) Immunolocalization of the arachidonic acid and mechanosensitive baseline traak potassium channel in the nervous system. Neuroscience 95:893–901.
Sappington RM, Sidorova T, Long DJ, Calkins DJ (2009) TRPV1: contribution to retinal ganglion cell apoptosis and increased intracellular Ca^{2+} with exposure to hydrostatic pressure. Invest Ophthalmol Vis Sci 50:717–728.
Saw SM, Gazzard G, Friedman DS (2003) Interventions for angle-closure glaucoma: an evidence-based update. Ophthalmology 110:1869–1878.
Sharif-Naeini R, Ciura S, Zhang Z, Bourque CW (2008) Contribution of TRPV channels to osmosensory transduction, thirst, and vasopressin release. Kidney Int 73:811–815.
Shibasaki K, Suzuki M, Mizuno A, Tominaga M (2007) Effects of body temperature on neural activity in the hippocampus: regulation of resting membrane potentials by transient receptor potential vanilloid 4. J Neurosci 27:1566–1575.
Strotmann R, Harteneck C, Nunnenmacher K, Schultz G, Plant TD (2000) OTRPC4, a nonselective cation channel that confers sensitivity to extracellular osmolarity. Nat Cell Biol 2:695–702.
Suzuki M, Mizuno A, Kodaira K, Imai M (2003) Impaired pressure sensation with mice lacking TRPV4. J Biol Chem 278:22664–22668.
Szikra T, Barabas P, Bartoletti TM, Huang W, Akopian A, Thoreson WB, Križaj D (2009) Calcium homeostasis and cone signaling are regulated by interactions between calcium stores and plasma membrane ion channels. PLoS One 4:e6723.
Tezel G, Wax MB (2000) Increased production of tumor necrosis factor-alpha by glial cells exposed to simulated ischemia or elevated hydrostatic pressure induces apoptosis in cocultured retinal ganglion cells. J Neurosci 20:8693–8700.
Thodeti CK, Matthews B, Ravi A, Mammoto A, Ghosh K, Bracha AL, Ingber DE (2009) TRPV4 channels mediate cyclic strain-induced endothelial cell reorientation through integrin-to-integrin signaling. Circ Res 104:1123–1130.
Thorneloe KS, Sulpizio AC, Lin Z, Figueroa DJ, Clouse AK, McCafferty GP, Chendrimada TP, Lashinger ES, Gordon E, Evans L, Misajet BA, Demarini DJ, Nation JH, Casillas LN, Marquis RW, Votta BJ, Sheardonw SA, Xu X, Brooks DP, Laping JN, et al. (2008) *N*-((1*S*)-1-{[4-((2*S*)-2-{[(2,4-Dichlorophenyl)sulfonyl]amino }-3-hydroxypropanoyl)-1-piperazinyl] carbonyl}-3-methylbutyl)-1-benzothiophene-2-carboxamide (GSK1016790A), a novel and potent transient receptor potential vanilloid 4 channel agonist induces urinary bladder contraction and hyperactivity: Part I. J Pharmacol Exp Ther 326:432–442.
Vriens J, Watanabe H, Janssens A, Droogmans G, Voets T, Nilius B (2004) Cell swelling, heat, and chemical agonists use distinct pathways for the activation of the cation channel TRPV4. Proc Natl Acad Sci U S A 101:396–401.
Vriens J, Owsianik G, Janssens A, Voets T, Nilius B (2007) Determinants of 4 alpha-phorbol sensitivity in transmembrane domains 3 and 4 of the cation channel TRPV4. J Biol Chem 282:12796–12803.
Wang JH, Thampatty BP (2006) An introductory review of cell mechanobiology. Biomech Model Mechanobiol 5:1–16.
Watanabe H, Davis JB, Smart D, Jerman JC, Smith GD, Hayes P, Vriens J, Cairns W, Wissenbach U, Prenen J, Flockerzi V, Droogmans G, Benham CD, Nilius B (2002) Activation of TRPV4 channels (hVRL-2/mTRP12) by phorbol derivatives. J Biol Chem 277:13569–13577.
Whitmore AV, Libby RT, John SW (2005) Glaucoma: thinking in new ways—a role for autonomous axonal self-destruction and other compartmentalised processes? Prog Retin Eye Res 24:639–662.
Willette RN, Bao W, Nerurkar S, Yue TL, Doe CP, Stankus G, Turner GH, Ju H, Thomas H, Fishman CE, Sulpizio A, Behm DJ, Hoffman S, Lin Z, Lozinskaya I, Casillas LN, Lin M, Trout RE, Votta BJ, Thorneloe K, et al. (2008) Systemic activation of the transient receptor potential V4 channel causes endothelial failure and circulatory collapse. J Pharmacol Exp Ther 326:443–452.
Wu X, Davis MJ (2001) Characterization of stretch-activated cation current in coronary smooth muscle cells. Am J Physiol Heart Circ Physiol 280:H1751–H1761.
Zabel M, Koller BS, Sachs F, Franz MR (1996) Stretch-induced voltage changes in the isolated beating heart: importance of the timing of stretch and implications for stretch-activated ion channels. Cardiovasc Res 32:120–130.
Zhao S, Cunha C, Zhang F, Liu Q, Gloss B, Deisseroth K, Augustine GJ, Feng G (2008) Improved expression of halorhodopsin for light-induced silencing of neuronal activity. Brain Cell Biol 36:141–154.
Zhou ZJ, Fain GL (1996) Starburst amacrine cells change from spiking to nonspiking neurons during retinal development. Proc Natl Acad Sci U S A 93:8057–8062.
Zimoń M, Baets J, Auer-Grumbach M, Berciano J, Garcia A, Lopez-Laso E, Merlini L, Hilton-Jones D, McEntagart M, Crosby AH, Barisic N, Boltshauser E, Shaw CE, Landouré G, Ludlow CL, Gaudet R, Houlden H, Reilly MM, Fischbeck KH, Sumner CJ, Timmerman V, Jordanova A, Jonghe PD (2010) Dominant mutations in the cation channel gene transient receptor potential vanilloid 4 cause an unusual spectrum of neuropathies. Brain 133:1798–1809.

CHAPTER 6

SWELLING AND EICOSANOID METABOLITES DIFFERENTIALLY GATE TRPV4 CHANNELS IN RETINAL NEURONS AND GLIA

Daniel A. Ryskamp, Nanna MacAulay, Andrew O. Jo, Amber Frye, Felix Vazquez-Chona, Wallace B. Thoreson and David Krizaj contributed to experiments, analysis and/or writing for this chapter.

6.1 Abstract

Dramatic shifts in ions and water accompany neuronal and glial activity and can generate osmotic forces that have biological consequences for brain physiology. Active regulation of osmotic gradients and cellular volume requires coordinated operation of aquaporin water channels and volume-sensitive ion channels. In the vertebrate retina, Müller astroglia provide critical support to retinal neurons by regulating the transport of ions, metabolites and water, but the identity of their osmosensor is unknown. Here, we identify TRPV4 channels as necessary and sufficient to transduce increases in mouse Müller cell volume into physiological responses. Hypotonic stimuli induced sustained $[Ca^{2+}]_i$ elevations that were inhibited by TRPV4 antagonists and absent in $TRPV4^{-/-}$ Müller cells. Glial TRPV4 signals were phospholipase A2 (PLA2)-dependent, characterized by slow-onset and Ca^{2+} waves, and, in excess, were sufficient to induce reactive gliosis. In contrast, neurons responded to TRPV4 agonists and swelling with fast, inactivating Ca^{2+} signals that were independent of PLA2, suggesting that neuronal TRPV4 is either direct gated by membrane stretch or by a novel force-transduction pathway. PLA2 and arachidonic acid signaling was previously implicated in pathological glial swelling. Here, we demonstrate that Ca^{2+} influx via TRPV4 is required for PLA2-mediated glial swelling. TRPV4 signals in Müller glia and heterologously expressing *Xenopus* oocytes were amplified by water fluxes and swelling mediated by glial-specific aquaporin-4 (AQP4). Our results support a model whereby swelling and proinflammatory signals differentially gate TRPV4 in retinal neurons and glia with potentially significant consequences for normal and pathological function.

6.2 Introduction

The ability to sense increases in cell volume represents a primal sensory modality employed by cells and organisms as they detect and adapt to activity-dependent changes in their physical environment. Within the central nervous system (CNS), swelling induces compensatory relocation of ions/water and long-term changes in enzyme activation/gene expression in neurons and glia, but can also result in excitotoxicity, cytotoxic/vasogenic edema and irreversible loss of neural function (Hoffmann et al., 2009; Pasantes-Morales & Cruz-Rangel, 2010). Astroglial swelling results in increased intracellular calcium concentration $[Ca^{2+}]_i$, PLA2 activation, release of arachidonic acid (all-cis-5,8,11,14-eicosatetraenoic acid; AA) and production of oxygen-derived free radicals (Staub et al., 1994; Hoffmann et al., 2009; Thrane et al., 2011); however, the detailed molecular mechanisms that underlie transduction of cellular swelling within the brain into the physiological response remain to be elucidated.

Müller cells mediate bidirectional ion and water transport between retinal neurons and vascular endothelial cells in part through strategically placed ion channels and aquaporin 4 (AQP4) water channels. Under pathological conditions, AQP4-mediated water fluxes drive glial swelling and AA/eicosanoid release and may contribute to excitotoxic edema and ischemic damage (Da & Verkman, 2004; Reichenbach & Bringman, 2006; Verkman et al., 2008). Still, the relationship between glial osmotransduction and arachidonic signaling in the retina or the brain is not well understood (Reichenbach & Bringman, 2006). Here, we provide evidence that the TRPV4 (transient receptor potential vanilloid type 4) channel mediates Müller cell osmosensing, define its link to PLA2 and its downstream metabolite 5’6’-

epoxyeicosatrienoic acid (5'6'-EET), and formulate a mechanistic framework for TRPV4-AQP4 interactions in astroglial volume regulation.

Gain/loss of TRPV4 function has been related to deficient osmoregulation, force transduction and numerous neurological and musculoskeletal phenotypes (Liedtke & Friedman, 2003; Tian et al., 2009; Loukin et al., 2010; Nilius & Voets, 2013). Nonetheless, the gating mechanism of this ubiquitous channel (Strotmann et al., 2000; Nilius et al., 2004; Kunnert-Keil et al., 2006; Ryskamp et al., 2011) remains unclear. The canonical view, that TRPV4 activation requires the involvement of PLA2 and epoxygenase (Watanabe et al. 2003a; Nilius et al., 2004; Vreins et al., 2004), has been challenged by studies in heterologously transfected yeast, oocytes and sensory neurons (Loukin et al., 2009; 2010; Lechner et al., 2011). Here, we show that activation of astroglial, but not neuronal, TRPV4 channels requires AA and/or its metabolite 5'6'-EET and is potentiated by water influx through AQP4. Moreover, TRPV4-dependent Ca^{2+} influx enables further swelling in a hypoosmotic gradient and is sufficient to trigger glial reactivity. This provides a cellular and molecular framework with mechanistic insight into known relationships among glial swelling, mechanical stress, proinflammatory signaling and edema (Pannicke, et al., 2006; Reichenbach & Bringmann, 2006; Pinar-Sueiro et al., 2011; Krizaj et al., 2014), and thus, a potential novel target for therapeutic interventions in ocular/brain injury.

6.3 Materials and Methods

6.3.1 Animals

All experiments adhered to the NIH Guide for the Care and Use of Laboratory Animals and the Association for Research in Vision and Ophthalmology Statement for the Use of Animals in Ophthalmic and Vision Research and were approved by the Institutional Animal Care and Use Committees at the University of Utah and the University of Nebraska Medical Center. Mouse strains C57BL/6J, B6.Cg-Tg(*Thy1*-CFP)23Jrs/J and pan-null TRPV4$^{-/-}$ with excised exon-encoding transmembrane domains 5 and 6 (Liedtke & Friedman et al., 2003) were maintained in a 12-hour light/dark cycle with free access to food and water. Data from male and female mice were pooled. No sex differences were noted.

6.3.2 Acutely Dissociated Retina Preparation

Mice were euthanized, eyes removed and retinas isolated in cold Leibovitz 15 (L15) medium (Life Technologies) containing 11 mg/ml L15 powder, 20 mM D-glucose, 10 mM Na-HEPES, 2 mM Na-pyruvate, 0.3 mM Na-ascorbate, and 1 mM glutathione. To digest the extracellular matrix, retinas were incubated in L-15 containing papain (7 U/ml; Worthington) for 1 hour at room temperature (RT). Retinas were rinsed, placed on ice and cut into 500 μm pieces. One to two of these pieces were triturated and plated on concanavalin A (1 mg/ml) -coated coverslips. Dissociated cells were loaded with Fura-2 AM or Fura-5F AM (5-10 μM; Life Technologies) for 30-40 minutes and washed for 10-20 minutes. Under our experimental conditions, most plated cells maintained homeostasis for several hours at 25°C without substantial shifts in baseline $[Ca^{2+}]_i$ or the amplitude of

$[Ca^{2+}]_i$ responses to agonists or depolarization (Molnar et al., 2012; Ryskamp et al., 2011; Szikra et al., 2009).

6.3.3 Retinal Slice Preparation

Eye cups were loaded for 70 minutes with Oregon Green BAPTA-1 AM (Life Technologies; 200 μM in L-15 with 7 mg/ml Pluronic acid) to load the dye in Müller glia. The isolated retina was flat-mounted (RGC side down) on filter paper using vacuum suction. Retinas were sliced at 200 μm and rotated 90 degrees before mounting by lines of vacuum grease on a BD Cell-Tak-treated coverslip (BD Biosciences).

6.3.4 Superfusion of Retinal Tissue and Cell Swelling Assays

During imaging experiments, Ringer's solution (133 mM NaCl, 2.5 mM KCl, 1.5 mM NaH_2PO_4, 1.5 mM $MgCl_2$ (6H20), 2 mM $CaCl_2$, 10 mM glucose, 10 mM HEPES hemisodium salt, 1 mM pyruvic acid, 1 mM lactic acid, 0.5 mM L-glutamine, 0.5 mM glutathione, and 0.3 mM Na-ascorbate, pH 7.4, 300 mOsm) was perfused at a rate of 1-2.5 ml/minute. Extracellular osmolarity was set by addition or removal of mannitol, a procedure that minimally disrupts ionic strength of the extracellular solution but also reduces the secondary effects of RVD in Müller glia (VRD; Fernández et al., 2013). Following hypotonic stimulation (HTS), the x-y cross-sectional area of calcein-loaded cells was determined offline using NIS-Elements AR 3.2 (Ryskamp et al., 2011). To examine the geometric properties of swelling more closely, dissociated retinal cells were labeled with 100 μM Sulforhodamine 101. Cell volume is proportional to $\sqrt{area^3}$ when swelling occurs uniformly in all directions, which we confirmed with confocal z-stacks

over time (data not shown). Confocal imaging with a Zeiss LSM 510 was used to acquire Z-stacks before and during swelling. 3D volume was analyzed in ImageJ.

6.3.5 Optical Imaging

Ratiometric Ca^{2+} fluorescence imaging was performed on an inverted Nikon Ti, or an upright Nikon E600 FN microscope using 20x (0.75 N.A. oil), 40x (1.3 N.A. oil & 0.8 N.A. water) and 60x (1.0 N.A. water) objectives. Excitation was provided by the Lambda DG-4 illumination system (Sutter Instruments, Novato, CA). Images were captured with a 14-bit CoolSNAP HQ^2 camera and processed using NIS-Elements AR 3.2 and Excel. $[Ca^{2+}]_i$ was measured as described previously (Molnar et al., 2012; Ryskamp et al., 2011; Szikra et al., 2009), accounting for the Ca^{2+} dissociation constant of Fura-2 (224 nM) and Fura-5F (400 nM) at RT. We followed the conventional Tsien protocol to calibrate $[Ca^{2+}]_i$. Ten µM ionomycin permeabilized cell membranes to Ca^{2+}, driving Ca^{2+} out of cells with 0 Ca^{2+}/0.8 mM EGTA Ringer, giving (R_{min} and 380_{max}), and into cells with 10 mM Ca^{2+} Ringer, giving (R_{max} and 380_{min}). If Ca^{2+} elevations saturated the Ca^{2+} indicator or exposure to calibrating solutions induced dye leakage, ΔR/R (Peak ratio – baseline/baseline) was used. Results represent averages of RGC or Müller cell responses from a minimum of three animals.

6.3.6 Electrophysiology

Retina pieces were incubated in Hibernate A medium with papain (30 U/ml) plus cysteine (0.2 mg/ml) for 25-30 minutes at RT. Tissue was washed in ice-cold, Hibernate A supplemented with 1% BSA and DNAse (1 mg/ml) followed by two additional washes

in ice-cold Hibernate A alone. Retinal cells were dissociated and plated as before. After 10-15 minutes of plating, cells were superfused with oxygenated Ames' medium. Upon obtaining a whole cell recording, the superfusate was switched to Ames' medium containing 5 mM CsCl and 10 mM TEA (minimizes inward and outward K^+ currents).

Recording electrodes were pulled using a PP-830 vertical puller (Narishige, Tokyo, Japan) from borosilicate glass pipettes (1.2 mm O.D., 0.9 mm I.D.) to obtain tips that were 2 μm in diameter and with resistance values between 8-10 MΩ. Müller cells were voltage-clamped at –70 mV using a Multiclamp 700A patch clamp amplifier. Voltage steps and ramps were applied and membrane currents acquired using pClamp 9.2 software with a Digidata 1322 interface. The pipette solution contained (in mM): 125 CsGluconate, 10 TEACl, 10 HEPES, 3 EGTA, 1 ATP, 0.5 GTP, 3 $MgCl_2$, 1 $CaCl_2$ (pH 7.2). Simultaneous ratiometric intracellular Ca^{2+} measurements were made as before with 0.2 mM Fura-2 pentapotassium salt in the pipette.

6.3.7 Heterologous Expression in Xenopus Oocytes

Xenopus laevis frogs were obtained from Nasco (Fort Atkinson, WI) or National Center for Scientific Research (France). Oocytes were surgically removed from anesthetized frogs and prepared as previously described (Fenton et al. 2010). cDNA, encoding rat TRPV4 and AQP4.M23 in the oocyte expression vector pXOOM, were linearized downstream from the poly-A segment and *in vitro* transcribed using T7 mMessage Machine (Ambion, Austin, TX). cRNA was extracted with MEGAclear (Ambion, Austin, TX) and micro-injected into defolliculated *Xenopus laevis* oocytes (4 ng TRPV4 and/or 10 ng AQP4 RNA/oocyte). Oocytes were kept at 19˚C in Kulori

medium (in mM: 90 NaCl, 1 KCl, 1 $CaCl_2$, 1 $MgCl_2$, 5 HEPES, pH 7.4) for 3-4 days prior to experiments. Due to basal activity of TRPV4 and associated cell lysis, the oocytes were kept in 1 μM ruthenium red (Sigma) but rinsed prior to experiments (Loukin et al., 2011).

6.3.8 Electrophysiology and Volume Measurements on Oocytes

Conventional two-electrode voltage clamp studies were performed with a Dagan CA-1B High Performance oocyte clamp (DAGAN, Minneapolis, MN) with Digidata 1322A interface controlled by pCLAMP software, version 9.2 (Axon Instruments, Burlingame, CA). The oocyte membrane potential was clamped at −30 mV and the current-voltage (*I-V*) relationship was determined by stepping the clamp potential to test potentials ranging from +60 mV to −140 mV in 20-mV increments (100-ms pulses). The experimental setup for measuring water permeability of oocytes has been described in detail previously (Zeuthen et al., 2006). Briefly, the oocyte was placed in a small chamber with a glass bottom and perfused with a control solution (40 mM NaCl, 2 mM KCl, 1 mM $CaCl_2$, 1 mM $MgCl_2$, 125 mM mannitol, 10 mM HEPES, pH 7.4). Oocyte images were captured continuously from below at a rate of 25 images/s. To induce cell swelling, the oocytes were challenged with a hypotonic solution (composition as in control solution although with removal of 125 or 15 mM mannitol) and cell swelling determined as the percentage increase in cross-sectional area of the oocyte. Data were acquired from three different batches of oocytes.

6.3.9 Immunofluorescence

Eyes were removed after euthanasia, punctured with a needle at the ora serrata and placed in 4% paraformaldehyde in 1X phosphate buffered saline (PBS) for 10 minutes In PBS, the anterior eye was cut away and the posterior eye was fixed for another 50 minutes After 3 x 10 minutes washes with PBS, eyecups were soaked in 15% sucrose for 45 minutes at RT and then 30% sucrose overnight at 4^{o}C. Cryoprotected eyecups were embedded in OCT (Ted Pella), frozen at -80^{o}C, sliced at 16 µm with a cryostat and mounted onto Superfrost Plus slides. Slides were warmed at 40^{o}C for 10 minutes and circled with a PAP pen. After washing with PBS, tissue was blocked for 30 minutes (10 ml PBS, 30 µl of Triton X-100, 100 mg BSA, 200 µl 5% w/v Na azide solution). Primary antibodies in PBS were incubated with the tissue overnight at 4^{o}C. Retinas were rinsed with PBS and secondary antibodies in PBS were applied at 1:1000 for 1 hour at RT. After rinsing, labeled slices were protected with Fluoromount-G (Southern Biotech), coverslipped and imaged. Dissociated cells were fixed in 95% methanol and 5% acetone at -20^{o}C for 10 minutes, washed 3 x 10 minutes in PBS and immunostained as before. The following primary antibodies were used in this study: anti-TRPV4 (Lifespan Biosciences), 1:100-1:1000; anti-GS (BD Biosciences), 1:2000; anti-GFAP (Dako), 1:500, 1:500; anti-AGB (Signature Immunologics), 1:100. The secondary antibodies were goat antimouse or goat antirabbit IgG (H+L) conjugated to fluorophores (Alexa 488 and Alexa 594; Life Technologies). Negative controls without a primary antibody showed no staining. For the AGB loading experiment, retinas were incubated in 5 mM AGB (agmatine) for 10 minutes at 37^{o}C, fixed and cryoprotected. Immunofluorescence and differential interference contrast (DIC) images were acquired on a confocal microscope

(Zeiss LSM 510 or Olympus FX1000) using 488 nm Ar (10%) and 543 nm He/Ne (100%) lines for fluorophore excitation, suitable filters for emission detection and 40x/1.2 NA oil objectives.

6.3.10 Reagents

Salts and reagents were purchased from Sigma, except where noted otherwise. AA and its metabolites were from Cayman Pharmaceuticals. Given the instability of AA and 5'6'-EET due to auto-hydrolyzation, the compounds were aliquoted, gassed with liquid nitrogen and stored at -80^{o}C until use.

6.3.11 Statistics

GraphPad Prism 6.0 was used to analyze statistics. Means are shown ± SEM. Unless specified, an unpaired t-test was used to compare two means and a one-way ANOVA along with the Holm-Šídák test was used to compare three or more means. $p > 0.05$ = NS, $p < 0.05$ = *, $p < 0.01$ = **, $p < 0.001$ = *** and $p < 0.0001$ = ****.

6.4 Results

6.4.1 TRPV4 is Functional in RGCs and Müller Glia

To map the pattern of functional TRPV4 expression in the retina, we incubated intact mouse retinas with AGB^{+}, which permeates most nonselective cation channels (Marc, 1999). Control light-adapted retinas probed with an anti-AGB antibody displayed little endogenous signal (Fig. 6.1*A*). AGB incubation (10 minutes at 37º C) revealed cation accumulation in RGCs and photoreceptors (Fig. 6.1*B,E*). Stimulation with the selective

TRPV4 agonist GSK1016790A (hereafter, GSK101; 100 nM) increased AGB-immunoreactivity (ir) in large somata within the ganglion cell layer (GCL; arrowheads in Fig. 6.1*C*) and in radial processes of Müller glia (Fig. 6.1*C,F*) marked by glutamine synthetase (GS) staining. Consistent with preferential Müller glia and RGC cation loading, GSK101 increased AGB-ir by 14.2 ± 5.3 fold between the outer edge of the GCL and the outer limiting membrane (OLM) together with a 4.1 ± 1.3 fold increase in the GCL ($p < 0.05$ for both; Fig. 6.1*G,H*). Demonstrating agonist specificity, AGB-ir was blocked by co-incubation with the selective TRPV4 antagonist HC-067047 (hereafter, HC-06; 1 μM; Fig. 6.1*D,G-H*). Thus, RGCs and Müller glia represent predominant transducers of TRPV4 signals in the mouse retina.

A TRPV4 antibody prominently labeled RGCs and Müller cell processes (GS-ir; Fig. 6.1*I*). The specificity of the staining was confirmed by omitting the primary antibody and in sections from $TRPV4^{-/-}$ retinas (Ryskamp et al., 2011). TRPV4-ir was strongest in the perivascular endfoot region (Fig. 6.1*I*), suggesting a role for the channel in negotiating ion/water fluxes between the inner retina and blood vessels. Localization to glial endfeet was similarly observed in the human retina (Fig. 6.1*K*).

6.4.2 TRPV4 Agonists Induce Sustained Elevations in Müller Cell $[Ca^{2+}]_i$

We next investigated the properties of TRPV4 signals in Müller glia. In acutely dissociated cells, GSK101 elicited robust, reversible and dose-dependent increases in intracellular Ca^{2+} ($[Ca^{2+}]_{MC}$; Fig. 6.2*A-C*) with an EC_{50} of ~16 nM (Fig. 6.2*D*). Twenty-five nM GSK101 elevated $[Ca^{2+}]_{MC}$ from a baseline of 225 ± 31 nM to 2547 ± 269 nM (p

< 0.0001; Tukey test; Fig. 6.2*B*). The amplitude of GSK101 responses markedly exceeded $[Ca^{2+}]_{MC}$ signals evoked by other known $[Ca^{2+}]_{MC}$ modulators including: depolarization (32.5 mM KCl), release from internal stores (20 μM carbachol) and saturating activation of purinergic (100 μM ATP) and glutamate receptors (100 μM glutamate; $p < 0.0001$, Tukey test; Fig. 6.2*C*).

To examine the mechanism underlying the GSK101 response, we recorded the transmembrane current in voltage-clamped Müller cells. GSK101 (25 nM) induced an increase in conductance ($p < 0.0212$), averaging 1378 ± 522 pS (n = 9/10 cells). Consistent with imaging data, I_{TRPV4} showed little inactivation during 3-10 minutes stimulation with the agonist, showing a current-voltage relation typical of nonselective cation channels with a reversal at -4.5 ± 5.5 mV (Fig. 6.2*E,F*). This observation was reinforced by concurrent $[Ca^{2+}]_i$ and whole-cell recordings that indicated substantial overlap between $[Ca^{2+}]_i$ and I_{TRPV4} (Fig. 6.S2*F*). GSK101-induced $[Ca^{2+}]_{MC}$ increases were abolished in Ca^{2+}-free saline ($p < 0.0001$, Fig. 6.3*AB*), insensitive to the voltage-operated Ca^{2+} channel blocker Cd^{2+} (100 μM; $p < 0.01$; Fig. 6.3*CD*) and inhibited by the nonselective TRP channel blocker Ruthenium Red (10 μM; $p < 0.0001$; Fig. 6.3*EF*) and the selective TRPV4 antagonist HC-06 ($p < 0.0001$, Tukey test; Fig. 6.3*GH*). The TRPV1 antagonist capsazepine (10 μM) had no effect on GSK101-induced $[Ca^{2+}]_i$ elevations in Müller cells (data not shown).

6.4.3 The Kinetics of TRPV4 Activation Differ in Neurons and Glia

In contrast to the pronounced inactivation of agonist-induced $[Ca^{2+}]_i$ responses in RGCs, signals in Müller cells declined to stable plateaus (Fig. 6.4*A,B*). GSK101 elevated

$[Ca^{2+}]_i$ to a peak 215 ± 15% and 217 ± 16% greater than the baseline in Müller glia and RGCs, respectively (Fig. 6.4*B*). Four minutes after the peak, these $[Ca^{2+}]_i$ levels declined to 179 ± 11% and 116 ± 5% of the baseline ($p < 0.05$ for Müller glia and $p < 0.0001$ for RGCs; two-way repeated measures ANOVA). Müller cells exhibited a slower response onset (95.3 ± 18.4 seconds vs. 26.9 ± 3.6 seconds; $p < 0.001$, two-way ANOVA; Fig. 6.4*C*) and time-to-peak $[Ca^{2+}]_i$ elevations (236.9 ± 17.7 seconds vs. 93.0 ± 4.4 seconds; $p < 0.0001$, two-way ANOVA). The slope of the GSK101 response diverged for Müller glia (0.0132 ± 0.0027 Ratio/second) and RGCs (0.0319 ± 0.0052 Ratio/second; $p < 0.01$; Fig. 6.4*D*). The time constant of inactivation following the peak was larger in Müller glia than RGCs (τ = 346.2 ± 31.6 seconds vs. 123.0 ± 12.3 seconds; $p < 0.0001$; Fig. 6.4*E*). Thus, glial TRPV4 is characterized by distinct modulation and/or gating compared to its neuronal counterparts.

6.4.4 Spatiotemporal TRPV4 Activation in Müller Cells Involves Transcellular Ca^{2+} Waves

Müller glial Ca^{2+} signals evoked by agonists or membrane stretch typically took the form of Ca^{2+} waves propagating from the endfoot or the distal end towards the perikaryon (Fig. 6.5*A*-*H*). Ca^{2+} store depletion by cyclopiazonic acid (CPA), a reversible antagonist of sarco/endoplasmic Ca^{2+}-ATPases (SERCAs), combined with stimulation of Ca^{2+} release by carbachol, reduced the amplitude of the GSK101 response by 34.5 ± 11.6% ($p < 0.05$; Fig. 6.5*I*). CPA also suppressed Ca^{2+} wave propagation (Fig. 6.5*K*-*Q*), suggesting that Ca^{2+}-induced Ca^{2+} release (CICR) amplifies the TRPV4 response.

To follow glial TRPV4 activation in the retinal slice (Fig. 6.5*R*), glia were loaded

with Oregon Green 1,2-bis(o-aminophenoxy)ethane-N,N,N',N'-tetraacetic acid (BAPTA)-1 (OGB-1; Kurth-Nelson et al., 2009). GSK101 induced Ca^{2+} waves that originated within focal points in the distal end of Müller glia and/or the endfoot. The agonist elevated $[Ca^{2+}]_i$ in 12/14 (86%) distal stalks, 26/30 (87%) somata, 21/26 (81%) proximal stalks and 20/28 (71%) endfeet. Peak response amplitudes for these regions in $\Delta F/F$ were: distal stalk 0.4005 ± 0.0662, soma 0.3707 ± 0.0643, proximal stalk 0.1980 ± 0.0551 and endfoot 0.2988 ± 0.0642 (Fig. 6.5*S*). Somatic Ca^{2+} signals remained elevated after $[Ca^{2+}]_i$ levels within apical and distal regions returned to the baseline. The response amplitudes for all Müller cell domains were greater than R_o ($p < 0.01$ in all cases; Dunnett's test). Response latencies were (in seconds): distal stalk 214.8 ± 15.2, soma 246.2 ± 18.1, proximal stalk 353.0 ± 14.3 and endfoot 262.6 ± 14.9 ($p < 0.001$-0.0001; Bonferroni test; Fig. 6.5*T*). Thus, TRPV4 channels can initiate and contribute to propagation of transretinal Ca^{2+} waves, representing a plausible candidate trigger mechanism for the regenerative phenomena reported previously (Newman & Zahs, 1998).

6.4.5 Differential TRPV4 Channel Activation Mediates Neuronal and Glial Responses to Swelling

Astroglial swelling can compromise neuronal function through edema and excitotoxicity (Reichenbach & Bringmann, 2006; Pasantes-Morales & Cruz-Rangel, 2010; Thrane et al., 2011). Given that TRPV4 is activated by swelling (Strotmann et al., 2000; Becker et al., 2005; Benfenati et al., 2011), we examined the relationship between hypotonicity and volume regulation in Müller cells. HTS dose-dependently and reversibly increased the cell area and volume of Müller glia (Fig. 6.6). Müller cells were

able to withstand larger hypotonic challenges than concomitantly recorded RGCs (Fig. 6.6*B*) that are also known to express TRPV4 (Ryskamp et al., 2011), possibly because of the greater elasticity of the glial membrane (Lu et al., 2006). As depicted in Figure 6.6, cell swelling was associated with increases in $[Ca^{2+}]_i$ of concurrently recorded Müller cells with an EC_{50} of 34.15 ± 3.31 % HTS, (Fig. 6.6*C,D*). The $[Ca^{2+}]_i$ response in Müller cells and RGCs was abolished by the removal of extracellular Ca^{2+} (Fig. 6.6*E*) and was inhibited by HC-06 (1 μM; $p < 0.05$; Fig. 6.6*F,G*). Consistent with optical imaging data, 50% HTS stimuli elicited inward currents (91.34 ± 17.66 pA) that were antagonized by HC-06 and were absent from $TRPV4^{-/-}$ cells (Fig. 6.6*H,I*). Thus, TRPV4 channels play a central role in the hypotonicity-induced Ca^{2+} signals of Müller glia and RGCs.

TRPV4 activation might be secondary to stretch-induced stimulation of PLA2 (Watanabe et al., 2003a). Consistent with this, PLA2 inhibition with 4-bromophenacyl bromide (pBPB; 100 μM) blocked HTS-induced glial TRPV4 signals ($p < 0.001$; Fig. 6.6*F*). pBPB ($n = 39$) did not affect GSK101 responses ($n = 23$; $p > 0.05$), suggesting that cell swelling and GSK101 activate Müller TRPV4 through different mechanisms. Surprisingly, swelling-induced $[Ca^{2+}]_i$ increases in RGCs were unaffected by pBPB ($p > 0.05$; Fig. 6.6*G*). Thus, the Müller glial TRPV4 response to swelling requires the "canonical" PLA2 signaling pathway, whereas in neurons TRPV4 may either be directly force sensitive (Loukin et al., 2010) or reliant on a novel, indirect force transduction cascade.

Ruthenium Red reduced the percentage of Müller glia responding to 35% HTS with $[Ca^{2+}]_i$ elevations from 59 ± 7% to 17 ± 5% ($p < 0.01$, Dunnett's test; Fig. 6.6*J*). HC-06 also reduced the percentage of HTS-responding Müller glia to 29 ± 8% ($p < 0.05$),

whereas capsazepine (5 μM), a competitive inhibitor of TRPV1 channels, had no effect ($p > 0.05$). Likewise, HTS-evoked $[Ca^{2+}]_i$ responses of RGCs were diminished by Ruthenium Red and HC-06, but not capsazepine (Dunnett's test; Fig. 6.6*K*). The comparable efficacy of Ruthenium Red and HC-06 suggests that TRPV4 is the primary TRP channel contributing to volume sensing in Müller glia and RGCs. Although the residual responsiveness in the presence of TRPV4 blockers suggests that additional Ca^{2+}-permeable ion channels may contribute to the HTS-induced Ca^{2+} response, neuronal and glial responses to HTS and GSK101 were almost completely absent in $TRPV4^{-/-}$ cells (Fig. 6.7*A-D*).

6.4.6 TRPV4 Gating in Müller Cells but not RGCs Requires Activation of Phospholipase A2

The prevailing model of TRPV4 gating involves PLA2 activation and biosynthesis of epoxyeicosatrienoic acids, which act as endogenous activators of TRPV4 (Watanabe et al., 2003a; Nilius et al., 2004; Jang et al., 2012; Fig. 6.8*A*). To test the function of this canonical transduction pathway, we stimulated retinal cells with AA and its downstream metabolite 5'6'-epoxyeicosatrienoic acid (5,6-EET). AA (100 μM) elevated $[Ca^{2+}]_i$ ($\Delta R/R = 0.39 \pm 0.3$; Fig. 6.8*B,C*) above spontaneous activity (noise; $\Delta R/R = 0.16 \pm 0.03$; $p < 0.0001$). HC-06 abolished these responses ($p < 0.001$), suggesting that AA-induced $[Ca^{2+}]_{MC}$ responses were mediated by TRPV4. AA (10 μM) induced $[Ca^{2+}]_i$ elevations in all RGCs (Fig. 6.8*D,E*), but these were not antagonized by HC-06 ($p > 0.05$), even though HC-06 effectively blocked the GSK101 response ($p < 0.05$). 5'6'-EET, a major astroglial metabolite of AA, was proposed as the final activator of TRPV4 (Nilius et al.,

2004). 5,6-EET (5 μM) induced $[Ca^{2+}]_i$ increases (ΔR/R = 0.83 ± 0.2 in Müller glia and 0.47 ± 0.08 in RGCs) that were inhibited by HC-06 (ΔR/R = 0.40 ± 0.07 in Müller glia and 0.28 ± 0.03 in RGCs; $p < 0.05$; Fig. 6.8*F-H*). We conclude that glial, but not neuronal, TRPV4 activation in the retina involves an intermediary PLA2 step.

6.4.7 Calcium Influx via TRPV4 Exacerbates Swelling in Müller Glia and RGCs

Astroglial swelling is a major problem in traumatic brain injury and retinal diseases such as diabetic retinopathy and glaucoma (Staub et al., 1994; Pasantes-Morales & Cruz-Rangel, 2010; Pannicke et al., 2006; Sofroniew, 2009; Pinar-Sueiro, et al., 2011). We exposed HTS-stimulated cells to HC-06 and analyzed the swelling response in $TRPV4^{-/-}$ Müller cells. As shown in Figure 6.9A, HTS-induced increases in cross-sectional area were counteracted by HC-06 (reduced by 46.9 ± 9.4%; $p < 0.01$; two-way ANOVA; Dunnett's test) and markedly reduced in $TRPV4^{-/-}$ cells (reduced by 47.3 ± 6.1%; $p < 0.01$), indicating that swelling is facilitated by TRPV4 activation itself. HC-06 did not cause a further reduction in HTS-stimulated swelling in $TRPV4^{-/-}$ Müller glia, consistent with the central role for TRPV4 in the swelling response. Moreover, HTS-induced swelling was more pronounced in heterologously expressing HEK293:TRPV4 overexpressors compared to control cells ($p < 0.001$ in 35% HTS at each time, two-way ANOVA, Fig. 6.9*B*). While the mechanism through which TRPV4 channels contribute to the HTS-induced swelling in recombinant cells, neurons and glia remains to be determined, the effect is likely to be mediated by Ca^{2+} influx. This is indicated by the suppression of HTS-induced increase retinal cell area by BAPTA-AM (200 μM; reduced

by 45.7 ± 7.2% for RGCs; $p < 0.0001$; reduced by 33.2 ± 6.3% for Müller cells; $p < 0.05$; Fig. 6.9*A*).

Given that Müller glial swelling was proposed to involve PLA2 (Pannicke et al., 2006; Reichenbach & Bringmann, 2006), we exposed wild type and TRPV4$^{-/-}$ Müller cells to hypotonic saline in the presence of pBPB to test the hypothesis that this proposed obligatory activator of TRPV4 (Watanabe et al., 2003a; Nilius et al., 2004) is involved in the swelling response via its role in TRPV4 activation. The PLA2 antagonist reduced cell swelling in wild type Müller cells (reduced by 66.5 ± 12.2%; $p < 0.001$), but was not effective in TRPV4$^{-/-}$ Müller glia (Figure 6.9*A*). Moreover, pBPB did not suppress HTS-induced swelling in RGCs (reduced by 2.9 ± 9.2%; $p < 0.05$). Thus, hypotonicity-induced increases in cell volume are likely augmented by reciprocal stimulation between TRPV4-mediated Ca^{2+} influx and PLA2 activation in retinal glial cells but not neurons.

6.4.8 Aquaporin 4 Channels Amplify Stretch-Induced TRPV4 Activation

TRPV4 channels in astrocyte-derived cultures may form a complex with aquaporin 4 (AQP4), the dominant aquaporin in the brain (Benfenti et al., 2011; Verkman et al., 2008). TRPV4-ir and AQP4 –ir showed prominent colocalization within Müller endfeet, in Müller processes surrounding RGC layer (RGCL) somata and in radial processes extending towards the INL (Fig. 6.10*A*, arrowheads). Arguing against an obligatory interaction, TRPV4 immunolocalization in AQP4$^{-/-}$ retinas was indistinguishable from wild type retinas and AQP4 localization in TRPV4$^{-/-}$ retinas was likewise qualitatively similar to controls (Fig. 6.10*B,C*). Nevertheless, it is possible that the two channels

interact functionally through changes in swelling and/or $[Ca^{2+}]_{MC}$. $AQP4^{-/-}$ cells continued to respond to GSK101 with robust $[Ca^{2+}]_i$ elevations (Fig. 6.10*D*), suggesting that AQP4 is not required for TRPV4 function in Müller glia. However, analysis of HTS responses in $AQP4^{-/-}$ Müller glia revealed both a prolonged latency-to-peak of the swelling response and a decrease in the amplitude of HTS-induced $[Ca^{2+}]_i$ responses from $\Delta R/R$ of 0.74 ± 0.051 to 0.34 ±0.025 ($p < 0.0001$; two-way ANOVA; Fig. 6.10*E*). This suggests that AQP4-mediated water influx facilitates TRPV4 activation and subsequent modulation of intracellular Ca^{2+} homeostasis.

To test the functional interaction between TRPV4 and AQP4 in an isolated setting, both channels were expressed in *Xenopus* oocytes either alone or in combination. The cell volume and membrane currents were simultaneously determined following 60 seconds stimulation with HTS or GSK101. As expected, exposure to GSK101 induced inward currents in TRPV4 -expressing oocytes (at V_m = 60 mV; 2.4 ± 0.6 μA for TRPV4-expressing oocytes and 3.6 ± 1.1 μA for TRPV4/AQP4-expressing oocytes). The GSK-induced currents were of similar magnitude whether AQP4 was co-expressed or not ($p = 0.9$), whereas no current was observed in AQP4-expressing controls (0.08 ± 0.01 μA; Fig. 6.11*A-C*). Hypotonic cell swelling was more prominent in AQP4 expressors (5.76 ± 0.37% for AQP4-expressing oocytes, 4.25 ± 0.24% for TRPV4/AQP4-expressing oocytes vs. 0.33 ± 0.04% in TRPV4-expressing oocytes, $p < 0.001$, Dunnett's test). The I-V relationship measured 60 seconds after imposition of HTS (Δ125 mOsm) yielded markedly larger currents in TRPV4/AQP4-expressing oocytes than oocytes expressing only TRPV4 (at V_m = 60 mV; 6.3 ± 1.5 μA vs. 1.7 ± 0.4 μA, $p < 0.05$; Fig. 6.11*B,D-E*). The increased HTS-induced current in oocytes co-expressing TRPV4 and AQP4 could be

due to a required presence of AQP4 for full TRPV4 activity or due to the increased AQP4-dependent oocyte swelling. We thus determined HTS-induced TRPV4-mediated current in TRPV4-expressing oocytes and TRPV4/AQP4-expressing oocytes exposed to *different* osmotic gradients in order to obtain a *similar* degree of cell swelling (Δ125 mOsm for TRPV4-expressing oocytes; 0.33 ± 0.04% cell swelling after 60 seconds, and Δ15 mOsm for TRPV4+AQP4-expressing oocytes; 0.27 ± 0.03% cell swelling after 60 seconds, $p = 0.2$, t test). The I-V curves showed distinct overlap ($p = 0.4$; Fig. 6.11*F*). This suggests that water entry through AQP4 stimulates TRPV4-activation primarily by facilitating the rate of swelling-induced membrane stretch.

6.4.9 TRPV4 Activation or Deletion is Sufficient to Trigger Reactive Gliosis

Reactive astrogliosis is an early indicator of CNS stress induced by mechanical stress and neuroinflammation (Tezel et al., 2003; Reichenbach & Bringmann, 2006; Inman & Horner, 2007; Sofroniew, 2009; Lindqvist et al., 2010). In control retinas, the gliotic marker glial fibrillary acidic protein (GFAP) was confined to astrocytes within the inner limiting membrane (ILM), whereas $TRPV4^{-/-}$ retinas exhibited a moderate level of GFAP-ir (Fig. 6.12*A,B*). Following intravitreal injection of GSK101, a marked upregulation in GFAP-ir was observed especially at the endfeet and proximal processes within the IPL ($p < 0.01$; two-way ANOVA, Dunnett's test; Fig. 6.12*A,B*).

6.5 Discussion

This study provides new insights into retinal physiology by identifying the Müller glial osmosensor and demonstrating a mechanistic framework that governs the relationship between glial osmosensing, Ca^{2+} homeostasis, AQP4-mediated water fluxes, arachidonic acid metabolism and swelling. The differential modulation of neuronal and glial TRPV4 channels has broader implications for our understanding of volume (dys)regulation and inflammatory signaling in the healthy and diseased CNS.

At EC_{50}, GSK101-evoked $[Ca^{2+}]_i$ signals far surpassed Müller responses to other known effectors of Ca^{2+} signaling, including depolarization, purinergic signaling and Ca^{2+}-induced Ca^{2+} release. The close match between TRPV4-mediated currents and $[Ca^{2+}]_i$ suggests that the peak and plateau phases of the TRPV4 response are mainly mediated by plasma membrane influx. Interestingly, the I-V relationship underlying glial I_{TRPV4} did not exhibit the outward rectification typical of homomeric TRPV4 (Watanabe et al., 2003b; Loukin et al., 2010), but rather resembled the stretch-sensitive voltage-independent cation current observed in cultured Müller cells (Puro, 1991). It is possible that the conductance is linearized by heteromerization of TRPV4 with auxiliary TRPC1 or TRPP2 subunits (Köttgen et al., 2008; DaSilva et al., 2008; Ma et al., 2011) and/or modulatory influence of AQP (Becker et al., 2005; Liu et al., 2006; Benfenati et al., 2011). Release from internal stores provided a minor contribution to the overall $[Ca^{2+}]_i$; however, as in brain astrocytes (Butenko et al., 2012; Dunn et al., 2013) and possibly mechanically stimulated retinal glia (Newman & Zahs, 1998), it fostered the propagation of TRPV4-initiated Ca^{2+} waves from the endfoot towards the distal retina.

The mechanism of TRPV4 gating has been controversial. The obligatory role of

PLA2 has been questioned because TRPV4 is stretch-activated in excised patches of membrane, which are devoid of eicosanoids (Loukin et al., 2010; Loukin et al., 2011), and the channel is force-sensitive in yeast, which do not express PLA2 (Loukin et al., 2009). Our conclusion, that TRPV4 function in Müller glia requires AA and/or its metabolite 5'6'-EET, is based on the following observations: (1) AA and 5'6'-EET-induced $[Ca^{2+}]_{MC}$ elevations are sensitive to TRPV4 antagonists; (2) AA potentiates Müller cell swelling, whereas PLA2 antagonists suppress TRPV4-evoked and HTS-induced $[Ca^{2+}]_{MC}$ elevations; (3) PLA2 antagonists did not further suppress HTS-evoked swelling in $TRPV4^{-/-}$ Müller cells; (4) The lengthy activation lag time in Müller cells is consistent with activation of intermediary steps; and (5) HTS-evoked inward current and $[Ca^{2+}]_i$ increases were not observed in $TRPV4^{-/-}$ Müller cells or in the presence of the selective TRPV4 antagonist HC-06. These findings therefore provide a molecular context for the reported effects of AA on glial swelling in cellular and tissue models of ischemia, TBI and diabetic edema (Pannicke et al., 2006; Sofroniew, 2009; Nedergaard et al., 2010; Pasantes-Morales and Cruz-Rangel, 2010; Reichenbach & Bringmann, 2006). The simplest model to account for our results is that cell swelling, generated by hypotonic shock and therefore partly mediated by AQP4, induces TRPV4-dependent cation influx into Müller glia. This ionic flux is subsequently augmented by PLA2 activation and results in further glial swelling.

Data from $TRPV4^{-/-}$ and HC-06-exposed retinal cells and HEK293 overexpressors show that TRPV4 activation contributes to cell swelling. This is in contrast to observations in salivary gland cells and keratinocytes where $TRPV4/Ca^{2+}$ contributed to RVD (Becker et al., 2005; Liu et al., 2006), and cultured astrocytes in which RVD

required AQP4, whereas hypotonic sensing was mediated by TRPV4 (Benfenati et al., 2011). Arguing against an obligatory TRPV4-AQP4 complex (Benfenati et al., 2011), our data from AQP4$^{-/-}$ and TRPV4$^{-/-}$ retinas show that the distribution of TRPV4 is largely independent of AQP4, whereas the additional AQP4 contribution to the swelling-induced TRPV4 current is largely eliminated when TRPV4 and TRPV4/AQP4-expressing oocytes are exposed to the same extent of swelling. Nonetheless, it seems clear that functional coupling between the osmosensor and water transport has potentially significant consequences for Ca^{2+} homeostasis and downstream signaling pathways in glia, as suggested by *in vivo* experiments (Thrane et al., 2011). Exposure to GSK101 was sufficient to evoke reactive Müller gliosis either as a result of direct Ca^{2+} influx or as a secondary response to excitotoxic degeneration of RGCs (Ryskamp et al., 2011; Krizaj et al., 2014). However, as indicated by the mild gliosis observed in unstimulated TRPV4$^{-/-}$ retinas, basal TRPV4 activity in healthy retinas is likely to restrain glial reactivity.

Excitation mapping and HTS confirmed previous evidence of functional TRPV4 expression in RGCs (Ryskamp et al., 2011); however, the fast, inactivating $[Ca^{2+}]_i$ responses in RGCs were easily distinguishable from lagging, sustained glial signals. Given the relative insensitivity of $[Ca^{2+}]_{RGC}$ to 5'6'-EET and the inability of pBPB to block HTS-induced $[Ca^{2+}]_i$ elevations, we conclude that, as reported for gastrointestinal neurons (Lechner et al., 2011), RGC responses are largely independent of the canonical transduction mechanism. Thus, TRPV4 might differentially contribute to volume sensing and AA-mediated proinflammatory signaling in retinal neurons vs. glia.

In summary, we report that TRPV4 is expressed in every Müller cell and that its activation is essential for the normal glial $[Ca^{2+}]$ response to hypotonic stress, whereas

both its absence and overactivation are associated with reactive gliosis. Given that Müller glia perform key housekeeping, osmoregulatory and mechanosensory functions in the retina, our findings implicate TRPV4 in both normal visual function and injury responses caused by excessive swelling and/or release of proinflammatory metabolites. While Müller cells are not classically excitable, Ca^{2+} waves induced by endfoot TRPV4 channels might translate the effects of mechanical stress into interglial, gliovascular and neuroglial signals (Newman & Zahs, 1998; Kurth-Nelson et al., 2009; Butenko et al., 2012; Dunn et al., 2013). In addition to offering a new mechanistic context for previous studies that have yielded contradictory results regarding TRPV4 activation, our findings provide novel insights into differential neuronal and astroglial Ca^{2+} responses to swelling and inflammation. Our data suggest that targeting TRPV4 channels might offer a rational new tool for mitigating swelling-mediated neuronal damage and gliosis in patients with traumatic ocular/brain injury, edema, ischemia and glaucoma.

References

Becker D, Blasé C, Bereiter-Hahn J, Jendrach M (2005) TRPV4 exhibits a functional role in cell-volume regulation. J Cell Sci 118:2435-2440.

Benfenati V, Caprini M, Dovizio M, Mylonakou MN, Ferroni S, Ottersen OP, Amiry-Moghaddam M (2011) An aquaporin-4/transient receptor potential vanilloid 4 (AQP4/TRPV4) complex is essential for cell-volume control in astrocytes. Proc Natl Acad Sci USA 108:2563-2568.

Butenko O, Dzamba D, Benesova J, Honsa P, Benfenati V, Rusnakova V, Ferroni S, Anderova M (2012) The increased activity of TRPV4 channel in the astrocytes of the adult rat hippocampus after cerebral hypoxia/ischemia. PLoS ONE 7:e39959.

Da Silva N, Herron CE, Stevens K, Jollimore CA, Barnes S, Kelly ME (2008) Metabotropic receptor-activated calcium increases and store-operated calcium influx in mouse Müller cells. Invest Ophthalmol Vis Sci 49:3065-3073.

Da T, Verkman AS (2004) Aquaporin-4 gene disruption in mice protects against impaired retinal function and cell death after ischemia. Invest Ophthalmol Vis Sci 45:4477-4483.

Dunn KM, Hill-Eubanks DC, Liedtke W, Nelson MT (2013) TRPV4 channels stimulate Ca^{2+}-induced Ca^{2+} release in astrocytic endfeet and amplify neurovascular coupling responses. Proc Natl Acad Sci USA, 110:6157-6162.

Fenton RA, Moeller HB, Zelenina M, Snaebjornsson MT, Holen T, MacAulay N (2010) Differential water permeability and regulation of three aquaporin 4 isoforms. Cell Mol Life Sci 67:829-840.

Fernández JM, Giusto GD, Kalstein M, Melamud L, Rivarola V, Ford P, Capurro C (2013) Cell volume regulation in cultured human retinal Müller cells is associated with changes in transmembrane potential. PloS ONE 8:e57268.

Hoffmann EK, Lambert IH, Pedersen SF (2009) Physiology of cell volume regulation in vertebrates. Physiol Rev 89:193-277.

Inman DM, Horner PJ (2007) Reactive nonproliferative gliosis predominates in a chronic mouse model of glaucoma. Glia 55:942-953.

Jang Y, Jung J, Kim H, Oh J, Jeon JH, Jung S, Kim KT, Cho H, Yang DJ, Kim SM, Kim IB, Song MR, Oh U (2012) Axonal neuropathy-associated TRPV4 regulates neurotrophic factor-derived axonal growth. J Biol Chem 287:6014-6024.

Köttgen M, Buchholz B, Garcia-Gonzalez MA, Kotsis F, Fu X, Doerken M, Boehlke C, Steffl D, Tauber R, Wegierski T, Nitschke R, Suzuki M, Kramer-Zucker A, Germino GG, Watkick T, Prenen J, Nilius B, Kuehn EW, Walz G (2008) TRPP2 and TRPV4 form a polymodal sensory channel complex. J Cell Biol 182:437-447.

Križaj D, Ryskamp DA, Tian N, Tezel G, Mitchell CH, Slepak VZ, Shestopalov VI. (2014) From mechanosensitivity to inflammatory responses: new players in the pathology of glaucoma. Curr Eye Res 39:105-119.

Kunert-Keil C, Bisping F, Krüger J, Brinkmeier H (2006) Tissue-specific expression of TRP channel genes in the mouse and its variation in three different mouse strains. BMC Genomics 7:159.

Kurth-Nelson ZL, Mishra A, Newman EA (2009) Spontaneous glial calcium waves in the retina develop over early adulthood. J Neurosci 29:11339-11346.

Lechner SG, Markworth S, Poole K, Smith ES, Lapatsina L, Frahm S, May M, Pischke S, Suzuki M, Ibañez-Tallon I, Luft FC, Jordan J, Lewin GR (2011) The molecular and cellular identity of peripheral osmoreceptors. Neuron 69:332-344.

Liedtke W, Friedman JM (2003) Abnormal osmotic regulation in TRPV4 -/- mice. Proc Natl Acad Sci USA 100:13698-13703.

Lindqvist N, Liu Q, Zajadacz J, Franze K, Reichenbach A (2010) Retinal glial (Müller) cells: sensing and responding to tissue stretch. Invest Ophthalmol Vis Sci 51:1683-1690.

Liu X, Bandyopadhyay BC, Nakamoto T, Singh B, Liedtke W, Melvin JE, Ambudkar I (2006) A role for AQP5 in activation of TRPV4 by hypotonicity: concerted involvement of AQP5 and TRPV4 in regulation of cell volume recovery. J Biol Chem 281:15485-15495.

Loukin S, Zhou X, Su Z, Saimi Y, Kung C (2010) Wild-type and brachyolmia-causing mutant TRPV4 channels respond directly to stretch force. J Biol Chem 285:27176-27181.

Loukin S, Su Z, Kung C (2011) Increased basal activity is a key determinant in the severity of human skeletal dysplasia caused by TRPV4 mutations. PLoS ONE 6:e19533.

Loukin SH, Su Z, Kung C (2009) Hypotonic shocks activate rat TRPV4 in yeast in the absence of polyunsaturated fatty acids. FEBS Lett 583:754-758.

Lu YB, Franze K, Seifert G, Steinhäuser C, Krichhoff F, Wolburg H, Guck J, Jammey P, Wei EQ, Käs J (2006) Viscoelastic properties of individual glial cells and neurons in the CNS. Proc Natl Acad Sci USA 103:17759-17764.

Ma X, Cheng KT, Wong CO, O'Neil RG, Birnbaumer L, Ambudkar IS, Yao X (2011) Heteromeric TRPV4-C1 channels contribute to store-operated $Ca^{(2+)}$ entry in vascular endothelial cells. Cell Calcium 50:502-559.

Marc RE (1999) Mapping glutamatergic drive in the vertebrate retina with a channel-permeant organic cation. J Comp Neurol 407:47-64.

Molnar T, Barabas P, Birnbaumer L, Punzo C, Kefalov V, Križaj D (2012) Store-operated channels regulate intracellular calcium in mammalian rods. J Physiol 590:3465-3481.

Nedergaard M, Rodríguez JJ, Verkhratsky A (2010) Glial calcium and diseases of the nervous system. Cell Calcium 47:140-149.

Newman EA, Zahs KR (1998) Modulation of neuronal activity by glial cells in the retina. J Neurosci 18:4022-4028.

Nilius B, Vriens J, Prenen J, Droogmans G, Voets T (2004) TRPV4 calcium entry channel: a paradigm for gating diversity. Am J Physiol Cell Physiol 286:C195-C205.

Nilius B, Voets T (2013) The puzzle of TRPV4 channelopathies. EMBO Rep 14:152-163.

Pannicke T, Iandiev I, Wurm A, Uckermann O, vom Hagen F, Reichenbach A, Wiedemann P, Hammes HP, Bringmann A (2006) Diabetes alters osmotic swelling characteristics and membrane conductance of glial cells in rat retina. Diabetes 55:633-639.

Pasantes-Morales H, Cruz-Rangel S (2010) Brain volume regulation: osmolytes and aquaporin perspectives. Neuroscience 168:871-884.

Pinar-Sueiro S, Urcola H, Rivas MA, Vecino E (2011) Prevention of retinal ganglion cell swelling by systemic brimonidine in a rat experimental glaucoma model. Clin Exp Ophthalmol 39:799-807.

Puro DG (1991) Stretch□activated channels in human retinal Müller cells. Glia 4:456-460.

Reichenbach A, Bringmann A (2006) Müller cells in the healthy and diseased retina. Prog Retin Eye Res 25:397-424.

Ryskamp DA, Witkovsky P, Barabas P, Huang W, Koehler C, Akimov NP, Lee SH, Chauhan S, Xing W, Rentería RC, Liedtke W, Križaj D (2011) The polymodal ion channel transient receptor potential vanilloid 4 modulates calcium flux, spiking rate, and apoptosis of mouse retinal ganglion cells. J Neurosci 31:7089-7101.

Sofroniew MV (2009) Molecular dissection of reactive astrogliosis and glial scar formation. Trends Neurosci 32:638-647.

Staub F, Winkler A, Peters J, Kempski O, Kachel V, Baethmann A (1994) Swelling, acidosis, and irreversible damage of glial cells from exposure to arachidonic acid in vitro. J Cereb Blood Flow Metab 14:1030-1039.

Strotmann R, Harteneck C, Nunnenmacher K, Schultz G, Plant TD (2000) OTRPC4, a nonselective cation channel that confers sensitivity to extracellular osmolarity. Nat Cell Biol 2:695-702.

Szikra T, Barabas P, Bartoletti TM, Huang W, Akopian A, Thoreson WB, Križaj D (2009) Calcium homeostasis and cone signaling are regulated by interactions between calcium stores and plasma membrane ion channels. PloS ONE 4:e6723.

Tezel G, Chauhan BC, LeBlanc RP, Wax MB (2003) Immunohistochemical assessment of the glial mitogen-activated protein kinase activation in glaucoma. Invest Ophthalmol Vis Sci 44:3025-3033.

Tian W, Y Fu, A Garcia-Elias, JM Fernández-Fernández, R Vicente, PL Kramer, RF Klein, R Hitzemann, ES Orwoll, B Wilmot, S McWeeney, MA Valverde, and DM Cohen (2009) A loss-of-function nonsynonymous polymorphism in the osmoregulatory TRPV4 gene is associated with human hyponatremia. Proc Natl Acad Sci USA 106:14034-14039.

Thrane AS, Rappold PM, Fujita T, Torres A, Bekar LK, Takano T, Peng W, Wang F, Rangroo TV, Enger R, Haj-Yasein NN, Skare Ø, Holen T, Klungland A, Ottersen OP, Nedergaard M, Nagelhus EA (2011) Critical role of aquaporin-4 (AQP4) in astrocytic Ca^{2+} signaling events elicited by cerebral edema. Proc Natl Acad Sci USA 108:846-851.

Verkman AS, Ruiz-Ederra J, Levin MH (2008) Functions of aquaporins in the eye. Prog Retin Eye Res 27:420-433.

Vriens J, Watanabe H, Janssens A, Droogmans G, Voets T, Nilius B (2004) Cell swelling, heat, and chemical agonists use distinct pathways for the activation of the cation channel TRPV4. Proc Natl Acad Sci USA 101:396-401.

Watanabe H, Vriens J, Prenen J, Droogmans G, Voets T, Nilius B (2003a) Anandamide and arachidonic acid use epoxyeicosatrienoic acids to activate TRPV4 channels. Nature 424:434-438.

Watanabe H, Vriens J, Janssens A, Wondergem R, Droogmans G, and Nilius B (2003b) Modulation of TRPV4 gating by intra-and extracellular Ca^{2+}. Cell Calcium 33:489-495.

Zeuthen T, Belhage B, Zeuthen E (2006) Water transport by Na+-coupled cotransporters of glucose (SGLT1) and of iodide (NIS). The dependence of substrate size studied at high resolution. J Physiol 570:485-99.

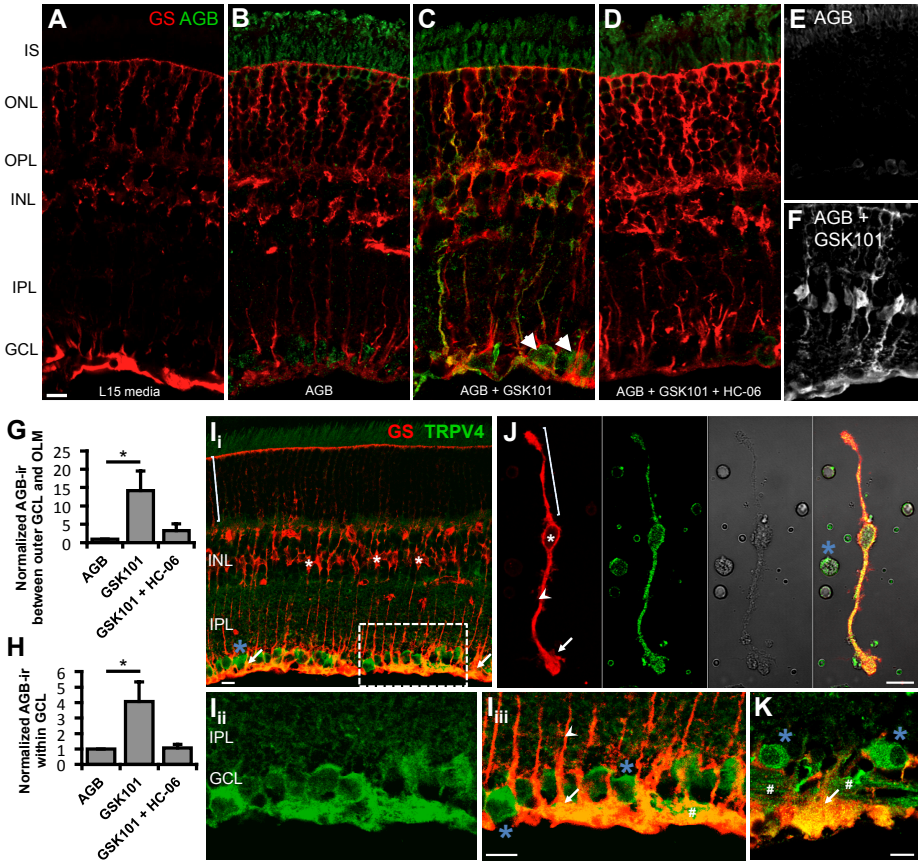

Figure 6.1 TRPV4 mediates cation influx in Müller glia and RGCs. ***A-D***. Vertical cryosections of mouse retinas immunolabeled for Müller glia marker GS (red) and AGB (green). Freshly isolated retinas were incubated for 10 minutes at 37°C with the indicated conditions. ***A***. Negative control (L15 media alone; n = 2). ***B***. Retinas incubated with AGB (N = 3). Basal cation (AGB^{+}) influx takes place in RGCs and photoreceptors. ***C***. GSK101 (100 nM) induces cation influx in RGCs and a subset of Müller glia (n = 3). ***D***. Agonist-induced cation entry is suppressed by HC-06 (1 µM; n = 3). ***E-F***. Additional examples of cation influx in the absence (***E***) and presence (***F***) of GSK101. ***G-H***. AGB influx between the outer edge of the GCL and the outer limiting membrane (OLM; ***G***) or within the GCL (***H***) was quantified by measuring the mean value (optical density) of AGB-ir. ***I_i-I_{iii}***. Vertical cryosection of mouse retina immunolabeled for the Müller cell marker glutamine synthetase (GS; red) and TRPV4 (green; ***I_i***). TRPV4 is preferentially localized to Müller cell endfeet (arrows) and RGCs (blue *). Müller cell somata (white *) lack TRPV4 in intact retinas. An example distal stalk/distal end is indicated with a bracket. ***I_{ii}-I_{iii}***. Close up of ***I_i*** (dashed rectangle) showing TRPV4 (***I_{ii}***) and the merge (***I_{iii}***). ***J***. TRPV4-ir is present throughout acutely dissociated Müller cells and a presumed RGC soma. Proximal stalk indicated by arrowhead. ***K***. In a human retina section TRPV4 similarly localizes to endfeet and proximal stalks of Müller glia as well as RGC somata and axon bundles (#). Scale bars = 10 µm. I = Inner, O = Outer, S = Segments, N = Nuclear, P = Plexiform, L = Layer, GC = Ganglion Cell.

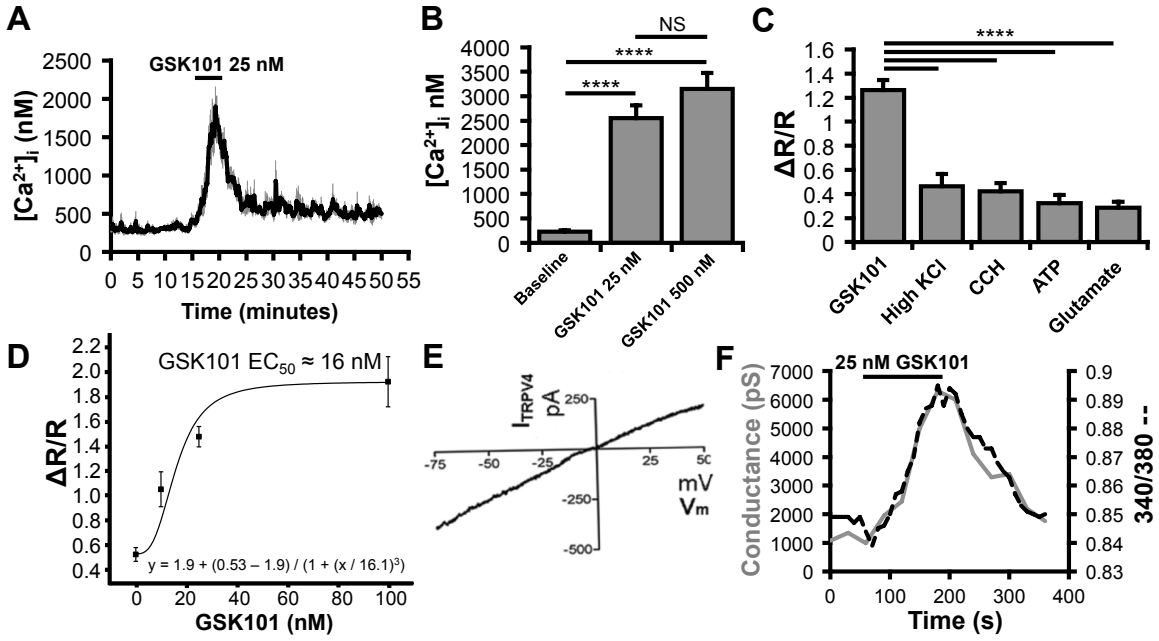

Figure 6.2 TRPV4 activation massively elevates Müller cell calcium levels. ***A***. GSK101 dose-dependently increases calcium above spontaneous calcium spikes. ***B***. The amplitude of Müller cell responses to GSK101 was quantified using Fura-5F. n = 14, 12 and 4, respectively. ***C***. Twenty-five nM GSK101 increased calcium levels far more than other known modulators of Müller cell calcium homeostasis. n = 33, 26, 25, 19 and 19, respectively. ***D***. According to the sigmoidal fit, the EC_{50} of GSK101 was ~16 nM. n = 12. ***E***. GSK101 induced a current with an IV plot characteristic of heteromeric TRPV4. n = 10. ***F***. TRPV4 opening by GSK101 resulted in a large inward conductance that coincided with an elevation in calcium.

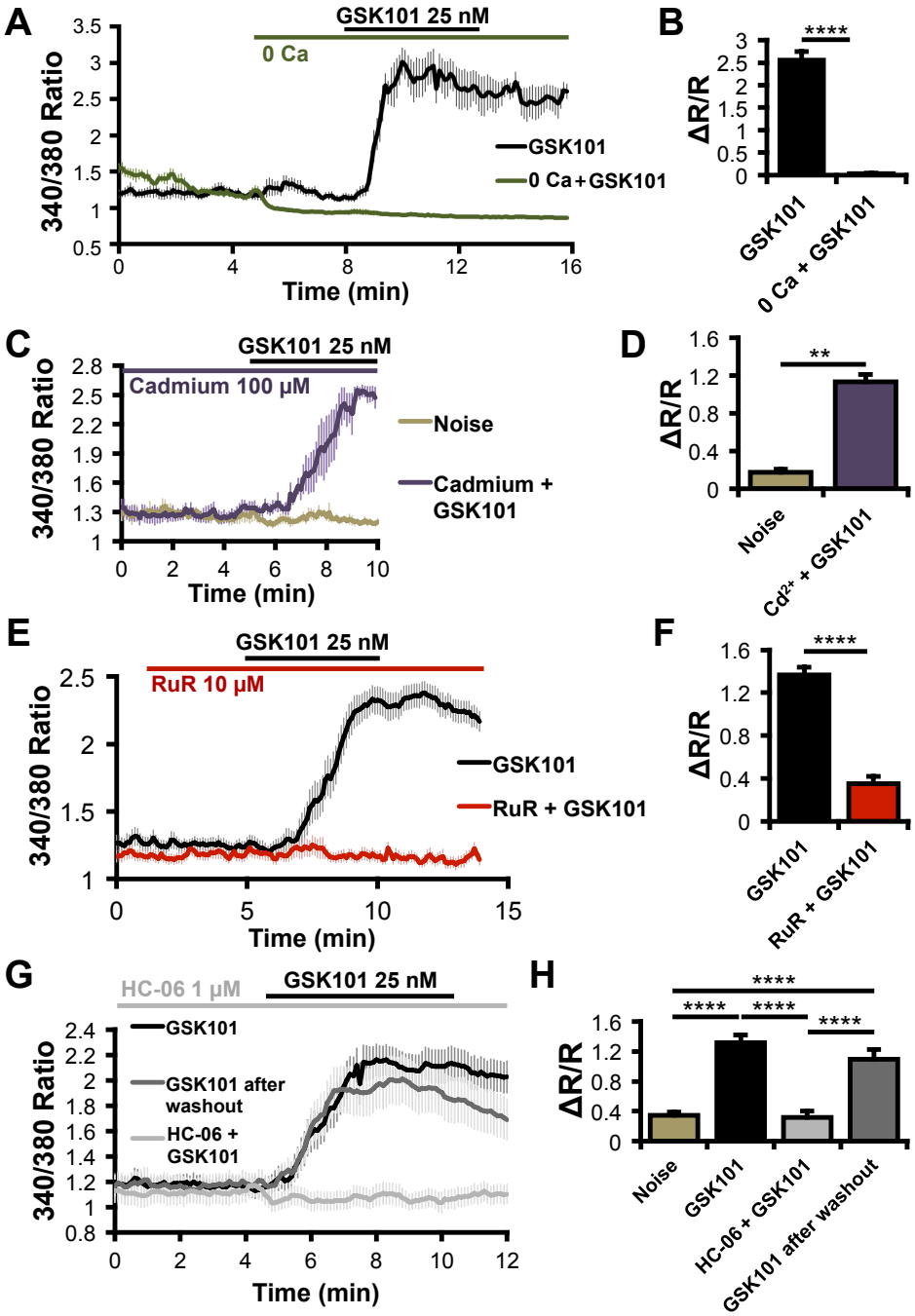

Figure 6.3 TRPV4 mediates responses to GSK101 in Müller cells. ***A-B***. External calcium is required for GSK101-induced calcium elevations, n = 16. ***C-D***. Responses to GSK101 persist in the presence of the voltage-gated channel blocker Cadmium (Cd^{2+}), n = 4. ***E-F***. The nonselective TRP channel antagonist Ruthenium Red (RuR) blocks responses to GSK101, n = 21 for GSK101 and 15 for GSK101 + RuR. ***G-H***. GSK101 responses are also blocked by the selective TRPV4 antagonist HC-06. This inhibition is reversible following a washout, n = 30 except noise = 40.

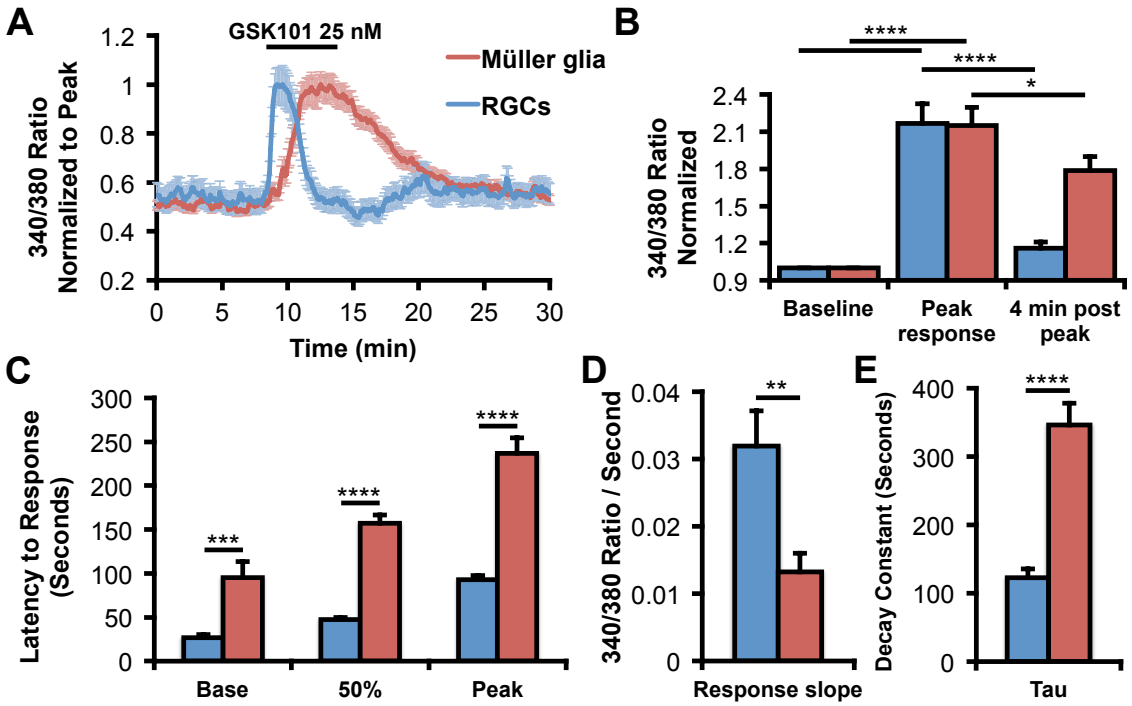

Figure 6.4 TRPV4 response kinetics differ in RGCs and Müller glia. ***A***. RGC responses to GSK101 are fast and transient, whereas Müller cells exhibit delayed and sustained TRPV4 activation. ***B***. GSK101 significantly increased calcium in both cell types (n = 25 Müller glia and 51 RGCs); however, RGC calcium returned closer to baseline levels 4 minutes after the response peak in the continued presence of GSK101. ***C***. The latency to the base (n = 17 Müller glia and 19 RGCs), 50% amplitude and peak response (n = 21 Müller glia and 24 RGCs) was longer in Müller cells. ***D-E***. The rate of TRPV4 activation (***D***, n = 20 Müller glia and 19 RGCs) and inactivation (***E***, n = 20 for each) was faster in RGCs.

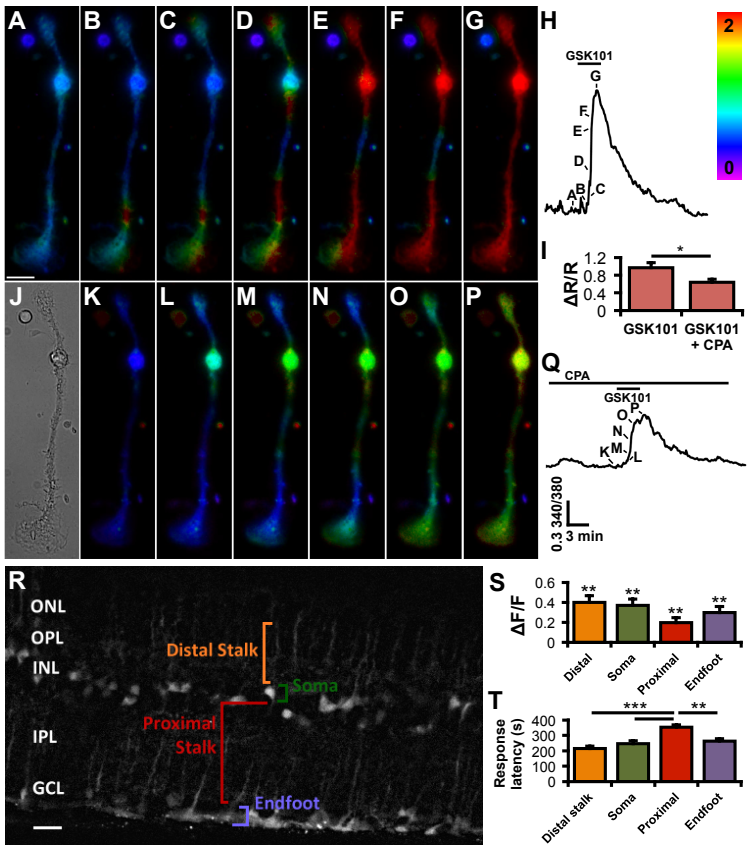

Figure 6.5 TRPV4 activation triggers Ca^{2+}-induced Ca^{2+} release and calcium waves. ***A-H***. Upon applying 25 nM GSK101 (***B-G***), calcium typically first flows into Müller glial endfeet (bottom) or their apical process (top). Calcium then elevates as a wave, filling the cytosol globally. Scale bar = 10 µm. The timing of the images (***A-G***) is indicated in the corresponding calcium trace (***H***). The rainbow scale specifies the 340/380 ratio level. ***I***. TRPV4 stimulation by GSK101 further elevates Ca^{2+} via Ca^{2+} release (stores depleted by bathing cells with 5 µM CPA while stimulating release with applications of 20 µM carbachol), n = 19. ***J-Q***. (***J***) A brightfield image of the Müller cell. (***K-P***) Store depletion by CPA attenuates the response to GSK101 (***L-P***) and the resulting wave. The corresponding trace (***Q***) indicates timing of images (***K-L***). ***R***. OBG-1 selectively loaded Müller glia in a retina slice. Four of the main Müller cell compartments are labeled for one cell. This image is the median composite of 10 temporally adjacent images separated by 3 seconds in time during the response to GSK101. The contrast between the Müller cells and the background was enhanced with the application of the rolling ball background subtraction function in ImageJ (10.0 pixel radius). Outer nuclear layer (ONL), outer plexiform layer (OPL), inner nuclear layer (INL), inner plexiform layer (IPL), ganglion cell layer (GCL). Scale bar 10 µm. ***S***. Responses to 10 µM GSK were significantly above the baseline for all cellular compartments. ***T***. The distal stalks and endfeet were the primary transduction sites, as indicated by shorter response latencies (time to ½ peak). n = 13 for distal stalk, 23 for somata, 16 for proximal stalk and 13 for endfeet.

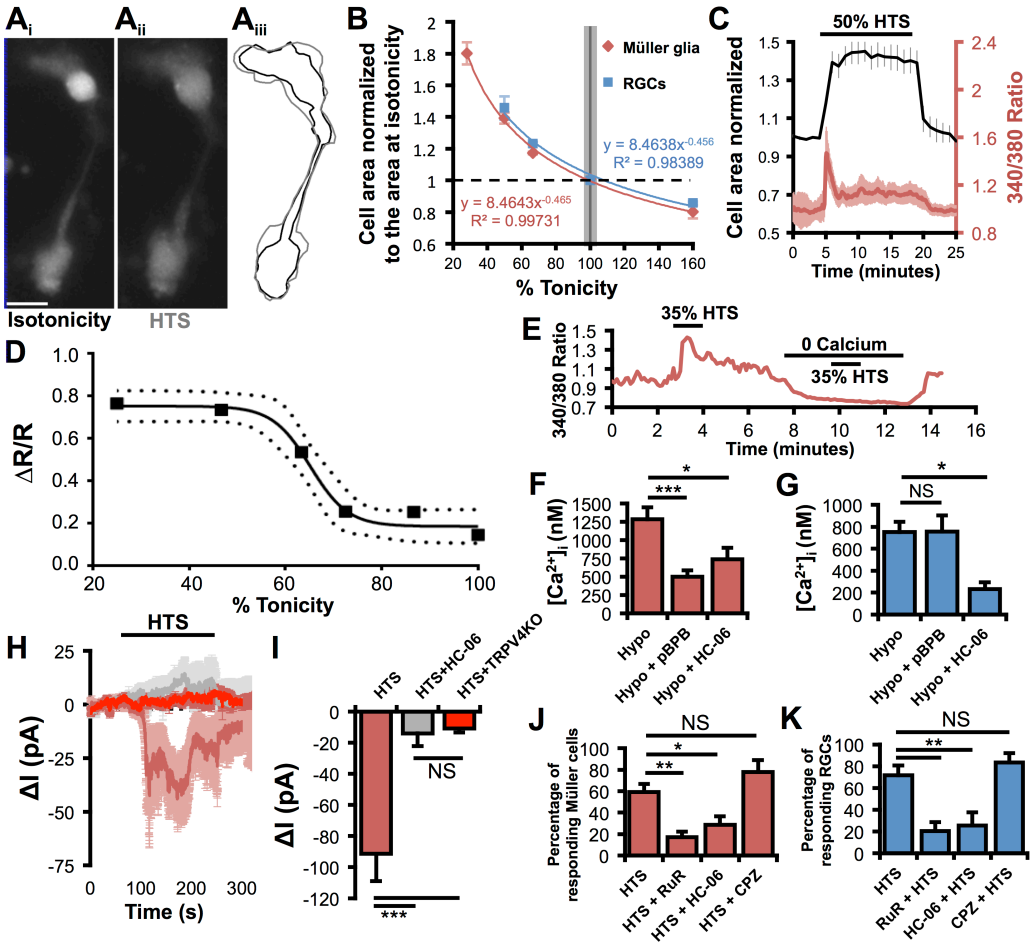

Figure 6.6 Differential TRPV4 channel activation mediates neuronal and glial responses to swelling. ***A***. Changes in the volume of calcein-loaded Müller cells were apparent when switching from isotonic (***Ai***) to hypotonic saline (***Aii***). ***Aiii***. The volume changes were approximated by measuring cell area. Isotonicity = black. Hypotonicity = gray. Scale bar = 10 µm. ***B***. Müller glia and RGCs swelled and shrunk as a function of tonicity. ***C***. HTS elevated Müller cell calcium as they swelled in a representative experiment. ***D***. Swelling-evoked calcium elevations were dose-dependent (95% confidence band around the sigmoidal fit), n = 13-20. ***E***. Swelling-evoked $[Ca^{2+}]_{MC}$ elevations required external calcium. ***F***. PLA2 and TRPV4 contribute substantially to the hypoosmotic response of Müller glia, n = 10, 13 and 11, respectively. ***G***. The PLA2 antagonist pBPB has no effect on RGC responses to cell swelling, even though these responses are mediated largely by TRPV4, n = 23, 16 and 9, respectively. ***H-I***. Fifty percent HTS evoked inward currents in Müller glia (n = 7) that were absent in the presence of HC-06 (n = 8) or in $TRPV4^{-/-}$ cells (n = 7). ***J***. Müller glia responsiveness to 35% HTS (n = 10 experiments) is reduced by the TRP channel antagonist Ruthenium Red (RuR 10 µM; n = 5) or 1 µM HC-06 (n = 6), but not the TRPV1 antagonist capsazepine (CPZ 10 µM; n = 3). ***K***. RGC responsiveness to HTS (n = 6) is impaired by Ruthenium Red (n = 6) and HC-06 (n = 6), but not TRPV1 inhibition (n = 3).

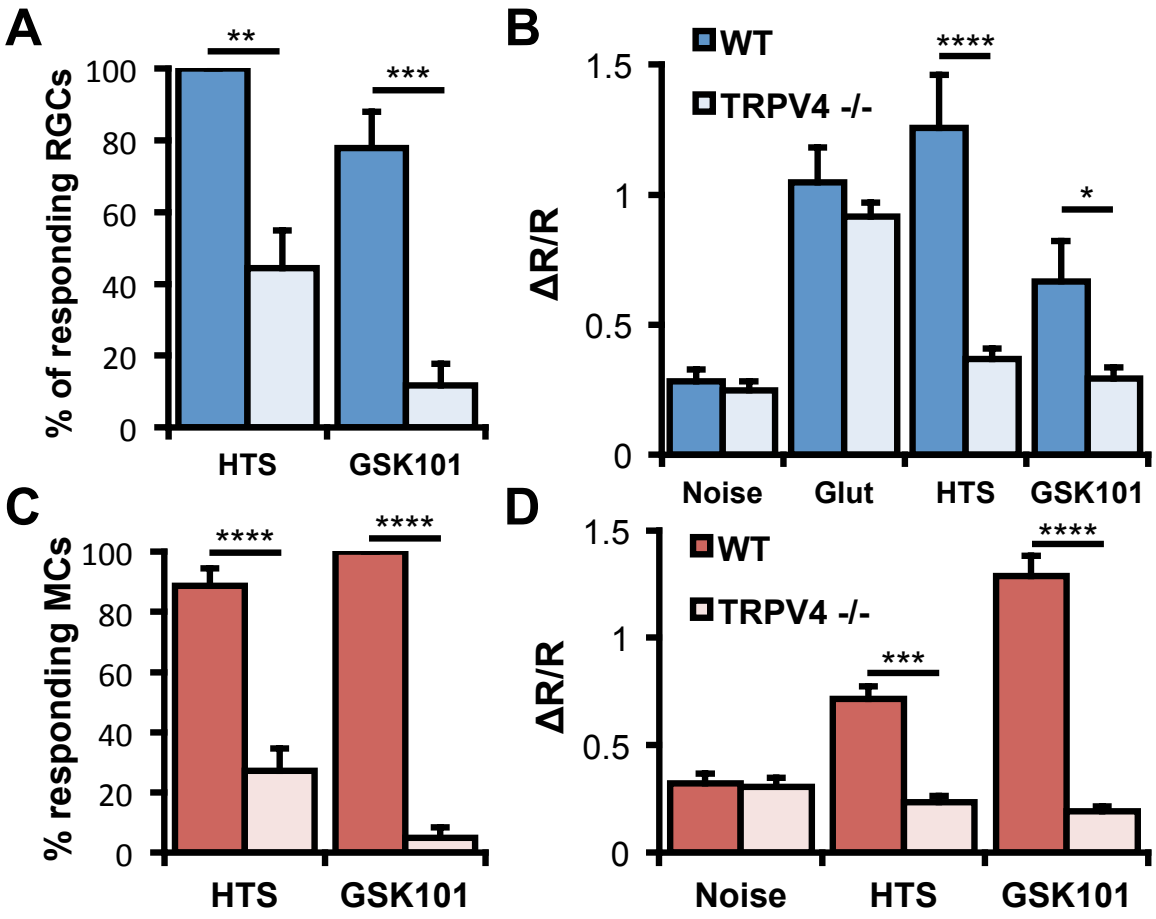

Figure 6.7 TRPV4 mediates RGC and Müller cells responses to HTS and GSK101. ***A***. The percentage of RGCs responding to 50% HTS and 25 nM GSK101 is reduced by TRPV4 ablation (n = 4-9 experiments, two-way ANOVA). ***B***. Calcium elevations induced by HTS and GSK are smaller in TRPV1$^{-/-}$ RGCs (N = 12-74 cells, two-way ANOVA). ***C***. The percentage of Müller cells responding to 50% HTS and 25 nM GSK101 is reduced by TRPV4 ablation (n = 3-8 experiments, two-way ANOVA). ***D***. Calcium elevations induced by HTS and GSK are smaller in TRPV1$^{-/-}$ Müller glia (n = 14-66 cells, two-way ANOVA).

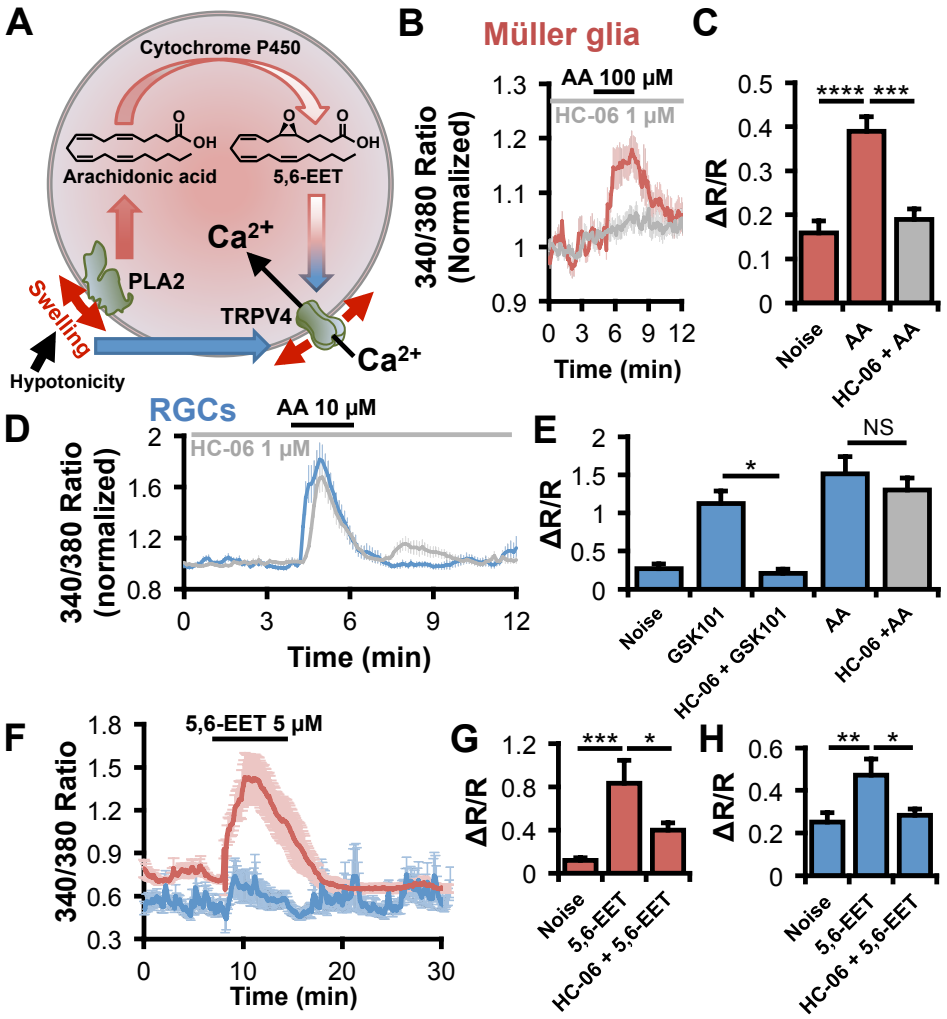

Figure 6.8 TRPV4 gating in Müller cells but not RGCs requires activation of phospholipase A2. ***A***. Working model for TRPV4 activation by cell swelling. In hypotonicity, both RGCs and Müller glia swell. This stretches the membrane and activates PLA2, at least in Müller cells. PLA2 then synthesizes AA, which is metabolized by a cytochrome P450 into 5,6-EET, an endogenous agonist for TRPV4. 5,6-EET can activate TRPV4 in both cell types, but its potency is greater in Müller cells. Although required in Müller cells, this indirect force transduction pathway does not contribute to swelling responses in RGCs. Thus, RGCs either utilize a novel force transduction pathway (indicated by the solid blue arrow) or direct gating of TRPV4 by membrane stretch (red arrows). ***B-C***. AA elevates $[Ca^{2+}]_{MC}$ by activating TRPV4, n = 34, 19 and 15, respectively. ***D-E***. Although HC-06 (n = 16) can completely inhibit TRPV4 activation by GSK101 (n = 10), HC-06 has no effect on AA responses (n = 46), suggesting that AA does not elevate RGC calcium through the activation of TRPV4. ***F***. Average traces from a representative experiment show that the 5,6-EET response is larger in Müller cells (red) than RGCs (blue). ***G-H***. 5,6-EET activates TRPV4 in both Müller glia (***G***, n = 14) and RGCs (***H***, n = 54).

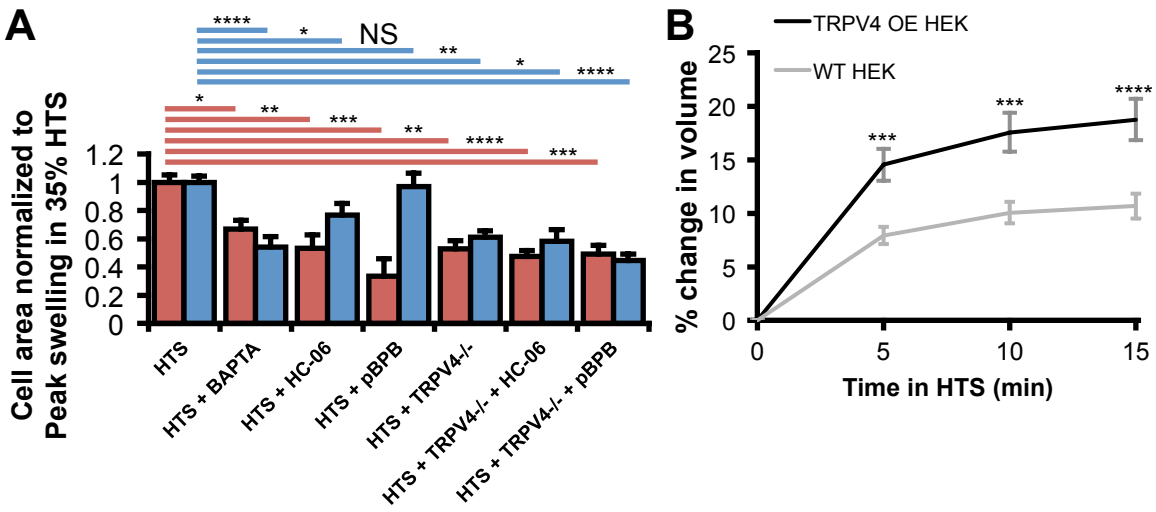

Figure 6.9 TRPV4 contributes to HTS-induced swelling. ***A***. The maximal extent of Müller cell (red) and RGC (blue) swelling in 35% HTS was reduced by chelating intracellular calcium with BAPTA-AM or by inhibiting TRPV4 and thereby limiting calcium entry. TRPV4-mediated swelling was PLA2-dependent in Müller glia, but not RGCs. Swelling was reduced in cells from TRPV4$^{-/-}$ mice. HC-06 and pBPB had no additional effect on the reduction of swelling. For Müller glia, n = 96, 14, 11, 8, 13, 18 and 14. For RGCs, n = 145, 31, 36, 24, 21, 9 and 22. ***B***. Thirty-five percent HTS increased the cross-sectional area of calcein-loaded, WT (n = 51) and TRPV4-overexpressing HEK293 cells (n = 64); however, the extent of swelling was increased by the activation of TRPV4.

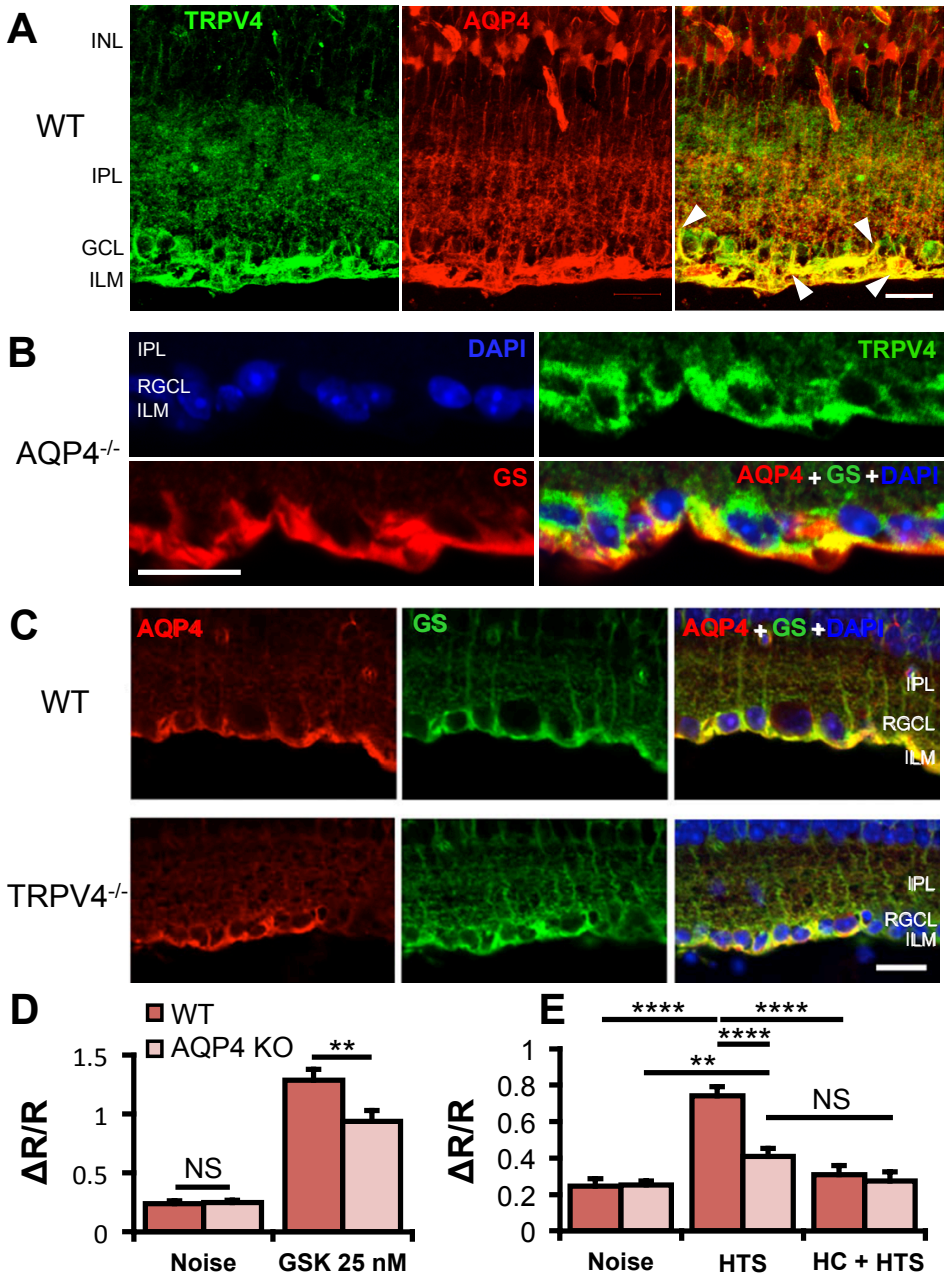

Figure 6.10 AQP4 expression is independent of TRPV4, yet it contributes to the swelling response of Müller glia. ***A***. Colocalization between TRPV4 and AQP4 within the glial endfeet and transverse processes in the inner retina (arrowheads). ***B***. TRPV4 expression in RGCs and the endfeet of Müller glia is normal in the AQP4$^{-/-}$ retina. ***C***. AQP4 is similarly expressed in the endfeet of Müller glia in retinal cryosections from both WT and TRPV4$^{-/-}$ mice. ***D***. Responses to GSK101 were slightly reduced, but still robust in AQP4$^{-/-}$ Müller glia. ***E***. Responses to 50% HTS (n = 20) were reduced in AQP4$^{-/-}$ Müller glia (n = 13). Scale bars = 20 µm. I = Inner, N = Nuclear, P = Plexiform, L = Layer, GC = Ganglion Cell, LM = Limiting Membrane.

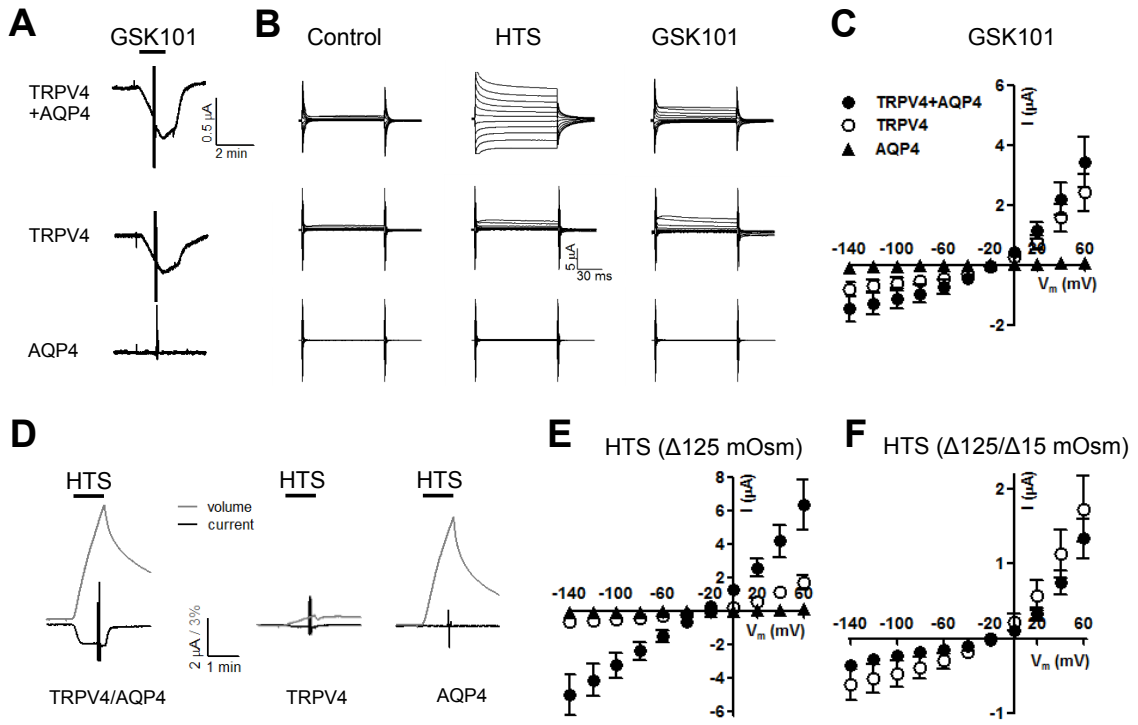

Figure 6.11 Aquaporin 4 channels amplify stretch-induced TRPV4 activation. ***A***. Oocytes expressing TRPV4 and AQP4 alone or in combination were voltage clamped at V_m= -30 mV and exposed to 100 nM GSK101 (indicated by black bar). After 60 seconds GSK exposure, an I-V curve was obtained by jumping the clamp potential to potentials ranging from +60 mV to -140 mV at 20 mV intervals (seen as the vertical lines in the current trace). ***B***. Representative I-V relations from oocytes expressing either TRPV4+AQP4 (n = 8), TRPV4 (n = 7), or AQP4 (n = 5) in control solution, in GSK solutions or when exposed to 125 mOsm HTS. ***C***. Summarized I-V relations obtained with GSK (as in ***B***, middle panel), n = 5-8. ***D***. Representative current (black lines) and volume traces (grey lines) recorded simultaneously from oocytes expressing TRPV4 and AQP4 alone or in combination upon exposure to a 125 mOsm hypotonic stimulus (indicated by the black bar), summarized in (***E***), n = 5-9. ***F***. Oocytes expressing TRPV4 alone or in combination with AQP4 were exposed to hypotonic challenges of different magnitudes in order to observe similar degree of cell swelling (125 mOsm for TRPV4-expressing oocytes and 15 mOsm for TRPV4/AQP4-expressing oocytes) and I-V relations were obtained after 60 seconds of cell swelling, n = 8-9.

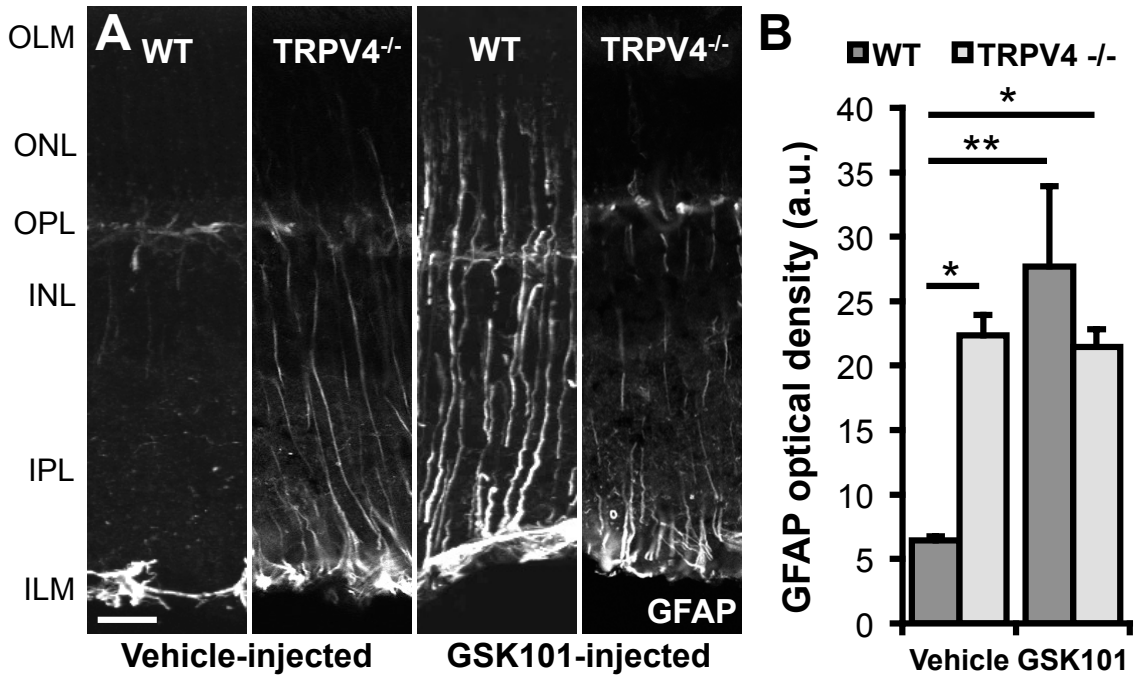

Figure 6.12 Role of TRPV4 in Müller glia reactivity. ***A***. Two weeks after a single intravitreal injection of a vehicle or 2 µl of 75 µM GSK101, mouse eyes were harvested and processed for immunohistochemistry. Only astrocytes on the vitreal surface expressed GFAP in control eyes, whereas Müller glia also expressed GFAP in the GSK101-injected eyes of wild type (WT) mice. TRPV4$^{-/-}$ Müller glia were reactive in both conditions, but GSK101 did not further increase gliosis. ***B***. The GFAP optical density was significantly greater in the GSK101-injected eyes, n = 3 for each. Scale bar = 20 µm. OLM = outer limiting membrane, ONL = outer nuclear layer, OPL = outer plexiform layer, INL = inner nuclear layer, IPL = inner plexiform layer, ILM = inner limiting membrane, a.u. = arbitrary units.

CHAPTER 7

TRPV4 SIGNALS GENERATE AND TRANSDUCE INTRAOCULAR PRESSURE IN GLAUCOMA

Amber Frye and I contributed equally to the research in this chapter. Sarah N. Redmon, Yong Xu, Erik Soderborg, Peter Barabas, Tam Phuong, Andrew O. Jo, Carol Toris, Glenn Prestwich and David Križaj also contributed to experiments, analysis, writing and/or synthesis of reagents.

7.1 Summary

Glaucoma treatment has faced two intractable challenges: to identify new pharmacological approaches to lower intraocular pressure (IOP) and to protect retinal ganglion cells (RGCs) from the effects of IOP (Chang & Goldberg, 2012). Here, we report that pharmacological or genetic inhibition of TRPV4, a mechano- and osmosensitive channel (Liedtke & Friedman, 2003), simultaneously addresses both key aspects of glaucoma therapy. Biochemical and functional analyses revealed TRPV4 expression in mouse and human trabecular meshwork (TM), a cellular network that permits aqueous humor outflow when its morphology and cytoskeletal organization are normal (Clark et al., 1994; Mitchell et al., 2002; Zhang et al., 2008). However, TRPV4-mediated Ca^{2+} influx into TM cells augmented hypoosmotic swelling, whereas suppression of TRPV4 activity decreased IOP in rodent and nonhuman primate models of glaucoma. TRPV4 inhibition additionally protected RGCs from apoptosis caused by glaucomatous mechanical strain, suggesting that the channel transduces elevated IOP into an excitotoxic calcium signal. The pathological effect of TRPV4 stimulation was reproduced by *in vivo* agonist stimulation of retinal TRPV4 channels and was sufficient to enable excitotoxic NMDA receptor currents. In support of these results, inhibition of TRPV4 prevented RGC loss in a rodent glaucoma model. These findings reveal a multifaceted role for TRPV4 in the regulation of conventional outflow and the sensitivity of RGCs to mechanical strain and suggest a potential first-in-kind comprehensive pharmacotherapeutic approach to simultaneously lower IOP and protect RGCs in glaucoma.

7.2 Main

Elevation of intraocular pressure (IOP), a major risk factor for glaucoma (Bonomi et al., 2001; Leske et al., 2007), most commonly results from impediment of aqueous humor drainage through the trabecular meshwork (TM; Clark et al., 1994; Mitchell et al., 2002; Zhang et al., 2008). The hydraulic conductivity of the iridocorneal angle and steady-state IOP are dynamically adjusted by TM cell volume regulation (Mitchell et al., 2002), actin reorganization (Clark et al., 1994; Zhang et al., 2008) and their capacity to transduce mechanical strain of the interwoven extracellular matrix (ECM) into a compensatory fluid transport response (Johnstone, 2004). If excessive, TM swelling and/or actin remodeling obstructs the conventional outflow pathway, which can pathologically elevate IOP (Brubaker 1975; Epstein & Rohen, 1991) and induce pressure-dependent degeneration of RGCs (Anderson et al., 2006; Della Santina et al., 2013). Thus, a better understanding of TM cell volume regulation and actin remodeling promises new molecular targets for IOP management; however, the mechanism by which TM cells respond to IOP, cell swelling and/or aqueous outflow remains poorly understood. Here, we identify the TM osmosensor/mechanosensor as TRPV4, a nonselective cation channel associated with polymodal transduction of warm temperature, cell swelling, shear stress and proinflammatory metabolites (Liedtke & Friedman, 2003; Watanabe et al., 2003). Real-time polymerase chain reaction (RT-PCR), western blotting and antibody staining showed TRPV4 expression in cultured human TM (hTM) cells (Fig. 7.1*A*,*B*), mouse TM cells (Fig. 7.1*C*), TM cells from glaucoma patient trabeculectomies (Fig. 7.1*D*) and HEK293 TRPV4 overexpressors (TRPV4:HEK293 cells), but not in naive HEK293 cells (Ryskamp et al., 2011). Both the selective TRPV4 agonist GSK10167901A (hereafter,

GSK101; 25 nM) and hypotonic swelling (220 mOsm) elevated the intracellular calcium concentration $[Ca^{2+}]_i$ in Fura-2 AM-loaded hTM cells (Fig. 7.1*E*,*F*,*H*,*I*). Similar to cultured cells (Fig. 7.1*E*,*F*), trabeculectomized human tissue responded to GSK101 with $[Ca^{2+}]_i$ elevations that were sensitive to the selective TRPV4 antagonist HC067047 (HC-06; 1 μM; Fig. 7.1*G*). GSK101- and swelling-induced $[Ca^{2+}]_{TM}$ elevations were prominently inhibited by HC-06 (Fig. 7.1*H*,*I*), suggesting that TRPV4 channels are necessary and sufficient for the transduction of swelling into $[Ca^{2+}]_i$ elevations in human TM cells. Inhibition of TRPV4 in hTM cells also reduced the extent of hypoosmotic swelling (Fig. 7.1*J*), indicating a potential pathogenic role for TRPV4 in human TM cell remodeling-induced IOP elevations.

To assess the potential involvement of TRPV4 in *in vivo* TM function, we studied the effect of the antagonist in mice with experimental glaucoma. As shown previously (Huang et al., 2011; Della Santina et al., 2013), injection of polystyrene microbeads rather than phosphate buffered saline (PBS; control) into the anterior chamber caused sustained IOP elevations (20.04 ± 1.24 (N = 13) vs. 9.8 ± 0.26 (N = 15) mm Hg; $p < 0.0001$; Fig. 7.2*A*). Animals were assigned to control or treatment groups while matching for the initial IOP elevation in the bead-injected eye before daily intraperitoneal (IP) injections commenced. Compared to MB/vehicle-injected controls (N = *9*), daily MB/HC-06-treated animals (10 mg/kg) showed a rapid drop in IOP (N = 4; $p < 0.0001$; Fig. 7.2*B*), which showed no desensitization in the continued presence of the antagonist (Fig. 7.2*A*). We tested whether the effectiveness of HC-06 was derived from direct targeting of the eye by injecting it (1.862 mM, 2 μl) directly into the anterior chamber (Fig. 7.2*C*,*D*). Single intraocular HC-06 injections rapidly reduced IOP and the effect

lasted for days, presumably by maximizing the local bioavailability of the antagonist. Further indicating that TRPV4 channels are required to maintain elevated IOP within the anterior eye, microbead injections never elevated pressure in TRPV4$^{-/-}$ eyes (N = 4; Fig. 7.2*E*). To test whether topical eye drops could lower IOP, we generated a prodrug (isopropyl ester; YX-02) version of the antagonist. Daily administration of the prodrug likewise decreased the IOP to baseline levels (Fig. 7.2*F*; N = 4; $p < 0.01$ to $p < 0.0001$; Holm-Šídák test). Given the functional expression of TRPV4 in hTM cells and trabeculectomized human TM (Fig. 7.1), we surmised that TRPV4 channels might regulate IOP in nonhuman primates. IOP was elevated in two macaque eyes by laser treatment of the TM. Microinjection of HC-06 (1.862 mM) into the anterior chamber elicited a long-lasting reduction of IOP (e.g., 25.6 ± 0.1 vs. 29.8 ± 0.1 mm Hg at 80 hours). These data suggest that TRPV4 channels, expressed within the conventional outflow pathway, contribute to the maintenance of elevated IOP in rodent and primate glaucoma.

We previously discovered that neuronal TRPV4 expression in the retina is restricted to most, if not all, RGCs where it contributes to their intrinsic mechanosensitivity and its activation increases RGC $[Ca^{2+}]_i$, spiking and apoptosis (Ryskamp et al., 2011). Given theses findings and the importance of calcium dysregulation in the pathogenesis of IOP-dependent RGC neurodegeneration (Crish & Calkins, 2011), we hypothesized retinal TRPV4 transduces glaucomatous forces into activation of IOP-dependent biochemical cascades associated with dendritic/synaptic remodeling, axon transport deficiencies and RGC apoptosis.

IOP mechanically strains the retina (Krizaj et al., 2014) and, during glaucoma

progression, RGCs are additionally subjected to osmotic pressures within the peripheral retina associated with swelling (Pinar-Sueiro et al., 2011) and apoptotic shrinking (Weber et al., 1998). To investigate the potential role of TRPV4 activation in glaucomatous force-induced RGC death, isolated mouse retinas were incubated in control L-15 media or hypoosmotic media for 2.5 hours and dead cells were labeled with ethidium homodimer. Thirty-five percent hypotonic stimulation (HTS) was sufficient to cause cell death in the ganglion cell layer (GCL; Fig. 7.3*A*,*B*). This required cytosolic calcium because death was suppressed by 200 μM BAPTA-AM. HC-06 (1 μM) also prevented HTS-induced death, indicating that TRPV4 is required for mechanical excitotoxicity of RGCs. TRPV4 overactivation by GSK101 (1 μM) was sufficient to drive RGC loss and this also required elevation of $[Ca^{2+}]_{RGC}$. Moreover, genetic ablation of TRPV4, but not TRPV1, another mechanosensitive channel expressed in RGCs (Sappington et al., 2009), prevented RGC death. These results indicate a role for TRPV4 in osmotic pressure-induced RGC death.

To examine whether TRPV4 overstimulation causes RGC death *in vivo*, GSK101 was injected into the intravitreal space of anesthetized mice. After 4 weeks, a profound loss of RGC nuclei was observed in GSK101-treated eyes compared to vehicle-treated eyes (2465.6 ± 92.5 vs. 5884.4 ± 166.3 $NeuN^+$ cells in the GCL / mm^2; $N = 6$; $p < 0.0001$; Fig. 7.3*C*,*D*). GSK101-induced RGC loss was blocked by a prior intraperitoneal injection of HC-06 (Fig. 7.3*D*). This further indicates that excessive TRPV4 activity can drive RGC pathology.

Although the precise coupling mechanism that underlies the transduction of mechanical (IOP-induced) stress within the retinal tissue and that leads to RGC pathology

is not known, one possibility entails the direct sensitivity of the output neurons to mechanical strain (local deformation induced by applied stress) produced by increased IOP (Burgoyne, 2011). Glaucomatous IOP elevations generate biomechanical strain through a pressure gradient that causes the volume of the eye to expand, stretching the retina (Krizaj et al., 2014). IOP fluctuations during saccades and head movements are superimposed on static IOP elevations (Downs et al., 2011) and thus contribute to dynamic retinal strain. To model this and to assess the RGC response to biomechanical strain, acutely dissociated mouse retinal cells were stimulated with biaxial substrate stretch (5 ± 1.5%; 2 Hz; 90 min). As shown in Fig. 7.3*E*,*F*, continuous cyclic strain increased RGC apoptosis as indicated by the percentage of Annexin V^+/propidium $iodide^+$ RGCs (10.55 ± 2.0 % vs. 31.47 ± 5.6 %; N = 6; $p < 0.01$). Stretch-elicited RGC loss was blocked by concurrent-treatment with HC-06 (Fig. 7.3*F*). Likewise, $TRPV4^{-/-}$ RGCs, but not $TRPV1^{-/-}$ RGCs, were protected from stretch-induced RGC apoptosis (Fig. 7.3*F*). Thus, TRPV4 represents an endogenous RGC sensor of mechanical strain that, when overactivated, is sufficient to compromise the viability of RGCs.

NMDA-mediated excitotoxicity and Ca^{2+} overload have been amongst the main mechanisms proposed to damage glaucomatous RGCs (Hare et al., 2001; Crish & Calkins, 2010). We investigated the possibility that TRPV4 activation induces Ca^{2+} overloads in part by augmenting NMDA receptor function. Thy1:CFP RGCs were stimulated with GSK101 (25 nM) and NMDA/glycine (100 μM/10 μM) in control (3 mM Mg^{2+}-containing) and Mg^{2+}-free saline. NMDA alone had no effect on $[Ca^{2+}]_{RGC}$ in control saline, but evoked marked $[Ca^{2+}]_i$ responses in 0 Mg^{2+} (Fig. 7.3*G*). Suggesting that TRPV4 activation is sufficient to override the effects of the Mg^{2+} block, concurrent

application of the GSK101 and NMDA (100 μM) in 3 mM Mg^{2+} exceeded the effects of each compound alone ($p < 0.001$; N = 16; repeated measures ANOVA; Fig. 7.3*G*).

Finally, to determine whether TRPV4 suppression or elimination treatment is neuroprotective, we analyzed RGC survival in the mouse glaucoma model treated daily with the antagonist. Eight weeks after IOP elevation, RGC counts in eyes with elevated IOP were decreased to 2370.1 ± 72.8 TuJ-1^{+} cells in the GCL / mm^2 (N = 6) compared to 3425.1 ± 251.3 in control eyes from vehicle-treated animals (N = 7). Consistent with the requirement for TRPV4 channels to support IOP elevation (Fig. 7.2), no RGC loss was observed in microbead-treated eyes of mice treated with HC-06 (Fig. 7.3*H*,*I*).

Glaucoma is a multifactorial disease involving multiple IOP-generating mechanisms within the anterior eye and several target cell populations within the retina (Clark et al., 1994; Mitchell et al., 2002; Johnstone et al., 2004; Zhang et al., 2008; Burgoyne, 2011; Crish & Calkins, 2011; Chang & Goldberg, 2012; Della Santina et al., 2013; Krizaj et al., 2014). As additional alleles that confer genetic susceptibility are discovered (van Koolwijk et al., 2012), it will be important to determine whether and how they contribute to IOP generation and/or retinal vulnerability. For example, a common variant near caveolin1/caveolin2 (CAV1/CAV2) was associated with primary open-angle glaucoma (Thorleifsson et al., 2010; Wiggs et al., 2011); however, despite the expression of CAV1/CAV2 in TM cells and RGCs, the mechanism by which changes in caveolin expression and/or function contributes to glaucoma remains unknown. CAV1/CAV2 form caveolae within membranes, which are important signaling domains for TRPV4 (Saliez et al. 2008). Thus, changes in their tissue-specific expression and/or function could potentially enhance or suppress TRPV4 function, which might explain the role of

CAV1/CAV2 variants in IOP generation and/or RGC susceptibility in open-angle glaucoma.

Given the vast number of studies that sought an effective modulator of elevated IOP within the conventional outflow pathway and the notable absence of successful neuroprotective approaches, it is remarkable that inhibition of the stretch- and swelling-sensitive TRPV4 channel simultaneously lowers IOP (Fig. 7.2) and protects RGCs from the effects of excessive mechanical stimulation (Fig. 7.3). Thus, TRPV4 blockers might represent an elegant and effective multifacted treatment paradigm for glaucoma.

7.3 Methods

7.3.1 Animals

All experiments followed recommendations of the NIH Guide for Care and Use of Laboratory Animals and the Association for Research in Vision and Ophthalmology Statement for the Use of Animals in Ophthalmic and Vision Research and were approved by the University of Utah and University of Nebraska Medical Center Animal Care and Use Committees. Experiments involved C57BL/6J, B6.Cg-Tg(*Thy1*-CFP)23Jrs/J, TRPV4$^{-/-}$ (Liedtke & Friedman, 2003) and TRPV1$^{-/-}$ mice (JAX) and cynomolgus monkeys.

7.3.2 hTM Cell Culturing

hTM cells (ScienCell Research Laboratories) were grown in Dulbecco's modified eagles medium (DMEM), penicillin (100 U/ml), streptomycin (0.1 mg/ml) and 10% fetal bovine serum at 37˚C and 5% CO_2.

7.3.3 mRNA and Protein Analysis

Semiquantitative RT-PCR and western blotting of hTM cells were performed as described previously (Ryskamp et al., 2011).

7.3.4 Cryosection Immunohistochemistry

Mice were deeply anesthetized with isoflurane and transcardially perfused with PBS, followed by 4% PFA in PBS. Eyes were postfixed for 2 hours at 4°C and rinsed with PBS. Fresh TM tissue explants were fixed in 4% PFA and PBS for 1 hour at room temperature (RT). Tissue was cryoprotected in 15% (1 hour RT) and 30% sucrose (4˚C overnight) and embedded in OCT (Tissue-Tek). Twelve to sixteen µm slices were cut with a cryostat and mounted on Superfrost plus slides (Fisher Scientific). Slides were dried and frozen at -80˚C until use. Slices were rinsed in PBS and incubated in blocking solution (10 ml PBS, 30 µl Triton X-100, 100 mg BSA, 100 µl 10% w/v Na^+ azide solution) for 30-60 minutes at RT. Primary (rabbit anti-TRPV4, 1:100; Lifespan) and secondary (goat antirabbit Alexa Fluor 488: 1:1000) antibodies were diluted in blocking solution and applied for 12 hours (4°C) and 1 hour (RT), respectively. Nuclei were counterstained with propidium iodide (PI). Sections were mounted in VectaShield (Vector Laboratories) and coverslipped.

7.3.5 Calcium Imaging

Cultured hTM cells were loaded with 5 µM Fura-2 AM 30 minutes and were perfused with isotonic saline (pH 7.4) containing the following (in mM): 98.5 NaCl, 5 KCl, 3 $MgCl_2$, 2 $CaCl_2$, 10 HEPES, 10 Glucose, 93 Mannitol. Mannitol was removed to make

30% hypotonic saline (HTS). To obtain primary retina cells, mice were euthanized with isoflurane, followed by cervical dislocation. Eyes were removed and retinas were isolated by dissection in cold L-15 media. Retina incubation in 7 U/ml papain (Worthington)/L-15 for 1 hour at RT digested the extracellular matrix to facilitate cellular dissociation by gentle mechanical trituration. Retinal cells were plated on a concanavalin A-coated coverslip and incubated with Fura-2-AM (5 μM) for 30-40 minutes. Human TM explants were loaded with 10 μM Fura-2 for 1 hour at RT and were perfused with recording buffer containing (in mM): 120 NaCl, 6 KCl, 1.4 $CaCl_2$, 1 $MgSO_4$, 20 HEPES, 5.6 glucose and 9 sodium pyruvate (pH 7.4). Calcium imaging was performed as described (Ryskamp et al., 2011). Cells from experiments summarized in Fig. 7.3*G* were exposed to verapamil (100 μM) to reduce spontaneous activity and to study more direct synergy between TRPV4 and NMDA receptors without depolarization/Ca^{2+} from L-type Ca^{2+} channels.

7.3.6 Volume Imaging

hTM cells were loaded with 10-15 μM calcein-AM during Fura-2 loading. Cell area, which was crisply delineated by calcein fluorescence, was measured with NIS-Elements (Nikon) to approximate cell volume. Percent change in cell area reflects the difference in volume after 5 minutes of exposure to 30% HTS compared to volume preceding HTS.

7.3.7 Microbead Occlusion Glaucoma Model

Mice were anesthetized with an intraperitoneal (IP) injection of ketamine/xylazine (90 mg/10 mg / kg of body weight) and eye drops were used to numb the eyes (0.5% proparacaine hydrochloride) and dilate the pupils (1% tropicamide ophthalmic solution

USP; Bausch & Lomb). IOP was elevated unilaterally by injecting 2 µl of polystyrene microbeads (10 µm FluoSpheres) with a blunt tip, Hamilton syringe (Hamilton Company) into the anterior chamber after making a guide hole using a 30.5 gauge needle, gently depressing the cornea to displace aqueous humor and drying the eye. Microbeads were injected over 60 seconds and the needle remained for an additional 60 seconds before injecting a small bubble to seal the cornea and prevent microbead outflow. The contralateral eye was injected with PBS. Erythromycin ophthalmic ointment USP 0.5% (Bausch & Lomb) was applied after the procedure.

7.3.8 Mouse IOP Measurements

We used a Tonolab rebound tonometer to measure IOP of Avertin-treated (Figure 7.2*A*,*B*; Huang et al., 2011) and awake mice (Figure 7.2*C*-*F*; Ding et al. 2011) between 10 AM and noon. For awake mice, 0.5% proparacaine hydrochloride was applied prior to measurements. IOP was determined from the mean of 15 to 20 tonometer readings.

7.3.9 Systemic TRPV4 Inhibition

HC-067047 (Sigma Aldrich, St. Louis, MO) was dissolved in 1.85% DMSO and PBS, then it or the vehicle was administered via a 10mg/kg intraperitoneal injection (IP) once daily for 8 weeks.

7.3.10 Topical TRPV4 Inhibition

The prodrug used for eye drops was identical to HC-06 except an isopropyl ester group replaced the trifluoromethyl group. To make the prodrug, 2-methyl-1-(3-

morpholinopropyl)-5-phenyl-1*H*-pyrrole-3-carboxylic acid (200 mg; 0.610 mmol) in 5 mL dichloromethane (DCM) was added to thionyl chloride (220 µL; 3.05 mmol) and dimethylformamide (20 µl). After stirring for 3 hours at RT, the reaction mixture was evaporated and dried under vacuum pressure. To the residue was added DCM (5 ml), isopropyl 3-aminobenzoate (218 mg; 1.20 mmol) and *N,N*-Diisopropylethylamine (0.42 ml), and the reaction mixture was stirred overnight. Water was added and the mixture was extracted with DCM. The organic phase was washed with water, brine, dried by anhydrous sodium sulfate, concentrated and purified by chromatography to provide the prodrug YX-02 (290 mg; 0.592 mmol, 97% yield). H-NMR (CD3OD/400 MHz): δ 8.32 (s, 1H); 7.89 (d, 1H); 7.71 (d, 1H); 7.42 (m, 6H); 6.65 (s, 1H); 5.21 (m, 1H); 4.07 (m, 2H); 3.54 (m, 4H); 2.64 (s, 3H); 2.15 (m, 6H); 1.64 (m, 2H); 1.38 (d, 6H). MS (ES^+, m/z): 490.1 (M^++1, 100.0). One drop of a 1.862 mM prodrug solution (1.85% DMSO and PBS) was applied unilaterally to each mouse eye. The vehicle was applied contralaterally as a control.

7.3.11 Primate Glaucoma Model and IOP Measurements

Two female cynomolgus monkeys between the ages of 6 and 14 years were included in the study. Both had laser treatment to the trabecular meshwork of the left eye to elevate IOP. Lasering had been done between 3 and 10 years earlier. HC-06 solution (1.862 mM) or the vehicle (1.85% DMSO and PBS) was injected into the anterior chamber, but the solution contents were masked until the study was completed. IOP was measured by tonometry, as in Toris et al. (2005), while animals were conscious and seated in specially designed chairs.

7.3.12 RGC Death/Neuroprotection Assays

To study acute RGC excitotoxicity, mouse retinas were isolated and incubated in L-15 media or specified conditions for 2.5 hours at RT in darkness. Membrane breakdown was indicated by ethidium homodimer (8 μM) labeling of RNA and DNA (15 minutes at RT). After rinsing, retinas were flatmounted and imaged on an Olympus FV1200 upright confocal (40X water objective, NA 0.8) or a Zeiss LSM 510 confocal (40X oil objective, NA 1.3) microscope. Five images were taken and the dead cell count in the GCL was averaged for each retina. Image acquisition parameters remained constant across samples. To quantify GSK101- and IOP-induced RGC loss *in vivo*, retinas were fixed as before, isolated in PBS, flatmounted and immunostained. To reduce autofluorescence, retinas were treated for 5 minutes with 50 mM NH_4Cl in PBS (Bosco et al., 2011). After rinsing with PBS, retinas were incubated for 1.5 hours at RT in 0.2% Triton X-100, 1% bovine serum albumin (BSA), and 5% normal goat serum (NGS) and PBS. Primary antibodies were diluted in 1% BSA, 5% NGS and PBS (1:500) and incubated with the retina for 1 hour at RT while rocking, then for 3 days at 4°C. Retinas were rinsed with PBS and secondary antibodies (1:500 in 1% BSA and PBS) were applied for 2 hours at RT. Retinas were rinsed in PBS, 0.2% Triton X-100 and then PBS again. Retinas were mounted in VectaShield and imaged with confocal microscopes. Neurons in the GCL were labeled by staining β-III-Tubulin (anti-Tuj1; Millipore) or NeuN (anti-NeuN Alexa Fluor 488; Millipore). Four images per quadrant were quantified manually for each retina while blinded to treatment. To examine the effects of sustained mechanical strain on RGC apoptosis, acutely isolated mouse retinal cells were plated on collagen type IV-coated silicone membranes. These membranes were then radially stretched using a

StageFlexer FX5000 system (Flexcell International Corporation) statically by 5% and sinusoidally ± 1.5% at 2 Hz for 90 minutes. RGCs were identified as before (Ryskamp et al., 2011) and the percentage of apoptotic RGCs was quantified using an Alexa Fluor 488 Annexin V/Dead Cell Apoptosis Kit.

7.3.13 Materials

Salts and reagents were purchase from Sigma or Life Technologies unless specified otherwise.

7.3.14 Statistical Analysis

GraphPad Prism 6.0 was used for statistics. Means are shown ± SEM. Unless specified, an unpaired t-test was used to compare two means and an ANOVA along with Tukey's multiple comparisons test was used to compare three or more means. $p > 0.05$ = NS, $p < 0.05$ = *, $p < 0.01$ = **, $p < 0.001$ = *** and $p < 0.0001$ = ****.

7.4 References

Anderson MG, Libby RT, Mao M, Cosma IM, Wilson LA, Smith RS, John SW (2006) Genetic context determines susceptibility to intraocular pressure elevation in a mouse pigmentary glaucoma. BMC Biol 4:20.

Bonomi L, Marchini G, Marraffa M, Morbio R (2001) The relationship between intraocular pressure and glaucoma in a defined population. Ophthalmologica 215:34-38.

Bosco A, Steele MR, Vetter ML (2011) Early microglia activation in a mouse model of chronic glaucoma. J Comp Neurol 519:599-620.

Brubaker RF (1975) The effect of intraocular pressure on conventional outflow resistance in the enucleated human eye. Invest Ophthalmol Vis Sci 14:286-292.

Burgoyne CF (2011) A biomechanical paradigm for axonal insult within the optic nerve

head in aging and glaucoma. Exp Eye Res 93:120-132.

Chang EE, Goldberg JL (2012) Glaucoma 2.0: neuroprotection, neuroregeneration, neuroenhancement. Ophthalmology 119:979-986.

Clark AF, Wilson K, McCartney MD, Miggans ST, Kunkle M, Howe W (1994) Glucocorticoid-induced formation of cross-linked actin networks in cultured human trabecular meshwork cells. Invest Ophthalmol Vis Sci 35:281-294.

Crish SD, Calkins DJ (2011) Neurodegeneration in glaucoma: progression and calcium-dependent intracellular mechanisms. Neuroscience 176:1-11.

Della Santina L, Inman DM, Lupien CB, Horner PJ, Wong RO (2013) Differential progression of structural and functional alterations in distinct retinal ganglion cell types in a mouse model of glaucoma. J Neurosci 33:17444-17457.

Ding C, Wang P, Tian, N (2011) Effect of general anesthetics on IOP in elevated IOP mouse model. Exp Eye Res 92:512-520.

Downs JC, Burgoyne CF, Seigfreid WP, Reynaud JF, Strouthidis NG, Sallee V (2011) 24-hour IOP telemetry in the nonhuman primate: implant system performance and initial characterization of IOP at multiple timescales. Invest Ophthalmol Vis Sci 52:7365-7375.

Epstein DL, Rohen JW (1991) Morphology of the trabecular meshwork and inner-wall endothelium after cationized ferritin perfusion in the monkey eye. Invest Ophthalmol Vis Sci 32:160-171.

Hare W, WoldeMussie E, Lai R, Ton H, Ruiz G, Feldmann B, Wijono M, Chun T, Wheeler L (2001) Efficacy and safety of memantine, an NMDA-type open-channel blocker, for reduction of retinal injury associated with experimental glaucoma in rat and monkey. Surv Ophthalmol 45:S284-S289.

Huang W, Xing W, Ryskamp DA, Punzo C, Križaj D (2011) Localization and phenotype-specific expression of ryanodine calcium release channels in C57BL6 and DBA/2J mouse strains. Exp Eye Res 93:700-709.

Johnstone MA (2004) The aqueous outflow system as a mechanical pump: evidence from examination of tissue and aqueous movement in human and non-human primates. J. Glaucoma 13:421-438.

Križaj D, Ryskamp DA, Tian N, Tezel G, Mitchell CH, Slepak VZ, Shestopalov VI (2014) From mechanosensitivity to inflammatory responses: new players in the pathology of glaucoma. Curr Eye Res 39:105-119.

Leske MC, Heijl A, Hyman L, Bengtsson B, Dong L, Yang Z, EMGT Group (2007) Predictors of long-term progression in the early manifest glaucoma trial.

Ophthalmology 114:1965-1972.

Liedtke W, Friedman JM (2003) Abnormal osmotic regulation in trpv4-/-mice. Proc Natl Acad Sci USA 100:13698-13703.

Mitchell CH, Fleischhauer JC, Stamer WD, Peterson-Yantorno K, Civan MM (2002) Human trabecular meshwork cell volume regulation. Am J Physiol Cell Physiol 283:C315-C326.

Pinar Sueiro S, Urcola H, Rivas AM, Vecino E (2011) Prevention of retinal ganglion cell swelling by systemic brimonidine in a rat experimental glaucoma model. Clin Experiment Ophthalmol 39:799-807.

Ryskamp DA, Witkovsky P, Barabas P, Huang W, Koehler C, Akimov NP, Lee SH, Chauhan S, Xing W, Rentería RC, Liedtke W, Križaj D (2011) The polymodal ion channel transient receptor potential vanilloid 4 modulates calcium flux, spiking rate, and apoptosis of mouse retinal ganglion cells. J Neurosci 31:7089-7101.

Saliez J, Bouzin C, Rath G, Ghisdal P, Desjardins F, Rezzani R, Rodella LF, Vriens J, Nilius B, Feron O, Balligand JL, Dessy C (2008) Role of Caveolar compartmentation in endothelium-derived hyperpolarizing factor–mediated relaxation Ca2+ signals and gap junction function are regulated by caveolin in endothelial cells. Circulation 117:1065-1074.

Sappington RM, Sidorova T, Long DJ, Calkins DJ (2009) TRPV1: contribution to retinal ganglion cell apoptosis and increased intracellular Ca2+ with exposure to hydrostatic pressure. Invest Ophthalmol Vis Sci 50:717-728.

Thorleifsson G et al. (2010) Common variants near CAV1 and CAV2 are associated with primary open-angle glaucoma. Nat Genet 42:906-909.

Toris CB, Zhan GL, Camras CB, McLaughlin MA (2005) Effects of travoprost on aqueous humor dynamics in monkeys. J Glaucoma 14:70-73.

van Koolwijk LM et al. (2012) Common genetic determinants of intraocular pressure and primary open-angle glaucoma. PLoS Genet 8:e1002611.

Watanabe H, Vriens J, Prenen J, Droogmans G, Voets T, Nilius B (2003) Anandamide and arachidonic acid use epoxyeicosatrienoic acids to activate TRPV4 channels. Nature 424:434-438.

Weber AJ, Kaufman PL, Hubbard WC (1998) Morphology of single ganglion cells in the glaucomatous primate retina. Invest Ophthalmol Vis Sci 39:2304-2320.

Wiggs JL, Kang JH, Yaspan BL, Mirel DB, Laurie C, Crenshaw A, Brodeur W, Gogarten S, Olson LM, Abdrabou W, DelBono E, Loomis S, Haines JL, Pasquale LR, Geneva

Consortium (2011) Common variants near CAV1 and CAV2 are associated with primary open-angle glaucoma in caucasians from the United States. Hum Mol Genet 20:4707-4713.

Zhang M, Maddala R, Rao PV (2008) Novel molecular insights into RhoA GTPase-induced resistance to aqueous humor outflow through the trabecular meshwork. Am J Physiol Cell Physiol 295:C1057-C1070.

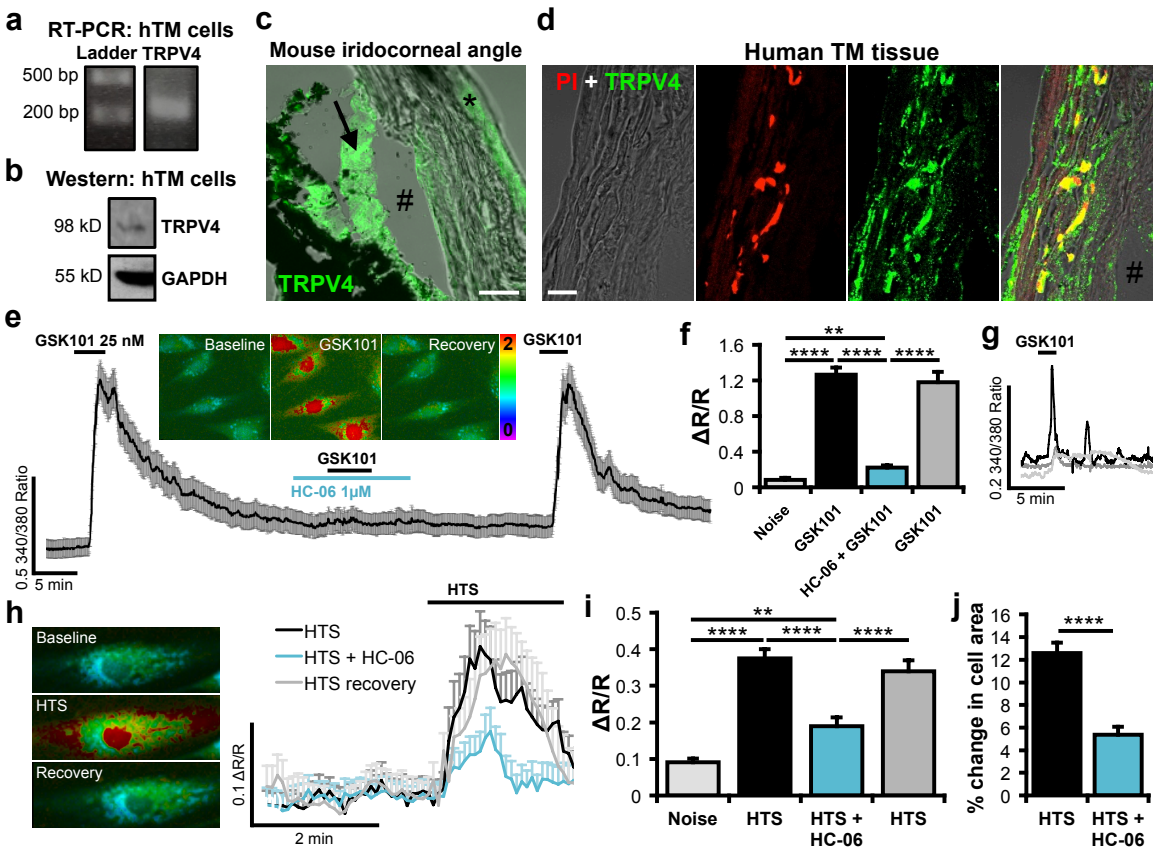

Figure 7.1 TRPV4 is functionally expressed in mouse and human TM and contributes to TM swelling. ***A***. Trpv4 mRNA is expressed in hTM tissue (202 bp amplicon). ***B***. TRPV4 protein was detected in hTM cells at the appropriate molecular weight. ***C***. TRPV4 is expressed in the mouse TM (arrow) preceding Schlemm's canal (#) and in corneal epithelial cells (*). ***D***. Trabeculectomized human TM tissue immunolabels for TRPV4. Nuclei were counter-stained with propidium iodide (PI). ***E-H***. GSK101- and hypotonic swelling (220 mOsm) -induced $[Ca^{2+}]_i$ increases in hTM cells are inhibited by HC-06. ***I***. Trabeculectomized human TM tissue cells respond to 100 nM GSK101 with elevations in $[Ca^{2+}]_i$. ***J***. TRPV4 activation increases the extent of hypoosmotic hTM swelling.

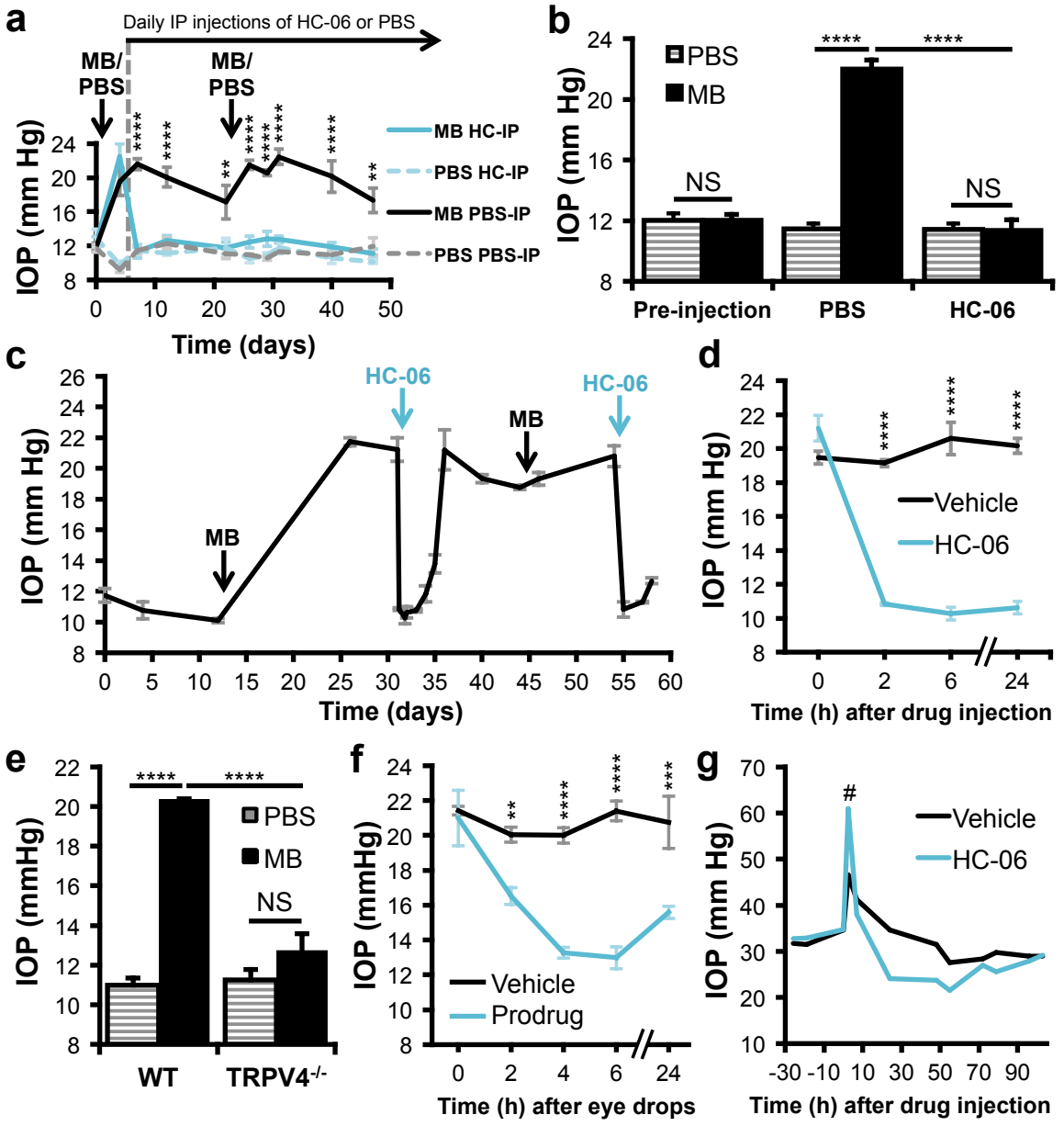

Figure 7.2 TRPV4 is required for IOP elevation in mouse and primate glaucoma models. ***A***. Intravitreal injection of MBs (black trace), but not PBS (dashed grey trace), caused a sustained elevation in IOP. Subsequent systemic injection of HC-06 (blue trace) lowered IOP to the baseline, whereas vehicle injection had no effect (dashed light blue trace). ***B***. TRPV4 is required for MB-induced IOP elevations. ***C-D***. Long-lasting IOP decreases were achieved by intravitreal injection of HC-06 into MB-treated eyes. ***E***. MB injection into TRPV4$^{-/-}$ eyes elicited little IOP elevation. ***F***. Application of the HC-06 prodrug eye drops was sufficient to decrease IOP. ***G***. HC-06 injection into two glaucomatous macaque eyes resulted in a prolonged and reversible decrease in IOP (asterisk = injection artifact).

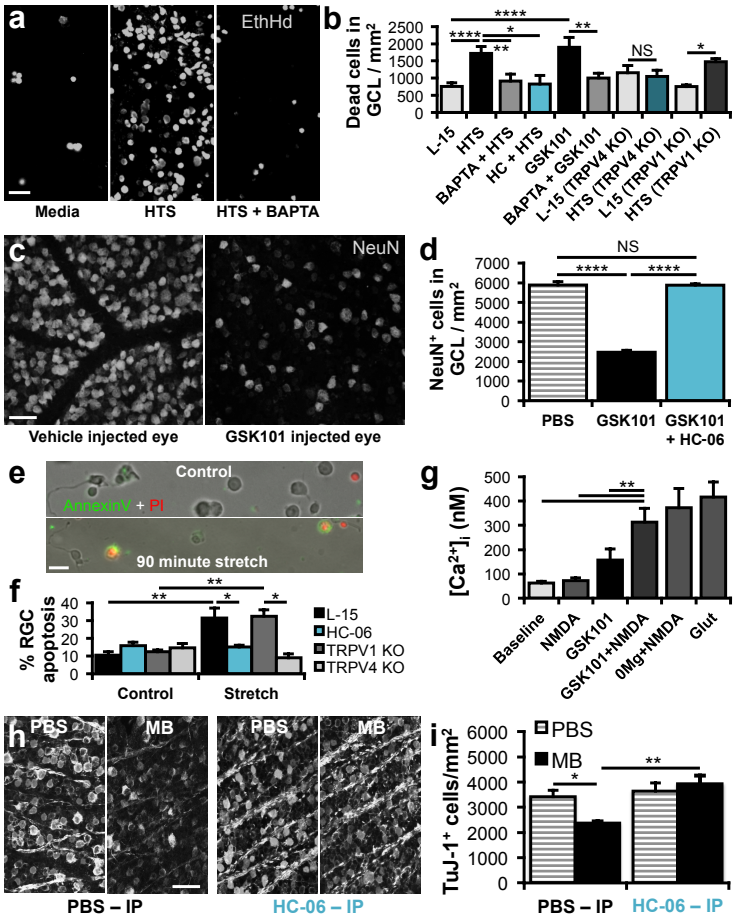

Figure 7.3 TRPV4 overactivity is necessary and sufficient for mechanical excitotoxicity of RGCs. ***A-B***. Isolated mouse retinas were incubated in the indicated conditions for 2.5 hours, stained with ethidium homodimer (EthHd) and dead cells in the GCL were imaged and counted. Thirty-five percent HTS increased RGC death and this required cytosolic Ca^{2+} and TRPV4. GSK101 (1 µM) overstimulated TRPV4, which was sufficient to kill RGCs. This required $[Ca^{2+}]_i$. Genetic TRPV4 ablation, but not deletion of TRPV1, rescued RGCs from swelling-induced excitotoxicity. ***C***. A 4-week prior intravitreal injection of GSK101 (75 µM, 2 µl) induces massive $NeuN^+$ neuron loss in the GCL of retinal wholemounts. ***D***. Intraperitoneal pretreatment of HC-06 rescues RGCs from TRPV4 overactivation. ***E-F***. RGC apoptosis induced by cyclic stretching for 90 minutes is inhibited by HC-06 and by genetic ablation of TRPV4, but not by elimination of TRPV1. Stretching did not increase apoptosis in other cell types such as bipolar cells (left of each image), consistent with a selective vulnerability of RGCs to mechanical strain. ***G***. Submaximal stimulation of TRPV4 facilitates removal of the Mg^{2+} block of the NMDA receptor. ***H***. IOP was raised by microbead (MB) injections or maintained at normal levels following PBS injections for 8-weeks. Mice were treated with daily IP injections of HC-06 or PBS. RGC loss was quantified by measuring the density of $TuJ1^+$ cells in the GCL of in retinal wholemounts. RGC density was diminished by sustained exposure to high IOP, whereas HC-06-treated mice were protected from IOP-mediated injury.

CHAPTER 8

CONCLUSION

8.1 Conclusion

We identified activation of the mechanosensitive ion channel TRPV4 as a primary mechanism by which RGCs, Müller glia and TM cells transduce biomechanical strain. In excess, this can activate calcium-dependent biochemical cascades, resulting in glial reactivity, increased hypoosmotic swelling and neuronal excitotoxicity. Because calcium dysregulation is implicated in the pathogenesis of glaucoma, TRPV4 may represent an elegant link between IOP elevation and RGC degeneration. Although glaucoma lacks neuroprotective treatments, we have identified TRPV4 as a promising therapeutic target to reduce the mechanosensitivity of retinal neurons and glia and to maintain IOP within a safe range. These findings thus provide important insights into the pathogenesis of glaucoma and may explain a potential mechanism for the generation of pressure phosphenes, a sensory phenomenon that may serve as a warning of impending retinal damage and blindness.

8.2 Future Directions

8.2.1 Vision Loss Caused by Ocular/Brain Trauma

Suppression of TRPV4 activity may additionally provide neuroprotection from the effects of traumatic impacts on the retina and the brain. Among the most common and debilitating consequences of traumatic ocular injuries (TOIs) and traumatic brain injuries (TBIs) in surviving patients is vision loss, resulting from damage to eyes or the brain network dedicated to vision, afflicting 57-66% of TBI patients (Lew et al., 2009). For example, combat-related blast exposure is the primary cause of TOI and TBI in U.S. soldiers (Okie, 2005; Owens et al., 2008). Developments in armor have reduced fatalities

and eye/brain injuries from shrapnel; however, wearing ballistic eyewear and Kevlar helmets does little to spare the eyes and brain from exposure to high blast overpressure, making it necessary to study the effects of primary blast waves on ocular and brain tissue (Okie, 2005; Mader et al., 2006; Thomas et al., 2009). While visual problems depend on the severity and type of injury, visual deficits in TBI patients can include diminished visual acuity, visual fields and/or oculomotor control (Glenn et al., 2009). Surgical interventions are available to correct corneal and lens damage as well as some oculomotor problems; however, retina and brain damage remains refractory to current medical interventions (Celesia et al., 1991; Ahmed et al., 2011; Nashed et al., 2011; Fasolo et al., 2012; Yu-Wai-Man & Griffiths, 2013; Gonzalez et al., 2013; Eiber et al., 2013; Shepherd et al., 2013; Xiong et al., 2013). Protective gear alone is not enough to effectively avert TOIs and TBIs; we need to both better understand the biological mechanisms that contribute to visual system dysfunction and develop neuroprotective pharmaceuticals that can readily prevent immediate and secondary injury mechanisms (e.g., mechanotransduction and inflammation, respectively) to preserve the sight and cognitive function of the wounded.

8.2.2 Increased Mechanosensitivity and/or Mechanical Strain Could Explain Age-Dependent Risk in Glaucoma

Along with elevated IOP, advanced age is a major risk factor for glaucoma; however, it is unclear how aging increases the likelihood of developing glaucoma. IOP stays fairly constant with age (Klein et al., 1992); thus, an age-dependent increase in IOP is probably not a major factor in the increased prevalence of glaucoma with aging. As mouse RGCs

are intrinsically sensitive to glaucomatous forces, an aging-dependent increase in their responsiveness to biomechanical strain could account for progressive vulnerability. Alternatively, age-dependent structural alterations within the tissues that contribute to RGC strain could magnify the IOP-related forces that normally impinge upon RGCs. To distinguish between these possibilities, it will be important to characterize the effect of aging on RGC sensitivity to mechanical forces and TRPV4 activation.

8.2.3 Cell-Type Specific Contributions of TRPV4 to the Pathogenesis of Glaucoma

We were unable to use TRPV4$^{-/-}$ mice or systemic TRPV4 inhibition to test the role of retinal TRPV4 in the pathogenesis of glaucoma *in vivo* because these manipulations serendipitously prevented pathological elevations in IOP. This, however, was exciting from a therapeutic standpoint, especially because TRPV4 inhibition may interfere with glaucoma pathogenesis at two key steps, which is a suggested and presently unmet requirement for the successful advancement of neuroprotective glaucoma treatments through late-stage clinical trials (Baltmr et al., 2010).

Although the present findings convincingly indicate that glaucomatous forces impinging upon the retina activate TRPV4 and damage RGCs, the functional expression of TRPV4 in RGCs, Müller glia and microglia (data not shown), in addition to possible expression in vascular endothelial cells, complicates the relative cellular involvement of TRPV4-signals in the initiation and progression of RGC degeneration. We are creating floxed TRPV4 mice to conditionally knockout TRPV4 using cell type-specific Cre expression to resolve this question and to definitively test our hypothesis that TRPV4

expression in RGCs is necessary for high-IOP to kill RGCs in glaucoma. Nevertheless, our data to date strongly support this possibility. Most notably we found that: 1) TRPV4 overactivation is sufficient to trigger apoptosis of dissociated RGCs and *in vivo* RGCs; 2) dissociated RGCs respond to tensile forces comparable to those experienced during glaucomatous IOP elevations with a Ca^{2+} elevation that is sensitive to TRPV4 inhibition; 3) TRPV4 is required for apoptosis induced by sustained mechanical strain (osmotic pressure or cyclic stretching); 4) TRPV4-mediated Ca^{2+} influx exacerbates osmotic swelling of RGCs; and 5) TRPV4 activation in RGCs is sufficient to potentiate other excitotoxic mechanisms such as NMDA receptor activation.

8.2.4 Mechanisms of Compartmentalized Calcium Dysregulation

Although we focused on Ca^{2+} regulation within RGC somata, an important site of excitotoxicity (Hare et al., 2001) during glaucoma progression, Ca^{2+} dysregulation also occurs within RGC dendrites and axons, contributing to their compartmentalized neurodegeneration (Crish & Calkins, 2010). IOP-dependent inner retina dysfunction occurs early (Kong et al., 2009; Kong et al., 2012; Frankfort et al., 2013) and is associated with dendritic arbor remodeling and/or electrophysiological changes (Della Santina et al., 2013). Given the important roles of Ca^{2+} in synaptic maintenance (Sun et al., 2014) and TRPV4 expression within proximal RGC dendrites (Chapter 5), it seems likely that TRPV4-dependent transduction of IOP-related forces will directly allow Ca^{2+} influx into RGC dendrites and/or trigger a Ca^{2+} influx in somata that spreads to RGC dendrites directly or via biochemical/genetic signals to induce remodeling and dysfunction.

High IOP also mechanically strains RGC axons within the complex physical environment of the optic nerve head laminar region, subjecting them to tensile, compressive and distortional forces as well as structural remodeling (another process thought to involve mechanosensation (Downs et al., 2008). Anterograde axonal transport from retina to the axon terminals in the brain is lost before retrograde transport (Crish & Calkins, 2010). This means that axonal transport is not physically obstructed (e.g., by the pinching of axons); otherwise, transport in both directions would be affected similarly. This finding and other evidence (e.g., Huang et al., 2008) implicate Ca^{2+} dysregulation within the axonal compartment in the axonal transport deficits and the ensuing consequences (e.g., impaired BDNF delivery to the soma (Quigley et al., 2000) and accelerated axonal degeneration; Knöferle, 2010). We observed TRPV4 expression within mouse and human RGC axon bundles (Chapters 5, 6), which might reflect its transport or functional expression within the membrane. Although the source of excessive axonal calcium is unknown, TRPV4 might confer mechanosensitivity to RGC axons or generate signals within the somata that spread into the axon. In support of this possibility, strain-induced Ca^{2+} elevations have been observed in the axons of other neurons in the absence of mechanically produced pores (Wolf et al., 2001). Alternatively, Ca^{2+} diffusion/waves, voltage-gated Ca^{2+} channels (Wolf et al., 2001) and/or reversal of the sodium-calcium exchanger could all be sources of axonal Ca^{2+} (Stys et al., 1992). Future experiments testing this will refine our understanding of a basic disease mechanism, which is important because it is necessary to protect all RGC compartments to maintain a functional visual system.

8.2.5 TRP Channels in the Retina

Although findings within this dissertation expand knowledge of TRP channel physiology and function in the retina, the retina-specific roles of most TRP channels remain unknown. This deficit is surprising given that the retina expresses most, if not all, mammalian TRP channels (Gilliam & Wensel et al., 2011) and that their expression is evolutionarily conserved (Montell & Ruben, 1989; Hardie & Minke, 1992; Niemeyer et al., 1996; Zimov &Yazulla, 2004; Szikra et al., 2008; Morgans et al., 2009; Shen et al., 2009; Sapington et al., 2009; Ryskamp et al., 2011; Kaur & Nawy, 2012; Molnar et al., 2012; Sánchez Ramos et al., 2012; Niederhäusern et al., 2013; Ward et al., 2014). Progress in this frontier has been hampered by an inadequate assortment of tools that can accurately characterize the expression and function of specific TRP channel subunits. For instance, many antibodies directed toward TRP channels are nonselective (Chapter 2) and most of the published immunohistochemical data regarding retinal TRP channel localization (Crousillac et al., 2003; Sekaran et al., 2007; Sappington et al., 2008; Leonelli et al., 2009; Sappington et al., 2009; Leonelli et al., 2010; Wang et al., 2010; Gilliam & Wensel et al., 2011) has not been validated by the absence of antibody staining in the retina of knockout animals. Furthermore, many TRP channels lack selective agonists and antagonists (Wu et al., 2010), making it difficult to examine their functional expression and physiological roles. We have begun collaborations with Drs. Christopher Reilly, Glenn Prestwich and Yong Xu to identify and/or create new modulators of TRPV channels. In addition to developing a prodrug version of a TRPV4 antagonist for topical delivery to the eye (Chapter 7) and novel TRPV4 antagonists (Krizaj et al., 2013), we identified a TRPV3 agonist with greater selectivity for the TRPV3 channel than other

known agonists (Appendix). As we have preliminary data indicating TRPV3 mRNA expression in mouse retinas and RGC $[Ca^{2+}]_i$ elevations in responses to camphor (nonselective TRPV3 agonist), this new agonist will help us to further examine the functional distribution of TRPV3 in the retina. Because body temperature potentiates TRPV3 activity (Smith et al., 2002; Xu et al., 2002), its thermosensitivity, like that of TRPV4 (Shibasaki et al., 2007), may contribute the resting excitability of RGCs. Thus, the repertoire of TRP channel expression, combined with their sensitivities to diverse stimuli, distinctive channel properties and subcellular localizations, will culminate in the emergent, polymodal properties of the mammalian retina. Future studies of these properties will not only teach us more about how the visual system functions normally, but also how the visual system behaves in disease. This information would further allow us to promote retinal homeostasis and orchestrate retinal output.

8.2.6 Polymodal Sensation in the Visual System as a Potential Tool for Visual Prostheses

Finally, the polymodal behavior of TRPV4 and other gene products may eventually allow us to hack the retina to provide useful visual information to RGCs that lack input from photoreceptors. Albert et al. (2012) discovered that RGCs are excited by infrared laser-based heating via the activation of TRPV4. Thus, expression of TRPV4 in RGCs, although potentially problematic in the presence of sustained, pathological forces, might allow us to interface with the retina to provide high spatial and temporal frequency information to the brain in otherwise blind patients. Optimization of this approach requires a clear understanding of the temperature parameters that gate TRPV4 as well as

molecular and genetic tools that may allow us to target relevant, specialized information to RGCs that normally represent preprocessed and integrated visual information. Thus, a rich understanding of polymodal sensation in the retina could lead to highly refined visual prostheses (Eiber et al., 2013; Shepherd et al., 2013), in addition to therapies that reduce neuronal vulnerability to biomechanical strain, a culprit implicated in many blinding and neurodegenerative diseases.

1.3 References

Ahmed N, Aziz T, Akram S (2011) Visual outcome after primary IOL implantation for traumatic cataract. Pak J Ophthalmol 27.

Albert ES, Bec JM, Desmadryl G, Chekroud K, Travo C, Gaboyard S, Bardin F, Marc I, Dumas M, Lenaers G, Hamel C, Muller A, Chabbert C (2012) TRPV4 channels mediate the infared laser-evoked response in sensory neurons. J Neurophysiol 107:3227-3234.

Baltmr A, Duggan J, Nizari S, Salt TE, Cordeiro MF (2010) Neuroprotection in glaucoma – is there a future role? Exp Eye Res 91:554-566.

Celesia GG, Bushnell D, Toleikis SC, Brigell MG (1991) Cortical blindness and residual vision is the "second" visual system in humans capable of more than rudimentary visual perception? Neurology 41:862-862.

Crish SD, Calkins DJ (2011) Neurodegeneration in glaucoma: progression and calcium-dependent intracellular mechanisms. Neuroscience 176:1-11.

Crousilla S, Lerouge M, Rankin M, Gleason E (2003) Immunolocalization of TRPC channel subunits 1 and 4 in the chicken retina. Vis Neurosci 20:453-463.

Della Santina L, Inman DM, Lupien CB, Horner PJ, Wong RO (2013) Differential progression of structural and functional alterations in distinct retinal ganglion cell types in a mouse model of glaucoma. J Neurosci 33:17444-17457.

Downs JC, Roberts MD, Burgoyne CF (2008) The mechanical environment of the optic nerve head in glaucoma. Optom Vis Sci 85:425-435.

Eiber CD, Lovell NH, Suaning GJ (2013) Attaining higher resolution visual prosthetics: a review of the factors and limitations. J Neural Engin 10:011002.

Fasolo A, Capuzzo C, Fornea M, Frigo AC, Monterosso C, Zampini A, Avarello A, Galan A, Sbordone S, Ragucci AE, Gorla C, Grigoletto F, Ponzin D (2012) Health status and patient satisfaction after corneal graft: results from the corneal transplant epidemiological study. J Ophthalmol 2012:230641.

Frankfort BJ, Khan AK, Tse DY, Chung I, Pang JJ, Yang Z, Gross RL, Wu SM (2013) Elevated intraocular pressure causes inner retinal dysfunction before cell loss in a mouse model of experimental glaucoma. Invest Ophthalmol Visual Sci 54:762-770.

Gilliam JC, Wensel TG (2011) TRP channel gene expression in the mouse retina. Vis Res 51:2440-2452.

Gonzalez MA, Flynn Jr HW, Smiddy WE, Albini TA, Tenzel P (2013) Surgery for retinal detachment in patients with giant retinal tear: etiologies, management strategies, and outcomes. Ophthalmic Surg Lasers Imaging Retina 44:232-237.

Hardie RC, Minke B (1992) The *trp* gene is essential for a light-activated Ca^{2+} channel in Drosophila photoreceptors. Neuron 8:643-651.

Hare W, WoldeMussie E, Lai R, Ton H, Ruiz G, Feldmann B, Wijono M, Chun T, Wheeler L (2001) Efficacy and safety of memantine, an NMDA-type open-channel blocker, for reduction of retinal injury associated with experimental glaucoma in rat and monkey. Surv Ophthalmol 45:S284-S289.

Huang W, Fileta J, Rawe I, Qu J, Grosskreutz CL (2008) Calpain activation in experimental glaucoma. Invest Ophthalmol Vis Sci 51:3049-3054.

Kaur T, Nawy S (2012) Characterization of Trpm1 desensitization in ON bipolar cells and its role in downstream signalling. J Physiol 590:179-192.

Klein BEK, Klein R, Linton KLP (1992) Intraocular pressure in an American community: the Beaver Dam Eye Study. Invest Ophtlmol Vis Sci 33:2224-2228.

Knöferle J, Koch JC, Ostendorf T, Michel U, Planchamp V, Vutova P, Tönges L, Stadelmann C, Brück W, Bähr M, Lingor P (2010) Mechanisms of acute axonal degeneration in the optic nerve in vivo. Proc Natl Acad Sci USA 107:6064-6069.

Kong YX, Crowston JG, Vingrys AJ, Trounce IA, Bui BV (2009) Functional changes in the retina during and after acute intraocular pressure elevation in mice. Invest Ophthalmol Vis Sci 50:5732-5740.

Kong YXG, van Bergen N, Bui BV, Chrysostomou V, Vingrys AJ, Trounce IA, Crowston JG (2012) Impact of aging and diet restriction on retinal function during and after acute intraocular pressure injury. Neurobiol Aging 33:1126-e15.

Krizaj D, Prestwich GD, Barabas P, Xu Y, Ryskamp D (2013) U.S. Patent Application

13/841,790.

Leonelli M, Martins DO, Kihara AH, Britto LR (2009) Ontogenetic expression of the vanilloid receptors TRPV1 and TRPV2 in the rat retina. Int J Dev Neurosci 27:709-718.

Leonelli M, Martins DO, Britto LR (2010) TRPV1 receptors are involved in protein nitration and Müller cell reaction in the acutely axotomized rat retina. Exp Eye Res 91:755-768.

Lew HL, Garvert DW, Pogoda TK, Hsu PT, Devine JM, White DK, Myers PJ, Goodrich GL (2009) Auditory and visual impairments in patients with blast-related traumatic brain injury: effect of dual sensory impairment on functional independence measure. J Rehabil Res Dev 46:819-26.

Mader TH, Carroll RD, Slade CS, George RK, Ritchey JP, Neville SP (2006) Ocular war injuries of the Iraqi insurgency, January–September 2004. Ophthalmology 113:97-104.

Molnar T, Barabas P, Birnbaumer L, Punzo C, Kefalov V, Križaj D (2012) Store-operated channels regulate intracellular calcium in mammalian rods. J Physiol 590:3465-3481.

Montell C, Rubin GM (1989) Molecular characterization of the Drosophila trp locus: a putative integral membrane protein required for phototransduction.Neuron, 2:1313-1323.

Morgans CW, Zhang J, Jeffrey BG, Nelson SM, Burke NS, Duvoisin RM, Brown RL (2009) TRPM1 is required for the depolarizing light response in retinal ON-bipolar cells. Proc Natl Acad Sci USA 106:19174-19178.

Nashed A, Saikia P, Herrmann WA, Gabel VP, Helbig H, Hillenkamp J (2011) The outcome of early surgical repair with vitrectomy and silicone oil in open-globe injuries with retinal detachment. Am J Ophthalmol 151:522-528.

Niemeyer BA, Suzuki E, Scott K, Jalink K, Zuker CS (1996) The Drosophila light-activated conductance is composed of the two channels TRP and TRPL. Cell 85:651-659.

Okie S (2005) Traumatic brain injury in the warzone. N Engl J Med 352:2043-2047.

Owens BD, Kragh JF Jr, Wenke JC , Macaitis J, Wade CE, Holcomb JB. (2008) Combat wounds in Operation Iraqi Freedom and Operation Enduring Freedom. J Trauma 64:295-299.

Quigley HA, McKinnon SJ, Zack DJ, Pease ME, Kerrigan-Baumrind LA, Kerrigan DF, Mitchell RS (2000) Retrograde axonal transport of BDNF in retinal ganglion cells is blocked by acute IOP elevation in rats. Invest Ophthalmol Vis Sci 41:3460-3466.

Ryskamp DA, Witkovsky P, Barabas P, Huang W, Koehler C, Akimov NP, Lee SH, Chauhan S, Xing W, Rentería RC, Liedtke W, Krizaj D (2011) The polymodal ion

channel transient receptor potential vanilloid 4 modulates calcium flux, spiking rate, and apoptosis of mouse retinal ganglion cells. J Neurosci 31:7089-7101.

Sánchez ramos C, Guerrera MC, Bonnin Arias C, Calavia MG, Laurà R, Germanà A, Vega JA (2012) Expression of TRPV4 in the zebrafish retina during development. Microsc Res and Tech 75:743-748.

Sappington RM, Calkins DJ (2008) Contribution of TRPV1 to microglia-derived IL-6 and NFκB translocation with elevated hydrostatic pressure. Invest Ophthalmol Vis Sci 49:3004-3017.

Sappington RM, Sidorova T, Long DJ, Calkins DJ (2009) TRPV1: contribution to retinal ganglion cell apoptosis and increased intracellular Ca2+ with exposure to hydrostatic pressure. Invest Ophthalmol Vis Sci 50:717-728.

Sekaran S, Lall GS, Ralphs KL, Wolstenholme AJ, Lucas RJ, Foster RG, Hankins MW (2007) 2-Aminoethoxydiphenylborane is an acute inhibitor of directly photosensitive retinal ganglion cell activity in vitro and in vivo. J Neurosci 27:3981-3986.

Shen Y, Heimel JA, Kamermans M, Peachey NS, Gregg RG, Nawy S (2009) A transient receptor potential-like channel mediates synaptic transmission in rod bipolar cells. J Neurosci 29:6088-6093.

Shepherd RK, Shivdasani MN, Nayagam DA, Williams CE, Blamey PJ (2013) Visual prostheses for the blind. Trends Biotechnol 31:562-571.

Shibasaki K, Suzuki M, Mizuno A, Tominaga M (2007) Effects of body temperature on neural activity in the hippocampus: regulation of resting membrane potentials by transient receptor potential vanilloid 4. J Neurosci 27:1566-1575.

Smith GD, Gunthorpe MJ, Kelsell RE, Hayes PD, Reilly P, Facer P, Wright JE, Jerman JC, Walhin JP, Ooi L, Egerton J, Charles KJ, Smart D, Randall AD, Anand P, Davis JB (2002) TRPV3 is a temperature-sensitive vanilloid receptor-like protein. Nature 418:186-190.

Stys PK, Waxman SG, Ransom BR (1992) Ionic mechanisms of anoxic injury in mammalian CNS white matter: role of Na+ channels and Na(+)-Ca2+ exchanger. J Neurosci12:430-439.

Sun S, Zhang H, Liu J, Popugaeva E, Xu NJ, Feske S, White CL, Bezprozvanny I (2014) Reduced synaptic STIM2 expression and impaired store-operated calcium entry cause destabilization of mature spines in mutant presenilin mice. Neuron, 82:79-93.

Szikra T, Cusato K, Thoreson WB, Barabas P, Bartoletti TM, Krizaj D (2008) Depletion of calcium stores regulates calcium influx and signal transmission in rod photoreceptors. J Physiol 586:4859-4875.

Thomas R, McManus JG, Johnson AJ, Mayer P, Wade CE, Holcomb JB. (2009) Ocular injury reduction from ocular protection use in current combat operations. J Trauma 66:S99-103.

Von Niederhäusern V, Kastenhuber E, Stäuble A, Gesemann M, Neuhauss SC (2013) Phylogeny and expression of canonical transient receptor potential (TRPC) genes in developing zebrafish. Dev Dynamics 242:1427-1441.

Wang X, Teng L, Li A, Ge J, Laties AM, Zhang X (2010) TRPC6 channel protects retinal ganglion cells in a rat model of retinal ischemia/reperfusion-induced cell death. Invest Ophthalmol Vis Sci 51:5751-5758.

Ward NJ, Ho KW, Lambert WS, Weitlauf C, Calkins DJ (2014) Absence of transient receptor potential vanilloid-1 accelerates stress-induced axonopathy in the optic projection. J Neurosci 34:3161-3170.

Wolf JS, Stys PK, Lusardi T, Meaney D, Smith DH (2001) Traumatic axonal injury induces calcium influx modulated by tetrodotoxin-sensitive sodium channels. J Neurosci 21:1923-1930.

Wu LJ, Sweet TB, Clapham DE (2010) International Union of Basic and Clinical Pharmacology. LXXVI. Current progress in the mammalian TRP ion channel family. Pharmacol Rev 62:381-404.

Xiong Y, Mahmood A, Chopp M (2013) Animal models of traumatic brain injury. Nat Rev Neurosci 14:128-142.

Xu H, Ramsey IS, Kotecha SA, Moran MM, Chong JA, Lawson D, Ge P, Lilly J, Silos-Santiago I, Xie Y, DiStefano PS, Curtis R, Clapham DE (2002) TRPV3 is a calcium-permeable temperature-sensitive cation channel. Nature 418:181-186.

Yu-Wai-Man P, Griffiths PG (2013) Surgery for traumatic optic neuropathy. Cochrane Database Syst Rev 6.

APPENDIX

DROFENINE: A 2-APB ANALOG WITH IMPROVED SELECTIVITY FOR HUMAN TRPV3

Christopher Reilly organized the drug screen for a TRPV3 agonist and research described in this article. Cassandra Deering-Rice designed and conducted many of the experiments along with others in Dr. Reilly's lab. Drs. Deering-Rice and Reilly wrote most of this paper. As part of a collaboration with Dr. Reilly's lab in the Department of Pharmacology and Toxicology, I collected electrophysiological data for figure 3 with oversight and suggestions from David Krizaj. I also wrote the results and methods for the experiment in figure 3, which demonstrated that drofenine induces inward currents in TRPV3-overexpressing HEK-293 cells.

Deering-Rice CE, Mitchell VK, Romero EG, Abdel Aziz MH, Ryskamp DA, Križaj D, Venkat RG, Reilly CA (2014) Drofenine: a 2-APB analog with improved selectivity for human TRPV3. Pharmacology Research & Perspectives 2(5):e00062. Reprinted with permission from Pharmacology Research & Perspectives and Wiley.

PRP Pharmacology Research & Perspectives Open Access

ORIGINAL ARTICLE

Drofenine: a 2-APB analog with improved selectivity for human TRPV3

Cassandra E. Deering-Rice[1], Virginia K. Mitchell[1], Erin G. Romero[1], May H. Abdel Aziz[1], Daniel A. Ryskamp[2], David Križaj[2], Raj Gopal Venkat[3] & Christopher A. Reilly[1,]

[1]Department of Pharmacology and Toxicology, University of Utah, Salt Lake City, Utah, 84112
[2]Department of Ophthalmology and Visual Sciences, Interdepartmental Neuroscience Program, University of Utah, Salt Lake City, Utah, 84132
[3]Department of Medicinal Chemistry, University of Utah, Salt Lake City, Utah, 84112

Keywords
2-APB, carvacrol, cutaneous physiology, drofenine, drug discovery, drug discovery, drug screening, receptor mechanisms, TRP channels, TRPV3, TRPV3 agonist, TRPV3 antagonist

Correspondence
Christopher A. Reilly, Department of Pharmacology and Toxicology, University of Utah, 30 South 2000 East, 201 Skaggs Hall, Salt Lake City, UT 84112.
Tel: (801) 581-5236; Fax: (801) 585-3945;
E-mail: chris.reilly@pharm.utah.edu

Funding Information
This work was supported by a grant from the National Institute of Environmental Health Sciences (ES017431).

Received: 29 January 2014; Revised: 2 June 2014; Accepted: 3 June 2014

Pharma Res Per, 2(5), 2014, e00062, doi: 10.1002/prp2.62

doi: 10.1002/prp2.62

Abstract

Transient receptor potential vanilloid-3 (TRPV3) is a member of the TRPV subfamily of TRP ion channels. The physiological functions of TRPV3 are not fully understood, in part, due to a lack of selective agonists and antagonists that could both facilitate the elucidation of roles for TRPV3 in mammalian physiology as well as potentially serve as therapeutic agents to modulate conditions for which altered TRPV3 function has been implicated. In this study, the Microsource Spectrum Collection was screened for TRPV3 agonists and antagonists using alterations in calcium flux in TRPV3 overexpressing human embryonic kidney-293 (HEK-293) cells. The antispasmodic agent drofenine was identified as a new TRPV3 agonist. Drofenine exhibited similar potency to the known TRPV3 agonists 2-aminoethoxydiphenylboronate (2-APB) and carvacrol in HEK-293 cells, but greater selectivity for TRPV3 based on a lack of activation of TRPA1, V1, V2, V4, or M8. Multiple inhibitors were also identified, but all of the compounds were either inactive or not specific. Drofenine activated TRPV3 via interactions with the residue, H426, which is required for TRPV3 activation by 2-APB. Drofenine was a more potent agonist of TRPV3 and more cytotoxic than either carvacrol or 2-APB in human keratinocytes and its effect on TRPV3 in HaCaT cells was further demonstrated using the antagonist icilin. Due to the lack of specificity of existing TRPV3 modulators and the expression of multiple TRP channels in cells/tissue, drofenine may be a valuable probe for elucidating TRPV3 functions in complex biological systems. Identification of TRPV3 as a target for drofenine may also suggest a mechanism by which drofenine acts as a therapeutic agent.

Abbreviations

2-APB, 2-aminoethoxydiphenylboronate; HEK-293, human embryonic kidney-293 cells; TRPA1, transient receptor potential ankyrin-1; TRPV1, transient receptor potential vanilloid-1; TRPV3, transient receptor potential vanilloid-3.

Introduction

The transient receptor potential vanilloid (TRPV) subfamily of TRP channels consists of six structurally similar, but functionally unique proteins (TRPV1-V6). Mammalian TRPV and other TRP family proteins (i.e., TRPA, TRPC, and TRPM) are differentially expressed in neurons and non-neuronal cells of animals and humans. Unlike many other TRP channels, TRPV3 expression in sensory neurons appears low, and it may exist in some cells as a heteromultimer with TRPV1 resulting in a functionally unique ion channel (Cheng et al. 2012). TRPV3 is abundantly expressed by keratinocytes, particularly intrafollicular keratinocytes (Peier et al. 2002; Chung et al. 2003, 2004b) as well as cells of the tongue, palate, testes, cornea, nasal epithelium, distal colon, and inner ear (Xu et al. 2006).

TRPV3 is currently being investigated for its role in cutaneous physiology, specifically its role in thermal perception, inflammation, irritation and pain, wound healing, maintenance of skin barrier integrity, and hair growth (Nilius and Bíró 2013; Nilius et al. 2013; Kaneko and Szallasi 2014). Known TRPV3 agonists include natural products such as thymol, carvacrol, camphor, 6-*tert*-butyl-*m*-cresol, menthol, eugenol, farnesyl pyrophosphate, incensole acetate, as well as synthetic 2-aminoethoxydiphenylboronate (2-APB), and α-hydroxy acids which are widely used in the cosmetic industry as skin peeling agents (Chung et al. 2004a; Xu et al. 2006; Vogt-Eisele et al. 2007; Moussaieff et al. 2008; Bang et al. 2010; Earley et al. 2010; Cao et al. 2012). These agents exhibit EC_{50} values between ~130 nmol/L (farnesyl pyrophosphate), ~34 to ~500 μmol/L (carvacrol), and up to >6 mmol/L (cresol), depending on the model used. The fact that essentially all known agonists of TRPV3 are skin sensitizing agents and irritants suggests that aberrant activation of TRPV3 may play key roles in regulating skin homeostasis and dermatopathologies, a notion supported by the identification of a constitutively active TRPV3 variant as a cause of Olmsted Syndrome (Lin et al. 2012). However, conflicting evidence has been obtained regarding the role of TRPV3 in skin using both transgenic mice and known TRPV3 agonists, essentially all of which also modulate the activity of other TRP channels including TRPA1 and TRPM8.

Known TRPV3 antagonists include 17(R and S)-resolvin D1, naturally occurring anti-inflammatory/proresolving ω-3 lipid derivatives (Bang et al. 2012), the TRPM8 agonist icilin (Sherkheli et al. 2012), 2,2-diphenyltetrahydrofuran (a 2-APB analog) (Chung et al. 2005), and isopentenyl pyrophosphate (Bang et al. 2011). However, much like the known TRPV3 agonists, these antagonists are not selective for TRPV3. Numerous TRPV3 modulators are currently under development as possible therapeutic agents (e.g., GRC15300 by Glenmark Pharmaceuticals and others by Hydra Biosciences), with potential utility in conditions such as itch, psoriasis, hirsutism, dermatitis, pain, etc. Thus, there is not only a need to identify selective agonists and antagonists of TRPV3 that can be used to understand its role in mammalian physiology but there is also an ongoing effort to target TRPV3 for treating human disorders and diseases.

The purpose of this study was to identify new commercially available agonists and antagonists with increased selectivity for TRPV3. Here we report that drofenine (CAS#: 0001679-76-1), a 2-APB analog, is an agonist of human TRPV3, with greater selectivity for TRPV3 versus other TRP channels than both 2-APB and carvacrol. As such, drofenine may be a valuable chemical probe to more specifically ascertain the complex physiological and pathophysiological roles of TRPV3. Furthermore, one might speculate that TRPV3 may have some role in the purported antispasmodic activity of drofenine (Spasmo-Cibalgin; Novartis, Muscat, Oman).

Materials and Methods

Chemicals

All chemicals used in this study were purchased from Sigma-Aldrich (St. Louis, MO), unless otherwise stated. 2-(5-trifluoromethyl-pyridine-2ylsulfanyl)-1-(8-methyl-3,4-dihydro-2H-quinolin-1-yl)-ethanone (TRPV3 antagonist) was synthesized as previously described (Chong et al. 2010) and the purified product verified by ^{1}H-NMR.

Screening library

The Microsource Spectrum Collection was obtained from the Drug Screening Resource at The University of Utah. This library consisted of 2320 compounds including drug components (60%), natural products (25%), and other bioactive compounds (15%). The compound library was prepared for screening as 3× (300 μmol/L) stock solutions in calcium assay buffer (1× HBSS [Hank's Balanced Salt Solution], 20 mmol/L HEPES [4-(2-hydroxyethyl)-1-piperazineethanesulfonic acid], pH 7.3) in 384-well plates.

Cell culture

Human embryonic kidney-293 (HEK-293) cells (ATCC, Rockville, MD) were engineered to stably overexpress human TRPV3 (in pcDNA3.1 D V5/His-TOPO) and other human TRP channels (TRPA1, TRPM8, TRPV1, TRPV2, and TRPV4) as previously described (Deering-Rice et al. 2011). HEK-293 cells were grown in DMEM:F12 (Invitrogen, Carlsbad, CA) containing 5% fetal bovine serum (FBS) and 1× penicillin/streptomycin (Invitrogen). HEK-293 cells stably overexpressing the various TRP channels were maintained in DMEM:F12 supplemented with 5% FBS, 1× penicillin/streptomycin, and 350 μg/mL Geneticin (Invitrogen). Cells were subcultured using trypsin and plated into 1% gelatin-coated 96- or 384-well plates for calcium imaging experiments. Human immortalized keratinocytes, HaCaT cells, were provided by Dr. Douglas Grossman, M.D., Ph.D., of the Department of Dermatology, University of Utah. HaCaT cells were cultured in DMEM containing 5% FBS and 1× penicillin/streptomycin/glutamine. Cells were subcultured using trypsin and plated into 96-well plates for experiments.

Site-directed mutagenesis and transient transfection of TRPV3

The following TRPV3 mutants were constructed using the QuickChange XL site-directed mutagenesis kit (Stratagene,

La Jolla, CA): H426N and R696K, residues previously identified as being critical for activation of TRPV3 by 2-APB (Hu et al. 2009). The primers were: TRPV3-H426N (+) 5′-CTGGAGCCGCTGAACACGCTGCTGC-3′ and (−) 5′-GCAGCAGCGTGTTCAGCGGCTCCAG-3′; and TRPV3-R696K (+) 5′-CATCTGGCGCCTGCAGAAAGCCAGGAC-3′ and (−) 5′-GTCCTGGCTTTCTGCAGGCGCCAGATG-3′. For assays, HEK-293 cells were transfected with mutant or wild-type constructs using 175 ng purified plasmid DNA complexed with Lipofectamine 2000 (Invitrogen), at a 2:1 ratio of lipid to DNA. Transiently transfected cells were assayed 48 h post transfection.

Calcium imaging

Calcium imaging experiments were performed as described previously (Deering-Rice et al. 2011, 2012; Shapiro et al. 2013). Briefly, cells were loaded with Fluo-4 AM using the Fluo-4 Direct Kit (Invitrogen) diluted in LHC-9 (HEK-293 cells) or calcium assay buffer (HaCaT cells) for 60 min at 37°C (HEK-293) or room temperature (HaCaT). The loading solution was removed and the cells were subsequently incubated 30 min at 37°C (HEK-293) or room temperature (~23°C) (HaCaT) in the dark with LHC-9 (HEK-293) or calcium buffer (HaCaT) containing 0.5 mmol/L probenecid and 0.75 mmol/L trypan red (ATT Bioquest, Sunnyvale, CA). Treatment solutions were prepared in LHC-9 (HEK-293) or calcium assay buffer (HaCaT) at 3× concentration and 10 or 25 μL was added to 20 or /50 μL of media on the cells in 384- or 96-well plates. Calcium flux responses were measured using either a NOVOstar plate reader (BMG LABTECH, Offenberg, Germany) or microscopically as described previously in the references above. Where specified, data were corrected for nonspecific responses observed with HEK-293 cells, and normalization to the maximum attainable change in fluorescence elicited by ionomycin (10 μmol/L).

Electrophysiology

Whole-cell recordings were made using borosilicate pipettes (3–5 MΩ). Coverslips were coated with concanavalin A as described previously (Ryskamp et al. 2011) and rinsed with phosphate buffer solution. Suspended TRPV3-overexpressing HEK-293 cells were plated on these coverslips in supplemented DMEM:F12 and used within 24 h. Throughout experiments, cells were perfused with external saline containing 145 mmol/L NaCl, 5 mmol/L KCl, 3 mmol/L $MgCl_2$, 10 mmol/L HEPES, 10 mmol/L glucose, and 2 mmol/L $CaCl_2$ (pH 7.4, 320 mOsm). Drofenine was bath applied via perfusion (250 and 500 μmol/L) or injection (1 mmol/L). The internal pipette solution consisted of 133 mmol/L CsCl, 10 mmol/L HEPES, 5 mmol/L ethylene glycol-bis(2-aminoethylether)-N,N,N′,N′-tetraacetic acid (EGTA), 1 mmol/L $CaCl_2$, and 1 mmol/L $MgCl_2$ (pH of 7.3 set with CsOH) (Bae et al. 2011). Pipette and membrane capacitances were automatically compensated and current recordings were Bessel-filtered at 10 kHz using an EPC-10 amplifier (Patchmaster; HEKA Instruments Inc., Bellmore, NY). Cells were voltage clamped at −60 or −70 mV to measure inward currents. The holding potential was adjusted to approximately normalize the baseline current from cell to cell. For each drofenine concentration, we only used cells that were recorded at the same holding potential. Fresh cells were used for each recording to prevent variability due to sensitization or desensitization. Data were collected at 1.0 kHz and analyzed with IGOR Pro 6 software (WaveMetrics Inc., Lake Oswego, OR). Every 100th data point was plotted in example traces (Fig. 3A).

Cell viability assay

HaCaT cells were subcultured in 96-well plates, grown until the cells reached 80–90% confluence, and incubated with increasing concentrations of 2-APB, drofenine, or carvacrol for 24 h. Cytotoxicity was measured using the Cell Counting Kit-8 assay (Cell Counting Kit CCK-8, Dojindo Laboratories, Gaithersberg, MD) as per manufacturer's instructions.

Results

The Microsource Spectrum Collection of compounds was screened to identify modulators of TRPV3 activity, as represented graphically in Figure 1. Calcium influx (i.e., increased fluorescence upon compound addition; t = ~8–17 sec) was used as an indicator of TRPV3 activation by an agonist. Attenuated calcium influx (i.e., reduced fluorescence change) upon addition of the known TRPV3 agonist carvacrol (300 μmol/L; t = ~17–30 sec) was indicative of an antagonist. Initial screening identified 22 of 2320 as possible TRPV3 agonists, and 102 of 2320 as possible antagonists; 1873 had insignificant effects on TRPV3 function. Upon further analysis of the potential agonists and antagonists, selected based on the magnitude of the effect and compound availability, all were either known agonists (e.g., 2-APB), false-positives (e.g., autofluorescent such as fluorescein), not reproducible, or nonspecific for TRPV3; activating or inhibiting other TRP channels (Tables 1 and 2), and/or causing an equivalent degree of calcium flux response in native HEK-293 cells (e.g., acetylcholine). A brief summary of the confirmation studies and selectivity data generated using other TRP channel overexpressing HEK-293 cell lines and specific agonists for each receptor, are summarized in Tables 1 and 2.

Drofenine, was selective for TRPV3 in that activation of TRPA1, M8, V1, V2, and V4, which are known to be

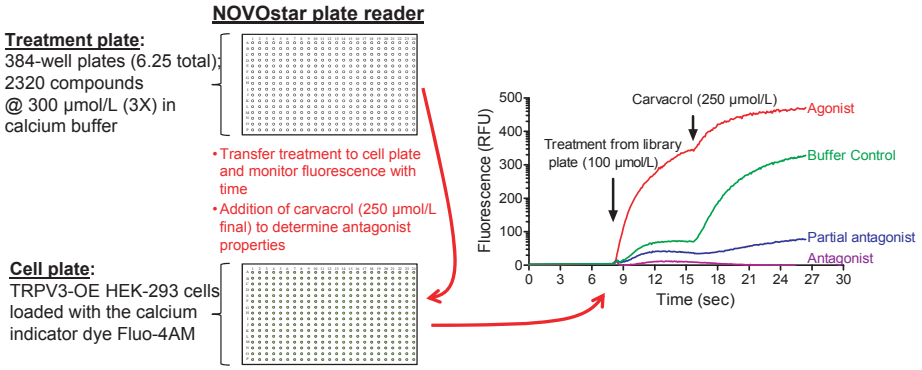

Figure 1. Schematic representation of the screening protocol. HEK-293 cells overexpressing TRPV3 were plated in a 384-well plate and loaded with Fluo-4 AM (cell plate). The compound library was prepared in 384-well plates (treatment plate) at a 3× (300 μmol/L) stock in calcium assay buffer (1× HBSS, 20 mmol/L HEPES, pH 7.3). Using the NOVOstar plate reader, compounds from the treatment plate were transferred to the cell plate and fluorescence was measured for 8 sec testing for agonist responses, followed by addition of carvacrol (250 μmol/L) to assess antagonist responses. The graph to the right depicts fluorescence traces representative of an agonist (red), a potent antagonist (purple), a partial antagonist (blue), and a buffer control (unmodified) response (green).

Table 1. List of potential TRPV3 agonists identified by initial screening and re-evaluated as TRPV3 agonists.

Name	CAS #	Description/Use	Comment(s)
Acetanilide	103-84-4	Analgesic, antipyretic acetaminophen precursor; toxic	Inactive in confirmation assay
Acetylcholine	60-31-1, 51-84-3	Neurotransmitter	Nonselective; HEK-293 response
Acriflavinium HCl	8018-07-3	Topical antiseptic, antifungal; irritant; antitumor	Fluorescence interference
Acrisorcin	7527-91-5	Topical antifungal	4-Hexylresorcinol inactive as TRPV3 agonist; 9-aminoacridine fluorescence interference
2-Aminoethoxydiphen-ylboronate (2-APB)	524-95-8	Broad-spectrum TRP channel modulator	Nonselective for TRPV3; activates HEK-TRPV1 others
Bepradil HCl	74764-40-2	Nonselective voltage-gated calcium channel blocker for angina	Inactive in confirmation assay
Calcein	1461-15-0	Fluorescent indicator	Not evaluated
Carbachol	51-83-2	Cholinomimetic; acetylcholine receptor agonist	Nonselective; HEK-293 response
Digitonin	11024-24-1	Detergent	Not evaluated
Drofenine HCl	1679-76-1	Antispasmodic agent	TRPV3-selective agonist
Fluorescein	2321-07-5	Fluorescent indicator	Not evaluated
Methacholine	62-51-1, 55-92-5	Muscarinic receptor agonist	Nonselective; HEK-293 response

activated by the TRPV3 agonists 2-APB and/or carvacrol, was not observed at concentrations up to 1 mmol/L (Fig. 2A). A detectable change in TRPV3 activity was observed at concentrations as low as ~30 μmol/L and increased in a concentration-dependent manner. At concentrations greater than 500 μmol/L, calcium flux exhibited some evidence of TRPV3 independence based on small and comparable responses in both native HEK-293 cells and other TRP channel overexpressing cell lines. The maximum change in cytosolic calcium (ΔF) for drofenine (EC_{50} = 207 μmol/L) was comparable to the known TRPV3 agonists 2-APB (EC_{50} = 78 μmol/L) and carvacrol (EC_{50} = 438 μmol/L) (Fig. 2B). A TRPV3 antagonist was synthesized and used to block calcium flux in TRPV3 overexpressing HEK-293 cells. Equal inhibition of calcium flux was observed for all three agonists with an IC_{50} of 1–3 μmol/L.

Consistent with calcium influx across the plasma membrane, drofenine dose-dependently induced inward currents in TRPV3-overexpressing HEK-293 cells held at

Table 2. List of potential TRPV3 antagonists identified by initial screening and re-evaluated as TRPV3 antagonists.

Name	CAS #	Description/Use	Comment(s)
Erythromycin	114-07-8	Macrolide antibiotic	Not inhibitory on rescreen
Tetracaine HCl	136-47-0, 94-24-6	Anesthetic; antipruritic; ryanodine receptor antagonist; Ca^{++}-induced Ca^{++} release/SOCE inhibitor	Structural similarity with dyclonine, pramoxine, tamoxifen, and mifepristone; inhibited TRPA1>V3=V1; apparent TRPV1 agonist <25 μmol/L
Etoposide	33419-42-0	Antineoplastic	Cytotoxic, false positive
Diphenhydramine HCl	147-24-0	Antihistaminic	Inhibitory at high concentrations. TRPV1>TRPV3>TRPA1.
Clomipramine HCl	17321-77-6, 303-49-1	Tricyclic antidepressant; nonselective neurotransmitter reuptake inhibitor	Inhibitory in rescreen; nonselective SOCE inhibitor. Inhibited TRPV1, V4, M8>V3
Spectinomycin HCl	22189-32-8, 21736-83-4	Aminocyclitol antibiotic	Not inhibitory on rescreen
Sulfinpyrazone	57-96-5	Uricosuric diuretic	Not inhibitory on rescreen
Chloramphenicol	56-75-7	Bacteriostatic antibiotic	Not inhibitory on rescreen
Dyclonine HCl	536-43-6, 586-60-7	Topical anesthetic	Not inhibitory on rescreen
Tamoxifen citrate	54965-24-1, 10540-29-1	Estrogen receptor antagonist	Structural similarity with dyclonine, pramoxine, tetracaine, and mifepristone; inhibited TRPV3>V1>A1 at <50 μmol/L
Warfarin	81-81-2, 2610-86-8	Anticoagulant	Nonselective; also inhibited TRPV1
Flufenamic acid	530-78-9	NSAID; voltage-gated Na^+ channel inhibitor	Nonselective; also inhibited TRPV1
Pramoxine HCl	637-58-1, 140-65-8	Topical anesthetic; antipruritic; Na^+ channel blocker	Structural similarity with dyclonine, tetracaine, tamoxifen, and mifepristone; inhibited TRPA1, V3, and V1
Mifepristone (RU 486)	84371-65-3	Progesterone receptor antagonist; abortifacient	Structural similarity with dyclonine, pramoxine, and tamoxifen; inhibited TRPA1>V3>V1

negative membrane potentials (Fig. 3A–D). Drofenine (250 μmol/L) tended to increase the frequency and amplitude of stochastic and transient inward currents, whereas 500 μmol/L and 1 mmol/L drofenine induced higher amplitude, more sustained responses with faster onset. Drofenine-induced inward currents were similar to 2-APB-evoked TRPV3 currents (Chung et al. 2004a). These data demonstrate that drofenine gates plasmalemmal cation influx.

The chemical structure of drofenine is similar to the known nonspecific TRPV3 agonist 2-APB (Fig. 4A). The contributions of the residues previously shown to determine 2-APB sensitivity were evaluated as determinants of drofenine sensitivity by comparing calcium flux elicited by carvacrol, 2-APB, and drofenine in HEK-293 cells transiently transfected with wild-type human TRPV3 (TRPV3-WT), TRPV3-H426N, or TRPV3-R696K. The TRPV3-H426N mutant exhibited reduced activation relative to TRPV3-WT using both drofenine and 2-APB at a concentration of 100 μmol/L (Fig. 4B). Mutation of H426 had no effect on calcium flux induced by carvacrol (100 μmol/L), as has been previously reported for the structurally similar monoterpenoid agonist camphor (Hu et al. 2009). At 200 μmol/L drofenine, the H426N mutation did not reduce TRPV3 activation, indicating only a shift in the binding of drofenine to TRPV3 or that drofenine may potentially interact with TRPV3 similar to, but not identically to 2-APB. The TRPV3-R696K mutant displayed diminished-to-no-function using all three agonists. Of significance, based on structural similarity and screening results, the 2-APB and drofenine analogs dicyclomine (Bentyl; anticholinergic, antispasmodic), was neither a TRPV3 agonist nor antagonist, while diphenhydramine was a nonselective TRPV3 inhibitor.

Drofenine also induced calcium flux in HaCaT cells, which are an immortalized human keratinocyte cell line that expresses high levels of TRPV3 and other TRP channels. Drofenine was a more potent agonist of TRPV3 in HaCaT cells than both 2-APB and carvacrol (Fig. 5A). The EC_{50} for drofenine was 605 μmol/L, versus >1000 μmol/L for carvacrol and 2-APB (Fig. 5A), and the maximum change in fluorescence achieved by treatment with drofenine was ~80% that of ionomycin. Fluorescence images of HaCaT cells 1 min after treatment with 100 μmol/L carvacrol, 100 μmol/L 2-APB, or drofenine (50 and 100 μmol/L) show the differences in potency for the three TRPV3 agonists in HaCaT cells (Fig. 5B). Icilin, a potent TRPM8 agonist, also inhibits TRPV3 at low micromolar concentrations (Sherkheli et al. 2012). Icilin ameliorated drofenine-induced calcium flux with an IC_{50} of 3.3 μmol/L (Fig. 5C). The synthesized TRPV3 antagonist could not be used in the HaCaT cells due to apparent off target effects characterized by increases in calcium flux at low (<300 nmol/L) and high (>1 μmol/L) concentra-

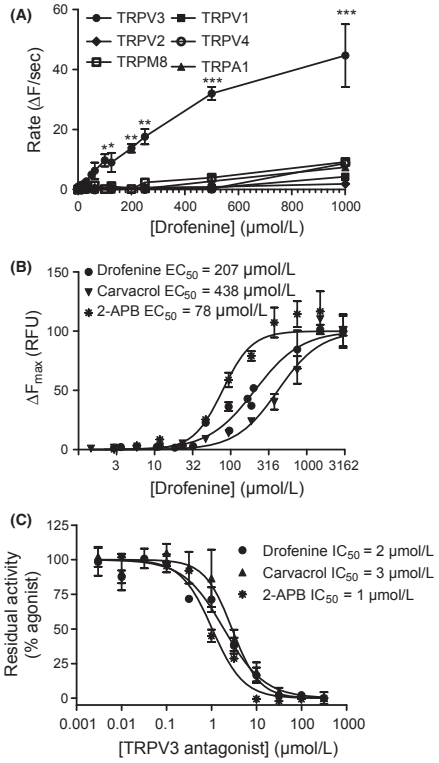

Figure 2. Characteristics and specificity of TRPV3 activation by drofenine. (A) Drofenine selectively increased calcium flux in HEK-293 cells overexpressing TRPV3, but not HEK-293 cells overexpressing TRPA1, M8, V1, V2, or V4 at concentrations up to 1000 μmol/L. (B) HEK-293 cells overexpressing TRPV3 were exposed to increasing concentrations of drofenine, carvacrol, and 2-APB. Changes in fluorescence were monitored. (C) TRPV3 overexpressing HEK-293 cells were preincubated with increasing concentrations of the TRPV3 antagonist for 30 min followed by treatment of drofenine (200 μmol/L), carvacrol (300 μmol/L), or 2-APB (300 μmol/L), inhibition of calcium flux was measured and an IC_{50} value was calculated. Data were collected using a NOVOstar plate reader, blank subtracted, and are expressed as the change in the maximal fluorescence (ΔF_{max}) or the initial rate of change in cellular fluorescence (ΔF/sec). Antagonist data were normalized to the agonist response in the absence of antagonist. Data are the mean and SEM ($n \geq 3$) and asterisks indicate a statistical difference between TRPV3 and the other TRP channels using two-way ANOVA with Bonferroni multiple comparison posttest. *$P < 0.05$, **$P < 0.01$, ***$P<0.001$. ANOVA, analysis of variance.

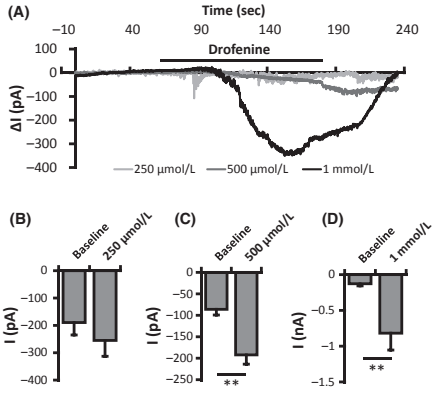

Figure 3. Drofenine induces inward currents in TRPV3-overexpressing HEK-293 cells. (A) Example traces of whole-cell recordings at a negative holding potential. 250 μmol/L, 500 μmol/L, and 1 mmol/L drofenine increased the change in inward current (ΔI). (B–D) Dose-dependent responses were characterized by comparisons between basal current and the peak response. (B) $n = 6$, $P = 0.197$. (C) $n = 5$, $P = 0.00151$. (D) $n = 8$, $P = 0.00574$. Data are represented as mean $\pm$ SEM and asterisks indicate a significant difference between the baseline current and the peak response detected using a one-tailed, paired *t*-test.

tions, and apparent inhibition at intermediate concentrations, which was not observed in TRPV3-overexpressing HEK-293 cells. Drofenine was the most cytotoxic of the three TRPV3 agonists to HaCaT cells, with an LC_{50} of ~230 μmol/L versus >300 μmol/L for both 2-APB and carvacrol (Fig. 5D). This result was consistent with the relative potencies of these agents as TRPV3 agonists in HaCaT cells, and implies a potential role for TRPV3 in mediating the cytotoxic effects of TRPV3 agonists in these cells.

Discussion

The roles TRPV3 plays in mammalian physiology are not completely understood. This is due, in part, to the lack of selective agonists and antagonists. In this study, we sought to identify new compounds that may be used as pharmacological tools for the study of TRPV3, as well as molecules that may have potential for treating pathologies in which TRPV3 may be involved. The Microsource Spectrum Collection, containing 2320 compounds including drugs, natural products, and other bioactive compounds, was screened.

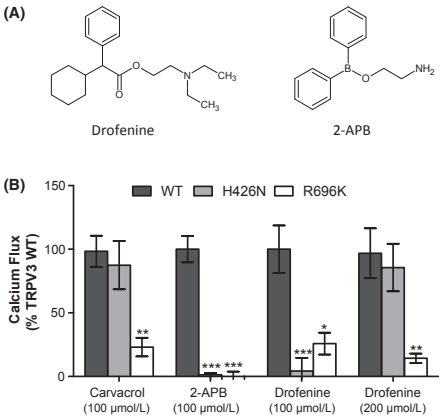

Figure 4. Mechanism of TRPV3 activation by drofenine. (A) Chemical structures of drofenine and 2-APB. (B) Mutation of the 2-APB "binding site" residue H426 blocks drofenine induced calcium flux at low concentrations. HEK-293 cells were transiently transfected with TRPV3-WT, TRPV3-H426N, and TRPV3-R696K and calcium flux was measured via fluorescence microscopy using 100 μmol/L carvacrol, 100 μmol/L 2-APB, and 100 and 200 μmol/L drofenine. Data are blank subtracted and expressed as the percentage of maximum cellular fluorescence elicited by ionomycin (10 μmol/L) and normalized to TRPV3-WT transfected cells. Data are the mean and SEM ($n \geq 3$) and asterisks indicate a statistical difference between TRPV3-WT and TRPV3-H426N or R696K using two-way ANOVA with Bonferroni multiple comparison posttest. $*P < 0.05$, $**P < 0.01$, $***P < 0.001$. ANOVA, analysis of variance.

Of the 2320 compounds tested, none of them selectively inhibit TRPV3. Tables 1 and 2 list some of the compounds identified as potential agonists or antagonists. Potential antagonists (Table 2) included antineoplastic agents (etoposide and tamoxifen), analgesics/anesthetics (acetanilide, flufenamic acid, pramoxine, and tetracaine), an antihistamine (diphenhydramine), a progesterone antagonist (mifepristone), an antiarrhythmic (procainamide), an antibiotic (spectinomycin), a uricosuric diuretic (sulfinpyrazone), and an anticoagulant (warfarin). Several of these compounds appeared to have structural commonality, yielding potential insights into the structural requirements for TRPV3 antagonists. Unfortunately, none of these agents were selective for TRPV3, and based on structural similarities may act by inhibiting store-operated calcium release as reported for structurally related 2-APB (Bootman et al. 2002). Regardless, the inhibition of multiple TRP channels by these agents may illuminate new, or further explain the known pharmacological effects for these molecules. For example, recent studies have identified substance P, resulting from TRPA1 activation in peripheral C-fibers, as a mediator of pruritus (Liu et al. 2013). Therefore, inhibition of TRPV3 in conjunction with other TRP channels such as TRPV1 and TRPA1 by diphenhydramine, tetracaine, or other molecules found to inhibit multiple TRP channels, in addition to inhibition histamine H_1 receptors or other receptor targets, may have complimentary effects in treating itch. This concept is supported by finding that the antitussive properties of dexbrompheniramine and chlorpheniramine are attributable to both inhibition of histamine H_1 receptors and TRPV1 (Sadofsky et al. 2008).

Multiple potential TRPV3 agonists were also identified and evaluated (Table 1). These included 2-APB (previously known) and drofenine. Here, drofenine was shown to activate TRPV3 (Figs. 2 and 3), but not other TRP channels that are known to have overlap in agonist preference with TRPV3 (Fig. 2A). For example, 2-APB was also identified in our screen, but 2-APB I known to be nonselective for TRPV3, based on numerous reports documenting the activation of other TRP channels including TRPA1, M6, V1, and V2, and inhibiting TRPC4, C5, C6, M2, and M8 (Clapham 2007).

Amino acid residues comprising a binding site for drofenine on TRPV3 were similar to 2-APB; H426 and R696 (Hu et al. 2009). However, these sites do not appear to solely explain the activation mechanism for TRPV3 since inhibition of TRPV3 was not achieved with the H426N mutant when higher concentrations of drofenine were used, similar to carvacrol (Fig. 4B). The differences in the relative potency of the three agonists between TRPV3 overexpressing HEK-293 and HaCaT cells may be due to differences in cell permeability and activation of different subcellular pools of TRPV3. Thus, additional studies are required to more fully elucidate the molecular basis for TRPV3 activation by drofenine.

In the human keratinocyte (HaCaT) cell line, drofenine also induced calcium flux (Fig. 5A–C) and caused cytotoxicity (Fig. 5D), exhibiting greater potency in both measures than the known TRPV3 agonists 2-APB and carvacrol. These results suggested a role for TRPV3 activation in cell death as has been suggested by others (Yamada et al. 2010). Pretreatment of HaCaT cells with icilin completely inhibited TRPV3-induced calcium flux (Fig. 5C) (Sherkheli et al. 2012), but icilin was also potently cytotoxic to HaCaT cells (data not shown) preventing the use of icilin to definitively link drofenine-induced calcium flux with cell death. The TRPV3 antagonist was also evaluated, but was not informative in this cell line due to apparent off target effects. This emphasizes the continued need for new TRPV3 antagonists for elucidating precisely what roles TRPV3 plays in biological systems such as skin cells and others.

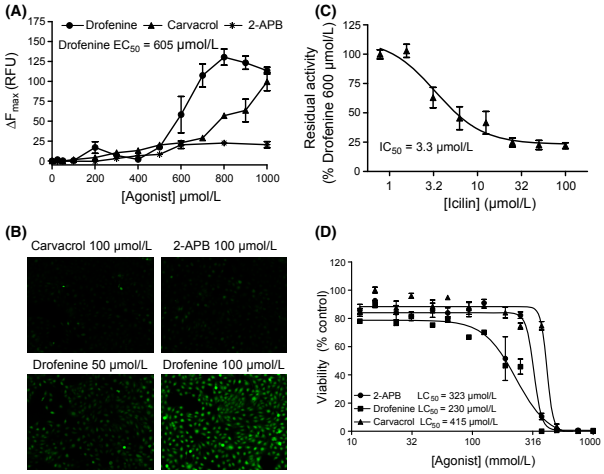

Figure 5. Activation of TRPV3 in keratinocytes by drofenine, 2-APB, and carvacrol. (A) HaCaT cells were exposed to increasing concentrations of 2-APB, drofenine, or carvacrol. The EC_{50} for drofenine was 605 μmol/L. Data were collected using a NOVOstar plate reader, blank subtracted, and expressed as the fold change in maximum cellular fluorescence (ΔF_{max}) compared to untreated controls. Data are the mean and SEM ($n \geq 3$) and asterisks indicate a statistical difference between drofenine and either 2-APB or carvacrol using two-way ANOVA with Bonferroni multiple comparison posttest. $^{**}P < 0.01$, $^{***}P < 0.001$. (B) Visual representation of the calcium flux observed in HaCaT cells treated with carvacrol (100 μmol/L), 2-APB (100 μmol/L), and drofenine (50 or 100 μmol/L). Green represents fluorescent cells where calcium flux was observed. (C) Specificity of TRPV3 activation in HaCaT cells was assessed by inhibition of calcium flux using icilin, a TRPV3 antagonist. HaCaT cells were pretreated with increasing concentrations of icilin for 30 min followed by treatment using 600 μmol/L drofenine. Calcium flux was measured as described above and the IC_{50} was calculated (IC_{50} = 3.3 μmol/L). (D) Viability of HaCaT cells treated with increasing concentrations of 2-APB, drofenine, and carvacrol for 24 h. Data were quantified with the absorbance ratio (λ = 450/630). The results were adjusted by subtracting the blank value, and reported as percent of untreated control. ANOVA, analysis of variance.

Drofenine, product name Spasmo-Cibalgin (Novartis, Oman), is an antispasmodic/anticholinergic agent used for relaxing smooth muscle, treating dysmenorrhea, and relieving pain in the gastrointestinal tract, biliary passages, and urogenital tract. Information regarding the clinical utility of drofenine is limited, but obscure sources suggest use for treatment of visceral spasm and urinary retention. Our results may suggest that TRPV3 could be involved in regulating these phenomena, if the concentration is high enough at the site of action, thus potentially providing new insights into mechanisms by which these events transpire. Additionally, drofenine has also been identified as an inhibitor of neomycin-induced hair cell loss in a zebrafish model of ototoxicity (Coffin et al. 2010). Similarly, several of the nonselective TRPV3 inhibitors listed in Table 2 were also identified as ototoxins (Coffin et al. 2010). Although not investigated, the results presented herein could indicate a critical role for TRPV3 in hair cell physiology and ototoxicity, as has been suggested for TRPA1, V1, and V4 (Mukherjea et al. 2008; Stepanyan et al. 2011; Lee et al. 2013).

In summary, drofenine has been characterized as a TRPV3 agonist with improved selectivity for TRPV3 relative to other TRP channels. The ability to target individual TRP channels is important not only for identifying key mediators of physiological and pathological processes but also in identifying the correct TRP channels for potential pharmacological interventions. Our results demonstrate that drofenine may be a new and valuable TRPV3 agonist for further unraveling some of the mysterious and occasionally paradoxical properties that have been attributed to TRPV3 thus far.

Acknowledgements

We thank Betsy Manos from the Drug Screening Resource at the University of Utah for access to the Microsource Spectrum Collection.

Disclosures

None declared.

References

Bae C, Sachs F, Gottlieb PA (2011). The Mechanosensitive ion channel Piezo1 is inhibited by the peptide GsMTx4. Biochemistry 50: 6295–6300.

Bang S, Yoo S, Yang T-J, Cho H, Hwang SW (2010). Farnesyl pyrophosphate is a novel pain-producing molecule via specific activation of TRPV3. J Biol Chem 285: 19362–19371.

Bang S, Yoo S, Yang T-J, Cho H, Hwang SW (2011). Isopentenyl pyrophosphate is a novel antinociceptive substance that inhibits TRPV3 and TRPA1 ion channels. Pain 152: 1156–1164.

Bang S, Yoo S, Yang TJ, Cho H, Hwang SW (2012). 17 (R)-resolvin D1 specifically inhibits transient receptor potential ion channel vanilloid 3 leading to peripheral antinociception. Br J Pharmacol 165: 683–692.

Bootman MD, Collins TJ, Mackenzie L, Roderick HL, Berridge MJ, Peppiatt CM (2002). 2-Aminoethoxydiphenyl borate (2-APB) is a reliable blocker of store-operated Ca2+ entry but an inconsistent inhibitor of InsP3-induced Ca2+ release. FASEB J 16: 1145–1150.

Cao X, Yang F, Zheng J, Wang K (2012). Intracellular proton-mediated activation of TRPV3 channels accounts for exfoliation effect of alpha hydroxyl acids on keratinocytes. J Biol Chem 287: 25905–25916.

Cheng W, Yang F, Liu S, Colton CK, Wang C, Cui Y, et al. (2012). Heteromeric heat-sensitive transient receptor potential channels exhibit distinct temperature and chemical response. J Biol Chem 287: 7279–7288.

Chong JA, Fanger C, Larsen GR, Lumma WC, Moran MM, Ripka A, et al. (2010). Compounds for modulating TRPV3 function, USP 7,803,790, issued September 28.

Chung M-K, Lee H, Caterina MJ (2003). Warm temperatures activate TRPV4 in mouse 308 keratinocytes. J Biol Chem 278: 32037–32046.

Chung M-K, Lee H, Mizuno A, Suzuki M, Caterina MJ (2004a). 2-Aminoethoxydiphenyl Borate activates and sensitizes the heat-gated ion channel TRPV3. J Neurosci 24: 5177–5182.

Chung M-K, Lee H, Mizuno A, Suzuki M, Caterina MJ (2004b). TRPV3 and TRPV4 mediate warmth-evoked currents in primary mouse keratinocytes. J Biol Chem 279: 21569–21575.

Chung M-K, Güler AD, Caterina MJ (2005). Biphasic currents evoked by chemical or thermal activation of the heat-gated ion channel, TRPV3. J Biol Chem 280: 15928–15941.

Clapham DE (2007). SnapShot: mammalian TRP channels. Cell 129: 220.

Coffin AB, Ou H, Owens KN, Santos F, Simon JA, Rubel EW, et al. (2010). Chemical screening for hair cell loss and protection in the zebrafish lateral line. Zebrafish 7: 3–11.

Deering-Rice CE, Romero EG, Shapiro D, Hughen RW, Light AR, Yost GS, et al. (2011). Electrophilic components of diesel exhaust particles (DEP) activate transient receptor potential ankyrin-1 (TRPA1): a probable mechanism of acute pulmonary toxicity for DEP. Chem Res Toxicol 24: 950–959.

Deering-Rice CE, Johansen ME, Roberts JK, Thomas KC, Romero EG, Lee J, et al. (2012). Transient receptor potential vanilloid-1 (TRPV1) is a mediator of lung toxicity for coal fly ash particulate material. Mol Pharmacol 81: 411–419.

Earley S, Gonzales AL, Garcia ZI (2010). A dietary agonist of transient receptor potential cation channel V3 elicits endothelium-dependent vasodilation. Mol Pharmacol 77: 612–620.

Hu H, Grandl J, Bandell M, Petrus M, Patapoutian A (2009). Two amino acid residues determine 2-APB sensitivity of the ion channels TRPV3 and TRPV4. Proc Natl Acad Sci 106: 1626–1631.

Kaneko Y, Szallasi A (2014). Transient receptor potential (TRP) channels: a clinical perspective. Br J Pharmacol 171: 2474–2507.

Lee JH, Park C, Kim SJ, Kim HJ, Oh GS, Shen A, et al. (2013). Different uptake of gentamicin through TRPV1 and TRPV4 channels determines cochlear hair cell vulnerability. Exp Mol Med 45: e12.

Lin Z, Chen Q, Lee M, Cao X, Zhang J, Ma D, et al. (2012). Exome sequencing reveals mutations in TRPV3 as a cause of olmsted syndrome. Am J Hum Genet 90: 558–564.

Liu B, Escalera J, Balakrishna S, Fan L, Caceres AI, Robinson E, et al. (2013). TRPA1 controls inflammation and pruritogen responses in allergic contact dermatitis. FASEB J 27: 3549–3563.

Moussaieff A, Rimmerman N, Bregman T, Straiker A, Felder CC, Shoham S, et al. (2008). Incensole acetate, an incense component, elicits psychoactivity by activating TRPV3 channels in the brain. FASEB J 22: 3024–3034.

Mukherjea D, Jajoo S, Whitworth C, Bunch JR, Turner JG, Rybak LP, et al. (2008). Short interfering RNA against transient receptor potential vanilloid 1 attenuates cisplatin-induced hearing loss in the rat. J Neurosci 28: 13056–13065.

Nilius B, Bíró T (2013). TRPV3: a 'more than skinny' channel. Exp Dermatol 22: 447–452.

Nilius B, Biro T, Owsianik G (2013). TRPV3: time to decipher a poorly understood family member !. J Physiol 592: 295–304.

Peier AM, Reeve AJ, Andersson DA, Moqrich A, Earley TJ, Hergarden AC, et al. (2002). A heat-sensitive TRP channel expressed in keratinocytes. Science 296: 2046–2049.

Ryskamp DA, Witkovsky P, Barabas P, Huang W, Koehler C, Akimov NP, et al. (2011). The polymodal ion channel transient receptor potential vanilloid 4 modulates calcium flux,

spiking rate, and apoptosis of mouse retinal ganglion cells. J Neurosci 31: 7089–7101.

Sadofsky LR, Campi B, Trevisani M, Compton SJ, Morice AH (2008). Transient receptor potential vanilloid-1-mediated calcium responses are inhibited by the alkylamine antihistamines dexbrompheniramine and chlorpheniramine. Exp Lung Res 34: 681–693.

Shapiro D, Deering-Rice CE, Romero EG, Hughen RW, Light AR, Veranth JM, et al. (2013). Activation of transient receptor potential ankyrin-1 (TRPA1) in lung cells by wood smoke particulate material. Chem Res Toxicol 26: 750–758.

Sherkheli MA, Gisselmann G, Hatt H (2012). Supercooling agent icilin blocks a warmth-sensing ion channel TRPV3. Scientific World J 2012: Article ID 982725.

Stepanyan RS, Indzhykulian AA, Velez-Ortega AC, Boger ET, Steyger PS, Friedman TB, et al. (2011). TRPA1-mediated accumulation of aminoglycosides in mouse cochlear outer hair cells. J Assoc Res Otolaryngol 12: 729–740.

Vogt-Eisele AK, Weber K, Sherkheli MA, Vielhaber G, Panten J, Gisselmann G, et al. (2007). Monoterpenoid agonists of TRPV3. Br J Pharmacol 151: 530–540.

Xu H, Delling M, Jun JC, Clapham DE (2006). Oregano, thyme and clove-derived flavors and skin sensitizers activate specific TRP channels. Nat Neurosci 9: 628–635.

Yamada T, Ueda T, Ugawa S, Ishida Y, Imayasu M, Koyama S, et al. (2010). Functional expression of transient receptor potential vanilloid 3 (TRPV3) in corneal epithelial cells: involvement in thermosensation and wound healing. Exp Eye Res 90: 121–129.